A dark matter quest through decaying axinos and vector-like portals

Dissertation

zur

Erlangung des Doktorgrades (Dr. rer. nat.)

der

Mathematisch-Naturwissenschaftlichen Fakultät

der

Rheinischen Friedrich-Wilhelms-Universität Bonn

vorgelegt von

Stefano Colucci

aus

Maglie, Italien

Bonn, 2018

Angefertigt mit Genehmigung der Mathematisch-Naturwissenschaftlichen Fakultät
der Rheinischen Friedrich-Wilhelms-Universität Bonn.

1. Gutachter: Prof. Herbert K. Dreiner, Ph. D.

2. Gutachter: Prof. Dr. Manuel Drees

Tag der Promotion: Freitag, 14. Dezember 2018

Erscheinungsjahr: 2019

ABSTRACT

To date there is no definite particle physics interpretation of dark matter. At the same time, LHC searches at $\sqrt{s} = 14$ TeV yielded no signals of physics beyond the Standard Model. Minimal models of new physics that predict extra states at the TeV scale are thus in some tension with the experimental data and some well-studied dark matter candidates face very stringent bounds. In the first and main part of this work, we discuss extended supersymmetric models that also address the strong CP-problem of the Standard Model. This has a well-motivated solution in axion models, which include a new neutral pseudoscalar, the axion, and an extra broken $U(1)_{PQ}$ global symmetry group. Both the axion and the axino, its supersymmetric partner, are valid dark matter candidates. We examine the case of a light axino dark matter that decays radiatively emitting a photon and producing the 3.5 keV X-ray line reported in 2014. Such a possibility is disfavored in most of the parameter space for several scenarios. We then construct an original R-parity violating supersymmetric model with a Dine-Fischler-Srednicki-Zhitnitsky axion and study in detail the one-loop decay of the light axino into photon plus neutrino. We examine cosmological constraints as well as those coming from X-ray signals, obtaining bounds on the R-parity-violating couplings and on f_a, the scale of the breaking of $U(1)_{PQ}$.

For the last project presented in this thesis, we consider the simplified model approach to describe dark matter phenomenology. Among simplified models with t-channel mediator, the vector-like portal has the interesting feature that the bremsstrahlung cross section can lift the chiral suppression of the two-body annihilation process and drive the relic density. Furthermore virtual internal bremsstrahlung produces a pronounced peak in the gamma-ray spectrum. We extend the existent analyses to the case of massive quark final states. We present a detailed calculation of the radiative corrections and discuss the effective approach for high mediator masses. Through approximated expressions for the differential and total cross section of the three-body process, we implement the VIB effects into software tools that simulate the hadronization process. Here this effects was not otherwise included for massive quark final states. Our result for the full inclusive cross section is part of a larger study that constraints the parameter space for this model through several complementary searches.

PUBLICATIONS

This thesis contains results from the following research papers.

- S. Colucci, H.K. Dreiner and L. Ubaldi
  "The supersymmetric R-parity violating DFSZ axion model"
  submitted to Phys. Rev. D, arXiv:1807.02530 [hep-th]

- S. Colucci, F. Giacchino, M.H.G. Tytgat and J. Vandecasteele
  "On Radiative Corrections to Vector-like Portal Dark Matter"
  submitted to Phys. Rev. D, arXiv:1805.10173 [hep-th]

- S. Colucci, B. Fuks, F. Giacchino, L. Lopez Honorez, M.H.G. Tytgat and J. Vandecasteele
  "Top-philic Vector-Like Portal to Scalar Dark Matter"
  Phys.Rev. D98 (2018) 035002 , arXiv:1804.05068 [hep-th]

- S. Colucci, H.K. Dreiner, F. Staub and L. Ubaldi
  "Heavy concerns about the light axino explanation of the 3.5 keV X-ray line"
  Phys.Lett. B750 (2015) 107-111 , arXiv:1507.06200 [hep-th]

ACKNOWLEDGEMENTS

I am deeply indebted to many people who supported me during my studies and here I want to show them my appreciation. Let me start with my Ph. D. advisor: working with Herbi and being part of his research group during all these years was an honour and a pleasure. I acknowledge his essential guidance and his support in the decisions I took about my studies. A big thanks goes to my co-advisor Manuel Drees, whose physics insights and sense of humour I will miss. I am thankful to Klaus Desch and Martin Langer for being part of my committee.
A very special thanks goes to my closest collaborator Lorenzo Ubaldi, with whom I already started working during my Master studies. The amount of time he spent sharing his physics knowledge with me is unimaginable. His advice has been always crucial to our common projects and to my career in general. I am much obliged to Florian Staub for his help and his patience in the initial part of my doctoral studies.
I consider myself extremely lucky for the time I spent working in the research group of Michel Tytgat. A huge *merci* goes to him and to my other collaborators in Brussels, Laura Lopez Honorez, Federica Giacchino and Jérôme Vandecasteele.
Among the many physicists that have crossed their paths with mine in Bonn I want to say here "thank you" to my very unique group: Victor Martín Lozano, Manuel Krauss, Simon Wang, Annika Reinert, Toby Opferkuch, Daniel Dercks, Kilian Nickel. I am glad that I had the chance to spend all this time with these wonderful people and I wish them the best of luck for their future.
I would like to thank Raghuveer Garani for being always keen to answer to my physics questions and for cooking exceptional lentils.
The good times I spent with Thorsten Schimannek inside and outside the institute will be deeply missed.
It would have been impossible to work in the BCTP at such privileged conditions without the extraordinary help from our precious secretaries. I thus hereby thank: Petra Weiss, Patricia Zündorf, Christa Börsch, Andreas Wisskirchen and Dagmar Fassbender.
Even though it is often very hard to let my family understand what my research is about, my parents and my sister never ceased to encourage me to pursue my objectives. I wish we could have more time to share together.
My deepest gratitude goes to Mila Shamku, who keeps providing me with all the inspiration I need in life.

CONTENTS

1

INTRODUCTION

1.1 THE SUCCESS OF THE SM ...

More than a century passed since in 1900 Planck solved the black-body radiation problem in 1900 with the first quantum hypothesis about the behaviour of light [1]. Only five years later Einstein published his paper stating the principle of invariant light speed [2]. The combination of the theories which were initiated from these two milestones, quantum mechanics and special relativity respectively, together with elements of field theory, constitutes the basis of (relativistic) quantum field theory (QFT). The addition of gauge symmetry completed the mathematical framework which sustains the Standard Model (SM) of particle physics, the theory through which to date we best understand how subatomic particles interacts.

The nucleus of its current structure is to be found in the seminal work done in the '60s by Glashow, Weinberg and Salam [3–5], whose GWS model introduced for the first time a unified theory of electroweak interactions with gauge group $SU(2) \otimes U(1)$. Clearly this symmetry is not realized at low energies though, as distinct charged-currents (CC) and neutral-currents (NC) were already observed at experiments at that time. The gauge symmetry itself also forbids adding mass terms for the gauge bosons or the fermions. The keystone that solves this conundrum is the Anderson-Brout-Englert-Guralnik-Hagen-Higgs-Kibble mechanism [6–8], or *Higgs mechanism* for short, which triggers electroweak symmetry breaking (EWSB). Its realization requires adding an extra scalar $SU(2)$ doublet ϕ, in a way that while the SM Lagrangian $\mathcal{L}_{SM}$ still respects the gauge symmetry, the state of lowest energy for ϕ is not zero, but rather a *vacuum expectation value* (VEV), $v/\sqrt{2} \approx 174$ GeV. Thanks to the Goldstone theorem [9, 10] and parametrizing the low energy scalar excitations around the VEV in the *unitary gauge* introduces explicit mass terms for the electroweak gauge bosons from the gauge-invariant kinetic terms of the scalar potential. At the same time, the $U(1)_{EW}$ subgroup of electrodynamics remains untouched and thus the photon stays massless. In terms of group theory the spontaneous symmetry breaking (SSB) of the electroweak theory is realized as

$$SU(2)_L \times U(1)_Y \xrightarrow{v \neq 0} U(1)_{EW} \,, \tag{1.1}$$

where the subscript Y refers to the *hypercharge* quantum number assigned to each field in the SM. The subscript L specifies that the left-chiral components of the three generations of leptons and quarks are organized in $SU(2)$ doublets, while the right-chiral counterparts are singlets. The structure of the resulting gauge-invariant *Yukawa couplings* $y_{ij}\psi_{i,L} \cdot \phi\, \psi_{j,R}$[1] [2] that mixes the left and right component of the fermionic field ψ allows for v-dependent mass terms for the fermions, for which a mass term before EWSB would also be forbidden. Among the greatest successes of the GWS model of electroweak interactions is the correct prediction of the values

1 For case of up-quark Yukawas, one also needs to introduce $\widetilde{\phi} \equiv i\sigma_2\phi^*$ in order to respect the $U(1)_Y$ gauge symmetry of the SM.

2 We use here "$\cdot$" to refer to the standard antisymmetric $SU(2)$ product.

of the Z and W masses, which were both discovered in 1983 [11, 12]. The SM theory of electroweak interactions was also shown to be *renormalizable* at all orders [13, 14]. This essentially means that all the infinities arising from the loop corrections to the parameters of the model can be absorbed by an opportune shifting of the bare Lagrangian terms and thus the remaining value is meaningful physical observables. The quantum field theory describing strong interactions within hadrons, *Quantum chromodynamics* (QCD) [15–17], was incorporated in the SM in the '70s. QCD interactions exhibit a non-abelian unbroken $SU(3)$ gauge symmetry, which extends the group structure of the SM to its complete form (before EWSB),

$$\mathcal{G}_{SM} = SU(3)_C \otimes SU(2)_L \otimes U(1)_Y \,, \tag{1.2}$$

where the subscript C stands for the *color* charge of quarks and gluons, the latter being the massless gauge bosons of the strong force. One of the earliest and most spectacular successes of QCD was the prediction of the gluon particle, which was discovered in 1978 [18].

Yet the most celebrated prediction of the SM was the one about the existence of its Higgs boson h, the neutral scalar resulting from the doublet ϕ after EWSB. In 2012 a resonance around the expected value of its mass, $m_h \approx 125$ GeV, was reported by both the ATLAS and CMS experiment independently. They analyzed the products of the proton-proton collisions at the LHC collider, with energies $\sqrt{s} = 7 - 8$ TeV. Further measurements of its couplings and spin confirmed that it was indeed the Higgs boson, thus finally completing the picture of the SM particle content.

Additional accidental *global symmetries* the SM exhibits are associated to the conservation of *baryon number* B and of individual *lepton numbers* L_i , with $i = e, \mu, \tau$, respectively. Hinting at concept that we will explore deeper in Ch. 2, we anticipate that *at classical level* $U(2)_L \otimes U(2)_R$ could be a *approximate* flavor symmetry of the QCD Lagrangian, in the sense that it is realized only at tree-level and in the limit $m_{u,d} \ll \Lambda_{QCD}$ [19]. The only *exact* symmetry associated to QCD is indeed the $U(1)_B$ corresponding to baryon number, which guarantees *e.g.* that nucleons and antinucleons have the same mass. *At quantum level* though, $U(1)_B$ and $U(1)_{L_i}$ are both affected by *anomalous currents* and the only conserved global charges of $\mathcal{L}_{SM}$ are $3L_i - B$ [3].

With 19 independent free parameters (3 gauge couplings, 9 charged fermion masses, 3 quark mixing angles, 1 CP-violating phase, 1 Higgs VEV and 1 Higgs mass, 1 QCD vacuum angle) the SM explains to a very high level of agreement all experimental data obtained in low-energy physics, high-precision measurements and high-energy physics, with the exception of neutrino oscillations [20]. Yet there are many aspects in which we know beyond Standard Model (BSM) physics is needed, due to either experimental facts which find no possible explanation within the SM or because of limitations in the SM theory itself.

1.2 ... AND WHERE IT FALLS SHORT.

Following from general principles, the SM is most evidently not expected to be the ultimate theory of nature, as it accounts for the electromagnetic, weak and strong

3 Adding right-handed neutrinos to SM as to give them a Dirac mass reduces this symmetry to $U(1)_{B-L}$ only.

forces, but gravitational phenomena are not covered at all. Clearly their inclusion in a theory of high-energy physics is a genuinely theoretical problem, since gravitational effects become important only around the *Planck scale* $M_{Pl} \approx 10^{19}$ GeV, an energy which is definitely out of our experimental reach. On the other hand, Einstein's General Relativity is a much consolidated theory that accurately describes the behaviour of celestial bodies and large-scale structure in the universe. Despite great theoretical efforts though, all the attempts towards a unified theory of nature including all four known forces failed so far [21].

1.2.1 *The dark matter puzzle, WIMPs and gamma-ray signals*

Leaving theory aside for a moment, when it comes to *dark matter* (DM), particle physics seems to disagree even with classical gravity. The introduction of the concept of dark matter dates back to 1933, when the Swiss astronomer F. Zwicky proposed that such "dunkle Materie" could account for the radial velocity dispersion of galaxies in the Coma Cluster [22, 23]. What is regarded to be the first convincing and direct DM evidence first came in 1939 [24], and was later confirmed [25] with the observation of *rotation curves* of the galaxies, namely the graph of circular velocities of stars and gas as a function of their distance from the galactic center. In order to reconcile with Newtonian physics the observation of constant rotational velocity of the galaxy for radii larger than the visible size of the galaxy, the presence of non-luminous matter was postulated. Experimental evidences for DM are nowadays numerous and stem from various phenomena and techniques: X-ray detection of hot gas in elliptical galaxies [26], strong lensing [27], weak modulation of strong lensing [28, 29], Oort discrepancy [30], weak gravitational lensing of distant galaxies by foreground structures [31], velocity dispersion of dwarf spheroidal galaxies [32, 33].

Today the most stringent constraint on dark matter comes from the *cosmic microwave background* (CMB) radiation [34, 35]. This is essentially the relic abundance of the photons which lastly decoupled from plasma. They then cool down until today to a temperature near $2,73\,K$. Very recently, some years after the last data release of the Wilkinson Microwave Anisotropy Probe experiment (WMAP) [36], the PLANCK experiment [37] measured the value and fluctuation of the cosmic microwave background radiation. PLANCK confirmed the isotropy of the CMB. This and other measurements highly constrained the ΛCDM model, also called *the cold*[4] *dark matter model with dark energy*. It is the simplest and most-widely accepted description of our universe, which explains with six degrees of freedom the expansion after big-bang, the large scale structure of galaxy clusters, the distribution of the lightest elements and the accelerating expansion of distant galaxies and supernovae, assuming a flat universe. The best fit given by PLANCK for cold DM density is

$$\Omega_{CDM} h^2 = 0.1200 \pm 0.0012 \,. \tag{1.3}$$

Everything we mentioned so far are among the main experimental evidences for dark matter. From a theoretical point of view, a strong argument supporting the existence of DM is about structure formation. If the universe consisted solely of

4 A DM relic with mass m_{DM} which decouples at a temperature T_d is defined to be *cold* if $T_d \ll m_{DM}$, *i.e.* it is non-relativistic at the time of freeze-out. When $T_d \gtrsim m_{DM}$, we refer to a *warm* (*hot*) DM relic if $m_{DM} \gtrsim 1$ eV ($m_{DM} \lesssim 1$ eV) [38].

luminous matter, then the epoch of structure formation would have been very short, probably requiring initial perturbation that would have given rise to CMB anisotropies larger than those observed [39, 40].

There is an enormous wealth of possible dark-matter candidates. Their mass range from axions with mass around $10^{-5}\text{eV} = 9 \times 10^{-72} M_\odot$, to black holes of masses up to $10^{14} M_\odot$. A first distinction can be done: baryonic versus non-baryonic candidates, with the main baryonic candidates being massive compact halo objects (MACHOs) [41, 42]. A second distinction can be done among cold, hot or warm nonbaryonic dark matter candidates. Light neutrinos were the first hot candidates, but N-body simulations of structure formation in a universe dominated by hot dark matter do a poor job of reproducing the observed structures [43]. Also, they are not abundant enough to be the dominant component of dark matter [44]. The nonbaryonic dark matter candidates are basically particles which have not yet been discovered. The leading non-baryonic cold dark matter are axions and *weakly interacting massive particles* (WIMPs). The reason why WIMPs are so widely studies lies in the fact that they realize the so-called *WIMP miracle*, yielding the correct value of the relic abundance $\Omega_{\text{CDM}} h^2$ with a cross section comparable to those typical of the weak interaction, $\sigma_W \sim 10^{-36}\text{cm}^2$. The first proposed cold dark-matter candidate in the WIMP class was a stable, heavy ($m \gtrsim$ GeV), fourth-generation Dirac or Majorana neutrino with SM couplings [45], which was ruled out some time ago [46]. The most theoretically well-developed candidate is by far the lightest supersymmetric particle (LSP). It arises in the context of theory of supersymmetry (see Sec. 1.2.3 below), and some popular example are *neutralinos* [47], *sneutrinos* [48], *gravitinos* [49–51].

The axion [52, 53] is motivated as a possible solution to the strong CP-problem, see Ch. 2. If such an axion exists, then a cosmologically interesting (i.e., $\Omega \sim 1$) density of axions would have been produced at the QCD phase transition. If these axions populate our halo, they can potentially be detected via resonant conversion to photons in a magnetic field. *Axinos*, the supersymmetric partner of the axion, were believed until recently to only be capable of acting as a warm, or hot, dark matter candidate [54]. It has been shown, however, that for quite low reheating temperatures, cold axino dark matter may be possible [55]. In many ways, axinos and gravitinos share similar phenomenological properties.

Particle physics experiments searching for DM essentially proceed with three methods: *direct detection* involves a DM particle scattering off of a nucleus from a detector material [56]; *indirect detection* techniques look for DM annihilation into SM particles [57–59]; *collider production* aims at producing DM in laboratories, with current searches undergoing at the LHC [60]. Among indirect methods, gamma rays are the most promising tool to observe DM, as they propagate through the galaxy without significant energy losses. Secondary photons are produced copiously when the annihilation or decay products undergo subsequent interactions in the interstellar medium. These happens via a variety of processes and these photons are therefore hard to trace back to a DM origin. On the contrary, primary or prompt photons can be produced directly or through radiative corrections by the process that destroys DM and thus preserve specific spectral features. An example of such processes is Virtual Internal Bremsstrahlung (VIB), which consists in the emission of a boson from the internal propagator in the diagram describing the process. The corresponding photonic spectra has a pronounced peak for

energies close to the DM mass that has no astrophysical counterpart. In Ch. 5 we study how to produce such a VIB photon spectrum in the context of a *simplified model* for DM. This class of models represent an approach to DM model building which falls in between complete models and effective field theories (EFT). In the first case, the main limitation is given by the fact that one can hardly constrain all the parameters of the theory, whereas in the second case its application to process with high-momentum transfer was proven inaccurate [61, 62]. Simplified models add to $\mathcal{L}_{SM}$ only masses and couplings which are strictly needed in order to describe the interaction between ordinary matter and DM, which is mediated by an extra particle acting as a *portal*. There are many options available when constructing simplified DM models, which are normally classified between s- and t-channel portals according to the way the DM annihilation proceeds [63]. The second case is particularly appealing, since under the assumption that the DM is a Majorana particle, it closely resembles the case of the MSSM neutralino, and thus received much attention. VIB is particularly relevant to this class of models, as the three-body final state processes can lift the helicity suppression of the two-body annihilation cross section [64–66]. On the other hand, a scalar DM candidate is equally viable and shares some of the characteristics of the Majorana case. In [67] it was proven that for the case of real scalar dark matter the $2 \to 2$ DM annihilation cross section is d-wave suppressed. This vindicates the fact that bremsstrahlung process can be a dominant annihilation channel within the *vector-like portal* (VLP) model.

In Ch. 3 we encounter another potential indirect signal for DM detection in the form of the 3.5 keV line. This excess in the X-rays was reported in 2014 from the observation of galaxies and galaxy clusters [68, 69]. While the discussion about its possible astrophysics origin has weakened the strength of the DM hypothesis [70–78], plenty of particle physics explanations were proposed. Among those, [79–82] demonstrated how the decay of a 7 keV axino with a photon in the final state can be responsible for it.

1.2.2 *GUTs, Naturalness of the electroweak scale and the hierarchy problem*

Switching now to a more theoretical preoccupation, from the perspective of unification of forces the SM is *per se* not satisfying, as one seeks for the highest possible symmetry to be realized in nature at some high scale $\Lambda \leqslant M_{Pl}$, rather than simply accept the aforementioned 19 parameters to be god-given. In particular, $\mathcal{G}_{SM}$ of Eq. (1.2) ought to be the result of some SSB pattern from an original single gauge group $\mathcal{G}_X$. This way, at the scale of such a Grand Unified Theory (GUT), all three *running* coupling g_i of the SM would meet at a single value. Most well-studied examples of GUTs take $\mathcal{G}_X$ to be $SU(5)$ or $SO(10)$ [83–86], with a typical unification scale at $M_{GUT} \sim 10^{16}$ GeV.

The fact that some new physics is expected to lie at some high scale $\Lambda > M_{EW} \sim 10^2$ GeV introduces one of the main theoretical drawbacks of the SM. From QFT we know that the mass m_f of chiral fermions is protected: when self-energies contributions m_f are considered, they can be at worst log-divergent, $m_f \propto \ln(\mu/m_f)$. μ is some *cut-off scale* at which our theory does not yield meaningful predictions, ideally $\mu \lesssim M_{Pl}$. In a theory with renormalizable interactions, such a term can safely be absorbed in a counterterm and quantum corrections will not depend on Λ in the limit $m_f \to 0$. The same argument does not apply to scalars though,

and the mass of the Higgs boson is a highly unnatural [5] parameter of the SM [90, 91]: corrections from particles with masses around a new physics scale Λ diverge quadratically, and any renormalization procedure leaves a residual finite correction $m_h^2 \propto \Lambda$ [92]. Therefore a very fine-tuned cancellation among the $\mathcal{O}(\Lambda)$ terms would be needed in order to keep $m_h^2 \sim M_{EW}$. This is called the *hierarchy problem* of the SM: it pressingly requires a mechanism to obtain such cancellation from a higher principle.

1.2.3 *Supersymmetric theories, the MSSM and R-parity violation*

Together with theories of extra-dimensions [93, 94] and composite Higgs [95, 96], the solution offered by *supersymmetry* (SUSY) [97, 98] is among the most well-motivated and widely studied over the last five decades. Consistent theories of spacetime exhibit the external symmetries described by the Poincaré algebra. Charge conjugation (C), parity transformation (P) and time reversal (T) are additional internal discrete symmetries of QFT. The fundamental *Coleman-Mandula no-go theorem* [99] restricts any additional Lie algebra that contains both the Poincaré algebra and the algebra describing such internal symmetries to be trivially the direct product of the two. A possible caveat to this argument is to consider *graded Lie algebras* for the internal symmetries, in which case an extra Z_2 discrete group is the maximum allowed [100, 101]. The corresponding extra supersymmetric generators Q_α [6] map fermionic representations into bosonic ones and *vice versa*. As a consequence, in a consistent supersymmetric theory the fermionic and bosonic degrees of freedom ought to be the same and thus each particles comes with its *superpartner*, which is bosonic if the original particle is fermionic and the other way around. Integer-spin and half-spin modes are then parts of SUSY-invariant objects called *superfields*, each component of which has the same mass and the some coupling with respect to any interaction. This is the key to solve the hierarchy problem in SUSY, as an automatic cancellation between bosonic and fermionic loops is thereby enforced: it removes the quadratic divergences in the loop diagrams contributing to the m_h^2. In other words, SUSY extends to scalars the protection from high-scale corrections that chiral fermions enjoy, thus rendering *natural* for the Higgs of the SM to have a mass around the electroweak scale or any other low scale, despite it being so low compared to the Planck scale [92]. Another aspect of the mass degeneracy within superfields is that, following the lack of evidence for any scalar partner of the SM fermions with masses at the electroweak scale, one concludes any realistic supersymmetric theory should also implement a mechanism through which SUSY is broken spontaneously at same scale above M_{EW}.

The *Minimal Supersymmetric Standard Model* (MSSM) is the most minimal choice when seeking for a SUSY theory which contains the SM and preserves as much as possible its symmetries, and thus its interactions and phenomenology (see *e.g.* [92, 102] for excellent and accessible introductions). In the MSSM quarks and leptons are parts of *chiral superfields* with the same SM quantum numbers, together with their superpartners *squarks* and *sleptons*. Gauge bosons and their spin-1/2 partners

5 This can be also understood using the notion of *naturalness* [87–89], by considering th example of the SM fermions. Masses of the SM fermion are naturally small because in the limit of it going to zero, the chiral symmetry of the theory is restored. If the scalar mass is set to zero there is no extra symmetry.

6 From now on, we only refer to $\mathcal{N} = 1$ supersymmetry representation.

enter the *vector superfields*. Things get slightly more complicated when it comes to the SM scalar, since in the MSSM we end up with two Higgs doublets $\hat{H}_u$ and $\hat{H}_d$, where the symbol "$\hat{}$" from now on denotes a superfield. The first reason for this stems from preserving the *anomaly cancellation* of the SM also in the MSSM: solely adding a fermionic Higgs doublet $\tilde{H}$ [7] will spoil this desirable feature, which can be recovered in the most minimal way by adding a second doublet superfield with opposite hypercharge [103] [8].

The second reason why we need an extra doublet is rooted in the formalism of SUSY itself. Aside from kinetic terms and self interactions arising from the gauge sector of the theory, the interactions of superfields are described by specifying a so-called *superpotential* W, a polynomial in the superfields $\hat{\Phi}_i$. If one wants to retain renormalizability, than W can have cubic terms at most. The shape of the superpotential is further specified by gauge symmetries, *R-parity* and *holomorphy*. R-parity (R_p), is a discrete Z_2 symmetry resulting from the SUSY algebra, that is assumed to be conserved in the MSSM [104]. Its interaction thus always conserve the number $R_p = (-1)^{3(B-L)+2S}$, where S stands for the spin of the field. This also implies that all SM particles are R-even, while their superpartners (*sparticles*) are R-odd. Holomorphy dictates that the superpotential is an analytic function of the superfields, which in turn implies that the superfields ought to share all the same chirality. Since the convention for the MSSM is to work with left-chiral superfields only, in the MSSM superpotential we need to take the conjugates of the SM right-handed singlets. This is indicated by a bar on top of a letter. The superpotential of the MSSM then reads

$$W_{\text{MSSM}} = (Y_u)^{ij}\hat{Q}_i \cdot \hat{H}_u \hat{\bar{U}}_j + (Y_d)^{ij}\hat{Q}_i \cdot \hat{H}_d \hat{\bar{D}}_j + (Y_e)^{ij}\hat{L}_i \cdot \hat{H}_d \hat{\bar{E}}_j + \mu\, \hat{H}_u \cdot \hat{H}_d\,. \quad (1.4)$$

W_{MSSM} manifestly reproduces the Yukawa interactions by means of the first three terms in the above equation. This brings us to the second reason that explains the presence of $\hat{\bar{H}}_u$ within W_{MSSM}: as holomorphy prohibits the use of right-handed fields, we can not use the conjugate of $\hat{\bar{H}}_d$ to specify the Yukawa coupling involving the up-quarks and we must therefore add $\hat{\bar{H}}_u$. The extra μ-*term* in the superpotential does not resembles any SM interaction and features the dimensionful coupling μ. The parts of the Lagrangian of the MSSM contained in W_{MSSM} can be obtained as

$$\mathcal{L}_{\text{MSSM}} \supset -\frac{1}{2}\left(\xi_i \xi_j \left.\frac{\partial^2 W_{\text{MSSM}}}{\partial\hat{\phi}_i \partial\hat{\phi}_j}\right|_{\hat{\phi}_i \to \varphi_i} + \text{h. c.}\right) - \left.\frac{\partial W_{\text{MSSM}}}{\partial\hat{\phi}_i}\right|_{\hat{\phi}_i \to \varphi_i}, \quad (1.5)$$

where the subscript $\hat{\phi}_i \to \varphi_i$ indicates that one needs to first take the derivative with respect to the superfield, then consider only its scalar component. ξ_i are the spin-1/2 components each superfield.

A remarkable feature that comes with the MSSM is that it achieves the unification of the running gauge couplings: the additional particle content modifies

7 Superpartners of SM particles are generally denoted by the same character of the original field with a tilde above, *e.g.* $\tilde{t}_L$ represents a *stop*, the spin-0 component of the third generation of the lepton doublets $\hat{L}_i$.

8 In our convention $\hat{H}_d$ is the SM-like Higgs superfield, with hypercharge $Y = -1/2$. A table with the MSSM particle content and the quantum numbers for the different gauge group can be found *e.g.* in Ref. [92].

the *renormalization group equations* (RGEs) in such a way that the gauge couplings associated to $\mathcal{G}_{SM}$ meet at the same point at $M_{GUT} \sim 10^{16}$ GeV.

As we mention earlier, if the MSSM is to explain the current SM mass spectrum, SUSY must be spontaneously broken a some energy above the electroweak scale. There are various mechanisms that can achieve that, *e.g.* via Planck-scale interaction [105–107], gauge-mediation [108–113], extra dimensions [93, 114–116] or anomaly mediation [117, 118]. More generally, when constructing a realistic SUSY theory, one adds to the scalar potential a generic set of *soft-breaking terms* that violates SUSY, while being consistent with all the other symmetries of the model. An example of this $\mathcal{L}_{soft}$ Lagrangian can be found in Eq. (4.14), where we see *e.g.* that explicit SUSY-breaking mass terms $m^2_{H_{d,u}}|H_{d,u}|^2$ for neutral scalars $H_{u,d}$ are introduced. The natural values of the parameters in $\mathcal{L}_{soft}$ are all expected to be around the scale of SUSY breaking M_{SB}. This parameter therefore enters in the analytical expressions for the particle masses, as it is the case for the mass of the Z boson when studying the scalar potential at tree-level [102]:

$$M_Z^2 = \frac{\left|m^2_{H_d} - m^2_{H_u}\right|}{\sqrt{1-\sin(2\beta)}} - m^2_{H_d} - m^2_{H_u} - 2|\mu|^2 \,, \tag{1.6}$$

where the parameter β is defined as the ratio of the VEVs of the two CP-even neutral components the Higgs scalars, $\tan\beta = v_u/v_d$. Eq. (1.6) captures the essence of the μ-*problem*: in order to reproduce the right value for M_Z, one needs all the parameters in the RHS to be around its order of magnitude, otherwise very ad-hoc cancellations are required. Thus the μ parameter, although of supersymmetric origin, is *a posteriori* required by correct EWSB to be at the order of the electroweak scale or M_{SB}.

Another important lesson from the study of the MSSM scalar mass spectrum pertains the mass of the Higgs. In fact at tree-level one obtains an upper bound on the Higgs mass, $m_h \leqslant M_Z|\cos 2\beta|$ [9], which manifestly disagree with experiments. Radiative corrections come to our rescue, provoking a shift [10]

$$m_h^2 \leqslant M_Z^2\cos^2 2\beta + \frac{3g_2^2 m_t^4}{8\pi^2 M_W}\left[\ln\left(\frac{M_{\tilde{t}_1}M_{\tilde{t}_2}}{m_t^2}\right) + \dots\right] , \tag{1.7}$$

where the $M_{\tilde{t}_i}$ are the masses of the stops and we are neglecting subleading terms. In order to accommodate the measured value of m_h one needs the stop masses to $\mathcal{O}(\text{TeV})$. A similar argument also applies for corrections dependent on gluino masses. Thus this argument constitutes a strong motivation for expecting new physics to be found at the TeV-scale.

Unfortunately so far no evidence whatsoever for BSM physics was found at the LHC, something which is tension with the predictions of the most simple models like the MSSM. Most supersymmetric models which have been searched for at the LHC make the assumption of conserved R-parity [119]. A very restrictive and

9 To be more precise, this is true when $m_A > M_Z$, with m_A the physical mass of the CP-odd neutral Higgs.

10 Eq. (1.7) is to be considered valid only under certain assumptions about the spectrum of the theory, *i.e.* the stop mass eigenvalues and mixings. In order to stick to the point of our discussion, here we omit further details, which can be instead found in the Ref. [20], as well as in the reviews quoted above.

widely considered version with universal boundary conditions at the unification scale, the constrained minimal supersymmetric model (CMSSM) [120], is put under pressure by collider data [121]. The R-parity violating (RpV) CMSSM is still very much allowed [122]. R-parity is invoked in the CMSSM to forbid baryon and lepton number violating operators which together lead to rapid proton decay. The bonus of imposing R-parity is that sparticles are always produced and disappears in pairs. Consequently the LSP, typically the neutralino, is stable and provides a DM candidate in the form of a WIMP. This is the most popular and most searched for DM candidate. However, to–date no neutralino dark matter has been found [123–125]. It is thus prudent to investigate other DM candidates, also within alternative supersymmetric models. R-parity does not forbid some dimension-5 operators dangerous for proton decay [126]. This issue can be resolved by imposing a Z_6 discrete symmetry, known as proton hexality (P_6), which leads to the same renormalizable superpotential as R-parity [127, 128], but is incompatible with a GUT symmetry. Alternatively, one can impose a Z_3–symmetry known as baryon-triality (B_3) [102, 127, 129–133]. The latter allows for lepton number violating operators in the superpotential thanks to which the neutrinos acquire Majorana masses (see below in Sec. 1.2.4), without introducing a new very high energy Majorana mass scale [130–132, 134–139]. This is a virtue of B_3 models [11]. The superpotential for such models extends that of Eq. (1.4) by the terms:

$$W_{B_3} = \frac{1}{2}\lambda_{ijk}\hat{L}_i \cdot \hat{L}_j\hat{\bar{E}}_k + \lambda'_{ijk}\hat{L}_i \cdot \hat{Q}_j\hat{\bar{D}}_k + \kappa_i\hat{H}_u \cdot \hat{L}_i \,, \tag{1.8}$$

where λ_{ijk} is antisymmetric in the first two index due to the $SU(2)$ structure of the operator and κ_i has mass dimension 1. A possible handicap of RpV models is that the LSP is unstable and is not a dark matter candidate. This can be naturally resolved by considering a candidate which long-lived such that it decays with a lifetime longer than the age of the universe.

1.2.4 *"It gets worse before it gets better"*

The third main BSM topic that enters the discussion of this manuscript together with DM and SUSY is the *strong CP-problem* [145]. This puzzle has to do with the presence of the θ-term in the SM Lagrangian - the aforementioned QCD vacuum angle, once the true topology of the $SU(2)_L$ vacuum is properly defined [146, 147]. This extra term $\bar{\theta}\,\widetilde{F}^{\mu\nu}_a F^a_{\mu\nu}$ is a source of charge-parity (CP) violation. As such it is very much constrained by measurements of electric dipole moment (EDM), which impose a restrictive $\bar{\theta} < 10^{-10}$ [148, 149]. The question why this parameter of the gauge theory should be so unnaturally small is labelled as the strong CP-problem. Every complete model should address it, as it plagues the SM, as well as its supersymmetric generalizations. In its simplest forms this needs the introduction of the pseudo scalar axion field [150, 151] and an extra broken $U(1)_{PQ}$ global symmetry [152, 153]. In the supersymmetric versions, the axion is part of a chiral supermultiplet and is accompanied by another scalar, the saxion, and a spin-1/2 fermion, the axino. Ch. 2 of this thesis is dedicated to introduce this subject.

11 Other than P_6 and B_3, one can also consider R-symmetries to restrict the renormalizable Lagrangian resulting in R-parity conservation or violation [140–144].

The fact that the SM predicts massless neutrinos represents another drawback for this theory. SM neutrinos are the only massless Weyl fermions with no right-handed counterpart. In the last few years, evidence for neutrino masses through their oscillations and mixings has become more and more compelling, through solar, atmospheric, reactor and accelerator neutrinos [20, 154]. The absolute scale of the sum of their masses is fixed by PLANCK measurements $\sum_i m_{\nu_i} < 0.23$ eV, [20] but their hierarchy is not fixed. The most economical explanation of these facts is that neutrinos have Majorana masses arising from lepton-number violating dimension five operators [12], *i.e.* suppressed by one power of some large mass. Explicitly, these have the form: $\mathcal{L}_{l\nu} = \frac{1}{M} LHLH$. Replacing the Higgs field by its expectation value v gives a mass for the neutrino of order $\frac{v^2}{M}$. If $M = M_{Pl}$, this mass is too small to account for either set of experimental results. So one expects that some lower scale is relevant. The *see-saw* mechanism provides a simple picture of how this scale might arise [155, 156], as we show in the case of a toy-model in Sec. 3.1. The MSSM does not provide any mass term for neutrinos. Allowing for RpV interactions opens up the possibility to obtain the measured neutrino physical parameters from the mixings in the neutralino mass matrix [157, 158], as shown in Sec. 3.6.2.

In our work presented here we will not be dealing with other pressing issues of high-energy theory that require BSM physics : the discrepancy between the measured and the predicted value for the muon magnetic moment [159]; the lack of an explanation for the origin of the baryon asymmetry of the universe (BAU) [160, 161]; the mystery associated with the nature of *dark energy* [162].

The content of this thesis is structured as follows. In Ch. 2 we introduce the strong CP-problem and its axion solution. Moving from the notion of classical symmetry, we show how symmetries can be broken by the anomaly. After the $U(1)_A$ of $n = 2$ QCD is presented, we explain how the θ-vacuum naturally arises in $SU(2)$ gauge theories and how this leads to the problematic $\bar{\theta}$-term of the SM Lagrangian. We show the early axion solution and then examine in details the the Dine-Fischler-Srednicki-Zhitnitsky (DFSZ) model, as it constitutes part of the basis for our original model introduced in Sec. 4.2. For the same purpose, we analyze a minimal supersymmetric axion model that achieves PQ-breaking while being consistent with SUSY. A description on how to obtain axino gauge interactions follows.

Ch. 3 is devoted to assess whether the axino is a valid candidate to explain the 3.5 keV-line signal. We start with a brief introduction to some feature with sterile neutrino models, since the axino behaves analogously when it decays. After a brief look at the astrophysical X-ray signals, we narrow our analysis to the axino case and consider constraints from DM relic abundance and the presence of a gravitino, both for R-parity conserving and violating scenarios. In particular, in the second case we also examine the scenario with a neutralino mass $\mathcal{O}(\text{GeV})$.

The study of a new RpV supersymmetric model with an axion sector is the subject of Ch. 4. Here we begin by motivating our choice for the specific DFSZ model and high-scale SUSY-breaking. After we discuss the Lagrangian of the model and its mass spectrum, we scrutinize cosmological constraints from axion, saxion, axino and gravitino. We analyze in detail the decay modes of the light axino, with specific focus on the different channels for its radiative decay. Using X-ray bounds, we

12 A Majorana mass is a mass for a two component fermion, which is permitted if the fermion carries no conserved charges.

use this observable to obtain constraints on the scale of the PQ symmetry-breaking scale f_a, as well as on RpV couplings.

In Ch. 5 we switch to the study of DM annihilation for the vector-like portal model with massive quark final states. We present a detailed next-to-leading-order (NLO) calculation of the three-body process with emission of a massless boson. We argue that this can be relevant to the fully inclusive cross section due to the velocity suppression of the $2 \to 2$ process. Finally we discuss several approximations to the total as well as differential cross section and obtain the photonic spectra from bremsstrahlung showing a VIB feature.

In Ch. 6 we summarize the main points of our research and conclude. Extra details about some technical aspects of our work are given the in App. A.

2

THE AXION

In this chapter we introduce the reader to some aspects in the vast topic of axion physics which are relevant to our research work presented in Chs. 3 and 4 . Sec. 2.1 is about motivation: we explain the shortcoming of the SM known as the strong CP problem, starting from the concept of anomalous symmetries in QFT. We then show why they are important to the resolution of the $U(1)_A$ problem of QCD, then introduce the θ-vacuum of non-abelian gauge theories and the strong CP problem. In Sec. 2.2 we discuss its resolution within the original axion model and present the subsequent variants. In Sec. 2.3 we focus on the original DFSZ invisible axion from a model building perspective. Supersymmetric axion models are introduced in Sec. 2.4, where we also study the mass spectrum derived from a superpotential with three axion-like superfields, later adopted in in the model of Sec. 4.2.

2.1 INTRODUCING THE STRONG CP PROBLEM

2.1.1 *Chiral symmetry breaking via the axial anomaly*

At the classical level in field theory, a *symmetry* is defined as a continuous transformation on the field ϕ that leaves the equation of motion invariant. If we express the infinitesimal form of the transformation in terms of a parameter ε,

$$\phi(x) \to \phi(x) + \varepsilon\, \delta\phi(x)\,, \tag{2.1}$$

then the corresponding change in the Lagrangian

$$\mathcal{L} \to \mathcal{L} + \varepsilon\, \partial_\mu \mathcal{P}^\mu\,, \tag{2.2}$$

involves at most an innocuous surface term $P^\mu(x)$, which doesn't contribute to the action integral. *Noether theorem* ensures that the corresponding current density

$$j^\mu = \frac{\partial \mathcal{L}}{\partial\,(\partial_\mu \phi)}\delta\phi - \mathcal{P}^\mu\,, \tag{2.3}$$

is conserved, i.e. $\partial_\mu j^\mu = 0$. Another way of expressing the conservation law is to say that the charge

$$Q \equiv \int d^3x\, j^0 \tag{2.4}$$

does not change with time. The first example of one such current is the energy-momentum tensor, which corresponds to the invariance of the Lagrangian under translations. Let us now consider the massless QED Lagrangian

$$\mathcal{L}_{\text{QED}} = i\overline{\psi}(x)\not{D}\psi(x) - \frac{1}{4}F^a_{\mu\nu}F^{\mu\nu}_a\,, \tag{2.5}$$

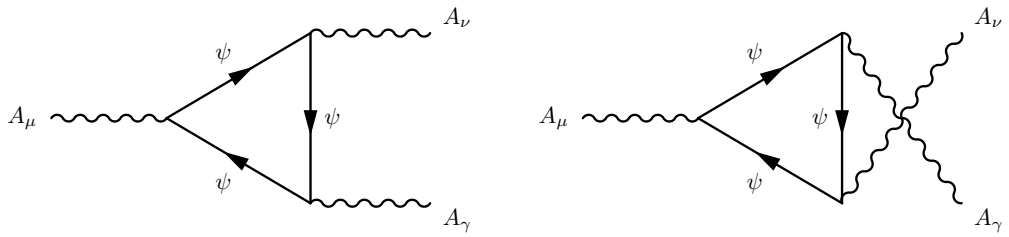

Figure 2.1: Diagrams responsible for the anomalous axial divergence. The anomaly follows from the need of preserving gauge invariance when using dimensional regularisation to calculate the loop integrals. Put in simple terms, one has to extend the intrinsic four-dimensional definition of $\gamma_5 \equiv i\gamma^0\gamma^1\gamma^2\gamma^3$ to an arbitrary number of dimensions. Then the resulting extra terms are responsible for the anomaly.

with the derivative $D_\mu = \partial_\mu - igA_\mu$, required from the $U(1)$ gauge invariance. The corresponding transformation $\psi \to e^{i\alpha}\psi$ generates a conserved *vector current*

$$j^\mu_V = \bar{\psi}(x)\gamma^\mu\psi(x)\,. \tag{2.6}$$

Secondly, the *chiral transformation* $\psi \to e^{i\alpha\gamma_5}\psi$ also leaves Eq. (2.5) unchanged with conserved *axial vector current*

$$j^\mu_A = \bar{\psi}(x)\gamma^\mu\gamma^5\psi(x)\,. \tag{2.7}$$

However, at quantum level this current is plagued by an *anomalous* divergence [163, 164]

$$\partial_\mu j^\mu_A = -\frac{g^2}{16\pi^2}\widetilde{F}^{\mu\nu}_a F^a_{\mu\nu} \tag{2.8}$$

where $\widetilde{F}^{\mu\nu} = \frac{1}{2}\varepsilon^{\mu\nu\rho\sigma}F_{\rho\sigma}$ is the dual field strength tensor. Eq.(2.8) is known as the *Adler-Bell-Jackiw anomaly*. This result can be obtained by calculating the three-photon vertex diagrams in Fig. 2.1. The emergence of anomalies from the axial current of a global symmetry can be also understood in terms of path integrals, where it turns out that the functional measure of fermion fields violates gauge invariance. Treating the gauge field as a fixed background, the path integral for the field ψ can be defined as

$$Z[A] \equiv \int \mathcal{D}\psi\mathcal{D}\overline{\psi}e^{iS[A]}\,, \tag{2.9}$$

where $S[A] \equiv \int d^4x i\overline{\psi}(x)\not{D}\psi(x)$ is the Dirac action. Under a $U(1)$ local transformation $\psi \to e^{i\alpha(x)\gamma_5}\psi$ that leaves the action invariant, the path integral transforms as

$$Z[A] \to \int \mathcal{D}\psi\mathcal{D}\overline{\psi}e^{iS[A]}\exp\left\{-i\int d^4x\ \alpha(x)\left[\frac{g^2}{8\pi^2}\widetilde{F}^{\mu\nu}F_{\mu\nu} + \partial_\mu j^\mu_A\right]\right\}. \tag{2.10}$$

Eq. (2.8) thus results from gauge invariance. Compared to the previous diagrammatic approach, this derivation of the anomaly [165] has the virtue of being valid to all orders in perturbation theory, since no assumption about the size of the gauge coupling g needs to be done in its derivation. It goes under the name of *Adler-Bardeen theorem*.

2.1.2 *Massless $n_F = 2$ QCD and the $U(1)_A$ problem*

Having introduced these concepts about quantum field theory, let us pause for a moment and instead look at a case in which they could potentially find a physical application, namely massless QCD. A theory describing free QCD below $\Lambda_{QCD} \simeq 0.4\,\text{GeV}$ must include both quarks from the first generation, which can be sensibly neglected, since $m_{u,d} \ll \Lambda_{QCD}$. The Lagrangian for the free massless theory

$$\mathcal{L}_{QCD}^{free} = i\overline{\psi_i}\not{D}\psi_i \,, \tag{2.11}$$

with $i = u, d$, is invariant under the group $U(2)_L \times U(2)_R$ of $n_F = 2$ flavor symmetries. We can identify the $SU(2)$ and the $U(1)$ part of each $U(2)$ symmetry group by defining the field transformation on the chiral components of the Dirac spinor

$$(\psi_i)_{L,R} \to e^{-i\left[\alpha_{L,R}\delta_{ij} + \left(\beta^a_{L,R}\tau_a\right)_{ij}\right]} \left(\psi_j\right)_{L,R} \,, \tag{2.12}$$

where $\tau_a = \frac{\sigma_a}{2}$ are the generators of $SU(2)$. The resulting eight conserved currents can be divided between the vector and axial types with a suitable basis choice of the infinitesimal parameters $\alpha_{L,R}$ and $\beta_{L,R}$:

1. The $U(1)_B$ transformation corresponding to *quark number* conservation is obtained for $\alpha_L = \alpha_R \neq 0$, $\beta^a_{L,R} = 0$, and has an associated vector current $j^\mu = \overline{\psi}\gamma^\mu\psi$. This symmetry is clearly realized in nature among baryons and mesons, since the quark number is just one third of the baryon number.

2. The $U(1)_A$ conserved axial current $j^\mu_A = \overline{\psi}\gamma^\mu\gamma_5\psi$ results from $\alpha_L = -\alpha_R \equiv \alpha \neq 0$, $\beta^a_{L,R} = 0$. In terms of the four component Dirac spinor it is simply
$$\psi \to e^{-i\alpha\gamma_5}\psi \,. \tag{2.13}$$
No known quantum number is associated with this symmetry. As we know from Eq. (2.8), this symmetry is anomalous.

3. The $SU(2)_I$ *isospin* symmetry results from a transformation with $\beta^a_L = \beta^a_R \neq 0$, $\alpha_{L,R} = 0$. The conserved vector current is in this case $j^{\mu,a} = \overline{\psi}\gamma^\mu\tau^a\psi$. Although not exactly, hadrons obey this symmetry: the nucleons live in a doublet representation of the group, while the spin-0 pions form a triplet representation.

4. Setting $\beta^a_L = -\beta^a_R \neq 0$, $\alpha_{L,R} = 0$, yields a $SU(2)_A$ conserved current $j^{\mu,a}_A = \overline{\psi}\gamma^\mu\gamma_5\tau_a\psi$. This symmetry does not resemble the quark behaviour in any way.

When particle physicists were still moving their first steps in constructing a theory of QCD, it seemed undesirable that out of the full

$SU(2)_I \times SU(2)_A \times U(1)_B \times U(1)_A$ symmetry group of the Lagrangian in Eq. (2.11), only the vector $U(2)_{L+R} = SU(2)_I \times U(1)_B$ was (approximately) realised. The pioneering work of [166] on theories with SSB offered a possible solution to this conundrum by speculating that the axial $U(2)_{L\text{-}R}$ symmetry could be spontaneously broken, in such a way that the observed light pions can be regarded as the *pseudo-Goldstone bosons* of the broken group. This is also in agreement with the fact that the observed pions are of odd parity only. The simplest scalar state of our theory in Eq. (2.11) which transforms non-trivially under $U(2)_{L\text{-}R}$ and can acquire a non-zero VEV v is the composite

$$\langle 0|\overline{\psi_i}\psi_j|0\rangle = v^3\delta_{ij} \neq 0\,; \tag{2.14}$$

which defines the ground state of the theory as a quark-antiquark condensate. As it mixes left and right spinor components, such a state evidently breaks both $SU(2)_A$ and $U(1)_A$ axial symmetries of $\mathcal{L}^{\text{free}}_{\text{QCD}}$, as one can see by applying the transformation of the type 1. and 4. in the list above. One can thus construct an effective Lagrangian for the pions by allowing small space-time perturbation around the ground state, something which has been successfully used to predict matrix elements for scattering among hadrons. But there is a caveat to this approach: one cannot treat the light mesons $\pi^{\pm,0}$ and η as the pseudo-Goldstone bosons of a spontaneously broken $U(2)_{L-R}$. In this case in fact, one would expect four light particles, while experimentally $m_\pi \ll m_\eta$. Therefore the chiral symmetry breaking can be performed on $SU(2)_A$ in order to give masses to $\pi^{\pm,0}$, but spontaneously breaking $U(1)_A$ would result in a wrong prediction for m_η. This constitutes the essence of what Weinberg dubbed the $U(1)_A$ problem. We have already anticipated one aspect of what leads to its resolution, which is the anomaly associated to the $U(1)_A$ global symmetry. Next, we move on to see how the structure of non-abelian gauge symmetries complement it.

2.1.3 *The θ-vacuum of non-abelian gauge theory*

In order for the theory of QCD to be realistic, gauge interactions should be included. As anticipated in Sec. 2.1.1 for the case of QED, the presence of a $U(1)$ gauge field strength term, the axial current resulting from a global chiral transformation is affected by an anomaly. While this is indeed the case for the interacting Lagrangian

$$\mathcal{L}_{\text{QCD}} \equiv \mathcal{L}^{\text{free}}_{\text{QCD}} - 1/4\,(F^{\mu\nu})^2\,, \tag{2.15}$$

it is not enough to explain why $U(1)_A$ is not a symmetry of this theory. It was indeed shown [167] that under a global chiral transformation as of Eq. (2.13), the action is changed by a total divergence, which then becomes a surface integral. Evaluating the variation of the action $S_{\text{QCD}}[A]$ under a chiral transformation and setting $A^a_\mu = 0$ for $|x| \to \infty$, one sees that $U(1)_A$ is still a symmetry of $\mathcal{L}_{\text{QCD}}$:

$$\delta S_{\text{QCD}}[A] = \frac{g^2 n_F}{32\pi^2}\int d^4x\, \partial_\mu J^\mu_\star = \frac{g^2 n_F}{32\pi^2}\int d\sigma_\mu J^\mu_\star = 0\,, \tag{2.16}$$

where the *Chern-Simmons current* is defined as

$$J^\mu_\star = 2\varepsilon^{\mu\alpha\beta\gamma}\,\text{Tr}\left[A_\alpha F_{\beta\gamma} - \frac{2}{3}igA_\alpha A_\beta A_\gamma\right]. \tag{2.17}$$

We have used Gauss' theorem to transform the volume integral into a surface integral over the boundary $d\sigma_\mu$. The observation that changes what seems to be an unavoidable conclusion about the conservation of the axial current is the fact that at spatial infinity the naive boundary condition $A^a_\mu = 0$ represents only a subset of all the possible equivalent configurations linked by gauge transformations [146, 147]. If we consider the minima of a pure $SU(2)$ gauge theory, the ground state is defined by $F^a_{\mu\nu} = 0$. This in turn implies that the vector potential is either zero or a gauge transformation of it. If for simplicity we restrict ourselves to a time independent gauge transformation $U = U(\vec{x})$, its action on the null vector field

$$A^i_a(\vec{x}) \to \frac{i}{g} U \partial_\mu U^\dagger, \quad A^i_a(\vec{x}) \to 0, \tag{2.18}$$

defines the *temporal gauge*. We further add the point at infinity to this map, by imposing the condition $U(|\vec{x}| \to \infty) \to 0$. Gauge transformations map the S^3 configuration space into the S^3 vacuum space. They can be classified according to their *homotopy class*, meaning that maps belonging to different classes cannot be continuously modified into each other. These classes can be defined by their behaviour at spatial infinity through the label n [145] :

$$\lim_{\vec{x}\to\infty} U_n = e^{2i\pi n}, \quad n \in \mathbb{Z}. \tag{2.19}$$

The integer n is called *winding number* and it can be better understood by taking a simple example. Let us take the case of a coordinate space with only two space dimensions in a theory with a single complex scalar ϕ field and only one minimum of the potential: $\phi(\vec{x} = r(\cos\varphi, \sin\varphi)) = ve^{i\alpha}$. Both the coordinate space and the vacuum space have a boundary with the topology of S^1. The simplest way [168] to create a map $f : S^1 \to S^1$ is to have $\alpha \equiv \alpha(\phi)$, with the periodicity condition $\alpha(\varphi + 2\pi) = \alpha(\varphi) + 2\pi n$, with n integer, in order to have a single-valued function. One such possible map is $\widetilde{f} = e^{in\varphi}$, where the winding number n tells us how many times one winds around the the vacuum S^1 for each circle around the spatial S^1. It is easy to check that the identity

$$n = \frac{i}{2\pi} \int_0^{2\pi} d\varphi U_n \frac{\partial}{\partial\varphi} U_n^\dagger, \tag{2.20}$$

is indeed fulfilled if we use $U = \widetilde{f}$. In the case of a $S^3 \to S^3$ gauge transformation Eq. (2.20) becomes [169]:

$$\begin{aligned} n &= -\frac{1}{24\pi^2}\int d\sigma^\mu\ \varepsilon^{\mu\nu\rho\sigma}\,\mathrm{Tr}\left[\left(U\partial_\nu U^\dagger\right)\left(U\partial_\rho U^\dagger\right)\left(U\partial_\sigma U^\dagger\right)\right] \\ &= \frac{ig^3}{24\pi^2}\int d\sigma^\mu\ \varepsilon^{\mu\nu\rho\sigma}\,\mathrm{Tr}\left[A_\nu A_\rho A_\sigma\right] \\ &= \frac{ig^2}{32\pi^2}\int d\sigma^\mu\, J^\mu_\bigstar \\ &= \frac{ig^2}{32\pi^2}\int d^4x\,\partial_\mu J^\mu_\bigstar \\ &= \frac{ig^2}{16\pi^2}\int d^4x\,\mathrm{Tr}\left(\widetilde{F}_{\mu\nu}F^{\mu\nu}\right). \end{aligned} \tag{2.21}$$

Here we made use of Eq. (2.18), Eq. (2.17) for a ground state configuration at the boundary, i.e. $F^a_{\mu\nu} = 0$, as well as the property

$$\mathrm{Tr}\left(\widetilde{F}_{\mu\nu}F^{\mu\nu}\right) = \frac{1}{2}\partial_\mu J^\mu_\bigstar\,. \tag{2.22}$$

The vacuum of an $SU(2)$ gauge theory is therefore more complex than the one for any abelian gauge theory. It corresponds to an infinite number of configurations for the vector field potential, each with a different winding number. It turns out that a non-trivial solution to the field equations connecting two states with different winding number n and m exists even in the limit of infinite space dimensions. When $m = n+1$ we call this solution an *instanton*, with a corresponding action $S = 8\pi^2/g^2$. It determines the tunnelling amplitude

$$\langle m|e^{-\frac{i}{\hbar}Ht}|n\rangle \sim e^{-\frac{8\pi^2}{g^2}|m-n|}\,. \tag{2.23}$$

Since these matrix elements depend only on the difference $|m-n|$, the Hamiltonian H can be diagonalized by defining the θ-*vacuum* as a superimposition of states with different n:

$$|\theta\rangle = \sum_n e^{-in\theta}\,|n\rangle\ . \tag{2.24}$$

Contrary to a vacuum in a state characterized by a single generic winding number n, which under a gauge transformation $U_{n=1}$ transforms as

$$U_{n=1}\,|n\rangle = |n+1\rangle\ , \tag{2.25}$$

a θ-vacuum state respects gauge invariance:

$$U_{n=1}\,|\theta\rangle = e^{i\theta}\,|\theta\rangle\ . \tag{2.26}$$

Due to this new definition of the vacuum, the generating functional for the $SU(2)$ gauge theory picks up a θ contribution. Indeed, considering a transition from a θ-

vacuum at $t \to -\infty$ to a θ-vacuum at $t \to +\infty$ one has to sum over all the possible path connecting vacua with different winding number

$$\begin{aligned}\langle \theta_+|\theta_-\rangle &= \sum_{mn} e^{i(m-n)\theta} \langle m|n\rangle \\ &= \sum_{\nu\equiv m-n} e^{i\nu\theta} \sum_n \langle (n+\nu)|n\rangle \\ &= \sum_\nu e^{\frac{i\theta g^2}{32\pi^2}\int d^4x\, \mathrm{Tr}\left(\widetilde{F}^{\mu\nu}F_{\mu\nu}\right)} \int \mathcal{D}A e^{iS_{QCD}[A]} \delta\left(\nu - \frac{g^2}{32\pi^2}\int d^4x\, \mathrm{Tr}\left(\widetilde{F}^{\mu\nu}F_{\mu\nu}\right)\right),\end{aligned} \tag{2.27}$$

where we have used Eq. (2.21). The Lagrangian therefore acquires a new θ term:

$$\mathcal{L}_{QCD} = -\frac{1}{4}\,\mathrm{Tr}\,(F^{\mu\nu}F_{\mu\nu}) + \theta\frac{g^2}{32\pi^2}\,\mathrm{Tr}\left(\widetilde{F}^{\mu\nu}F_{\mu\nu}\right). \tag{2.28}$$

This new term respects Lorentz and gauge symmetries, but violates CP invariance. The implication of this fact will be clear soon. Now that we saw that $|\theta\rangle$ is the correct vacuum of an $SU(2)$ gauge theory[1], we can focus on its implications on the $U(1)_A$ problem we were trying to address. Extending the massless QCD Lagrangian of Eq. (2.15) to n_F quark flavors, the $U(1)_A$ axial anomaly becomes

$$\partial_\mu j^\mu_A = 2n_F\frac{g^2}{32\pi^2}\widetilde{F}^{\mu\nu}F_{\mu\nu}\,. \tag{2.29}$$

Using Eq. (2.17), we can define a current

$$\widetilde{j}^\mu_A = j^\mu_A - 2n_F\frac{g^2}{32\pi^2}J^\mu_\star\,, \tag{2.30}$$

which is conserved for global chiral transformation. The fact that its associated charge changes under a gauge transformation [170],

$$U_{n=1}\widetilde{Q}_A U^{-1}_{n=1} = \widetilde{Q}_A + 2n_F \tag{2.31}$$

has the profound consequence that the θ-vacuum is not invariant under chiral transformation [171]. In order to see this, first consider the chain of equalities

$$\begin{aligned} U_1 e^{i\alpha\widetilde{Q}_A}|\theta\rangle &= \\ U_1 e^{i\alpha\widetilde{Q}_A}U_1^{-1}U_1|\theta\rangle &= \\ e^{i(\widetilde{Q}_A+2n_F)\alpha}e^{i\theta}|\theta\rangle &= \\ e^{i(\theta+2n_F)}e^{i\alpha\widetilde{Q}_A}|\theta\rangle\,, \end{aligned} \tag{2.32}$$

with the shorthand $U_1 = U_{n=1}$ and using Eq. (2.26). Then compare the first and the last line of Eq. (2.1.3) with Eq. (2.26) for generic n, we can indeed conclude

$$e^{i\alpha\widetilde{Q}_A}|\theta\rangle = |\theta + 2n_F\alpha\rangle\,. \tag{2.33}$$

1 The vacuum structure of any $SU(N)$ theory is solely due to its $SU(2)$ subgroup.

In other words, $U(1)_A$ is not a symmetry of the theory once the correct θ-vacuum is established. The instantons provide the η-meson with an anomalous contribution to its mass, which would otherwise be zero and η a Goldstone boson of the spontaneously broken $U(1)_A$. More technical aspects about how the existence of the θ-vacuum solves the $U(1)_A$-problem will not be further discussed here. Arguably the θ-term of a $SU(N)$ gauge invariant QCD Lagrangian with n_F massless quarks cannot appear in any physical observable, since its value can be changed by a global axial transformation under which such Lagrangian is invariant. Things are different when one considers models with n_F flavors of massive quarks with EW interactions, like in the SM, where the generic quark mass term after $SU(2) \times U(1)$ symmetry breaking reads

$$\begin{aligned} -\mathcal{L}_{m_q} &= \overline{q}_{i,R} M_{ij} q_{j,L} + \overline{q}_{i,L} M^{\dagger}_{ij} q_{j,R} \\ &= \left|M_{ij}\right| \left(\overline{q}_{i,R} e^{i\phi} q_{j,L} + \overline{q}_{i,L} e^{-i\phi} q_{i,R}\right) \\ &= \left|M_{ij}\right| \overline{q}_i \left[P_L (1 + i\phi) + P_R (1 - i\phi)\right] q_j \\ &= \left|M_{ij}\right| \overline{q}_i [P_L + P_R + i\phi \left(P_L - P_R\right)] q_j \\ &= \left|M_{ij}\right| \overline{q}_i [1 - i\phi\gamma_5] q_j \\ &= \left|M_{ij}\right| \overline{q}_i \, e^{-i\phi\gamma_5} q_j \,, \end{aligned} \tag{2.34}$$

where we have written $\phi_{ij} \equiv \phi$ for readability. This mass terms violates chiral symmetry, since under $q \to e^{-i\alpha\gamma_5} q$:

$$-\mathcal{L}_{m_q} \longrightarrow \left|M_{ij}\right| \overline{q}_i e^{-i(\phi + 2\alpha)\gamma_5} q_j \,, \tag{2.35}$$

or equivalently $\phi_M \equiv \arg(\det M) \to \phi_M + 2n_F\alpha$. Thus ϕ_M behaves the same way as θ, as shown in Eq. (2.33). Obtaining a real diagonal quark mass term involves a chiral transformation that while removing the exponential factor generates the anomalous current of Eq. (2.29). The effective theta-term $\overline{\theta}$ of the SM will then comprises of two terms with distinct origin

$$\overline{\theta} = \theta + \arg(\det M) \,, \tag{2.36}$$

since θ is a parameter which results from the $SU(3)$ gauge vacuum structure, while $\arg(\det M)$ has to do with the Yukawa couplings of the quarks. Thus $\overline{\theta}$ cannot simply be rotated away from the theory, because each of the two terms in Eq. (2.36) will shift the same way under a chiral transformation. At phenomenological level, it indeed enters the mass matrix for the pions which are emitted and reabsorbed in the amplitude for the neutron electric dipole moment (EDM). This observable imposes [148] a stringent limit of $\overline{\theta} < 10^{-10}$ [149]. The absence of a theoretical reason for such a small θ value constitutes the essence of the *strong CP problem*.

2.2 THE AXION SOLUTION TO THE STRONG CP PROBLEM

Several attempts have been made in order to solve the strong CP problem, starting from the ones which state that there is no such problem at all, but while doing so ignoring the $U(1)_A$ problem [172] or not fully motivating their approach [173]. Spontaneous CP breaking was also proposed [174–176], but it seemed of little appeal due to its conflict with the CKM model of quark interaction, where CP

is instead broken explicitly. Refs. [177, 178] explored the possibility of restoring the $U(1)$ chiral symmetry with $m_u = 0$ in the QCD Lagrangian. This option was proven inconsistent [179]. What is widely recognized as the most cogent solution to the strong CP problem also relies on an extra $U(1)$ symmetry, but no quark mass parameter is set to zero in this case. Instead an extra global *Peccei-Quinn* (PQ) symmetry $U(1)_{PQ}$ [152, 153] is added to the SM and then spontaneously broken through a scalar φ at a scale f_a,

$$\varphi = f_a e^{i\frac{a(x)}{f_a}} . \tag{2.37}$$

The resulting massless excitation mode a, dubbed the *axion* [150, 151], is the Nambu-Goldstone (NG) boson of the broken $U(1)_{PQ}$. Under this symmetry, it therefore shifts as

$$a(x) \to a(x) + \varepsilon f_a . \tag{2.38}$$

In order for this mechanism to work, one needs at least one quark flavor to acquire its mass through a Yukawa coupling with φ[2]. Being a NG boson, the axion couples to fermions only through its derivative. Those among these fermions that are charged under $U(1)_{PQ}$ enter the loop that couples the axion to the gluon field strength through the anomaly. The $U(1)_{PQ}$-invariant Lagrangian reads

$$\mathcal{L}_{eff} = \mathcal{L}_{SM} + \bar{\theta}\frac{g^2}{32\pi^2}\tilde{F}^{\mu\nu}_a F^a_{\mu\nu} - \frac{1}{2}\partial^2 a + \kappa\frac{a}{f_a}\frac{g^2}{32\pi^2}\tilde{F}^{\mu\nu}_a F^a_{\mu\nu} + \mathcal{L}_{\partial a - q} , \tag{2.39}$$

where κ is model-dependent function of the PQ charges of the quarks and $\mathcal{L}_{\partial a - q}$ contains the axion-quarks interactions. The coupling of the axion to the anomaly provides it with an effective potential, in such a way that its minimization condition

$$\langle a \rangle = -\frac{f_a}{\kappa}\bar{\theta} , \tag{2.40}$$

is exactly the one that removes any source of CP violation from $\mathcal{L}_{eff}$[3] and thus provides a dynamical solution to the strong CP problem. This confirms the fact that any point of the parameter space with some higher degree of symmetry is necessarily a stationary point, as Weinberg noted [180]. A further consequence of the axial $U(1)_{PQ}$ anomaly is that the axion acquires a model-dependent mass thanks to the effective potential

$$\begin{aligned} m_a^2 &= \left\langle \frac{\partial^2 V_{eff}}{\partial a^2} \right\rangle_{\langle a \rangle = -\frac{f_a}{\kappa}\bar{\theta}} \\ &= -\frac{\kappa}{f_a}\frac{g^2}{32\pi^2}\frac{\partial}{\partial a}\left\langle \tilde{F}^{\mu\nu}_a F^a_{\mu\nu} \right\rangle_{\langle a \rangle = -\frac{f_a}{\kappa}\bar{\theta}} \end{aligned} \tag{2.41}$$

Through an estimate based on simple dimensional analysis [171], the axion mass can be expected to be quite small if $f_a \gg \Lambda_{QCD}$:

$$m_a^2 \approx \frac{\Lambda^4_{QCD}}{f_a^2} . \tag{2.42}$$

2 It does not need to be a SM quark.

3 One should rewrite Eq. (2.39) in terms of a the shifted axion field $a' = a + \frac{f_a}{\kappa}\bar{\theta}$.

The very first realisation of an axion model [152, 153] used EWSB in the SM to break $U(1)_{PQ}$, thus setting $f_a = v \simeq 274\,\text{GeV}$. The chiral invariance of the SM Yukawa coupling was made possible by the introduction of a second independent Higgs doublet ϕ_2, in order for it to carry a different PQ charge than the original ϕ_1. *Variant axion models* [181] came as a generalisation in the Yukawa coupling scheme that could help with the bounds from quarkonium states, at the cost of reintroducing flavor changing neutral current (FCNC). These early models of axion were ruled out long ago using the observed branching ratio for of charged mesons into pions [182]. In *invisible axion models* the scalar σ which breaks PQ symmetry is a singlet under $SU(2)_L \times U(1)_Y$ and the breaking happens at some scale $f_a \gg v$ higher than the electroweak one. Those models are still viable, as the large value of f_a enforces a very light, very weakly-coupled and very long-lived axion. They fall into two categories: the Kim-Shifman-Vainshtein-Zakharov (KVSZ) axion model [183, 184], where together with σ two new heavy quarks carrying PQ charges are introduced, while the matter fields are $U(1)_{PQ}$ singlet; the Dine-Fischler-Srednicki-Zhitnitsky (DFSZ) models, where σ is the only BSM particle and quarks and leptons carry $U(1)_{PQ}$ charges. As a further phenomenological motivation for the invisible axion models, the most stringent lower bound for the axion decay constant from astrophysics is indeed quite high compared to electroweak energies, $f_a > 10^9\,\text{GeV}$. It results from the observation of the cooling process of the supernova SN 1987 A [185]. Similar bounds can be obtained from other type of stars [20]. We will now examine in some details the characteristics of the DFSZ axion, since it constitutes the basis of our model in Ch. 4.

2.3 THE DFSZ AXION

Just like the original axion model, the DFSZ axion model contains two scalars doublets $\phi_{u,d}$ with hypercharges $Y_u = -Y_d = 1/2$. They both acquire a VEV $v_{u,d}$ around the electroweak scale, such that for the neutral components of the doublets we can write

$$\phi^0_{u,d} = \frac{v_{u,d} + h_{u,d}}{\sqrt{2}}\, e^{\frac{i\xi_{u,d}}{\sqrt{2}v_{u,d}}}\,, \tag{2.43}$$

and the SM vev $v = \sqrt{v_u^2 + v_d^2}$, as in the MSSM. The pseudoscalar fields $\xi_{u,d}$ parametrise the excitations along the flat directions. After EWSB quarks and leptons acquire their mass thanks to the Yukawa couplings

$$\mathcal{L}_{Yuk} = y_u \overline{Q}\phi_u u_R + y_d \overline{Q}\phi_d d_R + y_e \overline{L}\phi_d e_R + h.c.\,, \tag{2.44}$$

while the linear combination of fields which gives mass to the Z boson can be read from Eq. (2.43) :

$$\xi_Z = \frac{v_u}{v}\xi_u - \frac{v_d}{v}\xi_d\,. \tag{2.45}$$

An extra complex scalar singlet ϕ_a is responsible for breaking the global $U(1)_{PQ}$ symmetry of the model through its VEV $v_a \gg v$:

$$\phi_a = \frac{v_a + h_a}{\sqrt{2}} e^{\frac{i\xi_a}{\sqrt{2}v_a}}\,. \tag{2.46}$$

If we call X_k, with $k = u, d, a$, the PQ charges of the scalar fields, the effect of $U(1)_{PQ}$ transformation

$$\phi_k \to e^{i\alpha X_k}\phi_k\,, \tag{2.47}$$

together with the charge assignments

$$X_u + X_d = -2X_a \equiv 1\,, \tag{2.48}$$

tells us which is the most general gauge- and PQ-invariant scalar potential:

$$\begin{aligned} V(\phi_k) = &\sum_{k=u,d,a} \lambda_k\Big(|\phi_k|^2 - v_k\Big)^2 + \Big(\lambda_1|\phi_u|^2 + \lambda_2|\phi_d|^2\Big)|\phi_a|^2 \\ &+ \lambda_3\big(\phi_u\cdot\phi_d\phi_a^2 + \text{h.c.}\big) + \lambda_4|\phi_u\cdot\phi_d|^2 + \lambda_5|\phi_u^*\phi_d|^2\,. \end{aligned} \tag{2.49}$$

Here $\phi_u\cdot\phi_d$ stands for the $SU(2)$ antisymmetric tensor product. The conserved current associated to the PQ symmetry of this model can be calculated with Noether's theorem as in Eq. (2.3) :

$$j^\mu_{PQ} = \sum_{k=u,d,a} X_k\phi_k^\dagger \overleftrightarrow{\partial}\phi_k + \sum_{\substack{\text{quarks,}\\ \text{leptons}}} X_i\overline{\psi}_i\gamma^\mu\psi_i\,, \tag{2.50}$$

where $\phi_k^\dagger\overleftrightarrow{\partial}\phi_k = \Big(\partial^\mu\phi_k^\dagger\Big)\phi_k - \phi_k^\dagger(\partial^\mu\phi_k)$. We can identify the axial-vector part of this current by splitting terms involving quarks into their left- and right-chiral contributions:

$$\begin{aligned} j^\mu_{PQ} &\supset X_Q\overline{\psi}_Q\gamma^\mu\psi_Q + X_{u_R}\overline{u_R}\gamma^\mu u_R + X_{d_R}\overline{d_R}\gamma^\mu d_R \\ &= X_Q\overline{u}\gamma^\mu P_L u + X_Q\overline{d}\gamma^\mu P_L d + X_{u_R}\overline{u}\gamma^\mu P_R u + X_{d_R}\overline{d}\gamma^\mu P_R d \\ &= \frac{X_Q + X_{u_R}}{2}\,\overline{u}\gamma^\mu u + \frac{X_Q + X_{d_R}}{2}\,\overline{d}\gamma^\mu d \\ &\quad - \frac{X_Q - X_{u_R}}{2}\,\overline{u}\gamma^\mu\gamma^5 u - \frac{X_Q - X_{d_R}}{2}\,\overline{d}\gamma^\mu\gamma^5 d\,. \end{aligned} \tag{2.51}$$

From the constraints on the PQ charges resulting from the structure of the Yukawa couplings in Eq. (2.44), one can write the coefficients of the axial-vector part of the current in Eq. (2.51) as

$$X_Q - X_{u_R} = X_u \quad , \quad X_Q - X_{d_R} = X_d \quad . \tag{2.52}$$

The anomalous divergence associated with the axial-vector part of j^μ_{PQ} which couples to the gluons therefore reads

$$\partial_\mu j^\mu_{PQ}\Big|_{SU(3)} = \underbrace{-(X_u + X_d)}_{=1} N_{DW}\frac{g_3^2}{32\pi^2}\widetilde{G}^a_{\mu\nu}G^{\mu\nu}_a\,, \tag{2.53}$$

thanks to Eq. (2.48). This makes clear how the charge assignments for the scalars were motivated by finding a solution to the strong CP problem. N_{DW} is the number

of quark flavor which carry a PQ charge and it is often referred to as *domain wall number* in relation to the non-perturbative field configurations which arise due to the remnant symmetries after the SSB of a global symmetry. If after the breaking the homotopy group π (see our discussion in Sec. 2.1.3) of the functions mapping the spatial infinity to the space of the vacua is non-trivial[4], then the resulting *domain wall* is a stable 2D field configuration. Its sizeable surface energy density could dominate the energy of the universe unless very small couplings for the interactions are imposed, an issue which goes under the name of the *domain wall problem*. The DFSZ axion model is confronted with it, because of the remnant $Z(N_{DW} = 6)$ symmetry after the breaking of $U(1)_{PQ}$ [187]. Without entering into more technical details, let us just say here that with a small modification of the model the domain wall can decay before it comes to dominate the energy density of the universe. Going back to the anomalous current in Eq. (2.53), one has to make sure that it does not couple to the would-be Goldstone boson ξ_Z by imposing

$$\langle 0|\partial_\mu j^\mu_{PQ}|\xi_Z\rangle = X_u \frac{v_u}{v}\langle 0|\phi_u^\dagger \overleftrightarrow{\partial}\phi_u|\xi_u\rangle - X_d\frac{v_d}{v}\langle 0|\phi_d^\dagger\overleftrightarrow{\partial}\phi_d|\xi_d\rangle \stackrel{!}{=} 0\,. \tag{2.54}$$

With the parametrisation given in Eq. (2.43), one finds

$$\begin{aligned}
&\left(\partial^\mu\phi_k^\dagger\right)\phi_k = \frac{v_k+h_k}{2}\left(\partial^\mu h_k - \frac{i\partial^\mu\xi_k}{\sqrt{2}v_k}(v_k+h_k)\right)\\
-\quad &\left[\phi_k^\dagger(\partial^\mu\phi_k) = \frac{v_k+h_k}{2}\left(\partial^\mu h_k + \frac{i\partial^\mu\xi_k}{\sqrt{2}v_k}(v_k+h_k)\right)\right]\\
\hline
\Rightarrow\quad &\phi_k^\dagger\overleftrightarrow{\partial}\phi_k = -\frac{1}{2\sqrt{2}}(v_k+h_k)^2\frac{\partial^\mu\xi_k}{v_k}\,.
\end{aligned} \tag{2.55}$$

Plugging this into Eq. (2.54)

$$X_u\frac{v_u^2}{v} - X_d\frac{v_d^2}{v}\stackrel{!}{=}0\,, \tag{2.56}$$

enforces a relation between the PQ charges and the VEVs of the fields $\phi_{u,d}$:

$$X_{u,d} = \frac{v_{d,u}^2}{v^2} \tag{2.57}$$

It is important to notice that the field ξ_a is not the axion, which instead results from the linear combination of the neutral pseudoscalar fields which is massless

4 Formally, if the group breaking pattern is $\mathcal{G}\to\mathcal{H}$, then topologically stable domain walls are obtained if $\pi(\mathcal{G}/\mathcal{H})$ is different from the identity [186].

and orthogonal to ξ_Z. Considering only the CP-odd neutral states of the spectrum, the scalar potential $V(\phi_k)$ yields a mass term

$$\begin{aligned}\mathcal{L}_{m_\xi} &= \lambda_3 \langle\phi_u\rangle \langle\phi_d\rangle \langle\phi_a\rangle^2 \\ &= \lambda_3 \frac{v_a^2}{4} v_u v_d \left[e^{\frac{i}{\sqrt{2}}\left(\frac{\xi_u}{v_u}+\frac{\xi_d}{v_d}+2\frac{\xi_a}{v_a}\right)} + e^{-\frac{i}{\sqrt{2}}\left(\frac{\xi_u}{v_u}+\frac{\xi_d}{v_d}+2\frac{\xi_a}{v_a}\right)} \right] \\ &= \lambda_3 \frac{v_a^2}{4} v_u v_d \cos\left[\frac{1}{\sqrt{2}}\left(\frac{\xi_u}{v_u}+\frac{\xi_d}{v_d}+2\frac{\xi_a}{v_a}\right)\right]. \end{aligned} \tag{2.58}$$

The corresponding (normalised) massive mode

$$\chi = \frac{1}{\underbrace{\sqrt{v^2 v_a^2 + 4 v_u^2 v_d^2}}_{(v')^2}} [v_a(v_d \xi_u + v_u \xi_d) + 2 v_u v_d \xi_a], \tag{2.59}$$

is manifestly orthogonal to ξ_Z. The axion is then identified as the field which completes the orthonormal basis of the mass eigenstates

$$a = \frac{v_a}{(v')^4} \left[2 v_u v_d (v_d \xi_u + v_u \xi_d) - v^2 v_a \xi_a\right]. \tag{2.60}$$

In the limit $v_a \gg v$ the axion field is mostly constituted by the pseudoscalar singlet:

$$a \simeq -\xi_a + 2\frac{v_u v_d}{v^2 v_a}(v_d \xi_u + v_d \xi_u) \tag{2.61}$$

One can verify that under a transformation of the broken $U(1)_{PQ}$ in the form of Eq. (2.47), or equivalently

$$\xi_k \to \xi_k + \sqrt{2}\alpha X_k v_k, \tag{2.62}$$

the field a shifts as the associated Goldstone boson [188],

$$\begin{aligned} a \to\ & a + \sqrt{2}\alpha \frac{v_a}{(v')^4} \left\{2 v_u v_d [v_d (v_u X_u) + v_u (v_d X_d)] - v^2 v_a (v_a X_a)\right\} \\ &= a + \sqrt{2}\alpha \frac{v_a}{(v')^4} \left[2 v_u^2 v_d^2 + \frac{1}{2} v^2 v_a^2\right] \\ &= a + \frac{\alpha}{\sqrt{2}} v_a . \end{aligned} \tag{2.63}$$

Under the same transformation the would-be Goldstone boson and the massive pseudoscalar stay constant [189]:

$$\begin{aligned}\chi &\to \chi + \frac{\sqrt{2}\alpha}{(v')^2}\{v_a[v_d(v_u X_u) + v_u(v_d X_d)] + 2v_u v_d(v_a X_a)\} \\ &= \chi + \sqrt{2}\alpha\frac{v_a v_u v_d}{(v')^2}(X_u + X_d + 2X_a) = \chi\,, \end{aligned} \tag{2.64}$$

$$\begin{aligned}\xi_Z &\to \xi_Z + \sqrt{2}\alpha\left[\frac{v_u}{v}(v_u X_u) - \frac{v_d}{v}(v_d X_d)\right] \\ &= \xi_Z + \frac{\sqrt{2}\alpha}{v}\left[v_u^2 v_d^2 - v_d^2 v_u^2\right] = \xi_Z\,, \end{aligned} \tag{2.65}$$

where we have used Eqs. (2.48) and (2.57). In order to obtain the precise mass eigenvalue for the χ mode, we write Eq. (2.58) in terms of its series representation. The mass matrix resulting from the second order term reads in the basis (ξ_u, ξ_d, ξ_a):

$$\mathcal{L}_{m_\xi} = -\frac{\lambda_3 v_a^2}{4}\begin{bmatrix} \frac{1}{2}\frac{v_d}{v_u} & \frac{1}{2} & \frac{v_d}{v_a} \\ \frac{1}{2} & \frac{1}{2}\frac{v_u}{v_d} & \frac{v_u}{v_a} \\ \frac{v_d}{v_a} & \frac{v_u}{v_a} & \frac{v_u v_d}{v_a^2} \end{bmatrix}. \tag{2.66}$$

Its eigenvectors are precisely a, ξ_Z and χ, with the latter one being associated to the only non-vanishing eigenvalue

$$m_\chi^2 = \frac{\lambda_3}{4}\frac{(v')^4}{v_u v_d}\,. \tag{2.67}$$

The mass scale for χ is thus of order $\lambda_3 v_a^2 \gg v^2$, assuming λ_3 being not too much below the weak scale. This heavy pseudoscalar decouples from the rest of the spectrum at high energies and does not yield any interesting phenomenology. The anomalous mass of the axion can be determined using more advanced algebra applications [190, 191], but we won't go into details here as they are not relevant to our discussion.

2.4 SUPERSYMMETRIC AXION MODELS

By promoting the axion to a superfield, invisible axion models can be supersymmetrized [192, 193]. Along with the axion pseudoscalar component, the axion supermultiplet

$$\hat{\Phi}_a = s + ia + \sqrt{2}\,\tilde{a}\,\theta + F_a\theta\theta\,, \tag{2.68}$$

now comprises of two additional fields: the *saxion* s, its scalar counterpart, and the *axino* $\tilde{a}$, its fermionic partner. F_a is only an auxiliary field and doesn't have any dynamics. While the mass of the axion is shifted from zero only by the effect of the anomaly, its partners within the superfield $\hat{\Phi}_a$ are strongly affected by the breaking of supersymmetry at some scale $M_{SUSY} \ll v_a$, where v_a is the scale of PQ breaking. The saxion will generically enters the scalar mass matrix, due to its soft-breaking mass m_S in the scalar potential, which is expected to be $m_S \sim M_{SUSY}$.

The axino mass is not bound to such a scale and its range can largely vary depending on the details of the specific model. It was shown [194] that an axino mass $m_{\tilde{a}} \sim M_{SUSY}^2/f_a$ results generically from the lowest order non-renormalizable interactions. In models with more than one extra singlet instead, an axino mass can arise at tree-level from renormalizable interactions. The model in Ref. [195] has three SM singlet superfields in its superpotential

$$W_{PQ} = \hat{\chi}\left(\hat{A}\hat{\overline{A}} - \frac{f_a^2}{4}\right) . \tag{2.69}$$

The superfields $\hat{\chi}$, $\hat{A}$, $\hat{\overline{A}}$ have PQ charges 0, Q_A, $Q_{\bar{A}}$, respectively. An additional R-symmetry, under which χ has charge 2, forbids squared or cubic terms in χ. Let us study the spectrum of this toy model at energies where SUSY is still unbroken. From the renormalizable *Kähler potential*

$$K = \chi\chi^\dagger + AA^\dagger + \overline{A}\,\overline{A}^\dagger , \tag{2.70}$$

the Kähler metric is simply [102]

$$K^i_j \equiv \frac{\partial^2 K}{\partial\phi_i \partial\phi^{*j}} = \mathrm{diag}(1,1,1) . \tag{2.71}$$

Thus the resulting scalar potential reads

$$\begin{aligned} V &\equiv W^i W^*_j \left(K^{-1}\right)^j_i = W^i W^*_i \\ &= \left|A\overline{A} - f_a^2\right|^2 + |\chi A|^2 + \left|\chi\bar{A}\right|^2 . \end{aligned} \tag{2.72}$$

In absence of soft breaking terms, minimizing the scalar potential yields

$$\left\langle A\overline{A}\right\rangle = f_a^2 , \quad \langle\chi\rangle = 0 , \tag{2.73}$$

and thus the scalar fields can be expanded around their minimum as[5]

$$\overset{(-)}{A} = f_a + \frac{\phi_{a,\overline{a}} + i\sigma_{a,\overline{a}}}{\sqrt{2}} , \quad \chi = \frac{\phi_\chi + i\sigma_\chi}{\sqrt{2}} . \tag{2.74}$$

Plugging Eq. (2.74) back into Eq. (2.72) the (identical) mass matrices squared for both the scalar and the pseudoscalar modes gives[6], in the basis $(\chi, A, \overline{A})$

$$m_\phi^2 = m_\sigma^2 = \frac{f_a^2}{2}\begin{bmatrix} 2 & 0 & 0 \\ 0 & 1 & 1 \\ 0 & 1 & 1 \end{bmatrix} . \tag{2.75}$$

5 Here for simplicity we have chosen both $\langle A\rangle = \langle\overline{A}\rangle = f_a/\sqrt{2}$.

6 Note that, e.g. for scalars, this corresponds to $V \supset -\frac{1}{2}\phi_i\left(m_\phi^2\right)_{ij}\phi_j$.

$m^2_{\phi,\sigma}$ can be diagonalized as $R^{-1} m_{\phi,\sigma} R = f_a^2 \mathrm{diag}(1,1,0)$ and the mass eigenstates can be read off from the rows of the matrix

$$R = \begin{bmatrix} 0 & 1 & 1 \\ 1 & 0 & 0 \\ 0 & 1 & -1 \end{bmatrix} . \tag{2.76}$$

As we already know, the massless pseudoscalar mode $a \equiv \frac{\sigma_A - \sigma_{\bar{A}}}{\sqrt{2}}$ is the axion, the Goldstone boson of the broken $U(1)_{PQ}$ symmetry. The saxion $s \equiv \frac{\phi_A - \phi_{\bar{A}}}{\sqrt{2}}$ is the massless CP-even scalar, which has zero mass as long as SUSY is still unbroken. $\phi_\chi(\sigma_\chi)$ is an eigenstates with a heavy mass $\sim \mathcal{O}(f_a)$, same as for the symmetric combination $\frac{\phi_A + \phi_{\bar{A}}}{\sqrt{2}} \left(\frac{\sigma_A + \sigma_{\bar{A}}}{\sqrt{2}} \right)$. The fermionic mass terms can be derived from the superpotential as [92]

$$\mathcal{L}_{m_F} = -\frac{1}{2} \left(\xi_i \xi_j \underbrace{\left. \frac{\partial^2 W_{PQ}}{\partial \phi_i \partial \phi_j} \right|_{\langle \Phi \rangle}}_{\equiv m_F} + \mathrm{h.c.} \right) , \tag{2.77}$$

with

$$m_F = \frac{f_a}{\sqrt{2}} \begin{bmatrix} 0 & 1 & 1 \\ 1 & 0 & 0 \\ 1 & 0 & 0 \end{bmatrix} , \tag{2.78}$$

and the second derivative of the superpotential is performed by substituting the scalar fields to the superfields and evaluating them at their minima defined in Eq. (2.73). By noticing that $m_F^\dagger m_F = m_{\phi,\sigma}$, we can promptly verify the *supertrace* mass sum rule

$$\begin{aligned} \mathrm{STr}(m^2) &\equiv \sum_{\sigma}^{spin} (2\sigma + 1) \, \mathrm{Tr} \left(m_j^2 \right) \\ &= m_\phi^2 + m_\sigma^2 - 2 m_F^\dagger m_F = 0 , \end{aligned}$$

which signifies that the spin-weighted sum of all the tree-level masses in the spectrum will add up to zero[7], as well as the fact that the linear combinations we found for the (pseudo)scalar mass eigenstates are also valid for the fermionic case. At intermediate scale Λ, with $M_{SUSY} \ll \Lambda < f_a$, one can therefore arrange the massless component fields in the axion supermultiplet as

$$\hat{\Phi}_a \equiv s + ia + \sqrt{2}\theta \tilde{a} + F_a \theta\theta , \tag{2.79}$$

where $\tilde{a}$ is the massless axino resulting from the diagonalization of the fermionic mass matrix. In order to give masses to the gauginos one allows soft breaking potential terms which break the R-symmetry. The linear terms in ϕ_χ are then also

7 For this to be true, it is also necessary that the gauge group of the theory considered is non-anomalous

legit and responsible for this field acquiring a VEV $\langle\phi_\chi\rangle = v_\chi$. Updating Eq. (2.78) accordingly,

$$m_F\Big|_{soft} = \frac{1}{\sqrt{2}}\begin{bmatrix} 0 & f_a & f_a \\ f_a & 0 & v_\chi \\ f_a & v_\chi & 0 \end{bmatrix}, \tag{2.80}$$

yields an axino mass $m_{\tilde{a}} = -v_\chi$, while the heavy fields get a correction of the same order. In [196] the case of a supersymmetric DFSZ axion model with a single axion superfield A coupled to the MSSM ones through the superpotential term $c_1\hat{A}\hat{H}_u\hat{H}_d$ of the superpotential was found inconsistent, as the resulting spectrum for the CP-even scalar states contains tachyons. This has to do with the fact that imposing the EWSB conditions yields an unstable soft scalar potential. Adding W_{PQ} as in Eq. 2.69 fixes this issue, as the new tadpole equations for the VEVs are all solvable.

Talking about supersymmetric axion models so far, we only dealt with the axion sector of the theory. In order to solve the strong CP problem though, a non-renormalizable coupling to the gluons is needed, as the one of Eq. (2.39). Depending on the PQ charge assignments of the model, the axion field can effectively couple to the field-strength tensor of each symmetry group,

$$\mathcal{L}^{eff}_{aVV} = \frac{a}{32\pi^2 f_a}\left(g_1^2 C_{aBB} B_{\mu\nu}\widetilde{B}^{\mu\nu} + g_2^2 C_{aWW} W^a_{\mu\nu}\widetilde{W}^{a\mu\nu} + g_3^2 C_{agg} G^\alpha_{\mu\nu}\widetilde{G}^{\alpha\mu\nu}\right), \tag{2.81}$$

where the coefficients C_{aBB} and C_{aWW} are basis-dependent. Instead $C_{agg} = 1$ always, otherwise we don't solve the strong CP problem. The coefficients can be determined by looking at the overall factors in front of the anomalous divergences as the ones of Eq. (2.53), when a chiral $U(1)_{PQ}$ transformation of the form of Eq. (2.47) is applied. Formally the θ-term for each gauge group transforms as [189]

$$\theta \to \theta - d_\psi X_\psi \alpha\,, \tag{2.82}$$

where d_R is the Dynkin index of the group representation for the field ψ. For fundamental representations of $SU(N)$: $d_\psi = 1/2$, while for $U(1)$: $d_\psi = Y_\psi$. The coefficients for the axion coupling to the gauge bosons in Eq. (2.81) transforms exactly as the opposite. We will calculate them for our specific model in Ch. 4. Remarkably one can always use a $U(1)_{PQ}$ rotation in order to set C_{aWW} to zero below the QCD scale [197]. This will also determine unambiguously the value of C_{aBB}. Recalling the photon composition below EWSB, $A^\mu = \cos\theta_W B^\mu + \sin\theta_W W_3^\mu$, this in turn means that the coupling of the axion to photons is also set. The Lagrangian in Eq. (2.81) can be supersymmetrised by considering the F-term of the coupling between the axion superfield of Eq. (2.68) with the vector superfields V_i of the different gauge groups [188]:

$$\mathcal{L}^{eff}_{\hat{a}\hat{V}\hat{V}} = \frac{g_i^2}{8\sqrt{2}\pi^2}\frac{C_{aV_iV_i}}{f_a/N_{DW}}\int d^2\theta\,\hat{\Phi}_A V_i V^i + h.c.\,. \tag{2.83}$$

Below EWSB one can alternatively evaluate the strength of the interactions of the component fields of the axion superfield with gauge bosons and electroweakinos with an explicit calculation of the one-loop amplitude including virtual quarks and leptons charged under the broken $U(1)_{PQ}$. One should mention however that

for some cases this procedure is not exactly equivalent to determining $C_{aV_iV_i}$, in particular in the context of axino production in the early universe [198].

3

AXINO EXPLANATION OF THE 3.5 KEV LINE

So far we have been focusing on the model building side of axion theories. In this chapter we move to their phenomenological aspects and see how they can produce a detectable signature, in particular for the case of the claimed detection of a X-ray line in 2014 [68, 69]. This chapter contains parts of our published work [199] and it is organized as follows: in Sec. 3.1 we introduce basics about models of sterile neutrinos, then in Sec. 3.2 we explain how they can produce a X-ray signal. In Sec. 3.3 we present the hypothesis put forward in the literature in order to explain the line with an axino in analogy with a sterile neutrino. Then in Sec. 3.4 we discuss the constraints from axino dark matter, while those due to the presence of a gravitino follows in Sec. 3.5. In Sec. 3.6 we explain how to account for the radiative axino decay in both R-parity conserving and R-parity violating SUSY scenarios. Finally in Sec. 3.7 we summarise our findings about how the axino is unlikely to explain the putative 3.5 keV line.

3.1 STERILE NEUTRINO DARK MATTER

In Sec. 1.2.4 we referred to the lack of neutrino masses as one of the main shortcomings of the SM. Since the experimental data rule out the possibility that neutrino masses may be originated from higher dimensional operators within the SM particle content [200], the other viable option is to extend the particle content of the SM. The most minimal approach consists of adding to the SM a set of n right-handed neutrino singlets $N_{R,i}$, $i = 1, \ldots, n$ [201]. The resulting new gauge invariant terms[1]

$$\mathcal{L}_{N_R} = i\overline{N_{R,i}}\gamma^\mu \partial_\mu N_{R,i} - \left(Y'_{ij} \bar{L}_i \widetilde{\phi} N_{R,j} + \frac{M_R}{2} \overline{N_{R,i}} N^c_{R,i} + \text{h.c.} \right) , \tag{3.1}$$

include a kinetic term, $3n$ new Yukawa couplings Y'_{ij} and a Majorana mass term, which can be taken to be diagonal without loss of generality. Under the assumption that the resulting Dirac mass terms $(M_D)_{ij} = \langle \phi \rangle F_{ij}$ are negligible with respect to M_R, neutrino masses compatible with the observed oscillations are obtained through a *type-I see-saw mechanism* [155, 202, 203]. In order to explain it in simple terms, let us write the mass term for the neutrinos as

$$\mathcal{L}_{\nu-N} = -\frac{1}{2} \begin{bmatrix} \overline{\nu_L} & \overline{(N^c)_L} \end{bmatrix} \underbrace{\begin{bmatrix} 0 & M_D \\ M_D^T & M_R \end{bmatrix}}_{\equiv \mathcal{M}} \begin{bmatrix} (\nu^c)_R \\ N_R \end{bmatrix} . \tag{3.2}$$

1 The charge conjugate field is defined as $\psi^c = C\overline{\psi}^T$, where C is a unitary matrix such that ψ^c transforms correctly under a Lorentz transformation. This requirement is fulfilled by taking $C^{-1}\gamma_\mu C = -\gamma_\mu^T$. From $(\psi^c)^c = \psi$ it follows that $C^T = -C$. For the Weyl representation of the Dirac spinors $C = i\gamma_2\gamma_0$.

By integrating out the heavy right handed field through their equation of motion and substituting back in the Lagrangian in Eq. (3.2), an effective Majorana mass term for the left-handed neutrinos is generated [203, 204]:

$$\mathcal{L}_{\nu-N} = -\frac{1}{2}\overline{\nu_{Li}}\left[\sum_{k=1}^{n}(M_D)_{ik}\left(M_R^{-1}\right)_{kk}\left(M_D^T\right)_{kj}\right](\nu^c)_{Rj}\,. \tag{3.3}$$

Although at least $n = 2$ sterile neutrinos are needed in order to fit the neutrino oscillation data [2] [205], let us now consider a toy model with one sterile and one active neutrino. By taking for simplicity $M_{D,R}$ to be real and positive, the eigenvalues of $\mathcal{M}$ are reduced to[3]

$$\lambda_1 \simeq \frac{M_D^2}{M_R}, \qquad \lambda_2 \simeq M_R\,. \tag{3.4}$$

It is reasonable to assume that M_D should be around the same order of magnitude for all the fermions of one generation, since they all acquire their masses by means of their coupling to the Higgs field ϕ, which undergoes SSB. A large hierarchy among the eigenvalues naturally results:

$$\lambda_1 \ll M_D \ll \lambda_2\,, \tag{3.5}$$

with one neutrino masses well below the electroweak scale and another heavy one. Using the cosmological bound on the sum of neutrino masses [206], $\sum_i m_{\nu_i} < 0.23\,\text{eV}$, for the neutrino with heaviest associated charged lepton, i.e. $M_D \sim m_\tau$, a strong lower bound on the the Majorana mass parameter M_R is obtained:

$$M_R \gtrsim 3\cdot 10^9\,\text{GeV}\,. \tag{3.6}$$

An alternative to the introduction of an intermediate scale between the electroweak and the Planck scale is to relax the hypothesis of the universality of the Yukawa [207] and therefore allow for any value of M_R. In particular, M_R can be as low as $\mathcal{O}(\text{keV})$, which is the lowest regime in which the sterile neutrino is a viable DM candidate. This follows from *Tremaine-Gunn bound* [208], i.e. the argument according to which the DM distribution cannot be more dense than a degenerate Fermi gas. By looking at the matrix which rotates the neutrinos in the mass eigenstates for $n = 1$,

$$U \simeq \begin{bmatrix} 1 & -\frac{M_D}{M_R} \\ \frac{M_D}{M_R} & 1 \end{bmatrix} + \mathcal{O}\left[\left(\frac{M_D}{M_R}\right)^3\right], \tag{3.7}$$

we can estimate that for a sterile neutrino DM with mass $\sim \mathcal{O}(\text{keV})$, the *sterile-active neutrino mixing* is expected to be small,

$$\theta \simeq \frac{M_D}{M_R} \simeq 10^{-2}\left(\frac{\lambda_1}{0.1\,\text{eV}}\right)^{1/2}\left(\frac{\lambda_2}{\text{keV}}\right)^{-1/2} \tag{3.8}$$

2 This is not true if we consider the lightest neutrino to be massive too.

3 An additional rotation on e.g. $[(\nu^c)_R\ N_R]$ is needed in order to have a meaningful physical interpretation of $\mathcal{M}$. This is possible because the most general Majorana condition allow for a free phase $\psi = \psi^c = e^{-i\alpha}\psi$. Therefore ψ^c can have the opposite eigenvalue of ψ under a CP transformation.

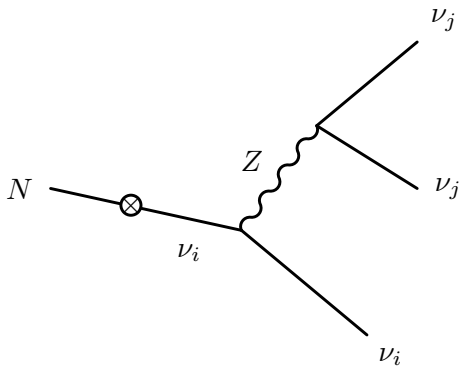

Figure 3.1: Feynman diagram describing the decay of the sterile neutrino into three active neutrinos. Here the dot on a fermion line stands for a mixing between fermionic mass eigenstates.

such that $\mathcal{L}_{\nu-N}$ describes a light active neutrino and a heavy sterile one with negligible overlap. The definition of θ can be extended to the case of n sterile neutrino species as in the following:

$$\theta_i = \langle\phi\rangle \sum_{j=e,\mu,\tau} |F_{ij}| M_R^{-1} \,. \tag{3.9}$$

The main decay channel for a sterile neutrino N is into three active neutrinos via a Z boson exchange, as depicted in Fig. 3.1. Its width reads [209]

$$\begin{aligned} \Gamma_{N\to 3\nu} &= \frac{9\alpha G_F^2}{8\pi^4}\theta^2 m_N^5 \\ &\simeq 10^{-20}\theta^2 \left(\frac{m_N}{\text{keV}}\right)^5 s^{-1} \,. \end{aligned} \tag{3.10}$$

In order for N to be DM, its lifetime should exceed the age of the universe, $\tau_U \simeq 4 * 10^{17} s$ in the Λ_{CDM} model [206]. For $m_N \sim \mathcal{O}(\text{keV})$, this requirement is fulfilled for any value of the mixing angle $\theta \lesssim 1$. The sterile neutrino can also decay into a photon and a light neutrino through the exchange of a virtual W boson, as shown in Fig. 3.2 . The associated width of the process [210]

$$\begin{aligned} \Gamma_{N\to\nu\gamma} &= \frac{9\alpha G_F^2}{1024\pi^4}\theta^2 m_N^5 \\ &\simeq 5\cdot 10^{-22}\theta^2 \left(\frac{m_N}{\text{keV}}\right)^5 s^{-1} \end{aligned} \tag{3.11}$$

shows how this channel is subdominant due to the loop suppression, $\text{Br}(N \to \gamma + \nu) \simeq 1/128$ [209]. Nevertheless, this is the most relevant decay mode for phenomenology, since a X-ray signal at energies $E_\gamma = \frac{m_N}{2}$ could be detectable through this decay.

3.2 X-RAY SIGNALS

Several astrophysical sources can be responsible for a light signal in the decaying DM hypothesis. First, the DM decay throughout the history of the universe gener-

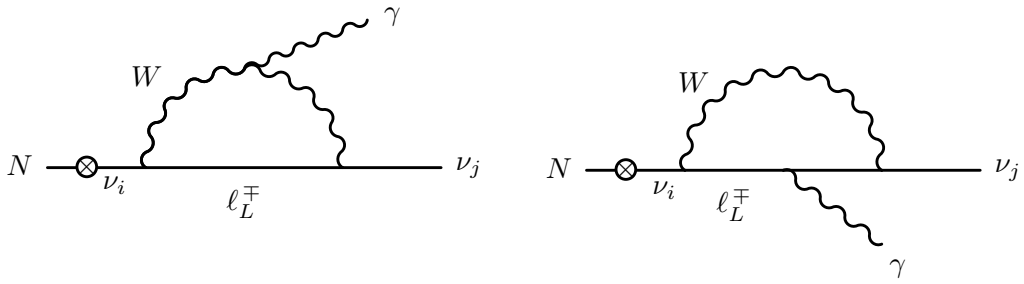

Figure 3.2: Diagrams for the process $N \to \gamma + \nu$ for a $SU(2)_L \times U(1)_Y$ plus sterile neutrino model in the *renormalizable* R_χ *gauges*. In the *Feynman - t'Hooft gauge* there are 4 more diagrams with the unphysical charged Higgses (*would-be Goldstone bosons*) in place of the W boson.

ates a contribution to the diffuse X-ray background (XRB), a series of luminous signals of unknown sources in the X-ray spectrum [211]. DM concentrations at small red-shifts, i.e. galaxy clusters, can strongly increase the light signal in their direction [212, 213]. Despite having smaller DM concentrations, also dwarf spheroidal (dSph) satellites of the Milky Way can produce a comparable photon flux thanks to their proximity [214–216]. Finally, the DM from the milky way halo can also decay yielding a sizeable contribution [214]. Except for this latter case, if the DM halo under scrutiny is composed of M_{DM}/m_N sterile neutrinos, the luminosity of the photon resulting from the decay $N \to \nu + \gamma$ can be estimated as

$$\mathcal{L} \simeq \frac{E_\gamma}{m_N} M_{DM} \Gamma_{N\to\nu\gamma}\,, \tag{3.12}$$

where the red-shift effects can be neglected [213]. The typical value of field of view (FoV) for modern X-ray telescopes is around $10' - 15'$, an interval at a negligible scale compared to the one of the DM distribution in the sources, which can thus be taken as uniform within the instrument's FoV. As a result, the FoV integral reduces to the *column density*, i.e. the one over the line of sight (LoS):

$$M_{DM}^{(FoV)} \equiv \int_{FoV} \rho_{DM}(r)\, d^3r \simeq \Omega_{FoV} D_L^2 \int_{LoS} \rho_{DM}(r)\, dr\,, \tag{3.13}$$

where D_L is the distance to the center of the object towards which the telescope is pointing. This quantity drops out in the expression for the DM flux

$$\begin{aligned} \phi_{DM} &\equiv \frac{\mathcal{L}}{4\pi D_L^2} \\ &\simeq \frac{1}{8\pi} \Omega_{FoV} \Gamma_{N\to\gamma\nu} \int_{LoS} \rho_{DM}(r)\, dr\,. \end{aligned} \tag{3.14}$$

This shows how contributions from faraway sources and as well as close ones could be equally relevant. Plugging in some typical values reveals the expected flux of photons resulting from the radiative decay of the sterile neutrino:

$$\phi_{DM} \simeq 20 \left(\frac{M_{DM}^{(FoV)}}{10^{10} M_\odot}\right) \left(\frac{D_L}{Mpc}\right)^{-2} \theta^2 \left(\frac{m_N}{keV}\right)^5 \frac{keV}{cm^2\, s}\,. \tag{3.15}$$

During the past few years, numerous experimental efforts were performed, including X-ray searches of all the aforementioned kinds: HEAO-1 [217], XMM-Newton [218], INTEGRAL [219], Chandra [220], Suzaku [216], just to mention a few. For a long time no hint to DM signature was found, since all detected signals were compatible with known astrophysics.

3.3 THE CLAIM OF THE OBSERVATION OF A 3.5 KEV LINE AND THE AXINO EXPLANATION

In early 2014, two independent groups reported a line of unknown origin at $\simeq 3.5\,\mathrm{keV}$ [68, 69]. In [68] the analysis was performed using data from the Andromeda galaxy and the Perseus cluster from the XMM-Newton telescope. The authors of [69] combined the observations of several individual galaxy clusters as well as clusters stacked spectra from the same instrument. A sterile neutrino with mass $m_N = 7\,\mathrm{keV}$ would be a natural candidate to explain such a line, provided that the decay rate into a photon is around $\Gamma_{N\to\gamma\nu} \sim 10^{-29}\,\mathrm{s}^{-1}$. Without entering the details of their statistical analysis, we combine our Eq. (3.12) and Eq. (3.14) to reproduce the expression for the observed differential flux in [68]

$$\frac{d\phi_{DM}}{dE_\gamma} \simeq \frac{2\cdot 10^{-6}}{\mathrm{cm}^2\,\mathrm{s}} \frac{\Omega_{DM}^{(FoV)}}{500\,\mathrm{arcmin}^2} \frac{\int_{LoS}\rho_{DM}(r)\,dr}{500\,M_\odot/\mathrm{pc}^2} \frac{\Gamma_{N\to\gamma\nu}}{10^{-29}\,\mathrm{s}^{-1}} \left(\frac{m_N}{\mathrm{keV}}\right)^{-1}, \tag{3.16}$$

where the values of of the column density and the FoV angle are centered around the averaged experimental values. A debate about the possible astrophysics explanation for the line followed [70–78], with [71] in particular pointing out how the line might also be due to atomic transitions from potassium ions (K XVIII). On the other side, among the long list of possible existing particle physics explanations, which would be impractical to report here, some authors [79–82] have pointed out how the the decay of the axino, the SUSY partner of the axion (see Sec. 2.4), can be responsible for it. Both RpC and RpV SUSY scenarios are possible and the decay happens in complete analogy with the decay of a sterile neutrino into an active neutrino and a photon depicted in Fig. 3.2. In the RpC SUSY case a neutralino lighter than the axino is needed in order to allow for the radiative decay channel of the NLSP axino. In RpV SUSY scenarios, the axino is unstable and can decay into an active neutrino plus photon with a lifetime longer than the age of the universe. Both possibilities are appealing since several problems could be addressed in a unique framework. Firstly, the presence of the axion solves the strong CP problem, as we learnt in Sec. 2.2. Second, both the axion and the axino are potential DM constituents [221, 222]. Thirdly, considering an axino in the keV range would make it a warm DM relic, which helps soothing the small-scale structure problem.

3.4 AXINO RELIC DENSITY

A generic supersymmetric axion model yields two possible DM candidates. While for the axion is always the case, the axino has to be enough long lived. From here until the rest of this chapter, we will focus on a scenario where the axino accounts for almost the entire budget of DM in the universe. In order to suppress the axion relic abundance Ω_a accordingly, a low value of the axion decay constant is needed,

i.e. $f_a \sim 10^{10}$ GeV, as can be read off from the expressions for Ω_a presented in Sec. 4.3.2. When it comes to the axino relic abundance $\Omega_{\tilde{a}}$, there is one aspect which needs to be carefully dealt with, which is the difference between two seemingly equal quantities, the Wilsonian axino-gaugino-gauge boson coupling and the one-particle-irreducible (1PI) axino-gaugino-gauge boson amplitude [198]. Wilsonian couplings are the coefficients in the effective Lagrangian which describe the interactions below f_a and it is obtained by integrating out the heavy modes after PQ breaking. This quantity is therefore local and depends on the field basis chosen in the effective Lagrangian. The coefficient $C_{aV_iV_i}$ in Eq. 2.83 is an example. The 1PI amplitude is an observable quantity which depends on the light particles running in the loop and in general carries a dependence on their momentum p. It turns out that in the range $M_\phi < p < f_a$, where M_ϕ is the highest PQ-charged and gauge-charged mass in the the spectrum, the 1PI amplitude has an extra suppression $\sim M_\phi^2/p^2$ with respect to the Wilsonian coefficient. This results from the fact that the effective Lagrangian does not keep track of the decoupling of the axion supermultiplet from the gauge- and matter-fields in the limit $M_\phi \to 0$. As a consequence, in a model with $M_\phi \ll f_a$ the axino production by gauge interaction is strongly reduced. This suppression is therefore naturally very efficient in DFSZ axion models, where M_ϕ is around the electroweak scale, while in KVSZ models the mass of the heavy vectorlike PQ-charged quarks is typically around $f_a \gtrsim 10^9$ GeV. Eventually this difference yields two distinct axino relic abundances for the two models, notably for their different dependence on the reheating temperature T_{RH}, the temperature that the universe reach after the end of inflation and before the Big-Bang epoch. For DFSZ models we have [188]

$$\Omega_{\tilde{a}}^{DFSZ}h^2 \simeq 0.78 \left(\frac{m_{\tilde{a}}}{7\ \text{keV}}\right)\left(\frac{10^{10}\ \text{GeV}}{f_a}\right)^2 , \tag{3.17}$$

which does not depend on T_{RH}, as long as T_{RH} is larger than roughly 1 TeV [223][4]. The relic density drops very quickly for lower values of T_{RH}. This can be understood in terms of the most efficient axino production mechanisms for the cases: a) $T_{RH} < M_\phi$, where most axinos are produced below T_{RH} through the process $g \to \tilde{g} + \tilde{a}$ (or $\tilde{g} \to g + \tilde{a}$) because in this regime the 1PI amplitude is equivalent to the Wilsonian coefficient; b) $T_{RH} > M_\phi$, in which case the suppression of the 1PI amplitude makes the production through gauge modes irrelevant compared to the mode $\phi \to \widetilde{\phi} + \tilde{a}$ (or $\widetilde{\phi} \to \phi + \tilde{a}$) for $T > M_\phi$. From eq. (4.65) we see that for a 7 keV DFSZ axino with $f_a < 10^{10}$ GeV the reheating temperature has to be below 1 TeV in order to avoid overabundance, i.e. $\Omega_{\tilde{a}}^{DFSZ}h^2 > \Omega_{\Lambda CDM}h^2$. Let us add that the extra suppression for the DFSZ case relaxes the constraint on the axino mass obtained in Ref. [194]. Here an upper bound of 2 keV on the axino mass was obtained by simply using entropy density conservation after axino decoupling and photon decoupling, respectively, without any assumption on the value of f_a.

The relic abundance for the KSVZ case [188] reads:

$$\Omega_{\tilde{a}}^{KSVZ}h^2 = 6.9 \times 10^{-3} \left(\frac{m_{\tilde{a}}}{7\ \text{keV}}\right)\left(\frac{10^{10}\ \text{GeV}}{f_a}\right)^2 \left(\frac{T_{RH}}{10^3\ \text{GeV}}\right) ,$$

4 The exact value of T_{RH} depends on the SUSY spectrum, but it is expected to lie in the TeV range.

which is valid for 1 TeV $< T_{RH} < M_\Phi \sim f_a$. In this case the abundance drops very quickly for reheating temperatures below about 1 TeV, too.

3.5 INCLUDING A LIGHT GRAVITINO

In the context of SUGRA one can show with a simple argument why the axino is generically expected to be heavier than the gravitino [224]. With $\sqrt{F}$ being the scale of SUSY breaking, we can write the superfield which breaks SUSY as

$$\hat{X} = \varphi_x + \sqrt{2}\theta\xi_x + \theta^2\sqrt{F}\,. \tag{3.18}$$

The effects of the phase transition are transmitted to the axion sector by means of a generic non-renormalizable operator suppressed by M_{Pl}:

$$\int d^4\theta \frac{(\hat{A}+\hat{A}^\dagger)^2(\hat{X}+\hat{X}^\dagger)}{M_{Pl}} \simeq \frac{1}{2} m_{3/2}\tilde{a}\tilde{a} + \dots\,, \tag{3.19}$$

where $\hat{A}$ is the axion superfield and the gravitino mass is [38]

$$m_{3/2} = \sqrt{\frac{8\pi}{3}}\frac{F}{M_{Pl}} \tag{3.20}$$

as expected from supergravity. Since the operator in Eq. (3.19) respects the PQ symmetry, the only components of the supermultiplet which can be effected by the SUSY breaking are the axino $\tilde{a}$ and the saxion s[5], but the axion mass stays zero, being it the Goldstone boson of the $U(1)_{PQ}$. Thus $m_{3/2}$ is a lower bound on the axino mass. This puts further constraints on our scenario. The generic form of the interactions between the goldstino $\tilde{\eta}$ and the chiral superfields is dictated by the fact that $\tilde{\eta}$ is the NG boson of the broken supersymmetry. Its coupling to the broken supercurrent J_μ^{SUSY} [225] can be used to determine the interaction between the gravitino and the components of the axino supermultiplet:

$$\begin{aligned}\mathcal{L}_{\tilde{\eta}} &= -\frac{1}{F}\tilde{\eta}\,\partial^\mu J_\mu^{SUSY} + \text{h. c.}\\ &= -\frac{1}{F}\tilde{\eta}\,\partial^\mu(\sigma^\nu\bar{\sigma}^\nu\tilde{a}\,\partial_\nu a + \dots)\\ &= \frac{m_{\tilde{a}}}{F}\,i\tilde{\eta}\,\sigma^\nu\tilde{a}\,\partial_\nu a + \dots\,,\end{aligned} \tag{3.21}$$

where we have used the Dirac equation in the form $i\bar{\sigma}\cdot\partial\tilde{a} = m_{\tilde{a}}\tilde{a}^\dagger$.

Once local SUSY gets broken the goldstino becomes the longitudinal component of the gravitino via the *super-Higgs* mechanism:

$$\tilde{G}_\mu \to \tilde{G}_\mu + i\sqrt{4\pi}\frac{M_{Pl}}{F}\partial_\mu\tilde{\eta}\,. \tag{3.22}$$

Since for most SUSY models the scale of SUSY breaking is relatively low, $\sqrt{F} \ll M_{Pl}$, the gravitino interacts with matter mostly through the would-be gold-

5 The mass term for the saxion s which results from Eq. 3.19 reads $1/2 m_{3/2}^2 ss$

stino. From the operator in Eq. (3.21) one can calculate the lifetime for the decay of the axino into a gravitino and an axion [224]:

$$\tau_{\tilde{a}\to\tilde{G}+a} \simeq 6\cdot 10^{28}\ \mathrm{s}\left(\frac{m_{3/2}}{\mathrm{keV}}\right)^2\left(\frac{7\,\mathrm{keV}}{m_{\tilde{a}}}\right)^5 . \tag{3.23}$$

If the 7 keV axino is to explain the X-ray line we must require its lifetime to be greater than the age of the universe, $\tau_{\tilde{a}\to\tilde{G}+a} > 10^{18}\,\mathrm{s}$, otherwise it would have decayed away. This in turn implies $m_{3/2} > 10^{-5}\,\mathrm{keV}$. A gravitino lighter than roughly 100 eV is a hot dark matter candidate. Its relic abundance [186],

$$\Omega_{\tilde{G}}^{\mathrm{HDM}}h^2 \sim 0.1\,\frac{m_{3/2}}{100\ \mathrm{eV}}, \quad \text{for } m_{3/2} < 100\ \mathrm{eV}, \tag{3.24}$$

is constrained to be less than 3% of the total DM abundance [226], which implies $m_{3/2} \lesssim 1\,\mathrm{eV}$. In the range $1\ \mathrm{keV} < m_{3/2} < 7\ \mathrm{keV}$, the gravitino is a warm dark matter candidate and its abundance depends on T_{RH} [227]:

$$\Omega_{\tilde{G}}h^2 = 0.27\left(\frac{T_{RH}}{100\ \mathrm{GeV}}\right)\left(\frac{\mathrm{keV}}{m_{3/2}}\right), \text{ for } m_{3/2} > 1\,\mathrm{keV}. \tag{3.25}$$

In this case we require a reheating temperature below $1-10$ GeV so that the gravitino contribution to the DM density is much smaller than that of the axino. However for such low values of T_{RH} the axino relic density, even with $f_a \sim 10^9$ GeV, is highly suppressed, $\Omega_{\tilde{a}}h^2 \ll 0.12$. Therefore, we exclude this case. Thus if the axino constitutes most of the DM and produces the 3.5 keV X-ray line, the gravitino mass is restricted to the small window

$$10^{-2}\ \mathrm{eV} < m_{3/2} < 1\ \mathrm{eV}. \tag{3.26}$$

As both the axino and the gravitino are in the keV range and below, one might worry about their contribution to the relativistic degrees of freedom g_* at Big Bang Nucleosynthesis (BBN). In the SM the effective numbers of degrees of freedom $g_*(T = 1\,\mathrm{MeV}) = 5.5 + \frac{7}{4}N_{eff}$, where N_{eff} is the number of effective neutrino species. Adding a light neutralino increases N_{eff} and consequently the expansion rate of the universe, in such a way that a higher ^{4}He primordial abundance results from the earlier proton-neutron decoupling [228]. Independent measurements of abundances of primordial elements [20] and of the CMB power spectrum [229] give strong bounds on BSM physics by constraining the conventionally chosen value

$$\Delta N_{eff} \equiv 3 - N_{eff}\ . \tag{3.27}$$

As of today the strongest constraint comes from the PLANCK collaboration's result [37]:

$$\Delta N_{eff} = 2.89^{+0.36}_{-0.38}\ . \tag{3.28}$$

This turns out not to be a problem in most cases. When the universe reheats to 10 - 100 GeV, both the axino and the gravitino are out of thermal equilibrium [188]. The subsequent annihilations of SM particles heat up the photon bath so that the photon temperature at BBN is higher than the respective temperatures of the axino and the gravitino. They are therefore not relativistic and does not enter into g_*. As a consequence their contribution to N_{eff} is well within the bound. If there is also

a very light or massless neutralino in the spectrum one has to worry about the constraint from N_{eff}, as we discuss later.

3.6 PRODUCING THE X-RAY LINE SIGNAL

In order to explain the 3.5 keV X-ray line via the decay of a DM particle X, one needs a decay rate of $\Gamma_{X\to\gamma+\ldots} \sim (10^{28}\ \mathrm{s})^{-1} \sim 10^{-53}\,\mathrm{GeV}$ [68], assuming that the decaying DM constitutes 100% to the relic abundance. If the decaying DM is a fraction $k < 1$ of the total DM, then the corresponding decay rate has to increase by $1/k$ to explain the signal.

There are two scenarios for a 7 keV axino to produce the 3.5 keV X-ray line, where R-parity is respectively conserved or violated. In either case the starting point is the following Lagrangian for the coupling of the axino to the SM gauge bosons and their gaugino supersymmetric partners:

$$\mathcal{L}^{\mathrm{eff}}_{a\lambda V} = \frac{\tilde{a}}{16\pi^2 f_a}\sigma_{\mu\nu}\left[g_1^2\, C_{aBB}\lambda_{\tilde{B}} B^{\mu\nu} + g_2^2\, C_{aWW}\widetilde{W}_0^a W_a^{\mu\nu} + g_3^2\,\lambda_{\tilde{G}}^{\alpha} G_{\alpha}^{\mu\nu}\right]. \quad (3.29)$$

Here $\tilde{a}$ is the axino mass eigenstate, while the gauginos and gauge fields are gauge eigenstates. The interactions described by $\mathcal{L}_{a\lambda V}$ are the supersymmetric version of the ones in $\mathcal{L}^{\mathrm{eff}}_{aVV}$ of Eq. (2.81), obtained from the F-term in Eq. (2.83).

3.6.1 *R-parity conserving SUSY*

In the R-parity conserved (RpC) case, if the bino is lighter than the axino, the X-ray line could be produced by the decay $\tilde{a} \to \lambda_{\tilde{B}} + \gamma$. This was pointed out in Ref. [82]. The axino partial decay rate with a massless bino is

$$\Gamma_{\tilde{a}\to\lambda_{\tilde{B}}+\gamma} = \frac{1}{128\pi^3}\frac{m_{\tilde{a}}^3}{f_a^2} C_{aBB}^2 \left(\frac{g_1^2}{4\pi}\right)^2 \cos^2\theta_W \quad (3.30)$$

$$\sim 7\times 10^{-52}\,\mathrm{GeV}\left(\frac{m_{\tilde{a}}}{7\ \mathrm{keV}}\right)^3\left(\frac{10^{14}\ \mathrm{GeV}}{f_a}\right)^2. \quad (3.31)$$

The factor $\cos\theta_W$ accounts for the B^μ-component of the photon after EWSB. Note, a massless bino is consistent with all data provided the sfermions are heavy enough [230–232]. To match the rate needed for the X-ray line this scenario requires $f_a > 10^{14}$ GeV. This immediately excludes the DFSZ axino, whose relic abundance would be too low to account for the DM relic density.

From Eq. (3.18), a KSVZ axino with $T_{RH} \sim 10^{12}$ GeV would seem viable. However this scenario is strongly disfavoured by two arguments. First, the abundance of axions produced via the misalignment mechanism (see Sec. 4.3.2.1 for details) would be far too high [221] for $f_a \sim 10^{14}$ GeV, unless one tunes the initial misalignment angle to very small values. Second, a massless bino together with a light gravitino would contribute to the relativistic degrees of freedom [228], giving a value $\Delta N_{eff} > 1$, in strong tension with the experimental result in Eq. (3.28).

3.6.2 *R-parity violating SUSY*

In the context of R-parity violation (RpV), the terms $\epsilon_i L_i H_u$, $i = e, \mu, \tau$, in the superpotential introduce mixing among the neutrinos and the Higgsinos. The modified scalar potential also results in non-zero sneutrino vacuum expectation values, which introduce mixing between the neutrinos and the bino and the neutral wino, respectively. In this case the RpC axino decay in Sec. 3.6.1 automatically includes the decay channel $\tilde{a} \to \nu_i + \gamma$. The new partial decay rate is simply modified by the appropriate mixing angles[6]

$$\begin{aligned}\Gamma_{\tilde{a}\to\nu_i+\gamma} &= \frac{1}{2048\pi^5}\frac{m_{\tilde{a}}^3}{f_a^2}\left[r_{\nu_i\tilde{B}}^2 C_{aBB}^2 g_1^4 \cos^2\theta_W + r_{\nu_i\widetilde{W}}^2 C_{aWW}^2 g_2^4 \sin^2\theta_W\right] \\ &\simeq 7\times 10^{-42}\ \text{GeV}\ \left(r_{\nu_i\tilde{B}}^2 + 3\, r_{\nu_i\widetilde{W}}^2\right)\left(\frac{m_{\tilde{a}}}{7\ \text{keV}}\right)^3\left(\frac{10^9\ \text{GeV}}{f_a}\right)^2 .\end{aligned} \tag{3.32}$$

Here $r_{\nu_i\tilde{B}}$ ($r_{\nu_i\widetilde{W}}$) parametrizes the mixing of the neutrino mass eigenstate with the gaugino gauge eigenstate $\lambda_{\tilde{B}}$ ($\widetilde{W}^0$). The lifetime of the axino to explain the X-ray line requires $r_{\nu_i\tilde{B}}^2$ ($r_{\nu_i\widetilde{W}}^2$) to be of order 10^{-12} for f_a fixed at its lowest possible value [185], 10^9 GeV. One of the outstanding features of RpV models with lepton number violation, is that they automatically provide for massive neutrinos. Assuming that the neutrino masses solely arise from the RpV sector, we can estimate bounds on the mixings $r_{\nu_i(\tilde{B},\widetilde{W})}$ as follows. Neglecting loop contributions, the terms $\epsilon_i L_i H_u$ lead to one massive neutrino [233–235] and two non-vanishing lepton mixing angles, which we take to be θ_{13} and θ_{23} [233]. Following [157, 158] we start from the neutralino mass term in the Lagrangian resulting from a generic superpotential with bilinear RpV,

$$\mathcal{L}_{\widetilde{\chi}^0} = -\frac{1}{2}\widetilde{\psi}_0^T \mathcal{M}_{\not{R}} \widetilde{\psi}_0 + \text{h. c.}\,. \tag{3.33}$$

The neutralino mass matrix $\mathcal{M}_{\not{R}}$ in the basis of the gauge eigenstates $\widetilde{\psi}_0 = \left(\lambda_{\widetilde{B}}, \widetilde{W}_0, \widetilde{H}_u^0, \widetilde{H}_d^0, \nu_{L,I}\right)$ reads in block form

$$\mathcal{M}_{\not{R}} = \begin{bmatrix} \mathcal{M}_{\widetilde{\chi}^0} & m \\ m^T & 0 \end{bmatrix}, \tag{3.34}$$

where $\mathcal{M}_{\widetilde{\chi}^0}$ is the 4x4 MSSM submatrix,

$$\mathcal{M}_{\widetilde{\chi}^0} = \begin{bmatrix} M_1 & 0 & \frac{g_1 v_u}{2} & -\frac{g_1 v_d}{2} \\ 0 & M_2 & -\frac{g_2 v_u}{2} & \frac{g_2 v_d}{2} \\ \frac{g_1 v_u}{2} & -\frac{g_2 v_u}{2} & 0 & -\mu \\ -\frac{g_1 v_d}{2} & \frac{g_2 v_d}{2} & -\mu & 0 \end{bmatrix}, \tag{3.35}$$

6 Note this decay would also occur with pure trilinear RpV via the resulting sneutrino vev 's [134].

and m is the matrix which contains the bilinear couplings ϵ_i and the sneutrino vevs $\langle\tilde{\nu}_i\rangle$,

$$m = \begin{bmatrix} -\frac{1}{2}g_1\langle\tilde{\nu}_e\rangle & -\frac{1}{2}g_1\langle\tilde{\nu}_\mu\rangle & -\frac{1}{2}g_1\langle\tilde{\nu}_\tau\rangle \\ \frac{1}{2}g_2\langle\tilde{\nu}_e\rangle & \frac{1}{2}g_2\langle\tilde{\nu}_\mu\rangle & \frac{1}{2}g_2\langle\tilde{\nu}_\tau\rangle \\ -\epsilon_e & -\epsilon_\mu & -\epsilon_\tau \\ 0 & 0 & 0 \end{bmatrix} . \tag{3.36}$$

Under the assumption that the RpV parameters are smaller than the electroweak scale, we can define a matrix $\xi = m^T \cdot \mathcal{M}_{\tilde{\chi}_0}^{-1}$, such that in the perturbative limit $\xi_{ij} \ll 1$, $\mathcal{M}_{\not R}$ can be block-diagonalized,

$$\begin{bmatrix} 1 - \frac{1}{2}\xi^\dagger\xi & \xi^\dagger \\ -\xi & 1 - \frac{1}{2}\xi\xi^\dagger \end{bmatrix} \mathcal{M}_{\not R} = \begin{bmatrix} \mathcal{M}_{\tilde{\chi}_0} & 0 \\ 0 & m_{\text{eff}} \end{bmatrix} . \tag{3.37}$$

The neutrino mass sub-block,

$$\begin{aligned} m_{\text{eff}} &= -m \cdot \mathcal{M}_{\tilde{\chi}_0}^{-1} \cdot m^T \\ &= \frac{M_1 g_2^2 + M_2 g_1^2}{2 \det \mathcal{M}_{\tilde{\chi}_0}} \begin{bmatrix} \Lambda_e^2 & \Lambda_e\Lambda_\mu & \Lambda_e\Lambda_\tau \\ \Lambda_\mu\Lambda_e & \Lambda_\mu^2 & \Lambda_\mu\Lambda_\tau \\ \Lambda_\tau\Lambda_e & \Lambda_\tau\Lambda_\mu & \Lambda_\tau^2 \end{bmatrix} , \end{aligned} \tag{3.38}$$

contains the *alignment parameters*

$$\Lambda_i = \mu\langle\tilde{\nu}_i\rangle - v_d\epsilon_i , \tag{3.39}$$

and the determinant

$$\det \mathcal{M}_{\tilde{\chi}_0} \equiv -\mu^2 M_1 M_2 + \frac{1}{2}\mu v_u v_d (g_2^2 M_1 + g_1^2 M_2) . \tag{3.40}$$

The PMNS matrix describes the mixing among the light neutrino species in terms of angles which have been measured by various independent experiments [20]. It can be put in the form [233]

$$V_\nu = \begin{bmatrix} \cos\theta_{13} & 0 & -\sin\theta_{13} \\ -\sin\theta_{13}\sin\theta_{23} & \cos\theta_{23} & -\cos\theta_{13}\sin\theta_{23} \\ \sin\theta_{13}\cos\theta_{23} & \sin\theta_{23} & \cos\theta_{13}\cos\theta_{23} \end{bmatrix} , \tag{3.41}$$

which manifestly depends only on two mixing angles. Their measured values are $\theta_{13} \sim \pi/20$ and $\theta_{23} \sim \pi/4$. The diagonalization requirement

$$V_\nu^T m_{\text{eff}} V_\nu = (0, 0, m_{\nu_3}) , \tag{3.42}$$

with

$$m_{\nu_3} = \frac{g_2^2 M_1 + g_1^2 M_2}{4 \det \mathcal{M}_{\chi_0}} |\vec{\Lambda}|^2 , \tag{3.43}$$

enforces the following relations between the angles in V_ν and the misalignment parameters:

$$\tan\theta_{13} = -\frac{\Lambda_e}{\sqrt{(\Lambda_\mu^2+\Lambda_\tau^2)}}\,, \qquad \tan\theta_{23} = \frac{\Lambda_\mu}{\Lambda_\tau}\,. \tag{3.44}$$

This in turn sets $\Lambda_e = 0.23\,\Lambda$, with $\Lambda \equiv \Lambda_\mu = \Lambda_\tau$. Additionally the cosmological bound on the sum of the neutrino masses [20],

$$\sum_i m_{\nu_i} < 0.23 \text{ eV}, \tag{3.45}$$

can be used on m_{ν_3} and yields

$$\Lambda < (3.2\times 10^{-13}\text{ TeV})^{1/2}\left(\frac{\det \mathcal{M}_{\tilde\chi^0}}{g_2^2 M_1 + g_1^2 M_2}\right)^{1/2}. \tag{3.46}$$

A remarkable feature about neutrino masses in bilinear RpV is that one does not need to explicitly diagonalize $\mathcal{M}_{\tilde\chi^0}$ in order to estimate the mixings between the MSSM gauginos and the light neutrino mass eigenstates, *i.e.* $r_{\nu_i\tilde B}$ and $r_{\nu_i\widetilde W}$. In fact if we generically define a matrix N^0 such that

$$N^{0*}\mathcal{M}_{\tilde\chi^0}N^{0\dagger} = \text{diag}(m_{\chi_1^0}, m_{\chi_2^0}, m_{\chi_3^0}, m_{\chi_4^0})\,, \tag{3.47}$$

the full 7x7 mass matrix $\mathcal{M}_{\not R}$ can be diagonalized by

$$\begin{bmatrix} N^{0*} & 0 \\ 0 & V_\nu^T \end{bmatrix}\begin{bmatrix} 1-\frac{1}{2}\xi^\dagger\xi & \xi^\dagger \\ -\xi & 1-\frac{1}{2}\xi\xi^\dagger \end{bmatrix} \simeq \begin{bmatrix} N^{0*} & N^{0*}\xi^\dagger \\ -V_\nu^T\xi & V_\nu^T \end{bmatrix}$$

We can read off $r_{\nu_i\tilde B}$ and $r_{nu_i\widetilde W}$ from the lower-left sub-block $-V_\nu^T\xi$:

$$r_{\nu_1\tilde B} = \frac{g_1 M_2\mu}{\det\mathcal{M}_{\tilde\chi^0}}\frac{\Lambda_e\Lambda_\mu^2}{\left|\vec\Lambda\right|\sqrt{\Lambda_\mu^2+\Lambda_\tau^2}} \simeq \frac{g_1 M_2\mu}{\sqrt{2}\det\mathcal{M}_{\tilde\chi^0}}\Lambda\,, \tag{3.48}$$

$$r_{\nu_2\tilde B} = \frac{g_1 M_2\mu}{\det\mathcal{M}_{\tilde\chi^0}}\frac{\Lambda_\mu\Lambda_\tau}{\sqrt{\Lambda_\mu^2+\Lambda_\tau^2}} \simeq \frac{g_1 M_2\mu}{\sqrt{2}\det\mathcal{M}_{\tilde\chi^0}}\Lambda\,, \tag{3.49}$$

$$r_{\nu_3\tilde B} = \frac{g_1 M_2\mu}{\det\mathcal{M}_{\tilde\chi^0}}\frac{\Lambda_e^2-\Lambda_\mu^2+\Lambda_\tau^2}{2\left|\vec\Lambda\right|} \simeq \frac{g_1 M_2\mu}{2\det\mathcal{M}_{\tilde\chi^0}}\frac{\Lambda_e^2}{\left|\vec\Lambda\right|}\,, \tag{3.50}$$

$$r_{\nu_1\widetilde W} = -\frac{g_2 M_1\mu}{\det\mathcal{M}_{\tilde\chi^0}}\frac{\Lambda_e\Lambda_\mu^2}{\left|\vec\Lambda\right|\sqrt{\Lambda_\mu^2+\Lambda_\tau^2}} \simeq -\frac{g_2 M_1\mu}{\sqrt{2}\det\mathcal{M}_{\tilde\chi^0}}\frac{\Lambda_e\Lambda_\mu}{\left|\vec\Lambda\right|}\,, \tag{3.51}$$

$$r_{\nu_2\widetilde W} = -\frac{g_2 M_1\mu}{\det\mathcal{M}_{\tilde\chi^0}}\frac{\Lambda_\mu\Lambda_\tau}{\sqrt{\Lambda_\mu^2+\Lambda_\tau^2}} \simeq -\frac{g_2 M_1\mu}{\sqrt{2}\det\mathcal{M}_{\tilde\chi^0}}\Lambda^2\,, \tag{3.52}$$

$$r_{\nu_3\widetilde W} = -\frac{g_2 M_1\mu}{\det\mathcal{M}_{\tilde\chi^0}}\frac{\Lambda_e^2-\Lambda_\mu^2+\Lambda_\tau^2}{2\left|\vec\Lambda\right|} \simeq -\frac{g_2 M_1\mu}{2\det\mathcal{M}_{\tilde\chi^0}}\frac{\Lambda_e^2}{\left|\vec\Lambda\right|}\,. \tag{3.53}$$

The bound on Λ in Eq. (3.46) translates into

$$r^2_{\nu_1 \tilde{B}\,(\nu_1 \widetilde{W})} < \frac{1.1 \times 10^{-14}\ \text{TeV}}{M_{\mu 1\,(\mu 2)}}\,, \tag{3.54}$$

$$r^2_{\nu_2 \tilde{B}\,(\nu_2 \widetilde{W})} < \frac{4.6 \times 10^{-13}\ \text{TeV}}{M_{\mu 1\,(\mu 2)}}\,, \tag{3.55}$$

$$r^2_{\nu_3 \tilde{B}\,(\nu_3 \widetilde{W})} < \frac{2.8 \times 10^{-16}\ \text{TeV}}{M_{\mu 1\,(\mu 2)}}\,, \tag{3.56}$$

with

$$M_{\mu 1\,(\mu 2)} = \frac{(g_2^2 M_1 + g_1^2 M_2)\det \mathcal{M}_{\widetilde{\chi}_0}}{g^2_{1\,(2)} M^2_{2\,(1)} \mu^2}\,. \tag{3.57}$$

Given the null SUSY searches at the LHC so far, it is reasonable to expect the parameters M_1, M_2, μ to be of order TeV or larger, and $\det \mathcal{M}_{\widetilde{\chi}_0} \sim \text{TeV}^4$, in absence of cancellations. In this case the bounds simplify to

$$\begin{aligned} r^2_{\nu_1 \tilde{B}} &< 2.3 \times 10^{-15} \quad , \quad & r^2_{\nu_1 \widetilde{W}} &< 9.0 \times 10^{-15}\,, \\ r^2_{\nu_2 \tilde{B}} &< 9.2 \times 10^{-14} \quad , \quad & r^2_{\nu_2 \widetilde{W}} &< 3.7 \times 10^{-13}\,, \\ r^2_{\nu_3 \tilde{B}} &< 5.6 \times 10^{-17} \quad , \quad & r^2_{\nu_3 \widetilde{W}} &< 2.6 \times 10^{-16}\,. \end{aligned} \tag{3.58}$$

By looking at Eq. (3.32) one sees how these mixings are several orders of magnitude smaller than those required in order to explain the X-ray line via the decay of the axino into neutrino plus photon through the RpV interaction of Eq. (3.29). One caveat to this line of reasoning can be the assumption that all the SUSY parameters and masses are at the TeV scale, which is perhaps too strict. Nothing forbids us to take the lightest neutralino $\widetilde{\chi}_0$ to have a mass of order GeV, while the other neutralinos are at the TeV scale. In this case $\det \mathcal{M}_{\widetilde{\chi}_0} \sim 10^{-3}\ \text{TeV}^4$ and the bound on $r^2_{\nu_2 \tilde{B}}$ becomes of order 10^{-10}, which is enough to fit the line. However this scenario faces another problem. Since in RpV there is no such thing as the LSP, the GeV-neutralino will now have two decay channels. First, the partial width for the decay into an axino and a photon reads

$$\begin{aligned} \Gamma_{\tilde{\chi}_1^0 \to \tilde{a} + \gamma} &\simeq \frac{1}{128\pi^3} \frac{m^3_{\tilde{B}}}{f_a^2} C^2_{aBB} \left(\frac{g_1^2}{4\pi}\right)^2 \cos^2 \theta_W \\ &= 1.7 \cdot 10^{-2}\ \text{s}^{-1} \left(\frac{m_{\chi_1^0}}{\text{GeV}}\right)^3 \left(\frac{10^9\ \text{GeV}}{f_a}\right)^2\,. \end{aligned} \tag{3.59}$$

Second, $\widetilde{\chi}_0$ decays into a a lepton-antilepton pair plus neutrino via an off-shell Z boson with partial width [236]

$$\begin{aligned} \Gamma_{\tilde{\chi}_1^0 \to \nu l^+ l^-} &\simeq \frac{r^2_{\nu_i \tilde{B}}\, \alpha^2}{1024\pi^3} \frac{m^5_{\chi_1^0}}{M_Z^4}\,, \\ &\approx 1.7 \cdot 10^{-2}\ \text{s}^{-1} \left(\frac{r^2_{\nu_i \tilde{B}}}{10^{-10}}\right) \left(\frac{m_{\chi_1^0}}{\text{GeV}}\right)^5\,. \end{aligned} \tag{3.60}$$

The decay into an axino plus photon dominates for $m_{\chi_1^0} > 1\,GeV$, while the one into a neutrino plus leptons does for $m_{\chi_1^0} < 1\,GeV$. Regardless in which of the two ranges $m_{\chi_1^0}$ lies, the lifetime of the lightest neutralino will be way longer than the time of the freeze-out, $t_F \sim 10^{-6}s$, at a temperature $T_F \simeq m_{\chi_1^0}/20$, as common to all WIMP candidates. Additionally the interaction which kept them in equilibrium with the plasma until that point freezes out with a relic abundance that matches the measured value $\Omega_{\chi_1^0}h^2 \sim 0.1$. If the admixture of the gauge eigenstates which constitutes the neutralino is mostly bino (wino), than the relic abundance will be slightly overabundant (underabundant).

A large range of neutralino masses is subject to constraints from BBN and CMB, due to the fact that its decay produces energetic photon. In detail:

- $7\,keV < m_{\chi_1^0} < 300\,keV$: this window is excluded by CMB constraint on late decaying particles [57];
- $300\,keV < m_{\chi_1^0} < 10\,MeV$: CMB spectrum distortions [237, 238] rule out this region of the parameter space;
- $10\,MeV < m_{\chi_1^0} < 100\,MeV$: bounds from photodestruction of D and photoproduction of $D + {}^3He$ [238] exclude this window.

For $m_{\chi_1^0} < 7$ keV the neutralino is lighter than the axino and we are back to the situation of the R-parity conserving scenario, which is strongly disfavored as we discussed in the previous section. The only region which cannot be excluded within our discussion is $100\ MeV < m_{\chi_1^0} < 10\ GeV$. But despite being viable in principle, in this range the neutralinos decay during BBN time, $10^{-3}\ s < \tau_{\chi_1^0} < 3 \times 10^4\ s$, which could be in some tension with the success of BBN itself. For $m_{\chi_1^0} > 10$ GeV one quickly hits the bound from neutrino masses. We conclude that also the RpV scenario is strongly disfavoured.

3.7 SUMMARY AND RESULTS

In this chapter we have investigated whether a decaying axino with a 7 keV mass could explain the X-ray line signal which was claimed to be detected in early 2014. The presence of a light bino together with a gravitino strongly disfavours the RpC scenario, since both particles contribute to the relativistic degrees of freedom of the universe and thus yield $\Delta N_{eff} > 1$, against BBN and CMB bounds. In order to account for the line with the decay $\tilde{a} \to \nu + \gamma$, RpV models with all neutralino masses around TeV require mixings between the light neutrino and the bino or wino which are excluded by the cosmological bound on neutrino masses. Alternatively one can evade this bound by taking the lightest neutralino to have a mass around GeV or below. BBN and CMB bounds exclude such a long-lived neutralino below 100 MeV, due to its decay into energetic photons.

The RpV scenario is still viable if the lightest neutralino has a mass between 100 MeV and 10 GeV, with corresponding lifetimes ranging between $\mathcal{O}(10^{-3}s)$ and $\mathcal{O}(10^4 s)$, which is effectively stable for collider physics. Such a neutralino is very hard to observe in the laboratory, with no present bounds [231]. Supernova cooling excludes the low mass range if the selectron is lighter than about 500 GeV [230]. The proposed SHiP facility at CERN is most likely not sensitive to these lifetimes, due to the restricted geometry [239] and a direct measurement at an

e^+e^- linear collider is also unlikely [240]. This range of lifetimes is also too short for possible astrophysical signatures. Therefore it is hard to verify whether this particular scenario is realized or excluded.

4

THE RPV DFSZ SUSY AXION

In the previous chapter we studied the radiative decay of a keV axino in light of its possible phenomenological application to the detection of the 3.5 keV emission. We disfavoured the light axino explanation of the keV line by relying on an effective Lagrangian for the axino-neutrino-photon interaction, as given by Eq. (3.29). We now want to enlarge the scope of our analysis in a twofold way: on the one hand, we turn our attention to a range of axino masses which spans two orders of magnitude starting from $\mathcal{O}$(keV), where our parameter space can be constrained by X-ray and gamma-ray bounds; on the other hand, we make our approach more robust by consistently building a complete supersymmetric model with an axion sector. In Sec. 1.2.3 we discussed possible discrete symmetries as alternatives to R-parity in SUSY. In particular, models with baryon triality B_3 allow for lepton number violating operators in the superpotential thanks to which the neutrinos acquire Majorana masses, without introducing a new very large Majorana mass scale [130–132, 134–139]. Based on our work [241], in this chapter we present a B_3 model with the inclusion of an axion supermultiplet of the DFSZ type. The axion contributes to the DM energy density in the form of cold DM [242, 243]. Depending on the value of its decay constant, f_a, it constitutes all or a fraction of the DM. The gravitino is heavy [$\mathcal{O}$(TeV)], decays early in the history of the universe, and does not pose cosmological problems. The axino mass is proportional to $\lambda_\chi v_\chi$ [see Eq. (4.27)], where v_χ is the vacuum expectation value (VEV) of a scalar field of the order of the soft masses $\sim \mathcal{O}$(TeV), and λ_χ is a dimensionless Yukawa coupling in the superpotential. An axino of the order of $\sim$ keV requires $\lambda_\chi \ll 1$ and that is the LSP: its lifetime is longer than the age of the universe and it contributes as warm DM [194]. The radiative decay of the axino into a neutrino plus a photon is treated explicitly at one loop, which allows us to study the dependence of the decay width on the sfermion masses and the RpV superpotential couplings. This chapter is organised as follows: in Sec. 4.1 we include some general comments on the axino mass, we discuss its dependence on the SUSY breaking scale and point out that DFSZ models accommodate more easily a light axino, as opposed to KVSZ models. In Sec. 4.2 we introduce the model, describe its parameters and mass spectrum, discuss the mixing between the axino mass eigenstate and some neutralino gauge eigenstates. In Sec. 4.3 we consider cosmological and astrophysical constraints on the model, with a focus on the more interesting case of a light axino. In Sec. 4.4 we compute in detail the axino decay rates and branching fractions. In Sec. 4.5 we obtain bounds on the RpV couplings and comment on the 3.5 keV line, before concluding our discussion in Sec. 4.6.

4.1 THE UNBEARABLE LIGHTNESS OF THE AXINO

The mass of the axino is a strongly model-dependent quantity [222, 244], which has been given a lot of attention in the literature [194, 245–248]. In Sec. 4.1.1 we argue why a DFSZ model is more suited than a KVSZ one for accommodating a

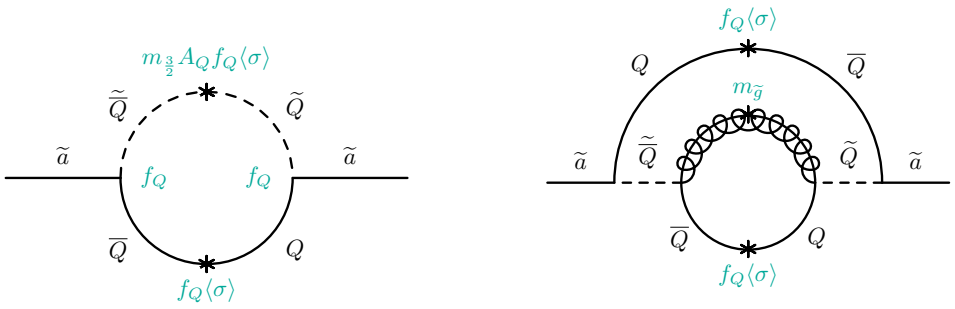

Figure 4.1: *Left:* One-loop contribution to the axino mass from soft supergravity breaking in supersymmetric KVSZ models. *Right*: Two-loop contribution to the axino mass from gluinos. The symbol "$*$" in the diagrams signifies the insertion of a VEV. Couplings and mass or VEV insertions are in green in the figure.

$\mathcal{O}(\text{keV})$ axino. In the following Sec. 4.1.2 we further argue that such a light axino can be more easily embedded in gravity-mediated SUSY models rather than in gauge mediation scenarios.

4.1.1 *DFSZ vs KVSZ*

As we mentioned in Sec. 2.2, axion models falls into two broad categories, DFSZ and KVSZ models. They both contain a scalar field σ, which is charged under PQ symmetry. In KVSZ models the phase of this field is exactly the axion a that removes the $\bar{\theta}$ term from the SM Lagrangian. σ couples to some new heavy fermions Q, also charged under PQ symmetry. This allows for the presence of an operator $f_Q \sigma Q \overline{Q}$ in the Lagrangian, which in turn generates the triangle loops that are responsible for the effective coupling $a G_{\mu\nu} \widetilde{G}^{\mu\nu}$, crucial in solving the strong CP problem. Here $G_{\mu\nu}(x)$ is the gluon field strength tensor and $\widetilde{G}^{\mu\nu}(x)$ its dual. The KSVZ model can be supersymmetrized and also embedded in supergravity. Supergravity breaking will induce a soft term $m_{3/2} A_Q f_Q \sigma \overline{Q} Q$ [194], where $A_Q \sim \mathcal{O}(1)$. This interaction allows us to write down the amplitude depicted in Fig. 4.1a, which results in a one–loop contribution to the axino mass of order [249]

$$m_{\tilde{a}} \sim 10\,\text{GeV} \left(\frac{m_{3/2} f_Q^2}{100\,\text{GeV}} \right) . \tag{4.1}$$

In Fig. 4.1b we show another contribution to $m_{\tilde{a}}$ which is independent from any high-scale condition and it is originated at two-loop level [250]:

$$m_{\tilde{a}} \sim 0.3\,\text{GeV} \left(\frac{m_{\tilde{g}} f_Q^2}{1\,\text{TeV}} \right) , \tag{4.2}$$

where $m_{\tilde{g}}$ is the gluino mass. Therefore even if we set the axino mass to keV at tree level, loop corrections will increase its value to around GeV. We can thus conclude that a KVSZ axino is naturally heavy.

In DFSZ models of axion the PQ-charged scalar σ is coupled to two Higgs doublets H_u and H_d, which are already required in order to form the Yukawa couplings in the MSSM superpotential when considering the supersymmetric version of the model. The choice of a SUSY DFSZ model is therefore more minimal than the KVSZ. In order to evade the astrophysical bound we mentioned in Sec. 2.2 one must have $f_a > 10^9$ GeV. This in turn sets the coupling c_1 of the superpotential operator $c_1 \hat{\sigma} \hat{H}_u \hat{H}_d$ to very small values. In the SUSY context it has been proposed that this operator could be replaced [192] by a non-renormalizable one $\frac{g}{M_{Pl}} \hat{\sigma}^2 \hat{H}_u \hat{H}_d$. With the latter operator one easily obtains a μ-term at the TeV scale, while with the former we are forced to take very small values the coupling c_1. We do not address the μ-problem, but we point out that Ref. [251] showed that the operator we consider can be derived consistently within a string theory framework. A small value of c_1 is essential to guarantee that the loop corrections to the mass of the axino, which are proportional to c_1, do not raise its mass beyond the value $m_{\tilde{a}}$ which was set to at tree level.

4.1.2 *Low-scale vs High-scale SUSY Breaking*

In Ref. [196] one finds a simple way to understand that in models where the SUSY breaking scale, M_{SB}, is lower than the PQ scale, f_a, the axino mass is of order $\mathcal{O}\left(M_{SUSY}^2/f_a\right)$, with M_{SUSY} the scale of the soft supersymmetry breaking terms. In models with $M_{SB} > f_a$ the axino mass is typically of order M_{SUSY}. The former models, with low M_{SB} are representative of global SUSY, for which the best known framework is gauge mediation of supersymmetry breaking [252]. The latter ones, with high M_{SB} usually fall in the scheme of gravity mediation of supersymmetry breaking, in local supersymmetry, and the scale of the soft terms is that of the gravitino mass, $M_{SUSY} \sim m_{3/2}$.

In light of these considerations one would think that a light axino is more natural in the context of gauge mediation. However it turns out that this is difficult to accommodate. The problem is with the saxion. Consider a model of minimal gauge mediation (see *e.g.* Ref. [252]), where the messengers do not carry any PQ charge and communicate with the visible sector only via gauge interactions. The leading contribution to the mass of the sfermions of the minimal supersymmetric Standard Model (MSSM) is generated at two loops. However the saxion is a gauge singlet and its mass can only be generated at three loops, as shown schematically in Fig. 4.2. The coupling c_1 that appears twice in the diagram is the one we discussed in the previous subsection. The saxion squared mass, m_s^2 is suppressed by a factor of $\sim c_1^2/16\pi^2$ compared to the squared masses of the MSSM sfermions, $m_{\tilde{f}}^2$, so we can estimate

$$m_s \sim 0.1 \text{ keV } \left(\frac{c_1}{10^{-9}}\right)\left(\frac{m_{\tilde{f}}}{1 \text{ TeV}}\right) . \tag{4.3}$$

This light saxion could pose serious cosmological problems [253] as it would come to dominate the energy density of the universe for a long time before it decays. We review some of the issues associated with saxion cosmology in Sec. 4.3. One way out of this problem would be to make the saxion heavier. This could be achieved by either coupling the axion superfield to the messengers or to fields in the hidden sector responsible for SUSY breaking. Apart from the extra field content that the procedure would bring into the model there is another issue that seems difficult to overcome: the same couplings needed to make the saxion heavier would very likely

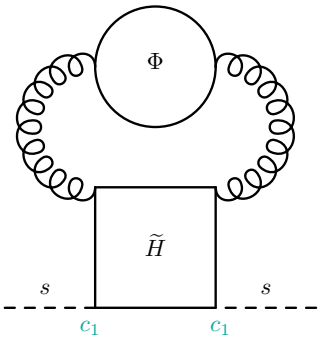

Figure 4.2: Three-loop contribution to the saxion mass in minimal gauge mediation. At the top we have a loop of messenger fields, Φ, drawn as a circle, at the bottom a loop of Higgsinos, drawn as a rectangle. The wiggly lines are gauge bosons. The coupling c_1 of the saxion to the Higgsinos is defined in Eq. (4.6).

produce a heavy axino [254]. There might be a clever way to arrange for a heavy saxion and a light axino in gauge mediation, but in light of our considerations it seems that such a model would have to be quite complicated. We do not investigate this aspect further in this work. Rather we choose a supergravity (SUGRA) model. We showed in Ref. [196] that in SUGRA the axino would typically have a mass comparable to the gravitino, thus in the TeV range. However, we can adjust a single parameter, λ_χ, to lower the axino mass down to the keV range. Doing so does not affect other masses, such as those of saxion and gravitino for instance. Also, as we argued above, since the axino we consider is of the DFSZ type, once we set its mass at tree level it will not be affected appreciably by loop corrections. Therefore the SUGRA model can be kept minimal, as opposed to a possible model with gauge mediation, at the expense of some tuning, needed to lower the mass of the axino. The model we present in the next section represents an exception to the generic argument according to which the axino is heavier than the gravitino, as discussed in Sec. 3.5.

4.2 THE RPV DFSZ SUPERSYMMETRIC AXION MODEL

4.2.1 *The Lagrangian*

The particle content of the supersymmetric DSFZ comprises of all the superfields of the MSSM (see Sec. 1.2.3) plus the three axion-like fields that we introduced in Sec. 2.4 and that are necessary to construct a self-consistent model [196]. The particle content, the quantum numbers with respect to the SM gauge sector $SU(3)_c \times SU(2)_L \times U(1)_Y$, and the charges under the global PQ symmetry, $U(1)_{PQ}$, are summarized in Table 4.1. We write the renormalizable superpotential as the sum of three terms,

$$W = W_{B_3} + W_I + W_{PQ} \,, \tag{4.4}$$

Superfield	$SU(3)_C$	$SU(2)_L$	$U(1)_Y$	$U(1)_{PQ}$
$\hat{Q}$	3	2	1/6	Q_Q
$\hat{U}$	$\bar{3}$	1	−2/3	Q_U
$\hat{D}$	$\bar{3}$	1	1/3	Q_D
$\hat{L}$	1	2	−1/2	Q_L
$\hat{E}$	1	1	1	Q_E
$\hat{H}_d$	1	2	−1/2	Q_{H_d}
$\hat{H}_u$	1	2	1/2	Q_{H_u}
$\hat{A}$	1	1	0	Q_A
$\hat{\bar{A}}$	1	1	0	$Q_{\bar{A}}$
$\hat{\chi}$	1	1	0	Q_χ

Table 4.1: Charge assignments for the chiral superfields.

with

$$W_{B_3} = Y_u \hat{Q} \cdot \hat{H}_u \hat{U} + Y_d \hat{Q} \cdot \hat{H}_d \hat{D} + Y_e \hat{L} \cdot \hat{H}_d \hat{E} + \frac{1}{2}\lambda \hat{L} \cdot \hat{L} \hat{E} + \lambda' \hat{L} \cdot \hat{Q} \hat{D} \,, \tag{4.5}$$

$$W_I = c_1 \hat{A} \hat{H}_u \cdot \hat{H}_d + c_2 \hat{A} \hat{L} \cdot \hat{H}_u \,, \tag{4.6}$$

$$W_{PQ} = \lambda_\chi \hat{\chi} \left(\hat{A}\hat{\bar{A}} - \frac{1}{4} f_a^2 \right) . \tag{4.7}$$

W_{B_3} contains only MSSM superfields, whereas W_{PQ} none. In W_I both kind of superfields are present. Same as in Sec. 2.4, quadratic and cubic terms in $\hat{\chi}$ are forbidden by an R-symmetry under which $\hat{\chi}$ has charge 2 and both A and $\hat{A}$ have zero charge. Here and in the following generation indices, as well as isospin and color ones, are suppressed for readability. Baryon triality enforces three RpV operators, with respective couplings λ, λ' and c_2. We have generalized the usual bilinear operators $\mu H_u H_d$ and $\kappa_i L_i H_u$ to obtain PQ invariance. Aside from the obvious PQ charges assignments resulting from W_{PQ}, the other ones needs to be determined from the equations

$$Q_{S_a} + Q_{S_b} + Q_{S_c} = 0 \,, \tag{4.8}$$

as resulting from each term in W_{B_3} and W_I, generally written as $\hat{S}_a \hat{S}_b \hat{S}_c$. The resulting homogeneous linear system of 9 equations has 10 unknowns and rank 7, therefore there are 3 unconstrained PQ charges. Let us take note here of one set of solutions which we will use later on in our discussion:

$$\begin{gathered} Q_U = Q_L - Q_Q + Q_A \quad , \quad Q_D = -Q_L - Q_Q \quad , \quad Q_E = -2Q_L \quad , \\ Q_{H_d} = Q_L \qquad , \quad Q_{H_u} = -Q_L - Q_A \quad , \quad Q_A = -Q_{\bar{A}} \quad , \quad Q_\chi = 0 \,. \end{gathered} \tag{4.9}$$

The PQ symmetry is spontaneously broken at the scale f_a, due to scalar potential resulting from W_{PQ}, and the scalar components of $\hat{A}$ and $\hat{\bar{A}}$ get VEVs v_A, $v_{\bar{A}}$, respectively,

$$A = \frac{1}{\sqrt{2}} (\phi_A + i\sigma_A + v_A) \,, \qquad \bar{A} = \frac{1}{\sqrt{2}} (\phi_{\bar{A}} + i\sigma_{\bar{A}} + v_{\bar{A}}) \,. \tag{4.10}$$

The VEVs must fulfil

$$v_A \cdot v_{\bar{A}} = \frac{1}{2} f_a^2 , \tag{4.11}$$

and we denote their ratio as

$$\tan^2 \beta' \equiv \frac{v_{\bar{A}}}{v_A} . \tag{4.12}$$

Below the breaking scale, we generate an effective μ-term, $\mu_{\text{eff}} \hat{H}_u \hat{H}_d$, and effective bilinear RpV κ-terms, $\kappa_{\text{eff},i} \hat{L}_i \hat{H}_u$, with

$$\mu_{\text{eff}} = \frac{c_1}{\sqrt{2}} v_A , \qquad \kappa_{\text{eff},i} = \frac{c_{2,i}}{\sqrt{2}} v_A . \tag{4.13}$$

The parameter μ_{eff} is required to be at the order of the EW scale in order for the theory to undergo electroweak symmetry breaking successfully. Neutrino physics constrains κ_{eff} to be $\leqslant$ O(MeV). As a consequence of the astrophysical bounds on axion discussed at the end of Sec. 2.2, both couplings in W_I (Eq. 4.6) are rather small, roughly $c_1 < 10^{-6}$ and $c_2 < 10^{-11}$[1]. We thus already expect the axion sector to interact very weakly with the other MSSM field content.

The soft-breaking terms of the scalar potential for this model consist of the scalar mass terms, gaugino masses, the bilinear and trilinear superpotential counterparts. Altogether the soft potential reads

$$\begin{aligned} -\mathcal{L}_{\text{soft}} =& (M_1 \widetilde{B}\widetilde{B} + M_2 \widetilde{W}\widetilde{W} + M_3 \widetilde{g}\widetilde{g} + \text{h.c.}) \\ &+ \widetilde{f}^\dagger m_{\widetilde{f}}^2 \widetilde{f} + m_\chi^2 |\chi|^2 + m_A^2 |A|^2 + m_{\bar{A}}^2 |\bar{A}|^2 + m_{H_u}^2 |H_u|^2 + m_{H_d}^2 |H_d|^2 \\ &+ m_{\ell H_u}^2 (\widetilde{\ell}^\dagger H_u + H_u^\dagger \widetilde{\ell}) + \left(m_{H_d H_u}^2 H_d \cdot H_u + \text{h.c.}\right) \\ &+ (T_u \widetilde{u} \widetilde{q} H_u + T_d \widetilde{d} \widetilde{q} H_d + T_e \widetilde{e} \widetilde{\ell} H_d + T_\lambda \widetilde{\ell}\widetilde{\ell}\widetilde{e} + T_{\lambda'} \widetilde{\ell}\widetilde{q}\widetilde{d} + T_{c1} A H_u H_d + T_{c2} A \, \widetilde{\ell} H_u \\ &+ T_{\lambda_\chi} \chi A \bar{A} + L_V \chi + \text{h.c.}) , \end{aligned} \tag{4.14}$$

with $\widetilde{f} \in \{\widetilde{e}, \widetilde{\ell}, \widetilde{d}, \widetilde{u}, \widetilde{q}\}$. Note that we include the terms in the last line of Eq. (4.14) because we assume that $\mathcal{L}_{\text{soft}}$ breaks the R-parity of W_{PQ}. Furthermore, even if we put them to zero at some scale, these terms would be generated at the two-loop level because of the small coupling to the MSSM sector, where no R-symmetry is present.

At scales below the one of PQ breaking, the axion interacts with the gauge fields according to $\mathcal{L}_{aVV}^{\text{eff}}$ in Eq. (2.81). We can now explicitly calculate the coefficients C_{aBB} and C_{aWW} making use of the prescription of Eq. 2.82, which tells us how

1 They are, nonetheless, radiatively stable.

the θ-terms for the various gauge groups transforms under a chiral transformation of the fermion fields $\psi \to e^{iQ_\psi \alpha}$. We obtain

$$\begin{aligned}\theta_1 &\to \theta_1 - 2\Bigg[N_g\left(6\left(\frac{1}{6}\right)^2 Q_Q + 3\left(\frac{2}{3}\right)^2 Q_U + 3\left(\frac{1}{3}\right)^2 Q_D + 2\left(\frac{1}{2}\right)^2 Q_L + Q_E\right) \\ &\quad + 2\left(2\left(\frac{1}{2}\right)^2 Q_{H_u} + 2\left(\frac{1}{2}\right)^2 Q_{H_d}\right)\Bigg]\alpha \\ &= \theta_1 - \left[\left(1 - \frac{8}{3}N_g\right)Q_A + N_g\left(Q_L + 3Q_Q\right)\right]\alpha\,, \end{aligned} \tag{4.15}$$

$$\begin{aligned}\theta_2 &\to \theta_2 - \left(N_g\left(3Q_Q + Q_L\right) + Q_{H_u} + Q_{H_d}\right)\alpha \\ &= \theta_2 - \left(Q_A - N_g\left(Q_L + 3Q_Q\right)\right)\alpha\,, \end{aligned} \tag{4.16}$$

where we simplified the starting expressions by means of the equalities in Eq. (4.9). The couplings between the axion field and the gauge field strength at low energy can be conveniently expressed in a basis where all the matter fields are invariant with respect to a PQ transformation. This is achieved with the axion-dependent transformation [255]:

$$\psi \to e^{iQ_\psi a/f_a}\psi \tag{4.17}$$

This rotation induces the anomalous axion couplings to gauge fields. Their coefficients are the opposite of the shifts in Eq. (4.15) and Eq. (4.16) , here with $N_g = 3$:

$$C_{aBB} = 3(3Q_Q + Q_L) - 7Q_A\,, \tag{4.18}$$

$$C_{aWW} = -3(3Q_Q + Q_L) + Q_A\,. \tag{4.19}$$

The effective coupling of the axino to to gauginos and gauge bosons are related to these by the supersymmetrisation procedure described in Eq. (2.83). In the case of broken SUSY we are interested in, it is more accurate to explicitly calculate the triangle loop diagrams from the full model, including tree-level couplings and soft masses. In Sec. 4.4.3 we therefore compute the one-loop decay of the axino into a photon and a neutrino using our full Lagrangian.

4.2.2 *The mass spectrum*

We implemented our model in `SARAH` [256–258], a `Mathematica` package for model building. It requires the user to define a particle physics model in terms of the following inputs: the superfield content and the superpotential; the symmetries of the model and the value of the BSM parameters introduced. `SARAH` checks the consistency of the model and calculates the full Lagrangian, including the soft-breaking terms. It then returns complete expressions for the mass matrices and the interaction vertices of the model below EWSB in the particle mass eigenstates, as well as tadpole equations for the stability of the scalar potential and the algebraic expressions for the RGEs.

We now turn our attention to the mass spectrum of the spin-1/2 neutral fermions of this model. In the gauge eigenstate basis for the neutralinos, there are terms entering their mass matrix which are proportional to the sneutrino VEVs:

$$\mathcal{L}_{\mathcal{M}_{\chi^0}} \supset v_{L,i}\left(-\frac{1}{2}g_1\bar{\lambda}_{\tilde{B}}\nu_{L,i}+\frac{1}{2}g_2\overline{\widetilde{W}}_0\nu_{L,i}+\frac{1}{\sqrt{2}}\sum_i c_{2,i}\overline{\widetilde{H}}_0\tilde{A}+\text{h.c.}\right), \tag{4.20}$$

where the repeated flavor indices are summed over. $\nu_{L,i}$ are the fermion components of the $SU(2)_L$ doublet superfields $\hat{L}_i$. While the presence of the last term in Eq. (4.20) can be easily traced back to the superpotential operator $c_2\hat{A}\hat{L}\hat{H}_u$, the ones including electroweakinos are originated by the gauge contributions to the matter kinetic terms. Here we show the case of the bino, dropping the lepton flavor index for readability:

$$\begin{aligned}
&\left[\hat{L}^\dagger e^{ig_1Q_Y V^Y}\hat{L}\right]_D = \Bigg[\left(\tilde{\nu}_L^* + i(\theta\sigma^\alpha\bar{\theta})^\dagger\partial_\alpha\tilde{\nu}_L^* + \sqrt{2}\bar{\theta}\nu_L^\dagger\right)\times \\
&\left(1+g_1Q_Y\left(\cdots+\theta\theta\bar{\theta}\bar{\lambda}_{\tilde{B}}+\bar{\theta}\bar{\theta}\theta\lambda_{\tilde{B}}\right)+\dots\right)\times\left(\tilde{\nu}_L - i(\theta\sigma^\beta\bar{\theta})\partial_\beta\tilde{\nu}_L+\sqrt{2}\theta\nu_L\right)\Bigg]_D \\
&\supset \sqrt{2}g_1Q_Y\left(\tilde{\nu}_L^*\bar{\lambda}_{\tilde{B}}\nu_L+\tilde{\nu}_L\bar{\nu}_L\lambda_{\tilde{B}}\right) \\
&= -\frac{g_1}{2}v_L\left(\bar{\lambda}_{\tilde{B}}\nu_L+\bar{\nu}_L\lambda_{\tilde{B}}\right),
\end{aligned}$$

where in the last step we have used that $\langle\nu_L\rangle = v_L/\sqrt{2}$. In RpV SUSY there is an ambiguity regarding the definition of lepton number, stemming from the fact that $\hat{L}_i$ and $\hat{H}_d$ superfields have the same quantum numbers. One can choose which linear combination of these fields to identify as the higgs doublet, so that the remnant orthogonal combinations will be the ones carrying lepton number. This clearly does not affect the definition of charged lepton mass eigenstates that we identify as e, μ and τ and define lepton number. It's rather an extra freedom in defining the interaction eigenstate basis [139], that allows us to choose to work in a convenient basis. To this purpose, we consider the matrix [135, 259]

$$R_{v,L} = \frac{|v_d|}{|\vec{w}|}\begin{bmatrix} 1 & \frac{v_{L,j}}{v_d} \\ -\frac{v_{L,i}}{v_d} & \frac{v_{L,i}v_{L,j}}{\vec{v}_L^2}\left(1-\frac{|\vec{w}|}{|v_d|}\right)+\delta_{ij}\frac{|\vec{w}|}{|v_d|}\end{bmatrix}, \tag{4.21}$$

with $|\vec{w}| \equiv \sqrt{\mu_{\text{eff}}^2+\vec{v}_L^2}$. It rotates away the sneutrino VEVs $v_{L,i}=0$:

$$R_{v,L}\begin{bmatrix} v_d \\ v_{L,i}\end{bmatrix} = \begin{bmatrix} \frac{v_d}{|v_d|}|\vec{w}| \\ 0\end{bmatrix} \equiv \begin{bmatrix} v'_d \\ v'_{L,i}\end{bmatrix} \tag{4.22}$$

Note that the condition $v_d \neq 0$, $v_{L,i}=0$, can alternatively be achieved by requiring *alignment* [234] between the four-dimensional vector μ_α which has the superpotential bilinear couplings as components, $\mu_\alpha = (\mu_{\text{eff}}, \kappa_{\text{eff},i})$ and the vector $v_\alpha = (v_d, v_{L,i})$ of the VEVs, *i.e.* $\mu_\alpha \propto v_L$. In the new basis what we call H_d is thus identified as the only scalar with hypercharge $Y=-1/2$ that receives a non-zero VEV and has zero lepton number. The scalars carrying lepton numbers coincides with the fields having zero VEV instead. In the following we drop the prime ($'$) for

the new basis. The choice of basis is scale dependent, in the sense that sneutrino VEVs are generated by RGEs running, even if set to zero at a given scale. Hence, one needs to specify at what scale the basis is chosen. For later convenience, when we compute the axino decays, we choose this scale to be the axino mass.

The tree-level 10×10 mass matrix in the basis $(\lambda_{\widetilde{B}}, \widetilde{W^0}, \widetilde{H}_u^0, \widetilde{H}_d^0, \nu_i, \widetilde{A}, \widetilde{\tilde{A}}, \widetilde{\chi})$, which is a generalization of the MSSM neutralino mass matrix, reads

$$\mathcal{M}_N = \begin{bmatrix}
M_1 & 0 & \frac{g_1 v_u}{2} & -\frac{g_1 v_d}{2} & 0 & 0 & 0 & 0 & 0 & 0 \\
0 & M_2 & -\frac{g_2 v_u}{2} & \frac{g_2 v_d}{2} & 0 & 0 & 0 & 0 & 0 & 0 \\
\frac{g_1 v_u}{2} & -\frac{g_2 v_u}{2} & 0 & -\frac{c_1 v_A}{\sqrt{2}} & \frac{c_{2,1} v_A}{\sqrt{2}} & \frac{c_{2,2} v_A}{\sqrt{2}} & \frac{c_{2,3} v_A}{\sqrt{2}} & -\frac{c_1 v_d}{\sqrt{2}} & 0 & 0 \\
-\frac{g_1 v_d}{2} & \frac{g_2 v_d}{2} & -\frac{c_1 v_A}{\sqrt{2}} & 0 & 0 & 0 & 0 & -\frac{c_1 v_u}{\sqrt{2}} & 0 & 0 \\
0 & 0 & \frac{c_{2,1} v_A}{\sqrt{2}} & 0 & 0 & 0 & 0 & \frac{c_{2,1} v_u}{\sqrt{2}} & 0 & 0 \\
0 & 0 & \frac{c_{2,2} v_A}{\sqrt{2}} & 0 & 0 & 0 & 0 & \frac{c_{2,2} v_u}{\sqrt{2}} & 0 & 0 \\
0 & 0 & \frac{c_{2,3} v_A}{\sqrt{2}} & 0 & 0 & 0 & 0 & \frac{c_{2,3} v_u}{\sqrt{2}} & 0 & 0 \\
0 & 0 & -\frac{c_1 v_d}{\sqrt{2}} & -\frac{c_1 v_u}{\sqrt{2}} & \frac{c_{2,1} v_u}{\sqrt{2}} & \frac{c_{2,2} v_u}{\sqrt{2}} & \frac{c_{2,3} v_u}{\sqrt{2}} & 0 & \frac{v_\chi \lambda_\chi}{\sqrt{2}} & \frac{v_{\tilde{A}} \lambda_\chi}{\sqrt{2}} \\
0 & 0 & 0 & 0 & 0 & 0 & 0 & \frac{v_\chi \lambda_\chi}{\sqrt{2}} & 0 & \frac{v_A \lambda_\chi}{\sqrt{2}} \\
0 & 0 & 0 & 0 & 0 & 0 & 0 & \frac{v_{\tilde{A}} \lambda_\chi}{\sqrt{2}} & \frac{v_A \lambda_\chi}{\sqrt{2}} & 0
\end{bmatrix} . \tag{4.23}$$

Since the axion sector is very weakly coupled to the rest, in order to obtain the light neutrino mass eigenstates we can apply the Takagi diagonalization procedure explained in Sec. 3.6.2 to $\mathcal{M}_7$, the upper-left 7x7 upper-block of $\mathcal{M}_N$. The single massive neutrino state obtained this way is the one of Eq. (3.43). While this procedure is essential for obtaining the mixings among the MSSM gaugino and the physical neutrinos, for the sake of an estimate of the neutrino mass, one can simply consider the ratio of the product of the five non-zero eigenvalues of $\mathcal{M}_7$ [234, 260],

$$\det{}' \mathcal{M}_7 \equiv m_Z^2 \mu^2 \left(\cos^2\theta_W M_1 + \sin^2\theta_W M_2\right) \cos^2\beta \sin^2\xi \,, \tag{4.24}$$

to the product of the eigenvalues of the 4x4 MSSM matrix of Eq. (3.40), here written in a slightly different fashion using the relations among SM parameters $m_Z = \frac{v}{2}\sqrt{g_1^2 + g_2^2}$ and $\sin\theta_W$:

$$\begin{aligned}
m_\nu \simeq \left|\frac{\det' \mathcal{M}_7}{\det \mathcal{M}_{\widetilde{\chi}^0}}\right| &= \frac{m_Z^2 \mu \left(\cos^2\theta_W M_1 + \sin^2\theta_W M_2\right) \cos^2\beta \sin^2\xi}{m_Z^2 \sin 2\beta \left(\cos^2\theta_W M_1 + \sin^2\theta_W M_2\right) - M_1 M_2 \mu} \\
&\approx m_Z \cos^2\beta \sin^2\xi \approx m_Z \cos^2\beta \frac{\kappa_{\text{eff}}^2}{\mu_{\text{eff}}^2} \,,
\end{aligned}$$

where

$$\tan\beta = \frac{v_u}{v_d} \,, \quad \text{and} \quad \cos\xi = \frac{\mu_{\text{eff}}}{\sqrt{\mu_{\text{eff}}^2 + \kappa_{\text{eff},1}^2 + \kappa_{\text{eff},2}^2 + \kappa_{\text{eff},3}^2}} \,, \tag{4.25}$$

and we have assumed that all masses are around the electroweak scale. Requiring $m_\nu \approx 0.1$ eV, with $\tan\beta \approx 1$ and $\mu_{\text{eff}} \approx 1$ TeV, one finds that $\kappa_{\text{eff},i}$ is of order MeV, and correspondingly smaller for larger $\tan\beta$. The two neutrinos which are

massless at tree level acquire a small mass at one loop [134, 138, 139], which are thus not included in $\mathcal{M}_N$.

The four eigenstates of $\mathcal{M}_N$ mainly built from the MSSM gauge eigenstates $(\lambda_{\widetilde{B}}, \widetilde{W}^0, \widetilde{H}_u^0, \widetilde{H}_d^0)$ typically have masses between 100 and 1000 GeV. The three mostly axino mass eigenstates can be determined analytically in the limit $\tan\beta' \to 1$ and $c_{1,2} \to 0$ by diagonalizing $\mathcal{M}_a$, the 3x3 lower-right sub-block of $\mathcal{M}_N$ with entries only from the axion sector fields. In this case the mass matrix is in the same form as the one in Eq. (2.80), once we read the latter in the basis $(A, \bar{A}, \chi)$. The smallest among the three eigenvalues [196]

$$-\frac{1}{\sqrt{2}}\lambda_\chi v_\chi\,, \quad \frac{1}{2\sqrt{2}}\left(\lambda_\chi v_\chi \pm \lambda_\chi\sqrt{v_\chi^2 + 4f_a^2}\right)\,, \tag{4.26}$$

corresponds to the fermionic component of the linear combination of superfields $\frac{1}{\sqrt{2}}(\bar{A} - A)$[2]. It is interpreted as the axino with a mass [196]

$$m_{\tilde{a}} \simeq -\frac{1}{\sqrt{2}}\lambda_\chi v_\chi\,. \tag{4.27}$$

For the general case of $\tan\beta \neq 1$ we find the leading order corrections in v_χ/f_a to be

$$m_{\tilde{a}} \simeq -\frac{\sqrt{2}\tan^2\beta'}{1+\tan^4\beta'}\lambda_\chi v_\chi + \mathcal{O}\left(\lambda_\chi v_\chi \frac{v_\chi^2}{f_a^2}\right)\,. \tag{4.28}$$

The parameter v_χ is expected to be $\mathcal{O}$ (TeV). Thus the mass of the axino is controlled by the parameter λ_χ, which is radiatively stable. The phenomenologically interesting case of the light axino that we consider in this chapter will then require a very small λ_χ, typically $\lambda_\chi < 10^{-6}$. We neglect other contributions to the axino mass coming from the superpotential couplings $c_{1,2}$, as they are suppressed as $c_{1,2}/f_a$.

We now move on to estimate some mixings between the neutralino mass and gauge eigenstates which are relevant for the computation of the decay width of the axino into a photon plus neutrino presented in Sec. 4.4.3. For the purpose of our estimates, we take $v \equiv \sqrt{v_u^2 + v_d^2} \sim v_u \sim v_d$ to be the weak scale.

The axino-higgsino mixing can be estimated by observing that the higgsino mass is of order μ_{eff}, and the off-diagonal element between axino and higgsino is of order $c_1 v = \frac{\mu_{\text{eff}}}{f_a} v$. Then we use a simple property for a symmetric real 2x2 matrix[3]

$$\mathcal{M}_2 = \begin{bmatrix} a & \varepsilon \\ \varepsilon & b \end{bmatrix}\,, \tag{4.29}$$

with $\varepsilon \ll a, b$. $\mathcal{M}_2$ can be rotated into

$$\mathcal{D}_2 = \mathcal{U}^T \mathcal{M}\, \mathcal{U} \approx \text{diag}(a, b)\,, \tag{4.30}$$

2 Negative fermionic masses can be eliminated by a chiral rotation.

3 This is the same procedure we applied for the sterile neutrinos in Sec. 3.1 for the n=2 case.

plus terms $\mathcal{O}(\varepsilon^2)$. To the same order of approximation, the mixing matrix is simply

$$\mathcal{U} \approx \begin{bmatrix} -1 & \frac{\varepsilon}{b-a} \\ \frac{\varepsilon}{b-a} & 1 \end{bmatrix} . \tag{4.31}$$

Thus the axino-higgsino mixing is

$$x_{\tilde{a},\tilde{H}} \approx \frac{c_1 v}{\mu_{\text{eff}}} = \frac{v}{f_a} . \tag{4.32}$$

Considering $M_1 \sim \mu_{\text{eff}} \sim M_{\text{SUSY}} = \mathcal{O}(\text{TeV})$, we can estimate the bino-higgsino mixing as $g_1 \frac{v}{M_{\text{SUSY}}}$. Multiplying this with $x_{\tilde{a},\tilde{H}}$ we obtain the axino-bino mixing

$$x_{\tilde{a},\tilde{B}} \approx g_1 \frac{v^2}{M_{\text{SUSY}} f_a} . \tag{4.33}$$

Estimating the axino-neutrino mixing is slightly more involved, due to some specific features of $\mathcal{M}_N$. First, the central 3x3 $\nu_{L,i}$ sub-block is simply 0_{3x3}. Second, the fermionic component of the superfield $\hat{A}$ is the only one in the axion sector that interacts directly with the neutral fermions from the doublet $\hat{L}$ through the superpotential term c_2, yielding the corresponding off-diagonal terms $c_{2,i} v_u/\sqrt{2}$ in $\mathcal{M}_N$. But here the diagonal entry for the field $\hat{A}$ is also zero, thus making it impossible for us to apply the procedure used for $x_{\tilde{a},\tilde{H}}$. We therefore adopt the following approach. We first perform the aforementioned Takagi-diagonalization of $\mathcal{M}_7$. The massive neutrino eigenstate will be mostly a combination of the gauge eigenstates $\nu_{L,i}$, with small components of bino, wino and higgsinos. We then rotate $\mathcal{M}_a$ into the basis of its mass eigenstates, using a rotation matrix which has entries of order one. In the off-diagonal block, the entries will thus stay of order $\kappa_{\text{eff}} v/f_a$. We can then estimate the axino-neutrino mixing by an approximate diagonalization of the matrix

$$\mathcal{M}_{\tilde{a}-\nu} = \begin{bmatrix} m_\nu & \mathcal{O}\left(\frac{\kappa_{\text{eff}} v}{f_a}\right) \\ \mathcal{O}\left(\frac{\kappa_{\text{eff}} v}{f_a}\right) & m_{\tilde{a}} \end{bmatrix} . \tag{4.34}$$

From the analogy with Eq. (4.31) and since $m_\nu \ll m_{\tilde{a}}$, we conclude that the axino-neutrino mixing reads

$$x_{\tilde{a},\nu} \approx \frac{\kappa_{\text{eff}} v}{m_{\tilde{a}} f_a} . \tag{4.35}$$

In App. A.1 we discuss a procedure for obtaining axino-gaugino mixings which is exact to $\mathcal{O}(\mu_{\text{eff}}/f_a)$ and does not require any assumption on the scale of the MSSM parameters.

4.3 COSMOLOGICAL AND ASTROPHYSICAL CONSTRAINTS

4.3.1 *The gravitino*

We embed our model in SUGRA with SUSY broken at a high scale $\sqrt{F} > f_a$. Planck-suppressed operators mediates the breaking and set the soft scale at $M_{\text{soft}} \sim F/M_{\text{Pl}} = \mathcal{O}(\text{TeV})$. Recalling Eq. (3.20), the gravitino acquires a mass $m_{3/2} \sim M_{\text{soft}}$. In models with high-scale SUSY breaking, the goldstino modes

of the field are not relevant to the gravitino interaction, see Eq. (3.22). A gravitino heavier than a few TeV has a lifetime [261]

$$\Gamma_{3/2}^{-1} \simeq \frac{M_{Pl}^2}{m_{3/2}^2} \simeq 10^{-1}\,s\left(\frac{m_{3/2}}{10\,TeV}\right)^3 , \tag{4.36}$$

and therefore does not does not pose any cosmological issues, since it decays before BBN starts at $t_{BBN} \sim 1s$.

4.3.2 *Axion dark matter*

In this model the axion is a dark matter candidate. Its cosmological history is best described in terms of the $U(1)_{PQ}$-invariant Lagrangian for the PQ-scalar ϕ [221]

$$-\mathcal{L} = \frac{1}{2}\partial_\mu\phi\partial^\mu\phi - \underbrace{\left[\frac{\lambda}{4}\left(|\phi|^2 + v_a^2\right)^2 + \frac{\lambda}{6}T^2|\phi|^2\right]}_{V_{eff}} , \tag{4.37}$$

which has a temperature-dependent term in the effective potential V_{eff}. At temperatures higher than v_a the minimisation condition

$$V'_{eff} = \frac{\lambda\phi}{2}\left(|\phi|^2 - v_a^2 + \frac{T^2}{3}\right) \stackrel{!}{=} 0 \tag{4.38}$$

can be only satisfied at $\phi = 0$. Below $T_c = \sqrt{3}v_a$ however this vacuum becomes unstable and the $U(1)_{PQ}$ is spontaneously broken, with the scalar developing a VEV $\langle\phi\rangle = v_a$. The axion a is as usual the corresponding massless NG boson, $\bar{\theta} = a/f_a = \arg\langle\phi\rangle$, where the axion decay constant is $f_a = v_a/N_{DW}$. For temperature $T \gg \Lambda_{QCD}$ the instantons effects are negligible and the axion is effectively massless. Approaching $T \sim \Lambda_{QCD}$, the axion develops an effective potential

$$V(\bar{\theta}) = m_a^2(T) f_a^2\left[1 - \cos\bar{\theta}\right] , \tag{4.39}$$

where the mass parameter m_a is a function of the temperature. A precise estimate of the axion mass was obtained in [262]

$$m_a(T) \simeq \begin{cases} 4.05\cdot 10^{-4}\,\frac{\Lambda_{QCD}^2}{f_a}\left(\frac{T}{\Lambda_{QCD}}\right)^{-3.34} & , \quad T > 0.26\,\Lambda_{QCD} \\ 3.82\cdot 10^{-2}\,\frac{\Lambda_{QCD}^2}{f_a} & , \quad T < 0.26\,\Lambda_{QCD} \end{cases} \tag{4.40}$$

In the following two sections we discuss two mechanisms to produce axion cold DM non-thermally. The resulting constraints are later shown in Figs. 4.11 and 4.12, where the the red area of the plane f_a vs $m_{\tilde{a}}$ is excluded by the requirement $\Omega_a h^2 \leqslant \Omega_{DM} h^2$.

4.3.2.1 *Misalignment mechanism*

We anticipated that the effective potential for the axion vanishes identically and therefore the dynamics does not specify any value for the angle $\bar{\theta}$ in Eq. (2.36), which can then take any value in the interval $[0, 2\pi)$. When the temperature approaches Λ_{QCD}, $\bar{\theta} \neq 0$ will roll down to its CP-conserving value $\bar{\theta} = 0$, but it will

overshoot it and start to oscillate around $m_a(T) \gtrsim 3H$. Assuming $T_{osc} > 0.26\Lambda_{QCD}$ and radiation domination, we can use Eq. (4.40) to estimate

$$T_{osc} \simeq 0.98\,\text{GeV}\left(\frac{f_a}{10^{12}\,\text{GeV}}\right)^{-0.19}\left(\frac{\Lambda_{QCD}}{400\,\text{MeV}}\right), \tag{4.41}$$

Using the Lagrangian obtained expanding the potential in Eq. (4.39) around its minimum,

$$\mathcal{L}_{osc} \simeq f_a^2\left[\frac{1}{2}\left|\partial_\mu\bar{\theta}\right|^2 - \frac{m_a^2(T)}{2}\bar{\theta}^2\right], \tag{4.42}$$

one can describe the axion dynamics below T_{osc} with the action [186]

$$S_a = \int d^4x\, R^3\mathcal{L}_{osc}\,, \tag{4.43}$$

which includes the comoving volume R^3. Treating this field as homogeneous, the resulting equations of motion can be expressed as

$$\begin{aligned}
&\partial_\mu\frac{\partial\left(R^3\mathcal{L}_{osc}\right)}{\partial\left(\partial_\mu\bar{\theta}\right)} - \frac{\partial R^3\mathcal{L}_{osc}}{\partial\bar{\theta}} = 0\,,\\
\mu = 0: \quad &-3R^2\dot{R}\dot{\bar{\theta}} - R^3\ddot{\bar{\theta}} - R^3 m_a^2 = 0\,,\\
\Rightarrow \quad &\ddot{\bar{\theta}} + 3H\dot{\bar{\theta}} + m_a^2\bar{\theta} = 0\,.
\end{aligned} \tag{4.44}$$

The energy density ρ_φ of a field φ is in the form $\mathcal{L}_{kin,\varphi} + V(\varphi)$. For the axion we can thus calculate

$$\rho_\theta = \frac{1}{2}\dot{\bar{\theta}}^2 + \frac{m_a^2}{2}\bar{\theta}^2 \quad \Rightarrow \quad \dot{\rho}_\theta = \left(\ddot{\bar{\theta}} + m_a^2\bar{\theta}\right)\dot{\bar{\theta}} + m_a\dot{m}_a\bar{\theta}^2\,, \tag{4.45}$$

such that multiplying Eq. (4.44) with $\dot{\bar{\theta}}$ yields

$$\dot{\rho}_\theta + 3H\dot{\bar{\theta}}^2 = \bar{\theta}^2 m_a\dot{m}_a\,. \tag{4.46}$$

Averaging over an oscillation sets $\left\langle\,\dot{\bar{\theta}}^2\,\right\rangle = \left\langle m_a^2\bar{\theta}^2\right\rangle = \rho_\theta$ and it follows that

$$\frac{\dot{\rho}_\theta}{\rho_\theta} = \frac{\dot{m}_a}{m_a} - 3\frac{\dot{R}}{R}\,. \tag{4.47}$$

Integrating this equation leaves us with the result that the the axion number density is conserved within a comoving volume

$$n_\theta = \frac{\rho_\theta}{m_a} \sim R^{-3} \times \left(\begin{smallmatrix}\text{some}\\ \text{integration}\\ \text{constant}\end{smallmatrix}\right)\,. \tag{4.48}$$

Since the number density scales with R the same way that the entropy density $s = \frac{2\pi}{45} g_\star T^3$ does [38][4], the present axion energy density

$$\begin{aligned}
\rho_{\theta,0} &= \rho_{\theta,osc} \frac{s_0}{s_{osc}} \\
&= \frac{m_a^2(T_{osc}) a^2}{2} \frac{T_0^3}{T_{osc}^3} \\
&\simeq m_a(T_{osc}) H_{osc} \frac{T_0^3}{T_{osc}^3} f_a^2 \bar{\theta}_{osc}^2 \\
&\simeq \sqrt{g_\star} \frac{T_0^3}{M_{Pl}} \bar{\theta}_{osc}^2 \frac{m_a(T_{osc}) f_a^2}{T_{osc}} \\
&\simeq \sqrt{g_\star} \frac{T_0^3}{M_{Pl}} \bar{\theta}_{osc}^2 \left(10^{-2} \frac{\Lambda_{QCD}^2}{f_a}\right) f_a^2 \left(\frac{f_a}{10^{12}\,\text{GeV}}\right)^{0.19} \left(\frac{\Lambda_{QCD}}{400\,\text{MeV}}\right)^{-1} \text{GeV}^{-1} \\
&\simeq 10^{-48}\, \bar{\theta}_{osc}^2 \left(\frac{f_a}{10^{12}\,\text{GeV}}\right)^{1.19} \left(\frac{\Lambda_{QCD}}{400\,\text{MeV}}\right) \text{GeV}^4
\end{aligned} \tag{4.49}$$

where we have used, in order: $\langle m_a^2 \bar{\theta}^2 \rangle = \rho_\theta$, $m_a(T_{osc}) \simeq 3H_{osc}$, $H_{osc} = 1.66\sqrt{g_\star}\frac{T_{osc}^2}{M_{Pl}}$, Eq. (4.40) for the temperature of the universe today, Eq. (4.41). As the critical density of the universe today can be written as

$$\rho_c = \frac{3}{8\pi} \frac{H_0^2}{G_N} \approx 10^{-47} \text{GeV}^4 \,, \tag{4.50}$$

the order of magnitude axion relic density can be estimated as

$$\Omega_{a,mis} h^2 = \frac{\rho_{\theta,0}}{\rho_c} \simeq 10^{-1}\, \bar{\theta}_{osc}^2 \left(\frac{f_a}{10^{12}\,\text{GeV}}\right)^{1.19} \left(\frac{\Lambda_{QCD}}{400\,\text{MeV}}\right) \text{GeV}^4 \tag{4.51}$$

To be more precise, one has to take into account that when the oscillation begins the adiabatic condition $m_a \gg T$ is not satisfied. In the following we will thus rely on the the result [263, 264]

$$\Omega_{a,mis} h^2 = 0.18\, \bar{\theta}_{osc}^2 \left(\frac{f_a}{10^{12}\,\text{GeV}}\right)^{1.19} \left(\frac{\Lambda_{QCD}}{400\,\text{MeV}}\right) \,, \tag{4.52}$$

where such effects are considered.

4.3.2.2 *String decay*

In Sec. 2.3 we briefly referred to the domain walls resulting from the breaking of a $U(1)_{PQ}$. But they are only one type of the possible topological defects which originate at cosmological scales from a phase transition. Together with the 2+1 space-time extended domain walls, we also find 1+1 cosmic string and 0+1 monopoles. These are relevant for our discussion since their most efficient decay mechanism is

4 In the following we simplify our calculation by treating the total number of effective degrees of freedom $g_\star$ as a constant, which is good enough for an order-of-magnitude estimate in the temperature range considered.

axion radiation. After PQ-symmetry breaking the universe is filled with a network of axionic strings, each with an energy per unit length [265]

$$\mu = \pi f_a^2 \ln(f_a d) \,, \tag{4.53}$$

where d is the distance between nearest neighbour strings. From numerical simulation we know that the energy density associated with the string network follows the exponential behaviour $\rho_{str} \simeq \xi\mu/t^2$ [266, 267], where ξ is the length parameter which represents the average number of strings in a horizon volume. This behaviour is maintained as long as for each Hubble time all the available energy density is dissipated via decay into axions [186]. Thus the variation of the number density of axions per entropy density is

$$dY_a \simeq d\left(\frac{n_a}{s}\right) = \frac{\rho_{str}}{\omega(t)}\frac{1}{T^3} H\, dt \,, \tag{4.54}$$

with $\omega(t)$ the average string energy radiated with axions. The energy spectrum of the radiated axion follows $dE/dk \sim 1/k$, in which case [265]

$$\frac{1}{\omega} = \frac{r}{\ln(f_a t) k_{min}} \,, \tag{4.55}$$

where r is the ratio of the rate of axion emission between the initial and final temperature and $k_{min} \simeq 2\pi/t$ on average. We integrate Eq. (4.54) between the time of the phase transition t_{PQ} and the time t_{osc} where the axion mass becomes comparable to the expansion rate, whereas later the string network decays. Plugging in Eq. (4.55) and using again the relation for radiation-dominated universe $t \sim H^{-1} \sim \left(T^2/M_{Pl}\right)^{-1}$,

$$\begin{aligned} Y_a &\simeq \int_{t_{PQ}}^{t_{osc}} \frac{\mu}{t^2}\left(\frac{t}{M_{Pl}}\right)^{3/2} \frac{r}{\ln(f_a t) k_{min}} \frac{dt}{t} \\ &\simeq \int_{t_{PQ}}^{t_{osc}} \frac{\xi\,\pi f_a^2 \ln\left(f_a^2 t\right)}{t^2}\left(\frac{t}{M_{Pl}}\right)^{3/2} \frac{r\,t}{2\pi \log(f_a t)} \frac{dt}{t} \\ &\simeq \int_{t_{PQ}}^{t_{osc}} \frac{\xi\, r\, f_a^2}{2M_{Pl}^{3/2}} \frac{dt}{\sqrt{t}} \\ &\simeq \xi\, \bar{r} \frac{f_a^2}{M_{Pl} T_{osc}} \end{aligned} \tag{4.56}$$

we find that the energy density of the axion produced from a string has the same dependence of the f_a, M_{Pl}, T_{osc} parameters as for the misalignment mechanism of Eq. (4.49). Adding an overall factor from Ref. [221], the relic density for axion produced by the decay of strings is therefore

$$\Omega_{a,str} h^2 \approx 0.2\, \xi\, \bar{r} \left(\frac{f_a}{10^{12}\text{GeV}}\right)^{1.19} \left(\frac{\Lambda_{QCD}}{400\text{MeV}}\right) . \tag{4.57}$$

The average value $\bar{r}$ has been the subject of a long debate. Two scenarios have been put forth, one predicts $\bar{r} \approx 1$, the other $\bar{r} \approx 70$. See Ref. [268] and references therein for details. While the misalignment mechanism produces axions when the temperature is $T \sim \Lambda_{QCD}$, the strings form at a much higher temperature $T \sim f_a$. If the PQ phase transition happened before the end of inflation, $T_{RH} < f_a$, then the strings would be inflated away and we would no longer have a contribution corresponding to Eq. (4.57). In this scenario the axion abundance is from Eq. (4.52), and $\bar{\theta}$ can take any value within the interval $[0, 2\pi)$. In a scenario where the PQ phase transition happens after inflation, $T_{RH} > f_a$, one has to average θ_{osc}^2 over many QCD horizons,

$$\left\langle \bar{\theta}_{osc}^2 \right\rangle = \frac{1}{2\pi} \int_{-\pi}^{+\pi} d\bar{\theta}_{osc}\, \bar{\theta}_{osc}^2 = \frac{\pi^2}{3} \,, \tag{4.58}$$

and the contribution from string decays can be comparable to that from misalignment or larger, depending on the value of $\bar{r}$.

4.3.3 *The saxion*

A light saxion may pose serious cosmological issues, due to its coherent oscillation. This is due to the fact that it is a pseudo-modulus, meaning it has a rather flat potential. After inflation, it will thus start to oscillate around its minimum. As for the misalignment mechanism in the previous section, the oscillations start when the the Hubble parameter is of the order of the saxion mass m_S, $H(T) \simeq m_S$. This tells us $T_s^{osc} \simeq \sqrt{m_S M_{Pl}}$. Taking the field to be at rest and averaging over an oscillation yields again $\rho_S \sim m_S^2 f_a^2$. Thus when the oscillations start the ratio of its energy density over the radiation density $\rho_r \sim T^4$ reads

$$\left.\frac{\rho_s}{\rho_r}\right|_{osc} \sim \frac{f_a^2}{M_{Pl}^2} \,. \tag{4.59}$$

From our result in Eq. (4.48) we know that the energy density of a field oscillating coherently around its minimum scales as $\rho_S \sim T^3$, assuming the saxion mass is constant. We can estimate the temperature at which it would come to dominate the energy density of the universe in absence of decays from the relation

$$\frac{(\rho_s/\rho_r)_{osc}}{(\rho_s/\rho_r)_{dom}} \sim \left(\frac{T_s^{osc}}{T_s^{dom}}\right)^{-1} \,, \tag{4.60}$$

together with the fact that by definition $(\rho_s/\rho_r)_{dom} \sim 1$. It follows that

$$T_s^{dom} \sim \frac{f_a^2}{M_{Pl}^2} T_s^{osc} \sim f_a^2 \frac{m_S^{1/2}}{M_{Pl}^{3/2}} \,. \tag{4.61}$$

The standard cosmological evolution in the ΛCDM model predicts the transition from matter domination to radiation domination to happen at a temperature $T_{eq} \simeq 1\,\text{eV}$. In order to make sure the saxion does not interfere with this, we

need to ensure that the saxion decays before it ever comes to dominate the energy of the universe. For the decay width of the saxion we rely on the simple estimate

$$\Gamma_s = \frac{1}{16\pi}\frac{m_s^3}{f_a^2}\,, \tag{4.62}$$

where we assume the saxion mass of the decay products can be neglected. The factor of f_a^2 in the denominator is due to the fact that the saxion couplings to matter are suppressed by f_a. The decay temperature can be obtained from $H(T_s^{dec}) \sim \Gamma_s$:

$$T_s^{dec} \sim \frac{m_s^{3/2} M_{Pl}^{1/2}}{10\, f_a} \approx \left(\frac{m_S}{\text{TeV}}\right)^{3/2}\left(\frac{10^{12}}{\text{GeV}}\right)\text{GeV}. \tag{4.63}$$

Since in our model the saxion mass is of order TeV , it decays at a temperature safely above BBN, $T_{BBN} \sim$ MeV. Putting Eq. (4.61) and Eq. (4.63) together shows that the saxion decays before it can dominate the energy density of the universe:

$$\frac{T_s^{dec}}{T_s^{dom}} \sim 10^4 \left(\frac{m_s}{1\,\text{TeV}}\right)\left(\frac{10^{12}\,\text{GeV}}{f_a}\right)^3\,. \tag{4.64}$$

4.3.4 *A heavy axino*

For $\lambda_\chi \sim 1$, we have $m_{\tilde{a}} \sim v_\chi \sim M_{SUSY}$, an axino mass of order TeV. Such an axino has many open decay channels into MSSM particles, with a total width that can be estimated as $\Gamma_{\tilde{a}} \sim \frac{1}{8\pi}\frac{m_{\tilde{a}}^3}{f_a^2}$. It decays safely before BBN, and does not pose cosmological issues.

4.3.5 *A light axino*

A keV axino can be a good DM candidate. In Sec. 3.4 we discussed how in DFSZ models the extra suppression $\sim M_\Phi^2/p^2$ in axino-gaugino-gauge boson loops relaxes the original 2 keV upper bound on the axino mass. In our model the axino is not stable. However, if its mass is below the electron mass the only three decay modes are

1. into a neutrino and an axion (tree-level, with dimension 5 operator), $\tilde{a} \to \nu_i + a$;
2. into three neutrinos (tree-level), $\tilde{a} \to \nu_i + \nu_j + \nu_k$;
3. into a neutrino and a photon (one-loop), $\tilde{a} \to \nu_i + \gamma$.

The resulting lifetime, as we show in the following section, is longer than the age of the universe, thus making the axino a dark matter candidate, with relic abundance

$$\Omega_{\tilde{a}} h^2 \simeq 2.1 \times 10^{-5}\left(\frac{m_{\tilde{a}}}{1\,keV}\right)\left(\frac{10^{12}\,GeV}{f_a}\right)^2\,. \tag{4.65}$$

This does not depend on T_{RH}, as long as $T_{RH} > 10^4$ GeV [198, 223]. An intuitive way to understand the f_a^{-2} dependence in Eq. (4.65) is to look at the processes that produce the axino in the early universe. These are listed *e.g.* in Table 1 of

(a) (b)

Figure 4.3: *Left*: Feynman diagram describing the process $\tilde{a} \to \nu + a$, with partial width given by Eq. (4.67). *Right*: One of the Feynman diagrams describing the decay of the axino into three neutrinos. In our convention a dot on a fermion line stands for a mixing between fermionic mass eigenstates.

Ref. [198]. Their cross section scales as f_a^{-2}, which makes them not efficient enough to ever reach thermal equilibrium. The larger the cross section the more the axino is produced, hence the $1/f_a^2$ dependence in Eq. (4.65). We show the constraint coming from overabundant axino production in Figs. 4.11 and 4.12, where the blue area is excluded by the condition $\Omega_{\tilde{a}} h^2 \leqslant \Omega_{\rm DM} h^2$.

4.4 LIGHT AXINO DECAY MODES

4.4.1 *Decay into neutrino and axion*

A dimension 5 operator is responsible for this decay:

$$\frac{1}{f_a} (\partial^\mu a)\, \bar{\psi}_{\tilde{a}} \gamma_\mu \gamma_5 \psi_{\tilde{a}} \,. \tag{4.66}$$

This is in the basis of the mass matrix in Eq. (4.34), before we diagonalize to the final mass matrix. Here a is the axion, $\psi_{\tilde{a}}$ is the four-component spinor denoting the axino mass eigenstate and the neutrino arises due to mixing with the axino, once we diagonalize. One can understand how this operator arises by considering the effect of the chiral rotation $\psi_{\tilde{a}} \to e^{i\gamma_5 a/f_a} \psi_{\tilde{a}}$ on the kinetic term $\bar{\psi}_{\tilde{a}} \gamma_\mu \partial^\mu \psi_{\tilde{a}}$. An axino-neutrino mixing [see Eq. (4.35)] is present in the final states, as shown in the diagram for this decay depicted in Fig. 4.3a. The partial width for this channel reads

$$\begin{aligned} \Gamma_{\tilde{a}\to\nu a} &= \frac{x_{\tilde{a},\nu}^2}{16\pi} \frac{m_{\tilde{a}}^3}{f_a^2} \approx \frac{1}{16\pi} \frac{v_u^2 \kappa_{\rm eff}^2}{f_a^4} m_{\tilde{a}} \\ &= 6 \cdot 10^{-54}\ \text{GeV} \left(\frac{\kappa_{\rm eff}}{\text{MeV}}\right)^2 \left(\frac{10^{11}\ \text{GeV}}{f_a}\right)^4 \left(\frac{m_{\tilde{a}}}{\text{keV}}\right) . \end{aligned} \tag{4.67}$$

4.4.2 *Decay into three neutrinos*

Similarly to the case of the sterile neutrino discussed in Sec. 3.1, the axino can also decay into three Majorana neutrinos via the exchange of a Z boson. We simplify our estimates by assuming that $x_{\tilde{a}-\nu}$ is a good measure of the axino-neutrino

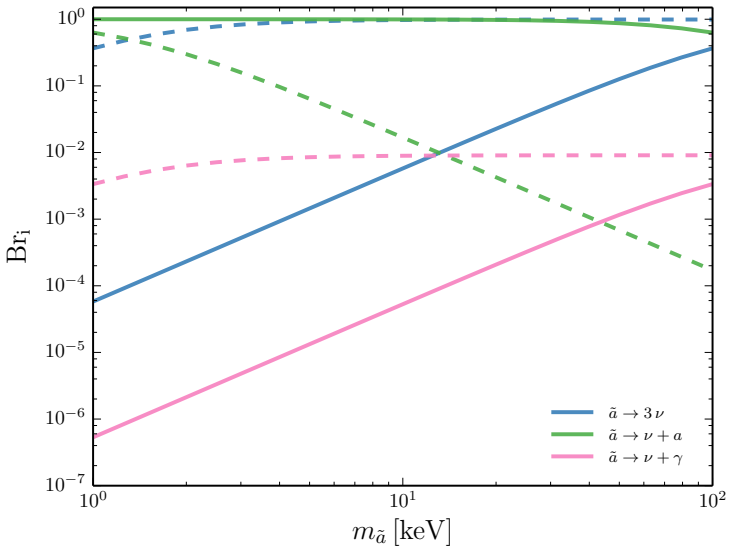

Figure 4.4: Branching ratios for the three axino decay channels: $\tilde{a} \to 3\nu, \tilde{a} \to \nu + a, \tilde{a} \to \nu + \gamma$. For the decay into photon plus neutrino (and thus the total decay width) we add here only the two dominant terms, i.e. the partial widths $\Gamma_{\tilde{B}(f\bar{f})}$ and $\Gamma_{\nu(Wl)}$, see Sec. 4.4.3. For this benchmark we choose the RpV couplings $\lambda_{QCD} = 10^{-2}$ and $\lambda_{LLE} = 0$, thus the only relevant contribution to $\Gamma_{\tilde{B}(f\bar{f})}$ is given by the bottom-sbottom loop, where we have also set $m_{\tilde{b}} = 1\,\mathrm{TeV}$. Continuous (dashed) lines correspond to $f_a = 10^{10}\,\mathrm{GeV}$ $(10^{12}\,\mathrm{GeV})$.

mixing for all neutrino flavors. The decay width for this process is substantially identical to that of Eq. (3.10),

$$\begin{aligned}\Gamma_{\tilde{a}\to 3\nu} &= \frac{9\alpha G_F^2}{8\pi^4} x_{\tilde{a},\nu}^2 m_{\tilde{a}}^5 \\ &= 3\cdot 10^{-56}\ \mathrm{GeV}\ \left(\frac{\kappa_{eff}}{\mathrm{MeV}}\right)^2 \left(\frac{10^{11}\ \mathrm{GeV}}{f_a}\right)^2 \left(\frac{m_{\tilde{a}}}{\mathrm{keV}}\right)^3 . \end{aligned} \tag{4.68}$$

The partial decay widths $\Gamma_{\tilde{a}\to\nu a}$ and $\Gamma_{\tilde{a}\to 3\nu}$ dominate the total decay width for all our parameter space, as one can observe in Fig. 4.4.

4.4.3 *Decay into photon plus neutrino*

The one-loop decay $\tilde{a}(p) \to \nu(k_1) + \gamma(k_2)$ is described by the amplitude [269]

$$\mathcal{M} = i g_{\tilde{a}\nu\gamma} \bar{u}(k_1)\,(P_R - \eta_\nu \eta_{\tilde{a}} P_L)\,\sigma^{\mu\nu} k_{2\mu} \epsilon_\nu^* u(p)\,, \tag{4.69}$$

with a Lorentz structure enforced by gauge invariance. Here η_ν and $\eta_{\tilde{a}}$ are the signs of the mass eigenvalues of neutrino and axino, k_2 the photon momentum, ϵ its polarization vector, $g_{\tilde{a}\nu\gamma}$ is a function with the details of the loop integrals, and has the dimension of inverse mass. Neglecting neutrino masses, the decay rate has then the form

$$\Gamma_{\tilde{a}\to\nu\gamma} = \frac{\left|g_{\tilde{a}\nu\gamma}\right|^2 m_{\tilde{a}}^3}{16\pi} . \tag{4.70}$$

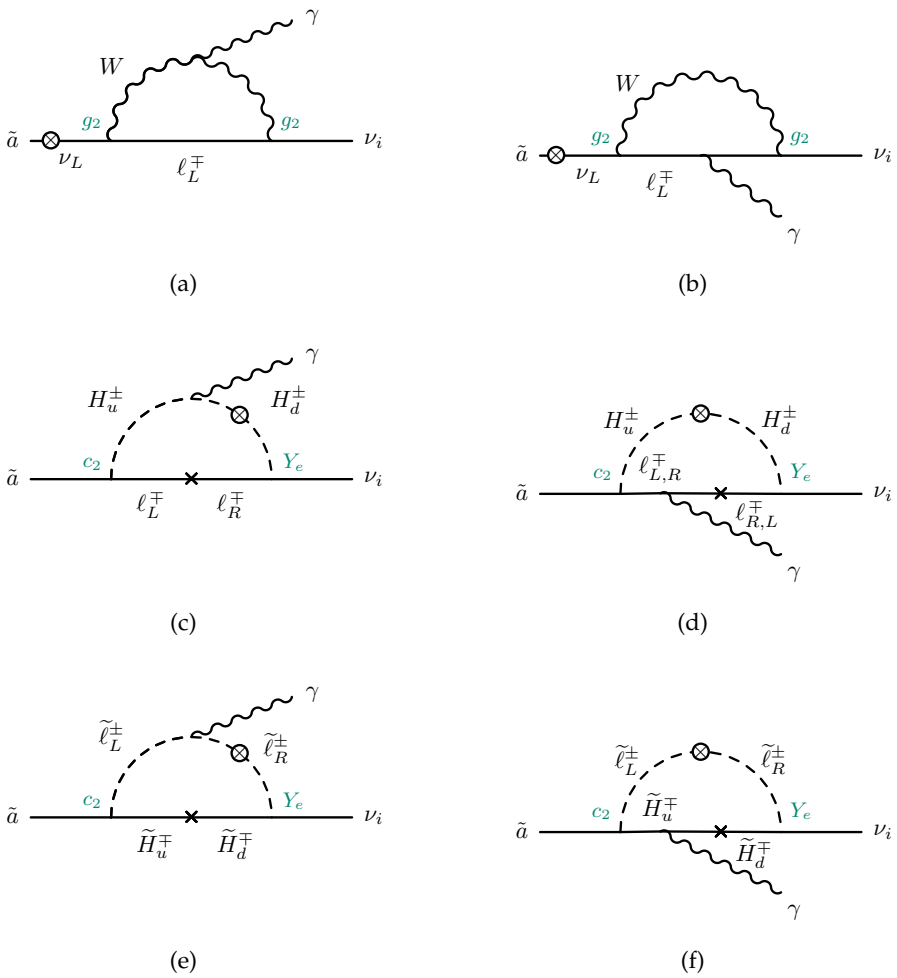

Figure 4.5: Diagrams with no dependence on the the RpV trilinear couplings $\lambda^{(\prime)}$. The cross on a fermion line indicates a mass insertion needed for the chirality flip, while the dot on a scalar line is a (dimensionless) mixing. We write the coupling constants in green at the vertices.

In principle the computation of $g_{\tilde{a}\nu\gamma}$ requires to sum all the amplitudes in Fig. 4.5 and Fig. 4.6 first, and then square them, as all the diagrams interfere. What we do in practice though is to square the amplitudes in pairs, considering each coupling combination individually. Although formally not legit, this approximation greatly simplifies the task of identifying which loops contributes the most for each point in the parameter space. At the same time, our results are still correct at the level of an estimate and their orders of magnitude will not differ from those obtained with an accurate quantum mechanical computation. If not otherwise specified, we make use of the formulae provided in Ref. [270] to compute the loop integrals. Since we work in a basis where the sneutrino VEVs are set to zero, the diagrams with insertions of such VEVs (see e.g. [271]) are therefore automatically set to zero.

The first diagrams we consider are those in Fig. 4.5a , 4.5b and are the same as the ones in Fig. 3.2, describing the decay of a sterile neutrino into a neutrino and a photon. These are the only ones containing only SM particle in the loop. Plugging

in the appropriate axino-neutrino mixing $\chi_{\tilde{a},\nu}$ into Eq. (3.11), for the case of the axino initial state we obtain

$$\begin{aligned}\Gamma_{\nu(W l)} &= \frac{9\alpha G_F^2}{1024\pi^4}\chi^2_{\tilde{a},\nu} m^5_{\tilde{a}} \approx \frac{9\alpha G_F^2}{1024\pi^4}\frac{\kappa^2_{eff} v_u^2}{f_a^2} m^3_{\tilde{a}} \\ &= 3\cdot 10^{-58}\ \text{GeV}\ \left(\frac{\kappa_{eff}}{\text{MeV}}\right)^2 \left(\frac{10^{11}\ \text{GeV}}{f_a}\right)^2 \left(\frac{m_{\tilde{a}}}{\text{keV}}\right)^3 . \end{aligned} \tag{4.71}$$

The notation for the partial decay widths is as follows: the subscripts in brackets stand for the virtual internal particles, while the subscript out of the brackets, if present, denotes the particle which mixes with the axino in the initial state. We anticipate here that $\Gamma_{\nu(W l)}$ is the dominant contribution to the partial decay width for $\tilde{a} \to \nu + \gamma$ in most of the parameter space: in the following we find therefore useful to provide analytical expressions of the ratios $\Gamma_i/\Gamma_{\nu(W l)}$ for all the other loop subprocesses with decay widths Γ_i.

A virtual τ yields the main contribution to the amplitude for the diagrams in Fig. 4.5c, 4.5d. The resulting decay width

$$\Gamma_{(H l)} \approx \frac{m^3_{\tilde{a}}}{2^{11}\pi^5}\frac{\kappa^2_{eff}}{f_a^2}\left(\frac{B\mu}{m^2_{H^\pm}}\right)^2 Y_\tau^2 \frac{m_\tau^2}{m^4_{H^\pm}} \ln^2\frac{m_\tau^2}{m^2_{H^\pm}} , \tag{4.72}$$

contains the factor m_τ^2 , which comes from the mass insertion that flips the chirality in the fermion line in the loop. $B\mu$ is the Higgs bilinear parameter in the soft potential of Eq. (4.14), so that $B\mu/m_{H^\pm}$ is an estimate of the mixing between the charged higgses. Setting $B\mu \sim m_{H^\pm}$ for simplicity, the ratio

$$\begin{aligned}\frac{\Gamma_{(H l)}}{\Gamma_{\nu(W l)}} &= \frac{1}{18\pi\alpha G_F^2}\frac{Y_\tau^2}{v_u^2}\frac{m_\tau^2}{m^4_{H^\pm}}\ln^2\frac{m_\tau^2}{m^2_{H^\pm}} \\ &\approx 3\cdot 10^{-8}\left(\frac{m_{H^\pm}}{\text{TeV}}\right)^{-4}\frac{\ln^2\frac{m_\tau^2}{m^2_{H^\pm}}}{160} .\end{aligned} \tag{4.73}$$

is very suppressed by the charged higgs mass, and $\Gamma_{(H l)}$ can be safely neglected in the total decay width of the axino. Assuming $\tilde{\tau}$ to be the lightest charged slepton, we find for the diagrams in Fig. 4.5e, 4.5f

$$\Gamma_{(\tilde{H}\tilde{l})} \approx \frac{m^3_{\tilde{a}}}{2^{12}\pi^5}\frac{\kappa^2_{eff}}{f_a^2}\chi^2_{\tilde{\tau}_L-\tilde{\tau}_R} Y_\tau^2 \frac{\mu^2_{eff}}{m^4_{\tilde{\tau}}}\frac{\left(1+\ln\frac{\mu^2_{eff}}{m^2_{\tilde{\tau}}}-\frac{\mu^2_{eff}}{m^2_{\tilde{\tau}}}\right)^2}{\left(1-\frac{\mu^2_{eff}}{m^2_{\tilde{\tau}}}\right)^4} , \tag{4.74}$$

where $x_{\tilde{\tau}_L-\tilde{\tau}_R}$ measures the mixing between the left and right staus[5]. Taking $x_{\tilde{\tau}_L-\tilde{\tau}_R} \approx 1$ for simplicity, we find the ratio

$$\frac{\Gamma_{(\tilde{H}\bar{l})}}{\Gamma_{\nu(Wl)}} = \frac{1}{18\pi\alpha G_F^2}\frac{Y_\tau^2}{v_u^2}\frac{\mu_{eff}^2}{m_{\tilde{\tau}}^4}\frac{\left(1+\ln\frac{\mu_{eff}^2}{m_{\tilde{\tau}}^2}-\frac{\mu_{eff}^2}{m_{\tilde{\tau}}^2}\right)^2}{\left(1-\frac{\mu_{eff}^2}{m_{\tilde{\tau}}^2}\right)^4} \approx 10^{-5}\left(\frac{\mu_{eff}}{\text{TeV}}\right)^2\left(\frac{m_{\tilde{\tau}}}{\text{TeV}}\right)^{-4}. \tag{4.75}$$

We now turn our focus to the loop processes for the axino radiative decay that

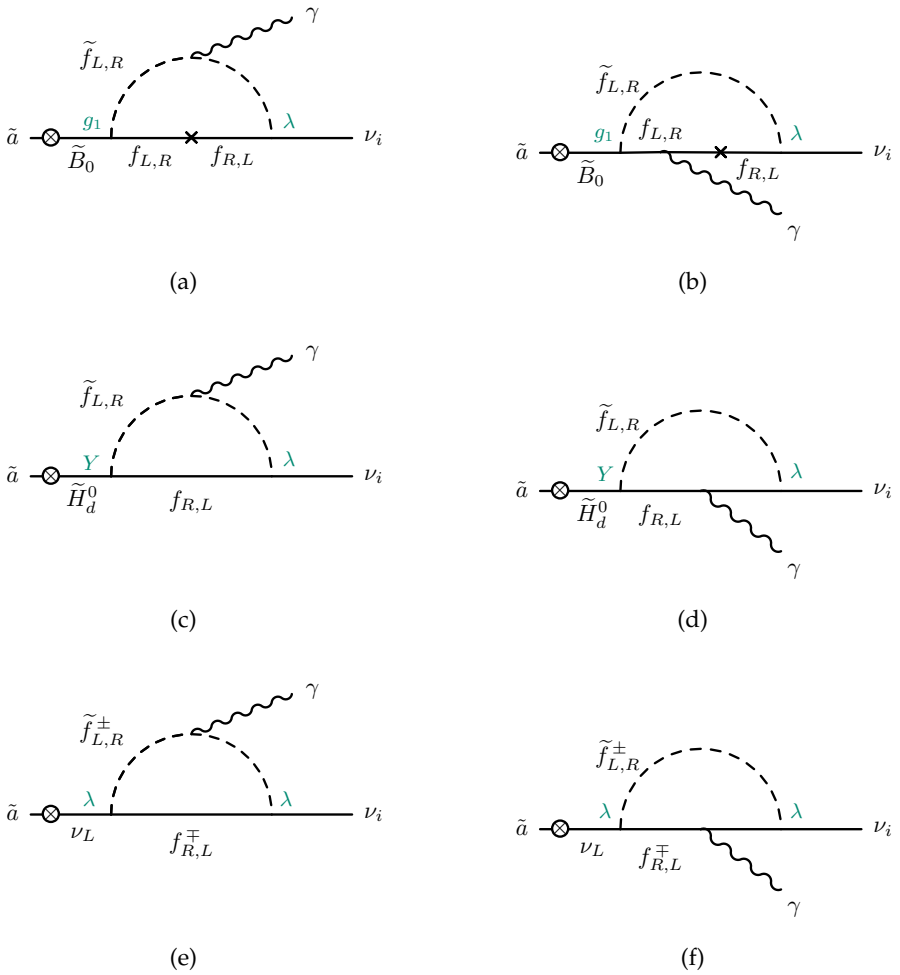

Figure 4.6: Diagrams with an explicit dependence on the RpV trilinear couplings $\lambda^{(\prime)}$. The notation is as in Fig. 4.5.

involve at least one RpV coupling, as depicted in Fig. 4.6. Since both λ or λ' are

5 Note that the expression is also finite for the particular case $\mu_{eff} = m_{\tilde{\tau}}$. Indeed in the limit $t \to 1$,

$$\frac{(1+\ln t - t)^2}{(1-t)^4} \to \frac{1}{4}.$$

allowed in each diagram, we will call them both λ in order to avoid cluttering. For the diagrams of Figs. 4.6a and 4.6b we find

$$\Gamma_{\widetilde{B}(f\tilde{f})} \approx \frac{m_{\tilde{a}}^3 Q^2}{2^{11}\pi^5} g_1^2 \lambda^2 \chi_{\tilde{a},\widetilde{B}}^2 \frac{m_f^2}{m_{\tilde{f}}^4} \ln^2 \frac{m_f^2}{m_{\tilde{f}}^2}\,, \tag{4.76}$$

where f ($\widetilde{f}$) denotes either a down-type quark (squark) or a lepton (slepton). Q is their electric charge in units of e. The main contributions to this subprocess comes from a bottom-sbottom or a tau-stau loop. Under the assumption that sleptons and squarks have comparable masses, $\Gamma_{\widetilde{B}(b\tilde{b})}$ and $\Gamma_{\widetilde{B}(\tau\tilde{\tau})}$ are of the same order of magnitude, as the smaller mass of τ is compensated by its larger electric charge. Comparing to the diagrams of Eq. (4.71) we find

$$\begin{aligned}\frac{\Gamma_{\widetilde{B}(f\tilde{f})}}{\Gamma_{\nu(W l)}} &= \frac{g_1^4 Q^2}{18\pi\alpha G_F^2} \frac{\lambda^2 v^2}{M_{SUSY}^2 \kappa_{eff}^2} \frac{m_f^2}{m_{\tilde{f}}^4} \ln^2 \frac{m_f^2}{m_{\tilde{f}}^2} \\ &\approx 0.2 \left(\frac{\lambda}{10^{-2}}\right)^2 \left(\frac{Q}{1/3}\right)^2 \left(\frac{\kappa_{eff}}{MeV}\right)^{-2} \left(\frac{M_{SUSY}}{TeV}\right)^{-2} \left(\frac{m_f}{m_b}\right)^2 \left(\frac{m_{\tilde{f}}}{TeV}\right)^{-4} \frac{\ln^2 \frac{m_f^2}{m_{\tilde{f}}^2}}{120}\,,\end{aligned} \tag{4.77}$$

where m_b is the mass of the bottom quark. As recent analyses [122, 272] disfavor squarks and sleptons lighter than ~TeV, we restrict to $m_{\tilde{f}} > 1$ TeV, where $\Gamma_{\nu(W l)}$ is larger than $\Gamma_{\widetilde{B}(f\tilde{f})}$.

The diagrams of Figs. 4.6c and 4.6d contain Y as either the Y_d or the Y_e Yukawa coupling. Its partial width reads

$$\Gamma_{\widetilde{H}(f\tilde{f})} \approx \frac{m_{\tilde{a}}^3 Q^2}{2^{11}\pi^5} Y^2 \lambda^2 \chi_{\tilde{a},\widetilde{H}}^2 \frac{m_{\tilde{a}}^2}{m_{\tilde{f}}^4} \ln^2 \frac{m_f^2}{m_{\tilde{f}}^2}\,, \tag{4.78}$$

where f ($\widetilde{f}$) can be either a down-type quark (squark) or a lepton (slepton). Again here the third generation of leptons or quarks and their supersymmetric partners contribute the most. Since there is no mass insertion over the virtual fermion line and thus no chirality flip with the corresponding mass-squared factor, $\Gamma_{\widetilde{H}(f\tilde{f})}$ is suppressed compared to $\Gamma_{\widetilde{B}(f\tilde{f})}$ by a factor $m_{\tilde{a}}^2/m_f^2$. Its ratio compared to Eq. (4.71):

$$\begin{aligned}\frac{\Gamma_{\widetilde{H}(f\tilde{f})}}{\Gamma_{\nu(W l)}} &= \frac{Q^2}{18\pi\alpha G_F^2} \frac{\lambda^2 Y^2}{\kappa_{eff}^2} \frac{m_{\tilde{a}}^2}{m_{\tilde{f}}^4} \ln^2 \frac{m_f^2}{m_{\tilde{f}}^2} \\ &\approx 10^{-12} \left(\frac{\lambda}{10^{-2}}\right)^2 \left(\frac{Q}{1/3}\right)^2 \left(\frac{Y}{Y_b}\right)^2 \left(\frac{\kappa_{eff}}{MeV}\right)^{-2} \left(\frac{m_{\tilde{a}}}{10\text{ keV}}\right)^2 \left(\frac{m_{\tilde{f}}}{TeV}\right)^{-4} \frac{\ln^2 \frac{m_f^2}{m_{\tilde{f}}^2}}{120}\,.\end{aligned} \tag{4.79}$$

The last diagrams we need to consider are the only ones involving the axino mixing with the neutrino in the initial state, as depicted in Fig. 4.6e, 4.6f. They also a feature a RpV vertex for both internal non-photonic vertices:

$$\Gamma_{\nu(f\tilde{f})} \approx \frac{m_{\tilde{a}}^3 Q^2}{2^{11}\pi^5} \lambda^4 \chi_{\tilde{a},\nu}^2 \frac{m_{\tilde{a}}^2}{m_{\tilde{f}}^4} \ln^2 \frac{m_f^2}{m_{\tilde{f}}^2}\,, \tag{4.80}$$

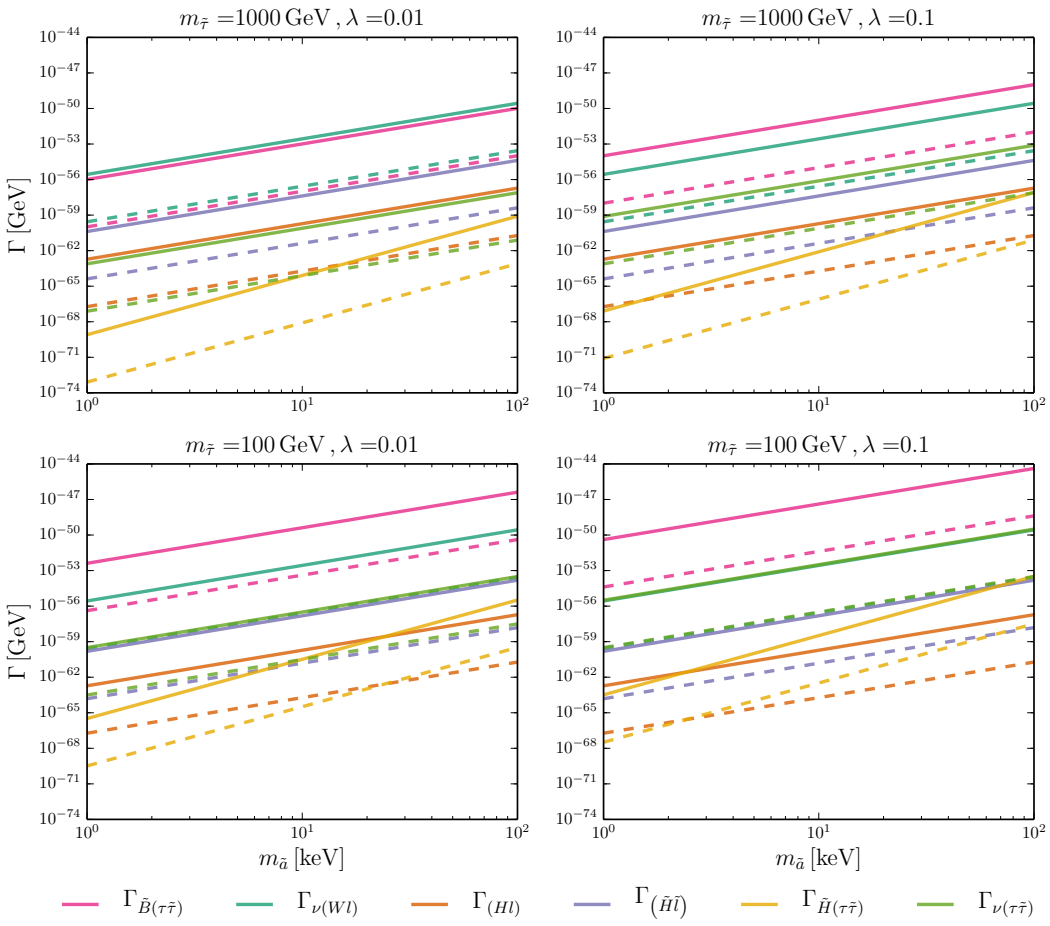

Figure 4.7: The six different contributions to $\Gamma(\tilde{a} \to \nu + \gamma)$ as a function of the axino mass for the case of the LLE RpV operator. We take 4 different combinations of the stau masses, $m_{\tilde{\tau}} \in \{10^2\,\text{GeV}, 1\,\text{TeV}\}$, and lambda couplings, $\lambda \in \{10^{-1}, 10^{-2}\}$. The continuous (dashed) lines are for $f_a = 10^{10}$ (10^{12}) GeV. We also set $\mu_{\text{eff}} = 1\,\text{TeV}$ and $B\mu \sim m^2_{H^\pm} \sim 800\,\text{GeV}$.

the main contributions being again from bottom-sbottom and tau-stau loops. Comparing with Eq. (4.71) yields

$$\frac{\Gamma_{\nu(f\tilde{f})}}{\Gamma_{\nu(Wl)}} = \frac{Q^2}{18\pi\alpha G_F^2}\frac{\lambda^4}{m^4_{\tilde{f}}}\ln^2\frac{m_f^2}{m^2_{\tilde{f}}} \tag{4.81}$$
$$\approx 10^{-9}\left(\frac{\lambda}{10^{-2}}\right)^4\left(\frac{Q}{1/3}\right)^2\left(\frac{m_{\tilde{f}}}{\text{TeV}}\right)^{-4}\frac{\ln^2\frac{m_f^2}{m^2_{\tilde{f}}}}{120}\,.$$

In Fig. 4.7 and Fig. 4.8 we plot all the contributions to the different diagrams considered so far for four benchmark points for each RpV operator. They show four corners of the parameter space defined by the slepton or squark masses, the RpV couplings and the f_a scale. We consider the minimum allowed mass of the stau(sbottom) to be 100 GeV (1 TeV), and a highest value of 1 TeV (5 TeV), respectively. We assign to the RpV couplings the values $\lambda \in \{10^{-1}, 10^{-2}\}$. In each case we plot the partial widths for f_a either 10^{10} GeV or 10^{12} GeV. In all our parameters space the dominant contributions are $\Gamma_{\tilde{B}(f\tilde{f})}$ and $\Gamma_{\nu(Wl)}$, and $\Gamma_{\tilde{a}\to\gamma\nu}$ can be

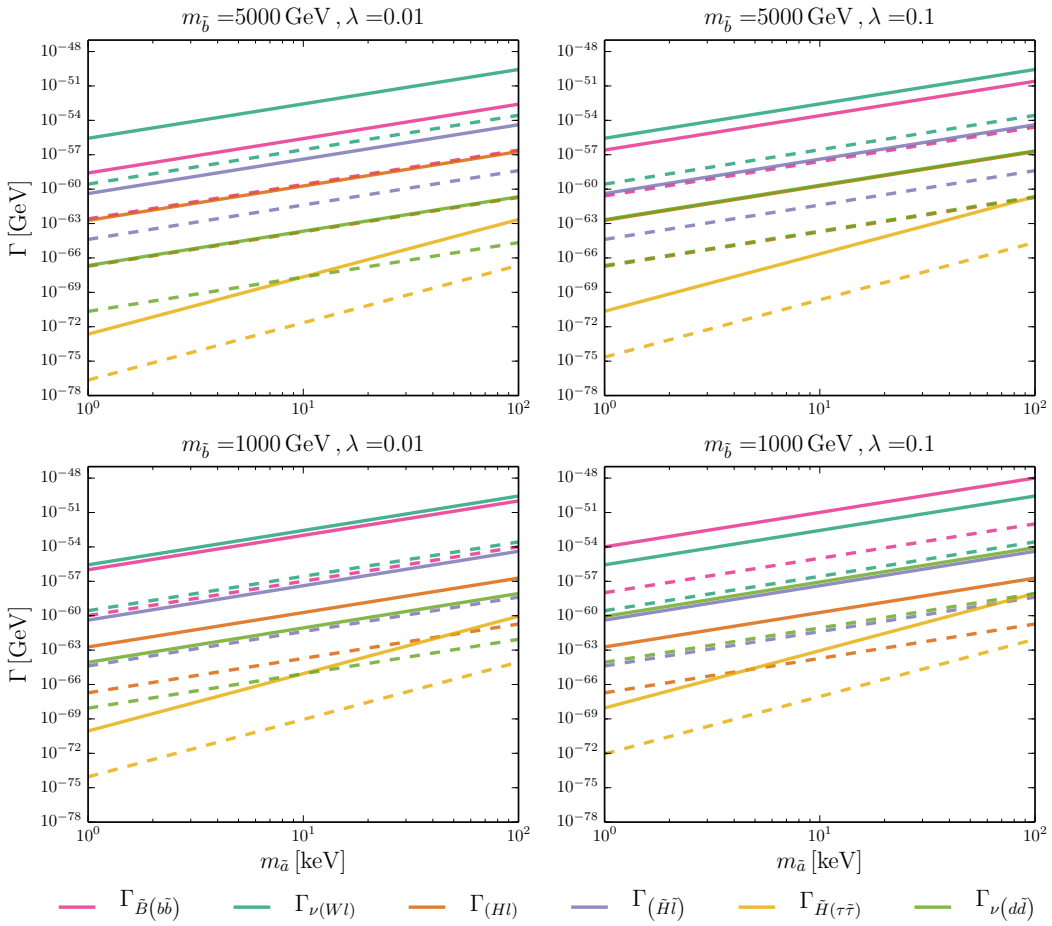

Figure 4.8: Same as Fig. 4.7, but for the case of the LQD RpV operator. For the sbottom mass we consider the benchmarks $m_{\tilde{b}} = 1\,\text{TeV}, 5\,\text{TeV}$. The mass of the slepton that runs in the loop is set to 1 TeV.

accurately approximated by their sum, as anticipated in Fig. 4.4. The respective position of these two curves can be understood by looking at their ratio in Eq. (4.77). Our conclusions extend to physically allowed regions with higher $m_{\tilde{f}}$ or lower λ too.

4.5 RESULTS

Let us now consider the phenomenological implication of our model. We start by reintroducing the generation indices in the superpotential terms

$$\frac{1}{2}\lambda_{ijk}\hat{L}_i\hat{L}_j\hat{\bar{E}}_k + \lambda'_{ijk}\hat{L}_i\hat{Q}_j\hat{\bar{D}}_k\,. \tag{4.82}$$

we can take into account the bounds on the trilinear couplings in Table 4.2. In our case the first index of λ_{ijk} and λ'_{ijk} refers to the neutrino in the lepton doublet. We see in Fig. 4.9 that when we consider the decay $\widetilde{a} \to \nu_2\gamma$, with λ_{233} and λ'_{233} saturating the upper bounds in Table 4.2, the diagrams giving $\Gamma_{\widetilde{B}(f\tilde{f})}$ provide the dominant contribution.

ijk	$\lambda_{ijk}(M_W)$	$\lambda'_{ijk}(M_W)$
133	$0.0060 \times \sqrt{\frac{m_{\tilde{\tau}}}{100\,\mathrm{GeV}}}$	$0.0014 \times \sqrt{\frac{m_{\tilde{b}}}{100\,\mathrm{GeV}}}$
233	$0.070 \times \frac{m_{\tilde{\tau}_R}}{100\,\mathrm{GeV}}$	$0.15 \times \sqrt{\frac{m_{\tilde{b}}}{100\,\mathrm{GeV}}}$
333	-	0.45 (1.04)

Table 4.2: Upper bounds on the magnitude of R-parity violating couplings at the 2σ confidence level, taken from Ref. [122]. The constraints arise from indirect decays. The concrete processes are described in detail in Ref. [273].

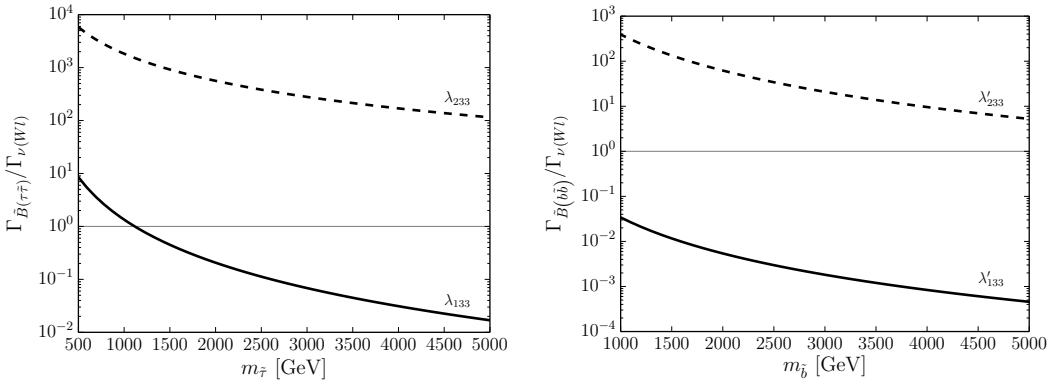

Figure 4.9: The ratio $\frac{\Gamma_{\tilde{B}(f\bar{f})}}{\Gamma_{\nu(W\ell)}}$ as in Eq. 4.77 as a function of the sfermion masses. The RpV couplings specified over the curves are also functions of the masses on each x-axes, as they saturates the bounds in Tab. 4.2. We have set $M_{SUSY} = 1$ TeV and $\kappa_{eff} = 1$ MeV.

In turn, X- and gamma-rays constraints [274, 275] applied to the decays $\tilde{a} \to \nu_{2,3}\gamma$ can set new bounds to the trilinear couplings $\lambda^{(')}_{233}$. Such constraints in fact describe a curve in the $\tau - m_{\tilde{a}}$ (or equivalently $\Gamma - m_{\tilde{a}}$) plane, $\tau_{bound}\,(m_{\tilde{a}})$. The simplifying assumption that the observed DM abundance comprises solely of axinos, $\Omega_{\tilde{a}}h^2 = \Omega_{DM}$, allows us to convert the photon bound on the lifetime into one on f_a, see Eq. (4.65). Then the excluded region corresponds to

$$\Gamma_{\tilde{B}(f\bar{f})} > \Gamma_{bound} = \frac{1}{\tau_{bound}}\,, \tag{4.83}$$

In Fig. 4.10 we see that, for $m_{\tilde{a}} = 100$ keV, we can set bounds on the trilinears $\lambda_{233}, \lambda'_{233}, \lambda'_{333}$ of order 10^{-2}. These would update the figures in Table 4.2. However, it is important to keep in mind that these new bounds, contrary to those in Table 4.2, rely on the presence of the axino and on the assumption that it is the whole dark matter. In Fig. 4.11 and 4.12 we show the X and gamma ray constraints on the plane f_a vs m_a. The excluded regions in on the right side of the yellow line correspond to

$$\frac{\Omega_{\tilde{a}}}{\Omega_{DM}}\Gamma_{\tilde{a}\to\nu\gamma} > \Gamma_{bound} = \frac{1}{\tau_{bound}}\,. \tag{4.84}$$

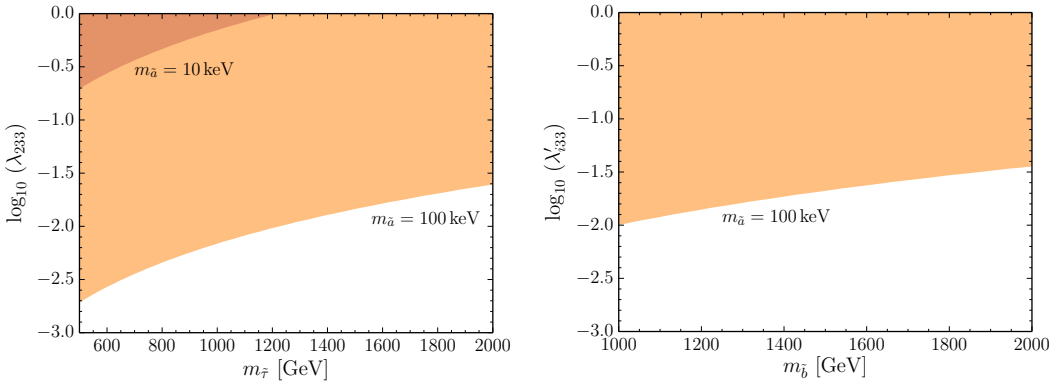

Figure 4.10: Regions of the parameters space excluded by the X and gamma ray constraints [274, 275], assuming that $\Omega_{\tilde{a}}h^2 = \Omega_{DM}$. The dark (light) orange region is excluded when $m_{\tilde{a}} = 10$ keV (100 keV). For λ'_{i33}, the index i can be either 2 or 3, in which case the dominant contribution to the decay $\tilde{a} \to \nu_i\gamma$ is from $\Gamma_{\tilde{B}(f\tilde{f})}$.

Here, $\Gamma_{\tilde{a}\to\nu\gamma} = \Gamma_{\tilde{B}(f\tilde{f})} + \Gamma_{\nu(Wl)}]$, and we multiply by $\Omega_{\tilde{a}}/\Omega_{DM}$ to account for the region of parameter space where the axino is under abundant.

4.5.1 *Comment on the 3.5 keV line*

This model can fit the 3.5 keV line observed in galaxy clusters and presented in our Sec. 3.3 A possible benchmark point, for instance, is the following:

$$m_{\tilde{a}} = 7\ \mathrm{keV}\,,\ f_a = 3.5\cdot 10^{10}\ \mathrm{GeV}\,,\ m_{\tilde{b}} = 2\ \mathrm{TeV}\,,\ \lambda'_{233} = 0.22\,. \tag{4.85}$$

With these values, the axino constitutes the entire dark matter and has a partial decay width $\Gamma_{\tilde{a}\to\nu\gamma} \approx \Gamma_{\tilde{B}(f\tilde{f})} \approx 6\cdot 10^{-53}$ GeV, needed to explain the putative line. The benchmark complies with the bounds we mentioned above. In our previous Ch. 3 we concluded that explaining the 3.5 keV line in a RpV SUSY scenario is possible under the assumption that the lightest neutralino should have a mass in the range $100\ \mathrm{MeV} < m_{\chi_1^0} < 10\ \mathrm{GeV}$, which can be achieved by having at least one of the SUSY parameters of the model at a much lower scale than TeV. For the case of our explicit model introduced in this chapter, the first straightforward consideration is that the neutralino which should be in the aforementioned mass range is the NLSP, since the the axino is the LSP now. Nomenclature aside, the mass range in the assumption remains untouched: the extremely weak coupling of the axion sector with the MSSM superfields makes any axino contribution to $\det \mathcal{M}_{\tilde{\chi}^0}$ irrelevant. Ultimately though, retaining all the mass eigenstates of $\mathcal{M}_N$ built from $(\lambda_{\tilde{B}}, \widetilde{W}^0, \widetilde{H}_u^0, \widetilde{H}_d^0)$ at $\mathcal{O}(1\,\mathrm{TeV})$ while claiming to provide a benchmark point for the 3.5 keV line is not in contrast with our conclusion from Ch. 3. In Eq. (3.32) we presented an estimate for the decay width $\Gamma_{\tilde{a}\to\nu_i+\gamma}$ which was obtained through the effective Lagrangian in Eq. (3.29). This approach is substantially different from what we do for the full model, where we calculate the loop amplitudes and the axino mixings explicitly. Even though the value of $\Gamma_{\tilde{a}\to\nu\gamma}$ obtained through the $C_{aV_iV_i}$ operators is only around two orders of magnitude lower than $\Gamma_{\nu(Wl)}$ for

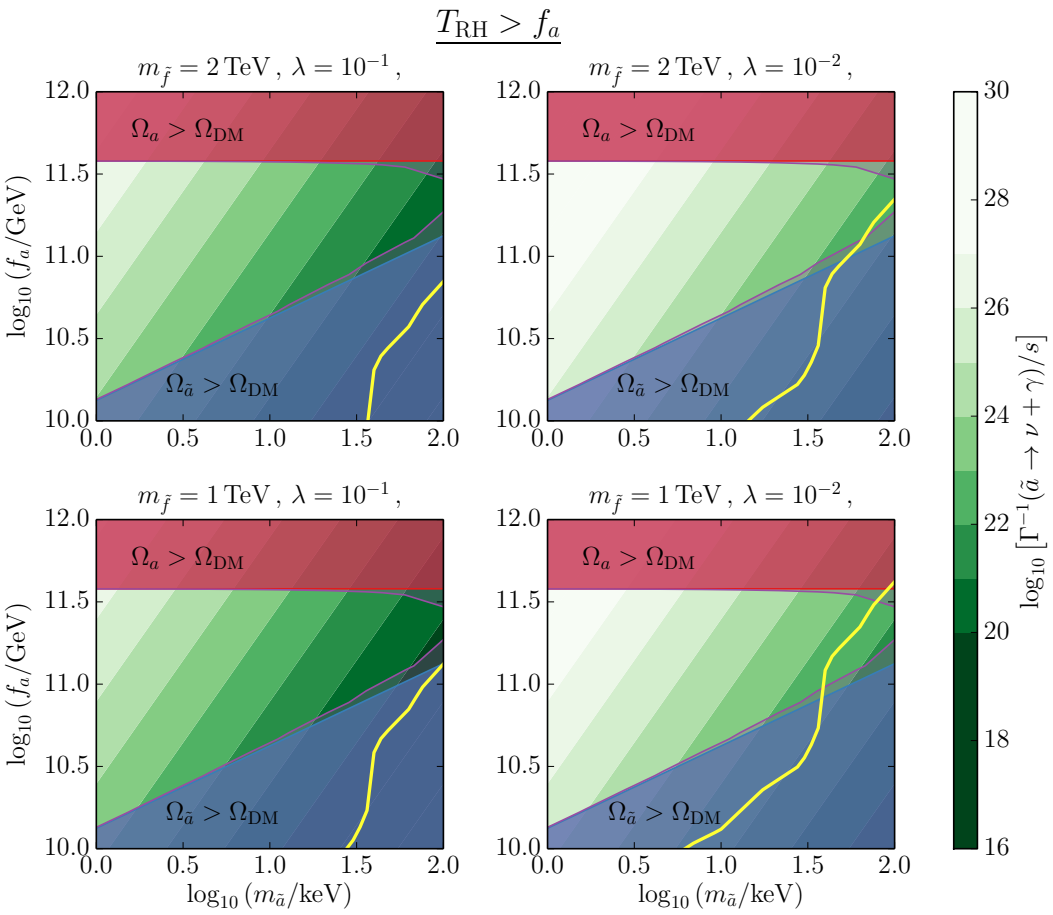

Figure 4.11: Summary plot of the constraints on our model in the plane f_a vs $m_{\tilde{a}}$, for the case $T_{\rm RH} > f_a$. The red (blue) region is excluded due to overabundance of the axion (axino) only. The red (blue) lines which serve as boundaries of such exclusion regions are the points where the axion (axino) relic density matches exactly the observed DM relic abundance, i.e. $\Omega_a h^2 = \Omega_{\rm DM} h^2$ ($\Omega_{\tilde{a}} h^2 = \Omega_{\rm DM} h^2$). The purple shaded region is excluded by the combination of both axino and axino DM. We take the reheating temperature to be higher than the PQ symmetry breaking scale, hence the contribution to the axion DM comes both from the misalignment mechanism and from string decay, see Eq. (4.52) and Eq. (4.57), respectively. We have set the average rate of axion emission to $\bar{r} = 1$. Choosing the other suggested value for such parameter, $\bar{r} = 70$, would exclude our whole parameter space. The points on the right side of the yellow line are excluded by X and gamma ray constraints. For each point we give the estimate of the inverse of the decay width for the radiative decay of the axino in terms of the corresponding shade of green. The contributions taken into account are again only $\Gamma_{\nu(Wl)}$ and $\Gamma_{\tilde{a}\to\gamma\nu}$. For our benchmarks we consider two pairs of parameters for the fermion masses and the RpV coupling respectively, $m_{\tilde{f}} \in \{1, 2\}$ TeV and $\lambda \in \{10^{-1}, 10^{-2}\}$.

the highest values of $r_{\nu_3\tilde{B}}$ and $r_{\nu_1\widetilde{W}}$ allowed, the effective approach leaves out the contributions to the decay width from trilinear RpV, and thus all diagrams in Fig. 4.6. Among these the two describing $\Gamma_{\widetilde{B}(f\tilde{f})}$, one of the two main contributions to the partial decay width $\Gamma_{\tilde{a}\to\nu\gamma}$. We can therefore conclude that the study we perform in Ref. [241] complements the one of our Ref. [199] for the case of of trilinear RpV and the DFSZ axion.

4.6 SUMMARY

In this chapter we have built a complete RpV SUSY model with baryon triality and with a DFSZ axion superfield. We have studied the mass spectrum and then investigated some cosmological bounds. The axion is a good dark matter candidate when its decay constant $f_a = \mathcal{O}(10^{11})\,\mathrm{GeV}$. For lower values of f_a the axino, with a mass roughly between 1 and 100 keV, can be the dominant dark matter candidate. We have looked at the possible decay modes of the light axino in detail. For such a light axino, its lifetime is longer than the age of the universe, but its decay into photon and neutrino still leads to interesting phenomenology. We have shown that X- and gamma-ray constraints on this decay give new bounds on some trilinear RpV couplings. These are model dependent and rely on the axino constituting the whole dark matter in the universe. We have also shown that in this model there is a corner of parameter space where a 7 keV axino could fit the 3.5 keV line observed in galaxy clusters.

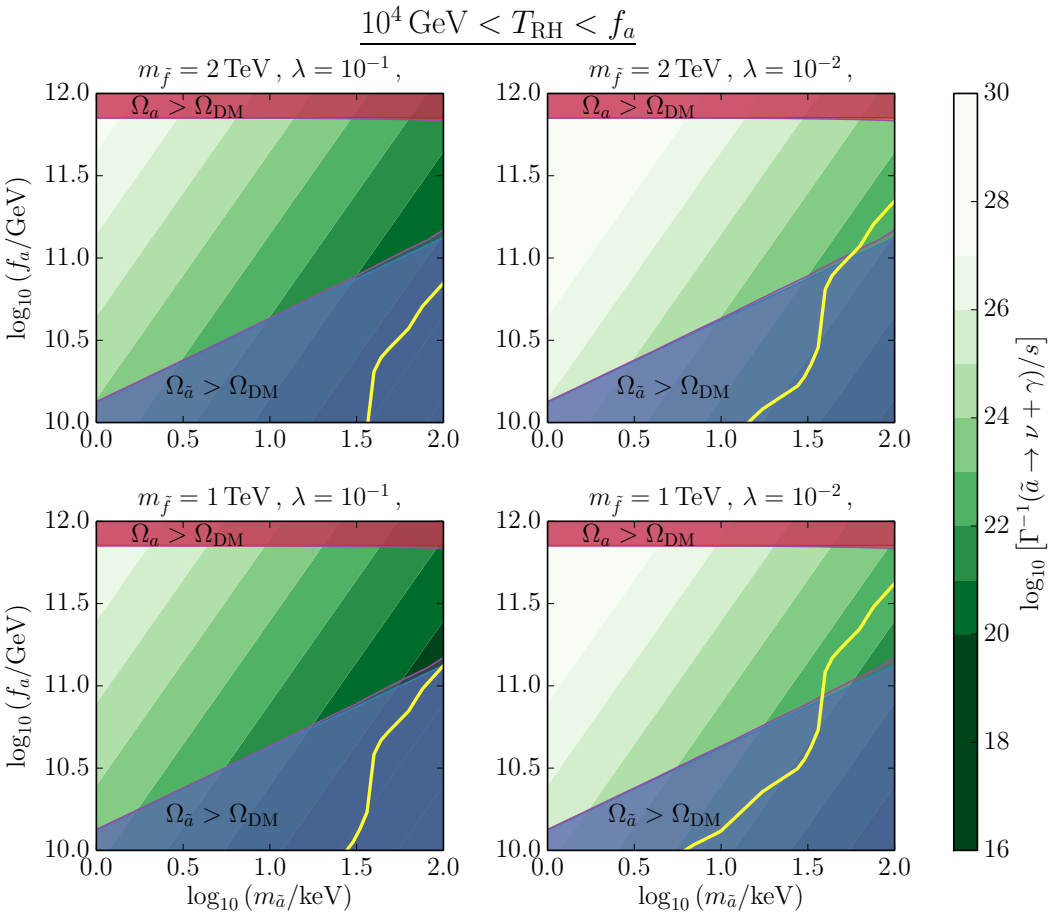

Figure 4.12: Same as Fig. 4.11, but for $10^4\,\mathrm{GeV} < T_{\mathrm{RH}} < f_a$. In this case the axion relic abundance is due only to the misalignment mechanism, as axions from string decay do not contribute, see Sec. 4.3.2.

5

ON RADIATIVE CORRECTIONS TO VECTOR-LIKE PORTAL DARK MATTER

As the LHC continues to probe the multi-TeV scale, the absence of signal of new physics creates considerable tension for the most minimal supersymmetric models and thus many LSP dark matter candidates became less natural. In the previous chapter we motivated RpV models as a possible alternative to escape LHC bounds, and presented the axion and the axino as potential DM candidates. In this chapter, we consider a different and more agnostic approach, in light of the raising scepticism about more traditional well-motivated theories for DM. Furthermore, DM searches at LHC need a theoretical interpretation in order to be related to the complementary constraints from DM direct and indirect searches. Following Ref. [63], one can define *simplified models* in terms of the limiting cases in the space of DM theories describing the LHC signatures, classified by their level of complexity. In the simplest case one finds DM-EFT theories [276–279], which describe SM-DM interactions by means of a contact interaction, with the underlining assumption that DM is the only BSM state which is kinematically accessible. An assumption which was strongly questioned given the high energies currently at reach at collider. At the opposite end of the spectrum, complete DM models offer the most general and well-motivated theoretical framework, introducing correlations between observables which might have been missed by simpler approaches. This comes at the price of introducing plenty of additional particles and thus parameters, with the classic example being the MSSM. Simplified DM models [61, 143, 280–283] fall in between these two categories, as they expand the content of BSM sector only by the particle which mediates the interaction between the SM and the dark matter. This allows a correct description of the kinematics for DM collider production, although the number of extra parameters increases with respect to DM-EFT theories. Requirements for a simplified DM models are [63]:

- The DM candidate is enough long-lived to escape the detector;
- All terms compatible with Lorentz invariance, SM gauge symmetries and DM stability should be added to the Lagrangian, although exceptions may be of interest;
- If extra symmetries are added, the resulting interactions should not violate the global symmetries of the SM, *i.e.* lepton and baryon number are conserved and flavour symmetries are not strongly broken.

Simplified models can be categorized in terms of how they describe the kinematics of the DM interacting with the SM. In the class of t-channels mediators [62, 63, 284, 285], the scenario with a Majorana DM and a scalar mediator has received much attention, due to its proximity to the neutralino DM case. Less so for the case of scalar DM, despite the analogous features. In the Vector-like Portal [67, 286] a real

scalar particle couples to Standard Model fermions through a vector-like fermion. The simplest realization of the VLP is given by

$$\mathcal{L}_{\rm DM} = -\left(y_f\, S\, \bar{\psi}\, f_R + \text{h.c.}\right) - \frac{1}{2}M_S^2 S^2 - M_\psi \bar{\psi}\psi\,, \tag{5.1}$$

where S is a singlet real scalar (the DM candidate), f_R is an $SU(2)_L$ singlet SM fermion (lepton or quark) and ψ a vector-like massive fermion. In order not to address flavour physics aspects, it is assumed that S couples dominantly to a single SM flavour. Also, in the sequel we will assume that the possible quartic coupling of S with the SM Higgs is small and may be neglected. The model described by $\mathcal{L}_{\rm DM}$ thus falls in the category of so-called simplified DM models with a t-channel mediator.

This model may be considered as the scalar version of a bino-like Majorana DM candidate, with which it shares some basic properties, the first being that their s-wave annihilation is helicity suppressed. They differ in the fact that annihilation of a bino-like candidate is p-wave in the chiral limit [287], whereas that of the real scalar S is d-wave [67, 288]. However, in both cases, the helicity suppression is lifted by radiative corrections [64, 289]. As discussed in several works, this has interesting phenomenological implications. In the case of coupling to leptons, radiative processes, either in the form of internal bremsstrahlung or annihilation at one-loop into, say, two gamma-rays, may lead to striking spectral features. Such spectral features are of interest for indirect searches for WIMPs (see, *e.g.* Refs.[66, 290–293] for the Majorana case and specifically [67, 288, 294, 295] for the scalar case). In the case of coupling to (light) quarks, radiative processes involving gluons on top of gammas may be relevant at the time of thermal freeze-out, thus impacting both the effective annihilation cross section and indirect signatures, see *e.g.* Refs. [296, 297]. Radiative corrections lift the helicity suppression most efficiently for the case of massless final states. In the chiral limit one also finds the most spectacular spectral signatures, with a pronounced peak in the photon spectrum for energies around the dark matter mass. This happens when the bremsstrahlung is dominated by the emission from the mediator, a process called *virtual internal bremsstrahlung* (VIB), as opposed to *final state radiation* (FSR), corresponding to the emission from final states. In the following, we will focus on a massive final state, having in mind a top-philic DM candidate. Indirect detection signatures from annihilation into $b\bar{b}$ and $\tau^+\tau^-$ are considered too. This can be important for the case considered in our work [298], where an extensive study of this model for the top-philic case is carried out, including direct and indirect searches, and collider constraints. We specifically focus on the technical aspects of determining the total cross section, taking into account radiative corrections, as well as the spectra into gamma-rays relevant for indirect searches. Our goal is to keep track of the non-zero quark mass effects, the most important being that the s-wave part of the annihilation cross section into quark-antiquark is helicity suppressed. The issue we will have to face is that the total annihilation cross section is plagued by infrared (IR) divergences, associated to FSR for soft gluons or gammas. According to the Kinoshita-Bloch-Nordsieck theorem [299, 300] the full cross section is free of IR divergence. This involves properly taking into account radiative corrections at a given order in the gauge coupling. For the case at hand, this requires calculating the one-loop corrections to the annihilation cross section $SS \to f\bar{f}$.

This chapter is organized as follows: in Sec. 5.1 we present the annihilation cross section of a real scalar DM particle into SM fermions through t-channel exchange of a vector-like fermion and introduce the effective approach. In Sec. 5.2 we introduce the amplitude for the annihilation with associated emission and consider the various term from an operator point of view in limit of large mediator masses. In Sec. 5.3 we present the decomposition of the total inclusive cross section into virtual corrections plus soft and hard modes. In Sec. 5.4 we study the differential cross sections (with gluon and gamma emission) and implications for indirect detection, in particular for the gamma-ray spectra. We conclude our discussion in Sec. 5.5.

5.1 TWO-BODY CROSS SECTION IN THE NON-RELATIVISTIC LIMIT

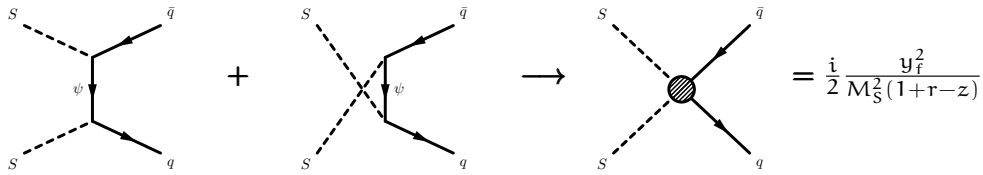

Figure 5.1: Amplitudes for the 2-body process $SS \to q\bar{q}$ and the resulting effective interaction ($r = M_\psi^2/M_S^2$ and $z = m_q^2/M_S^2$).

The annihilation of a pair of S into SM quarks proceeds at lowest order via the exchange of a heavy mediator ψ in the t- and u-channels, as depicted in Fig. 5.1. Its cross section rate in the limit of small DM velocity has a dominant s-wave contribution :

$$\langle \sigma v \rangle_{q\bar{q}} = \frac{3}{4\pi} \frac{y_f^4}{M_S^2} \frac{z\,(1-z)^{\frac{3}{2}}}{(1+r-z)^2} + \mathcal{O}(m_q^2\, v^2, v^4) \quad , \tag{5.2}$$

where the mediator and quark masses enter the above equation through the ratios

$$r \equiv \frac{M_\psi^2}{M_S^2} \quad , \quad z \equiv \frac{m_q^2}{M_S^2} \quad , \tag{5.3}$$

respectively. This result was already discussed in Ref. [67], where it was shown that in the chiral limit $m_q \to 0$ the amplitude for this process has a leading contribution $\propto v^4$, *i.e.* the cross section is d-wave suppressed. For the finite masses we consider in this work this is not generically true and we can identify two cases. First, if the dark matter annihilation takes place today in the galactic center, then it proceeds via s-wave for all points of our parameter space. Then the 2-body cross section can be described with the dimension five operator

$$\mathcal{O}_{2B,s} = \frac{m_q}{\Lambda^2} S^2\, \bar{q}\, q \ , \tag{5.4}$$

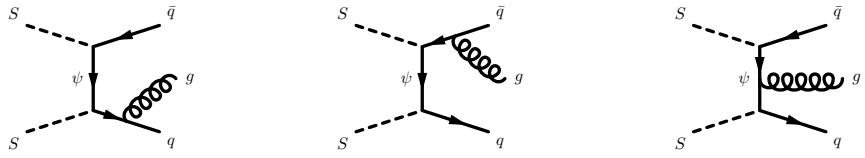

Figure 5.2: Amplitudes contributing to the 3-body process $SS \to q\bar{q}g$. We refer to final state radiation (FSR) for Fig. 5.2a and Fig. 5.2b and to virtual internal bremsstrahlung (VIB) for Fig. 5.2c.

where Λ is a mass scale that is specified through the matching between the cross section obtained with the Lagrangian 5.1 and the operator in Eq. (5.4):

$$\frac{m_q}{\Lambda^2} \to \frac{1}{2}\frac{y_f^2 m_q}{M_S^2 + M_\psi^2 - m_q^2} \tag{5.5}$$

The helicity suppression $\sim m_q^2$ of the s-wave part of the cross section in Eq. (5.2) can be seen in Eq. (5.4), where the S coupling to SM fermions is chiral while the quark-antiquark pair must have zero total helicity; matching the two requires a chirality flip. Note that the p-wave threshold behavior, $\propto (1 - m_q^2/M_S^2)^{3/2}$, of this cross section is similar to that of Higgs decay into SM fermions, as both the scalar DM pair in an s-wave and the Higgs are $J^{PC} = 0^{++}$. Second, the process $SS \to q\bar{q}$ can have a significant d-wave contribution for finite quark masses when considered in the early universe, as $v \sim 0.24$ leads to a weaker suppression compared to the case of the galactic center. Therefore the dimension five operator $\mathcal{O}_{2B,s}$ becomes a less exact approximation, the validity of which needs to be tested in the range of mass parameters of interest.

A similar result holds for s-wave annihilation of a pair of Majorana DM [297], with the initial state is instead in a $J^{PC} = 0^{-+}$ state, equivalent to a pseudo-scalar particle. Another important difference between the two cases is that the cross section for scalar DM is d-wave suppressed in the chiral limit $m_q \to 0$, while the suppression is p-wave for the Majorana case [67, 288]. A well-know consequence of the above is that the relevant cross sections for thermal freeze-out and for indirect detection will generally differ. In particular, in the chiral limit, the LO cross section is suppressed if $v \ll 1$. This suppression may however be alleviated by taking into account radiative corrections [64, 289].

5.2 THREE-BODY AMPLITUDE

We now move on to consider the annihilation of two scalars with associated emission of a gluon. In our discussion on bremsstrahlung we will focus on QCD corrections, but the procedure described in this section and that of Sec. 5.3 can be applied for the radiation of a photon too, provided $C_F \alpha_s \to Q^2 \alpha$, where $C_F = 4/3$ is a color factor and Q is the electric charge of the SM fermion. Taking the initial states S to be at rest, the part of the amplitude for the process $S(k_1)S(k_2) \to q(p_1)\bar{q}(p_2)g(k)$

associated the VIB diagram in Fig. 5.2c contribute to the three-body amplitude with

$$\mathcal{M}_{\mathrm{VIB}} = g_a\, y_f^2\, t^a \bar{u}(p_1)\Big\{ P_L\left[2(M_S^2 + M_\psi^2 - m_q^2)\not{\epsilon}^* - \epsilon^*\cdot(p_1+p_2)\not{k}\right] + m_q\left[\epsilon^*\cdot(p_1-p_2) + \not{\epsilon}^*\not{k}\right]\Big\} v(p_2) D_1 D_2\,, \tag{5.6}$$

where

$$D_i = \frac{i}{(p_i - K)^2 - M_\psi^2}\,, \tag{5.7}$$

and $K = k_1 = k_2 \equiv (M_S, 0)$. In this expression, ϵ^* is a shorthand for the polarization vector $\epsilon^*(k)$ and t^a are the representation matrices for the fundamental of $SU(3)$.

The FSR amplitudes in Figs. 5.2a and 5.2b read altogether

$$\mathcal{M}_{\mathrm{FSR}} = g_s\, y_f^2\, \bar{u}(p_1) t^a \Big\{ 2m_q \epsilon^*\cdot(p_1 D_{1k} D_2 - p_2 D_{2k} D_1) + m_q \not{\epsilon}^*\not{k}(D_{1k}D_2 + D_1 D_{2k}) + 2P_L \not{\epsilon}^*\left[M_S^2 - M_\psi^2 + m_q^2 - K\cdot(p_1+p_2)\right] D_1 D_2\Big\} v(p_2)\,, \tag{5.8}$$

where

$$D_{ik} = \frac{i}{(p_i - k)^2 - m_q^2}\,. \tag{5.9}$$

The presence of the $D_1 D_2$ term in $\mathcal{M}_{\mathrm{FSR}}$ is remarkable, as one would expect such combinations of the ψ propagators to arise only for VIB diagrams. This combination of D_i derives from the equality

$$D_1 + D_2 = -\left[2M_\psi^2 - 2M_S^2 + 2K\cdot(p_1+p_2)\right] D_1 D_2\,, \tag{5.10}$$

together with $D_{ik}^{-1} = p_i \cdot k$. This term is also gauge-dependent and must be therefore compensated by terms in Eq. (5.6). Thus already at amplitude level there no well-defined distinction between FSR and VIB. The total three-body amplitude reads

$$\mathcal{M}_{\mathrm{IB}} = g_s\, y_f^2\, \bar{u}(p_1) t^a \Big\{ P_L\left[(p_1+p_2)\cdot k \not{\epsilon}^* - \epsilon^*\cdot(p_1+p_2)\not{k}\right] D_1 D_2 + m_q\Big[\epsilon^*\cdot(p_1(2D_{1k}+D_1)D_2 - p_2(2D_{2k}+D_2)D_1) + \not{\epsilon}^*\not{k}(D_1 D_{2k} + D_2 D_{1k} + D_1 D_2)\Big]\Big\} v(p_2)\,. \tag{5.11}$$

In summing Eq. (5.11) we have manipulated the terms proportional to $P_L \not{\epsilon}^*$ in the following way:

$$\begin{aligned}
i\mathcal{M}_{IB} \subset & -\frac{i}{2}\bar{u}(p_1)P_L D_1 D_2 \not{\epsilon}^* \Big\{ 2\left[M_S^2 + m_q^2 - M_\psi^2 - K\cdot(p_1+p_2)\right] + 2\left[M_S^2 + M_\psi^2 - m_q^2\right] \Big\} v(p_2) \\
= & -\frac{i}{2}\bar{u}(p_1)P_L D_1 D_2 \not{\epsilon}^* \Big\{ 4\underbrace{M_S^2}_{K^2} - 2K\cdot(p_1+p_2) \Big\} v(p_2) \\
= & -\frac{i}{2}\bar{u}(p_1)P_L D_1 D_2 \not{\epsilon}^* \Big\{ 2K\cdot\underbrace{(2K - p_1 - p_2)}_{k} \Big\} v(p_2) \\
= & -\frac{i}{2}\bar{u}(p_1)P_L D_1 D_2 \not{\epsilon}^* \Big\{ k\cdot(p_1+p_2) \Big\} v(p_2)\,.
\end{aligned}$$

One can verify that the total amplitude is gauge invariant, $k_\mu \mathcal{M}_{IB}^\mu = 0$, using

$$D_1 - D_2 = -2i\, D_1 D_2\, K\cdot(p_1 - p_2)\,. \tag{5.12}$$

It is instructive to look at Eq. (5.11) from an effective interaction perspective. We consider an expansion of Eq. (5.11) in $r^{-1} = (M_S/M_\psi)^2$ assuming $M_\psi \gg M_S$. We group the dominant terms into three gauge invariant contribution:

$$\mathcal{M}_{IB} \approx -\frac{2g_s y_f^2}{r}\frac{m_q}{M_S^2}\,\bar{u}(p_1)t^a v(p_2)\,\mathcal{I}_{eik} + \tag{5.13}$$

$$-\frac{g_s y_f^2}{r}\frac{m_q}{M_S^2}\,\bar{u}(p_1)t^a \not{\epsilon}^* \not{k}\,(D_{1k} + D_{2k})\,v(p_2) + \tag{5.14}$$

$$+\frac{g_s y_f^2}{r^2}\frac{1}{M_S^4}\,\bar{u}(p_1)t^a P_L\left[(p_1+p_2)\cdot k \not{\epsilon}^* - \epsilon^*\cdot(p_1+p_2)\not{k}\right] v(p_2)\,, \tag{5.15}$$

where we are neglecting terms $\mathcal{O}(r^{-3})$. The first two terms are proportional to m_q. While they cannot be written in terms of local effective operators, they have a simple structure. The term on the RHS of (5.13) contains the familiar Weizsäcker-Williams factor,

$$\mathcal{I}_{eik} = \frac{\epsilon^*\cdot p_1}{k\cdot p_1} - \frac{\epsilon^*\cdot p_2}{k\cdot p_2}\,, \tag{5.16}$$

which multiplies the LO amplitude for $SS \to q\bar{q}$ and is responsible for the IR divergences of the total annihilation cross section. The term (5.14) has the structure of a dipole interaction,

$$\mathcal{O}_{DI} \sim \bar{q}_R\, \sigma_{\mu\nu} F^{\mu\nu} q_R\,, \tag{5.17}$$

with $F^{\mu\nu} = t^a F^{a,\mu\nu}$ and $\sigma_{\mu\nu} = i[\gamma_\mu, \gamma_\nu]/2$. This term comes entirely from the $\mathcal{M}_{FSR}$ amplitude in Eq. (5.8). Figs. 5.3a and 5.3b diagrammatically represent Eqs. (5.13–5.14). The term (5.15) in the expansion of $\mathcal{M}_{IB}$ in Eq. can be derived from the following dimension eight operator [301, 302]

$$\mathcal{O}_{VIB}^{(8)} = S^2 \partial_\mu\left(\bar{q}_R \gamma_\nu F^{\mu\nu} q_R\right)\,. \tag{5.18}$$

We identify it with the VIB diagram depicted it in Fig. (5.3c), as it reduces to emission from internal lines only in the chiral limit, though generically it has contributions from both $\mathcal{M}_{FSR}$ and $\mathcal{M}_{VIB}$. Since it does not suffer from helicity suppression, it may be the dominant contribution to DM annihilation if $m_q \ll M_S$.

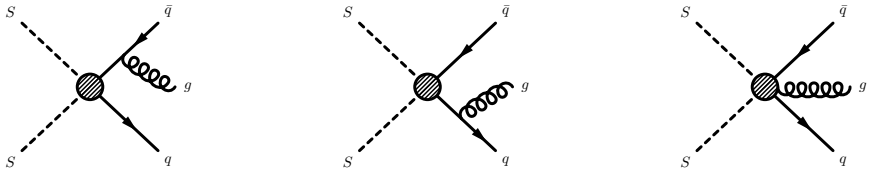

Figure 5.3: Diagrammatic representation of the amplitudes in Eqs. (5.13– 5.15). We refer to the first two amplitudes Figs. 5.3a and 5.3b as FSR, while Fig. (5.3c) corresponds to VIB.

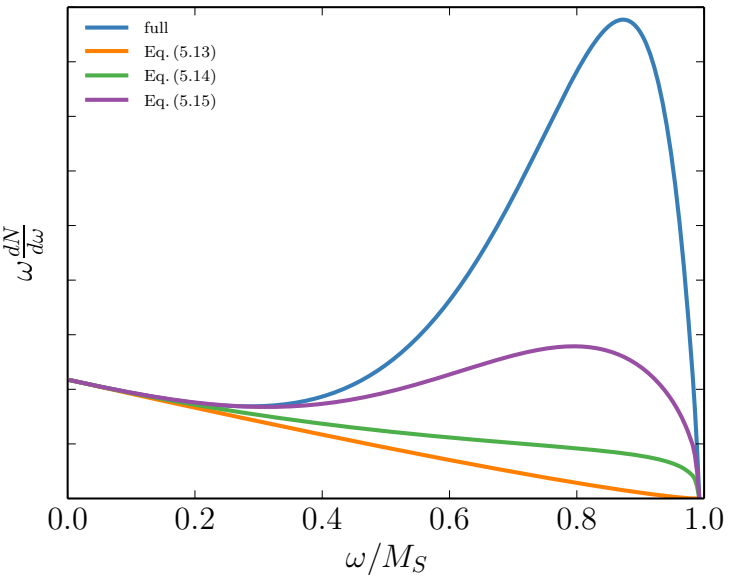

Figure 5.4: Comparison of the differential cross section $\sigma v_{\rm NLO}$ obtained in the full theory (in blue in the plot) with the various contributions from the effective approximation $\mathcal{M}_{\rm IB}$. The term in (5.13) and corresponding to the Weizsäcker-Williams approximation is in orange. The term $\propto r^{-1}$ $(\propto r^{-2})$ in the expression of $\mathcal{M}_{\rm IB}$ is in green (purple).

In the limit of large r the expansion of Eqs. (5.13– 5.15) is robust and one can use this amplitude to compute the annihilation cross section. The first term leads to IR divergences, but these can be tamed in the way we describe in Sec. 5.3.1. However, one would like to be more general: first, because the large r expansion spoils the spectral feature of VIB, which are most prominent when M_ψ and M_S are almost degenerate; secondly, because we have in mind DM candidates that could annihilate into heavy quarks, in particular the top, so that neglecting m_q may not be a good approximation. Anticipating on the results of the next sections, our considerations are illustrated in Fig. 5.4 where we depict the typical gluon or gamma-ray spectrum (at the partonic level) $\omega dN/d\omega$ as a function of $\chi = \omega/M_S$ for a DM candidate with a strong VIB feature, thus for almost degenerate masses, $r \approx 1$.

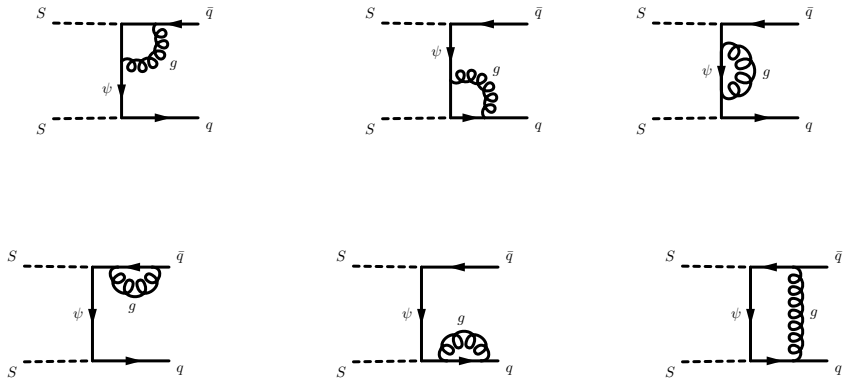

Figure 5.5: Full set of one-loop corrections to SS annihilation into $q\bar{q}$.

5.3 ORDER-α_s CORRECTIONS

For the purpose of probing DM through indirect detection, we aim at determining the spectrum of quark and gluons emitted when DM annihilates through internal bremsstrahlung, $d\sigma v_{q\bar{q}g}/d\omega$, where ω is the gluon energy. The integrated cross section is also relevant for determining the relic abundance of the DM particle [296]. However, for finite quark mass, its expression suffers from IR and collinear divergences. The standard procedure to address these divergences involves the computations of the three-body process as well as the one-loop corrections to the two-body annihilation. This follows from the Kinoshita-Lee-Nauenberg theorem (or Bloch-Nordsieck for QED) which guarantees us that IR divergences from the phase-space integration cancel out in the gauge couplings when all the possible initial and final states at each order are considered. Thus a sensible choice for the physical observable is the inclusive cross section summing up the processes $SS \to q\bar{q}$ and $SS \to q\bar{q}g$, including correction up to order $\mathcal{O}(\alpha_S)$, depicted in Fig. 5.5. Following Ref. [297], we split the integral over the gluon energy into the emission of soft and hard gluons, respectively. For the emission of soft gluons, we will use the effective interaction of Eq. 5.4 to control and cancel the IR divergences that affect the cross section for soft modes, whereas we keep the full UV-complete amplitudes to capture the VIB spectral features. The matching between the two regimes will be controlled by a cut-off on the energy of the emitted gluon, ω_0. Formally, the total next-to-leading order cross section reads

$$\sigma v_{\rm NLO} = \sigma v_{q\bar{q}g} + \Delta\sigma v|^{\rm eff}_{\rm soft}(\omega_0) + \Delta\sigma v|^{\rm full}_{\rm hard}(\omega_0)\,, \tag{5.19}$$

The soft contribution is defined as

$$\Delta\sigma v|^{\rm eff}_{\rm soft}(\omega_0) \equiv \Delta\widetilde{\sigma v}|^{\rm eff}_{\rm soft}(\omega_0,\lambda) + \Delta\sigma v|^{\rm eff}_{\rm 1L}(\lambda)\,, \tag{5.20}$$

where λ is a fictitious mass of the gluon, introduced in order to regularize the cross section obtained by integrating over soft modes. The term $\Delta\widetilde{\sigma v}|^{\rm eff}_{\rm soft}(\omega_0,\lambda)$ is unphysical, as its phase-space integral includes only gluon energies $E_g < \omega_0$ and it diverges for $\lambda \to 0$. The λ dependence requires to take into account one-loop corrections to the LO cross section, which are computed using the effective theory. The dependence on λ will cancel in the sum of the two contributions. $\Delta\sigma v|^{\rm full}_{\rm hard}$ is

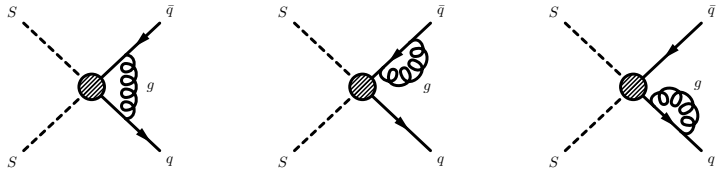

Figure 5.6: One-loop corrections to the effective coupling $\mathcal{O}_{2B,s}$ relevant for cancelling IR divergences.

the contribution to the total cross section which includes the hard gluon modes $E_g > \omega_0$. Both $\Delta\sigma v|^{\rm eff}_{\rm soft}$ and $\Delta\sigma v|^{\rm full}_{\rm hard}$ depend on the matching energy ω_0 but their sum does not.

A remarkable advantage of our approach is that in order to cancel infrared divergences we will need to calculate the one-loop corrections depicted in Fig. 5.6 rather than those of Fig. 5.5. Since the coupling of Eq. (5.4) has precisely the same structure as the Higgs coupling to SM fermions, much of the underlying physics is the same as that discussed in Refs. [303, 304]. What is specific to the DM scenario is the emission of gluons by the vector-like mediator.

5.3.1 *Soft modes*

We now consider the DM annihilation into a pair of massive SM quarks with the emission of a soft gluon. The gluon energy is $\omega = |\vec{k}| \leqslant \omega_0$, where ω_0 is the cut-off energy introduced above, which we take to be small compared to other characteristic mass scale in the theory, $\omega_0 \ll \{M_S, M_\psi, m_q\}$, but larger than $\Lambda_{\rm QCD}$. We describe the emission of a soft gluon using the eikonal approximation,

$$\mathcal{M}^a|^{\rm eff}_{\rm soft} = -g_s y_f^2 \frac{m_q}{M_S^2(1+r-z)}\,\bar{u}(p_1)t^a v(p_2)\left(\frac{\epsilon^*\cdot p_1}{k\cdot p_1} - \frac{\epsilon^*\cdot p_2}{k\cdot p_2}\right), \tag{5.21}$$

where the momentum labels are unambiguously determined by the convention for the Dirac spinor u and v. This expression differs from the RHS of (5.13) by a factor $1/(1+r-z)$, which stems from neglecting the soft gluon 4-momentum in the propagator of the mediator. Integrating over the phase space for the soft modes we get the following differential cross section:

$$\left.\frac{d\sigma v_{q\bar{q}g}}{d\chi}\right|^{\rm eff}_{\rm soft} = \frac{y_f^4 N_c}{4\pi(1+r-z)^2 M_S^2}\frac{\alpha_S C_F}{\pi}\left\{\frac{(2-z)(1-z)z}{\chi}\ln\frac{\chi+\beta\sqrt{\chi^2-4\mu_\lambda}}{\chi-\beta\sqrt{\chi^2-4\mu_\lambda}} + \right.$$
$$\left. -2(1-z)z^2\frac{\beta\sqrt{\chi^2-4\mu_\lambda}}{(1-\beta^2)\chi^2+4\beta^2\mu_\lambda}\right\}, \tag{5.22}$$

where $\chi = \omega/M_S$. This expression contains β, the velocity of the final state quarks in the rest frame of the $q\bar{q}$ system (see *e.g.* [305])

$$\beta = \sqrt{\frac{1-\chi-z+\mu_\lambda}{1-\chi+\mu_\lambda}} \xrightarrow{\omega,\lambda\to 0} \beta_0 \equiv \sqrt{1-z}\,. \tag{5.23}$$

In order to regulate the IR divergence that arises when integrating Eq. (5.22) over the gluon energy, we have introduced a fictitious mass $\lambda \ll \omega_0$ for the soft gluon, which enters in the expression for β through $\mu_\lambda \equiv \lambda^2/4M_S^2$.

Recovering the physical limit of a massless photon, the integrated cross section for emission of a soft gluon in the energy range $\lambda \leqslant \omega \leqslant \omega_0$ is given by

$$\begin{aligned}\Delta\tilde{\sigma}v|^{\text{eff}}_{\text{soft}} = \sigma v_{q\bar{q}}\,\frac{\alpha_s C_F}{\pi}\Bigg\{&\left(\frac{1+\beta_0^2}{2\beta_0}\ln\frac{1+\beta_0}{1-\beta_0}-1\right)\ln\frac{4\omega_0^2}{\lambda^2}\\&+\frac{1+\beta_0^2}{\beta_0}\left[\text{Li}_2\left(\frac{1-\beta_0}{1+\beta_0}\right)+\ln\frac{1+\beta_0}{2\beta_0}\ln\frac{1+\beta_0}{1-\beta_0}\right.\\&\left.-\frac{1}{4}\ln^2\left(\frac{1+\beta_0}{1-\beta_0}\right)-\frac{\pi^2}{6}\right]+\frac{1}{\beta_0}\ln\frac{1+\beta_0}{1-\beta_0}\Bigg\}.\end{aligned} \tag{5.24}$$

By construction this cross section is proportional to the leading order cross section $\sigma v_{q\bar{q}}$, which corresponds to the s-wave term of Eq. (5.2). This expression agrees with the analogous one in Ref. [303] for the Higgs decay, with both of them exhibiting a IR divergence term $\propto \ln(\omega_0^2/\lambda^2)$. We give full details about this computation in App. A.3. In order to obtain a IR finite result, we need take into account the $\mathcal{O}(\alpha_s)$ contributions virtual one-loop corrections to the leading order cross section into $q\bar{q}$. This stems from the interference term between LO and the one-loop corrections

$$|\mathcal{M}_{\text{tree}}+\mathcal{M}_{1L}|^2 = |\mathcal{M}_{\text{tree}}|^2 + 2\,\text{Re}(\mathcal{M}^*_{\text{tree}}\mathcal{M}_{1L}) + \mathcal{O}(\alpha_s^2)\,. \tag{5.25}$$

At one-loop, the IR divergent contributions come from the vertex correction and final state fermion wave-function corrections, depicted by the diagrams of Fig. 5.6. Using dimensional regularisation in $D = 4-2\epsilon$, we reproduce the corresponding result of Ref. [303]

$$\begin{aligned}\text{Re}\mathcal{M}|^{\text{eff}}_{1\text{-loop}} = \mathcal{M}_{\text{tree}}\frac{\alpha_s C_F}{2\pi}\Bigg\{&2\left(\frac{1}{\epsilon}-\ln\frac{m_q^2}{\mu^2}\right)-\frac{1+\beta_0^2}{2\beta_0}\ln\frac{1+\beta_0}{1-\beta_0}\ln\frac{m_q^2}{\lambda^2}\\&+\frac{1+\beta_0^2}{\beta_0}\left[\text{Li}_2\left(\frac{1-\beta_0}{1+\beta_0}\right)+\ln\frac{1+\beta_0}{2\beta_0}\ln\frac{1+\beta_0}{1-\beta_0}-\frac{1}{4}\ln^2\frac{1+\beta_0}{1-\beta_0}+\frac{\pi^2}{3}\right]\\&+\frac{1-\beta_0^2}{\beta_0}\ln\frac{1+\beta_0}{1-\beta_0}+3\Bigg\},\end{aligned} \tag{5.26}$$

which is both UV and IR divergent. According to the LSZ reduction formula [306], we must also take into account the $\mathcal{O}(\alpha_s)$ correction from the one-shell wave-function of the final state quark and anti-quark, with

$$(Z_2-1)\,\mathcal{M}_{\text{tree}} = \delta_2\mathcal{M}_{\text{tree}} = \mathcal{M}_{\text{tree}}\frac{\alpha_s C_F}{2\pi}\left[-\frac{1}{2}\left(\frac{1}{\epsilon}-\ln\frac{m_q^2}{\mu^2}\right)+\ln\frac{m_q^2}{\lambda^2}-2\right]. \tag{5.27}$$

Adding this to the Eq. (5.26) yields

$$\begin{aligned}\mathrm{Re}(\mathcal{M}_{1L}) = \mathcal{M}_{\mathrm{tree}}\frac{\alpha_s C_F}{2\pi}\Bigg\{&\frac{3}{2}\left(\frac{1}{\epsilon} - \ln\frac{m_q^2}{\mu^2}\right) - \left(\frac{1+\beta_0^2}{2\beta_0}\ln\frac{1+\beta_0}{1-\beta_0} - 1\right)\ln\frac{m_q^2}{\lambda^2}\\ &+ \frac{1+\beta_0^2}{\beta_0}\left[\mathrm{Li}_2\left(\frac{1-\beta_0}{1+\beta_0}\right) + \ln\frac{1+\beta_0}{2\beta_0}\ln\frac{1+\beta_0}{1-\beta_0} - \frac{1}{4}\ln^2\frac{1+\beta_0}{1-\beta_0} + \frac{\pi^2}{3}\right]\\ &+ \frac{1-\beta_0^2}{\beta_0}\ln\frac{1+\beta_0}{1-\beta_0} + 1\Bigg\}. \end{aligned} \tag{5.28}$$

Comparing the term $\propto \ln\left(m_q^2/\lambda^2\right)$ of this expression to the first term in Eq. (5.24), we see that, summing up the $\mathcal{O}(\alpha_s)$ one-loop corrections to the tree level cross section and the cross section for emission of soft gluons, the dependence on the fictitious gluon mass [*i.e.* the terms in $\ln(\lambda^2)$] disappears, leaving only the dependence on the cut off of the energy of the emitted gluon with terms proportional to $\ln(\omega_0^2)$.

At this point we are still left with a dependency on the UV divergence, as manifest in terms $\propto \ln\left(\mu^2\right)$. The renormalization prescription used in Ref. [297] is the same as the one advocated in Ref. [303] for the case of QCD corrections to Higgs decay into quarks. Since here the quark mass derives from the Yukawa coupling to the Higgs, the counterterm is that for quark mass renormalization,

$$\frac{\delta m_q}{m_q} = -\frac{C_F\alpha_s}{2\pi}\left[\frac{3}{2}\left(\frac{1}{\epsilon} - \ln\frac{m_q^2}{\mu^2}\right) + 2\right]. \tag{5.29}$$

This term cancels the UV divergence in Eq. (5.28), but it is not a unique prescription. Any other choice which differs from Eq. (5.29) by a constant term would be just as good. In fact, for fixed particle masses, the only free parameter in the annihilation cross section is the Yukawa coupling y_f. Its value is fixed by matching the cosmic relic abundance. All other parameters being kept fixed, a different renormalization prescription merely amounts to a shift in the value of y_f, which in simplified models does not change any observable. Here we choose to use the same prescription of Ref. [297] to renormalize our effective theory and thus the one-loop contribution to Eq. (5.20) reads

$$\begin{aligned}\Delta\sigma v|^{\mathrm{eff}}_{1L} = \sigma v_{q\bar{q}}\,\frac{\alpha_s C_F}{\pi}\Bigg\{&\left(1 - \frac{1+\beta_0^2}{2\beta_0}\ln\frac{1+\beta_0}{1-\beta_0}\right)\ln\frac{m_q^2}{\lambda^2}\\ &+ \frac{1+\beta_0^2}{\beta_0}\left[\mathrm{Li}_2\left(\frac{1-\beta_0}{1+\beta_0}\right) + \ln\frac{1+\beta_0}{2\beta_0}\ln\frac{1+\beta_0}{1-\beta_0} - \frac{1}{4}\ln^2\frac{1+\beta_0}{1-\beta_0} + \frac{\pi^2}{3}\right]\\ &+ \frac{1-\beta_0^2}{\beta_0}\ln\frac{1+\beta_0}{1-\beta_0}) - 1\Bigg\}. \end{aligned} \tag{5.30}$$

Adding this contribution to Eq. (5.24) we get a full expression for Eq. (5.20) which does not depend on the cut-off energy ω_0,

$$\Delta\sigma v|^{\mathrm{eff}}_{\mathrm{soft}} = \Delta\tilde{\sigma} v|^{\mathrm{eff}}_{\mathrm{soft}} + \Delta\sigma v|^{\mathrm{eff}}_{1\text{-loop}} = \sigma v_{q\bar{q}}\,\frac{\alpha_s C_F}{\pi}\left[\left(1 - \frac{1+\beta_0^2}{2\beta_0}\ln\frac{1+\beta_0}{1-\beta_0}\right)\ln\frac{m_q^2}{\omega_0^2} + \ldots\right], \tag{5.31}$$

where the terms not explicitly written are $\mathcal{O}(\omega_0^0)$.

5.3.2 *Hard modes*

In this section we calculate the spectrum of hard gluons and their contribution to the total NLO cross section. We carry this computation in the full theory defined by the Lagrangian $\mathcal{L}_{DM}$ of Eq. (5.1) and thereby starting from the amplitude corresponding to the diagrams of Fig. (5.3). Since ω_0 now represent a *lower* cut off on the energies of the gluons, there is no need to add a fictitious gluon mass for the sake of the finiteness of the phase-space integrals. At the level of the differential cross section we obtain

$$\left.\frac{d\sigma v_{q\bar{q}g}}{d\chi}\right|_{\text{full}} = \frac{y_f^4 N_c}{4\pi(1+r-z^2)M_S^2}\frac{\alpha_s C_F}{\pi}\left[\frac{(2-z)(1-z)z}{\chi}\ln\frac{1+\beta}{1-\beta}+\right.$$
$$\left.-2(1-z)z^2\frac{\beta}{(1-\beta^2)}\frac{1}{\chi}+S_0(\chi)\right], \tag{5.32}$$

where the first two terms are exactly those of Eq. (5.22) in the limit $\mu_\lambda \to 0$ and are divergent in the limit of large scalar masses, $\chi = \omega/M_S \to 0$. On the contrary, terms which are regular in this limit are collectively expressed as the function $S_0(\chi)$, a lengthy expression to which we dedicate part of our App. A.2. For finite quark masses, it also includes hard emission from final state quarks and interference terms between the latter and VIB.

Integrating Eq. (5.32) over $\omega \geqslant \omega_0$, we get

$$\begin{aligned}\Delta\sigma v|^{\text{full}}_{\text{hard}} = \sigma v_{q\bar{q}}\frac{\alpha_s C_F}{\pi}\Bigg[&\left(\frac{1+\beta_0^2}{2\beta_0}\ln\frac{1+\beta_0}{1-\beta_0}-1\right)\ln\frac{\beta_0^4 M_S^2}{\omega_0^2} \\ &+2\left(\ln\frac{1-\beta_0^2}{4}+\frac{1+\beta_0^2}{2\beta_0}\ln\frac{1+\beta_0}{1-\beta_0}+1\right) \\ &+\frac{1+\beta_0^2}{\beta_0}\left(2\text{Li}_2\left(\frac{1-\beta_0}{1+\beta_0}\right)+2\,\text{Li}_2\left(-\frac{1-\beta_0}{1+\beta_0}\right)-\frac{\pi^2}{6}+2\ln\frac{1+\beta_0}{2\beta_0}\ln\frac{1+\beta_0}{1-\beta_0}\right)\Bigg] \\ &+\frac{N_C}{4\pi^2}C_F\frac{\alpha_s y_f^4}{M_S^2}\int_0^{\beta_0^2} d\chi S_0(\chi)\,.\end{aligned} \tag{5.33}$$

The first term in this expression involves the cut-off energy ω_0. Adding $\Delta\sigma v|^{\text{full}}_{\text{hard}}$ to the soft contribution gives a result that is independent of ω_0. Our final expression for the cross section for s-wave annihilation is then

$$\begin{aligned}\sigma v_{\text{NLO}} &= \sigma v_{\text{LO}} + \Delta\sigma v|^{\text{eff}}_{\text{soft}}(\omega_0) + \Delta\sigma v|^{\text{full}}_{\text{hard}}(\omega_0) \\ &= \sigma v_{q\bar{q}}\Bigg\{1+\frac{\alpha_s C_F}{\pi}\Bigg[\left(1-\frac{1+\beta_0^2}{2\beta_0}\ln\frac{1+\beta_0}{1-\beta_0}\right)\ln\frac{1-\beta_0^2}{4\beta_0^4} \\ &+\frac{1+\beta_0^2}{\beta_0}\left(4\text{Li}_2\left(\frac{1-\beta_0}{1+\beta_0}\right)+2\text{Li}_2\left(-\frac{1-\beta_0}{1+\beta_0}\right)+4\ln\frac{1+\beta_0}{2\beta_0}\ln\frac{1+\beta_0}{1-\beta_0}-\frac{1}{2}\ln^2\frac{1+\beta_0}{1-\beta_0}\right) \\ &+2\ln\frac{1-\beta_0^2}{4}+\frac{3}{\beta_0}\ln\frac{1+\beta_0}{1-\beta_0}+\frac{1}{2}\Bigg]\Bigg\}+\frac{\alpha_S C_F}{4\pi^2}\frac{y_f^4 N_c}{M_S^2}\int_0^{\beta_0^2} d\chi S_0(\chi)\,.\end{aligned} \tag{5.34}$$

which is one of our main results.

5.3.3 *Limiting behaviour and approximations*

With the analytical treatment presented in Secs. 5.3.1 and 5.3.2 both the IR and UV divergences are taken care of, thus the expression of Eq. (5.34) is a finite and measurable observable, which can be useful to determine the relic abundance of the particle S and its indirect signatures. Despite its complexity though, it still has some limitations. $\sigma v_{\rm NLO}$ indeed diverges close to the threshold for quark-antiquark production, $\beta_0 \to 0$, as well as in the opposite limit, $\beta_0 \to 0$, for effective massless final states. These issues are both dealt with for the case of the Higgs in Ref. [92], so we address them only briefly here.

We first tackle the problem posed by the divergent behavior of the NLO cross section close to threshold for fermion-antifermion production. For $M_S \gtrsim m_q$, corresponding to $\beta_0 = \sqrt{1 - m_q^2/M_S^2} \to 0$, the annihilation cross section behaves as

$$\sigma v_{\rm NLO}|_{M_S \gtrsim m_q} \approx \sigma v_{\rm LO} \left[1 + \frac{\alpha_s C_F}{\pi}\left(\frac{\pi^2}{2\beta_0} - 1\right)\right] \tag{5.35}$$

The $\mathcal{O}(\alpha_s)$ terms arise from expanding near zero velocity $\beta_0 \to 0$ the two Spence functions in Eq. (5.34). As shown in Ref. [303], this singular behavior is spurious, as the cross section should be in a p-wave quark-antiquark final state, $\propto \beta_0^3$. It can be entirely traced back to the virtual corrections of Eq. (5.30), corresponding to the effective vertex in Fig. 5.6. Physically it signals the tendency to form a bound state, thus in principle one should sum over an infinite number of diagrams when approaching the threshold from above. Below it, one needs to take into account a possible quarkonium bound state [307]. Both cases are beyond our scopes. For practical purposes, the only relevant threshold limit to be considered is the one for the case of top-antitop final states: as the relic abundance strongly depends on M_S, having S with a mass close to those of lighter quarks automatically rules out the scenario, since not enough dark matter is produced [298].

The cross section $\sigma v_{\rm NLO}$ is ill-behaved in the opposite limit $\beta_0 \to 1$. In particular, the terms which are proportional to $\sigma v_{\rm LO}$ receives a large negative logarithmic contribution [303, 304],

$$\sigma v_{\rm NLO} \approx \sigma v_{q\bar{q}} \left[1 + \frac{3}{2}\frac{\alpha_s C_F}{\pi}\left(\frac{3}{2} - \ln 4z\right)\right] + \dots \tag{5.36}$$

where the dots represent the terms that are regular for small $z = m_q^2/M_S^2$. Remarkably they reduce to the cross section for the pure VIB process in the limit $z \to 0$, where $\sigma v_{q\bar{q}} \to 0$ too, thus one expect the new logarithmic term to be harmless for most of the parameter space. Otherwise one must re-sum large logarithmic contributions to the cross section. Heuristically, we notice that the leading log term in Eq. (5.36) is precisely the one-loop $\mathcal{O}(\alpha_s)$ correction to the quark mass operator [297]. A convenient way to regularize the NLO cross section is thus to subtract

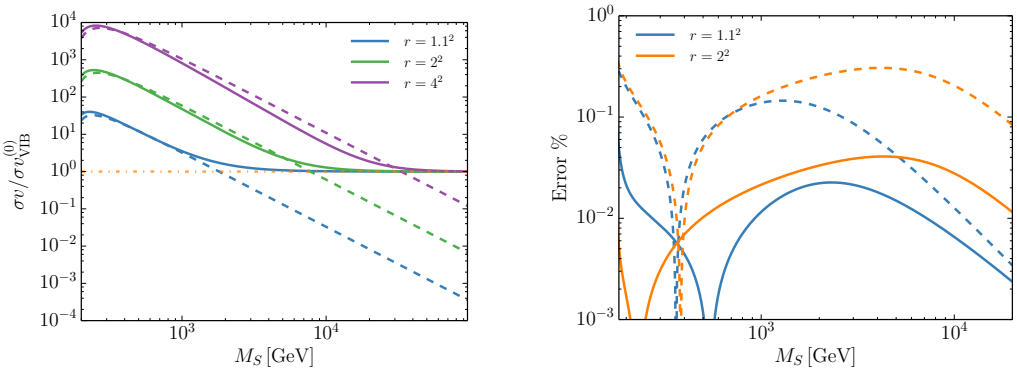

Figure 5.7: Left panel: Ratio $\sigma v_{\rm NLO}/\sigma v^{(0)}_{\rm VIB}$ as function of the DM mass M_S for three values of r. The curves are shown for $m_q = m_t$, the top quark mass. The dashed lines corresponds to $\sigma v_{q\bar{q}}$. By definition, the horizontal dot-dashed line corresponds to the VIB cross section in the massless limit, $\sigma v^{(0)}_{\rm VIB}$. Right panel: Relative error due to use of the approximate expression of Eq. (5.38) (dashed line) or Eq. (5.39) (continuous line).

from Eq. (5.34) the log-divergent term in Eq. (5.34) and replacing in the expression for $\sigma v_{q\bar{q}}$ the quark mass parameter m_q by the running mass [303]

$$m_q \to \bar{m}(M_S) = m_q \left(\frac{\ln(m_q^2/\Lambda^2)}{\ln(M_S^2/\Lambda^2)} \right)^{\frac{4}{b_0}} \tag{5.37}$$

with $b_0 = 11 - 2/3 n_f$ the leading order function with n_f the number of quarks lighter M_S and $\alpha_s(M_S^2) = 4\pi/b_0 1/\ln(\mu^2/\Lambda^2)$.

We now move on to discuss a useful approximation for the expression of Eq. (5.34), which is more practical than the original expression and differs from it by a known value. In Fig. 5.7a we show the ratio of the full $\sigma v_{\rm NLO}$ cross section expression over the limiting expression $\sigma v^{(0)}_{\rm VIB}$ of Eq. (A.6): as presented in the App. 5.3.2 in fact, in the limit of large z ratio the $\sigma v_{\rm NLO}$ reduces to the exclusive VIB contribution $\sigma v^{(0)}_{\rm VIB}$ from effectively massless final states. This a consequence of the fact that in this limit the FSR effects are proportional to $\sigma v_{q\bar{q}} \to 0$. For lower DM masses, the cross section is dominated by the chirally suppressed component $\propto \sigma v_{q\bar{q}}$. For increasing $r = (M_\psi/M_S)^2$, the VIB contribution is relatively suppressed, as it scales like $\sigma v_{\rm VIB} \propto r^{-4}$ while $\sigma v_{q\bar{q}} \propto r^{-2}$, see Eqs. (5.13– 5.15). Crossing of $\sigma v_{q\bar{q}}$ and the VIB cross section occurs roughly for $z \approx 0.21 \alpha_S C_F/2\pi r$ with $m_q \equiv m_t$ in the figure and the factor $0.21 \equiv 7/2 - \pi^2/6$, see Eq. (A.7). We thus learn that the NLO cross section $\sigma v_{\rm NLO}$ is reasonably approximated by the following simple expression, in which the leading two-body cross section $\sigma v_{q\bar{q}}$ is added to the VIB cross section in the massless limit,

$$\sigma v_{\rm NLO} \approx \sigma v_{q\bar{q}} + \sigma v^{(0)}_{\rm VIB} \,. \tag{5.38}$$

The relative error, or in other words the K-factor for QCD corrections defined through $\sigma v_{\rm NLO} = \sigma v_{q\bar{q}}(1 + K)$, is at worst of order 20 %, see Fig. 5.7b. A better

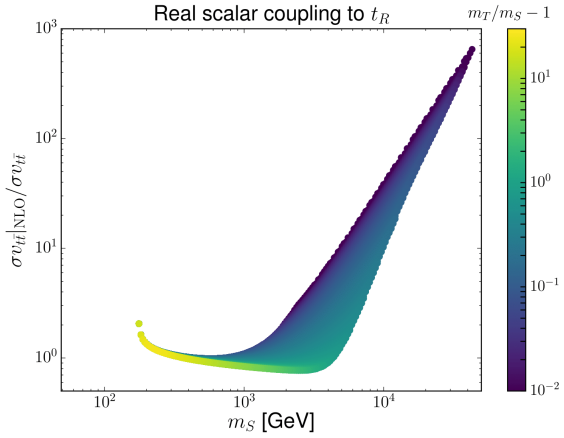

Figure 5.8: Ratio of the exact NLO DM annihilation cross section $\sigma v_{t\bar{t}g}|_{\rm NLO}$ to the two-body LO cross section $\sigma v_{t\bar{t}}$. This shows that gluon radiation constitutes the dominant component of the annihilation cross section for DM masses satisfying $M_S \gtrsim 5$ TeV. In the figure, all points correspond to models matching the correct DM abundance and the color code represents the value of $r - 1$. The feature observed for $M_S \gtrsim m_t$ is spurious as correct predictions must include threshold effects that we could not include here. *This plot is courtesy of L. Lopez Honorez.*

approximation can be obtained by replacing $\sigma v_{q\bar{q}}$ with the NLO two-body cross-section for the effective theory in Eq. (5.38):

$$\sigma v_{\rm NLO} \approx \sigma v_{q\bar{q}}^{\rm eff,NLO} + \sigma v_{\rm VIB}^{(0)} \,. \tag{5.39}$$

This is little surprise, as our NLO calculation is built upon the effective operator in Eq. (5.4), which should lead to the dominant contribution to the cross section when VIB emission may be neglected. Our calculations also show that interference terms play little role, even when VIB is relevant. What it is more difficult to assess is how large is the error made by using the effective theory instead of the full one-loop amplitudes depicted in Fig. 5.5. Based on the conclusions in the analogous case of Majorana dark matter [297], we expected it not to be larger than a few percent. In our [298] we have used the approximation of Eq. (5.39) in combination with numerical codes for DM abundance calculations, like `MicrOMEGAs`. A typical result based on our analysis can be observed in Fig. 5.8, where for all benchmark points giving rise to the right DM abundance, we plot the ratio of the exact NLO result to the LO predictions $\sigma v_{t\bar{t}}$. For high DM masses we enter the regime of validity of the chiral limit approximation. Here the viable region of has almost degenerate S and ψ masses, thus yields large VIB contribution.

5.4 GAMMA-RAY SPECTRA

In the previous section we mentioned that determining $\sigma v_{\rm NLO}$ is relevant for determining the relic abundance of the dark matter S. Total cross sections generically set the scale for indirect searches, as they constitute the normalization factor in the expression for the spectrum

$$\frac{dN}{d\omega} = \frac{1}{\sigma}\frac{d\sigma}{d\omega} \,, \tag{5.40}$$

where ω stands for the energy of the emitted gamma or gluon and σ is the total annihilation cross section into a specific channel. In order to asses the indirect indirect signature from DM annihilation, say into gamma-rays, we need to take into account both the gamma-ray contribution produced directly by the annihilation process (*i.e.* prompt photons or gluons produced at the partonic level) and those that will emerge from the process of fragmentation into hadrons from both the quark-antiquark final state and the gluon from bremsstrahlung. The latter kind of processes requires to resort to Monte Carlo simulation tools, like `PYTHIA` [308], which we discuss later on in this section. While Eq. (5.32) is in principle all we need to determine for the spectrum of prompt gluons or gammas, its expression is however not very convenient, as it involves the cumbersome expression S_0. A first useful approximation consists in replacing the expression of Eq. (5.32) by

$$\frac{d\sigma}{d\omega} \approx \frac{d\sigma_{FSR}}{d\omega}\bigg|_{m_q \neq 0} + \frac{d\sigma^{(0)}_{VIB}}{d\omega} \,. \tag{5.41}$$

The first term in this expression is the differential cross section for emission of a massless boson using the effective theory, calculated from the amplitude corresponding to the term in (5.13) and depicted in Figs. 5.3a and 5.3b. The second term in Eq. (5.41) is the differential cross section for VIB obtained from the operator of Eq. (5.18), corresponding to the diagram in Fig. 5.2c. The superscript in $d\sigma^{(0)}_{VIB}/d\omega$ refers to the limit of a massless quark, see Eq. (A.5) in Sec. A.2. The *rationale* behind Eq. (5.41) is that is mostly relevant in the limit $m_q \ll M_S$, provided the mediator is not much heavier than the DM particle. As for intermediate regimes, we refer to Fig. 5.9 to show the goodness of our *ansatz*: the solid black line obtained from the full calculation of the differential cross section and the the dotted blue line coming from Eq. (5.41) have indeed an almost indistinguishable profile. This comes at the price of shifting the energy ω in the differential cross section for the VIB contribution to $\omega + m_q^2/M_S$, in order to take into account the finite quark mass effect at the end-point of the gamma-ray spectrum. An even simpler approximation for the expression of the spectra involves the standard splitting function for emission of gamma by a final state fermion [309],

$$\mathcal{F}(\omega) = \frac{M_S^2 + (M_S^2 - \omega)^2}{M_S} \frac{1}{\omega} \,, \tag{5.42}$$

such that the FSR component of Eq. (5.41) can be written as

$$\frac{d\sigma_{FSR}}{d\omega} \approx \sigma v_{q\bar{q}} \left(\frac{\alpha Q^2}{\pi}\right) \left\{ \mathcal{F}(\omega) \ln\left(\frac{4M_S(M_S - \omega)}{m_q^2}\right) - \frac{2M_S}{\omega} \right\} \,, \tag{5.43}$$

where the factor αQ^2 must be replaced by $\alpha_s C_F$ in the case of a gluon emission. This expression exactly reproduces $d\sigma_{FSR}/d\omega$ in the limit $m_q \ll \omega \sim M_S$. Integrating over ω down to a cut-off energy ω_0 leads to the characteristic Sudakov double logarithmic divergence $\propto \ln(m_q^2/M_S^2) \ln(m_q^2/\omega_0^2)$ which is found in the expression of Eq. (5.33). The last term in Eq. (5.43) is non-universal, but is kept for a better matching to the exact result. The dashed red line in Fig. 5.9 shows the differential cross section obtained by summing the contribution from Eq. (5.43) to VIB in the massless limit. The matching is not as good as the approximation

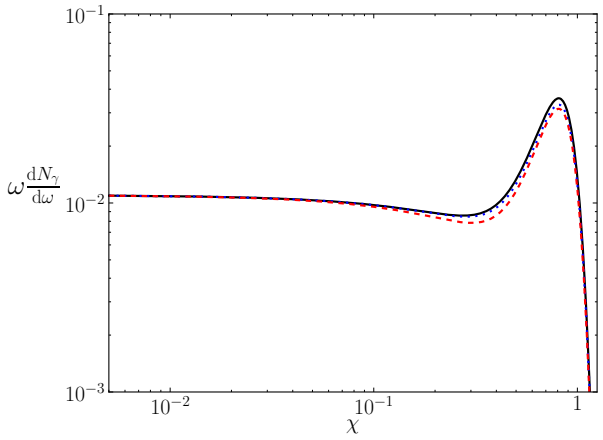

Figure 5.9: Gamma-ray spectra at partonic level resulting from an $M_S = 2$ TeV DM candidate annihilating into top-antitop. The spectra has been normalized to the LO 2-body cross section $\sigma v_{q\bar{q}}$. The black solid line corresponds to the full expression of Eq. (5.32), while the blue dotted line comes from the expression of Eq. (5.41) and the dashed red line from Eq. (5.43). The spectra have been convolved with a Gaussian window function with resolution of 10%. For all curves the vector-like mediator has a mass $M_\psi = 2.4$ TeV.

of Eq. (5.41), but it comes with the advantages of being much simpler and more physically transparent.

We now want to study the spectra resulting from the DM annihilation into a three-body final states, with both gluons and gammas produced in the fragmentation process. The standard procedure for this kind of study consists of producing a Monte-Carlo distribution of events by using `CalcHEP` [310] first, then the output is fed into `PYTHIA` [308], which takes care of the hadronization processes. This strategy was used in Ref. [296] for the case of coupling of the vector-like portal to light quarks, where one could simply neglect the quark mass and thus the 2-body annihilation process, due to the chiral suppression. In general however, the fermion mass and the associated FSR may not be neglected. This introduces a difficulty in our numerical analysis: the sharp peaks in the distribution associated with collinear and infrared divergences from FSR emission needs to be tamed with a cut off on the energy of the emitted particle, as well as on the angle at which the boson was radiated, otherwise the statistics of the distribution is not reliable. Applying such a procedure by hand for each point in the parameter space if of course impractical and not rigorous, and we discard it.

Let us instead go back to the decomposition of the differential cross section into soft and hard modes and see how it can help us with the production of the spectra. This splitting has an immediate advantage, which is that hard modes can undergo the straightforward implementation through `CalcHEP` first and then `PYTHIA` described above, since they are free of collinear and infrared divergences. For soft modes on the other hand, only FSR is relevant, thus we rely on the `PYTHIA` implementation of radiative correction to a two-body process through Sudakov factors.

A question which needs to be addressed is where to place the cut off that separates soft and hard modes in order to have a good matching between these two regimes. This is of particular importance because both non-inclusive cross sections show a dependence on the cut off as an argument of the divergent Sudakov dou-

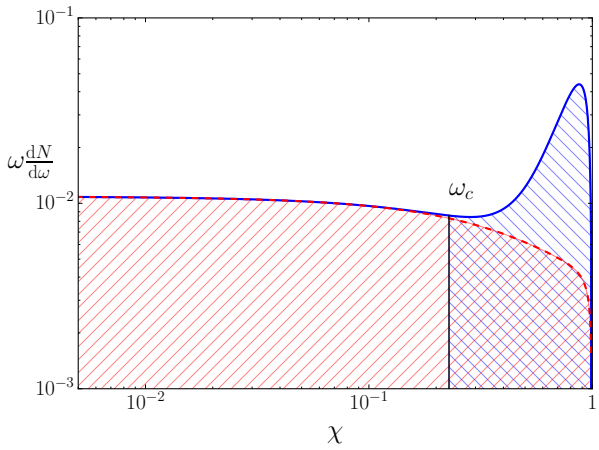

Figure 5.10: Comparison between the differential cross section for gluon emission in full theory (blue line) and effective theory (red line). The hatched red and blue are respectively the soft and hard contributions. The crossed region is the one included in both soft and hard spectra, so it should be subtracted in order to avoid double-counting.

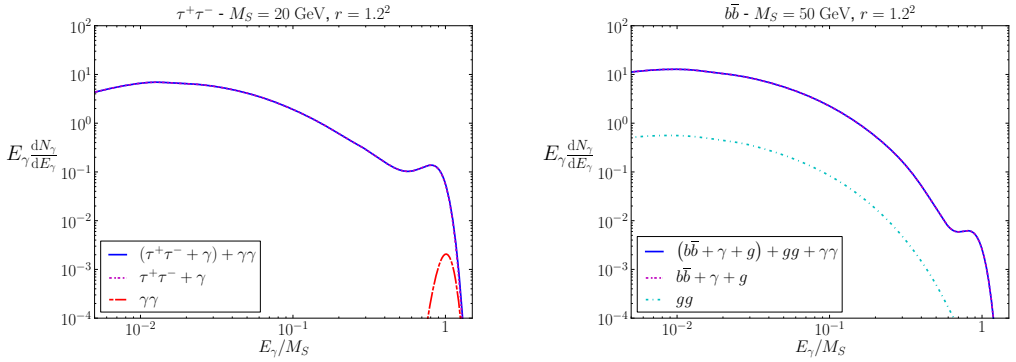

Figure 5.11: Gamma ray spectrum from annihilation into $\tau^+\tau^-$ (left) or $b\bar{b}$ (right) channels.

ble log factor, see *e.g.* the factor $\ln\left(\frac{1+\beta_0}{1-\beta_0}\right)\ln\left(\frac{\beta_0^4 M_S^2}{\omega_0^2}\right)$ in Eq. (5.33). In Fig. 5.10 we compare the spectrum obtained in our full theory with the one resulting from the effective theory, corresponding to the blue and red curve, respectively. Here we choose ω_c as the energy where the differential cross section in the effective theory departs from the one in the full theory, within a 5% error. Once ω_c is determined, it is straightforward to obtain the spectra for $\omega > \omega_c$ as described above for the hard modes. For soft modes instead, within `PYTHIA 8` we did not find a simple way to extract partonic level events with gluons or photons with energy $\omega < \omega_c$. The procedure we adopted was instead the following: first, we generate the complete gamma-ray spectrum from the 2-body process with `PYTHIA`, including FSR. Second, we use `CalcHEP` to simulate the distribution of hard gluons and gammas events with $\omega > \omega_c$, using the analytical cross section for the two-body process with FSR only. Third, we feed this distribution into `PYHTIA`, that generates the hadronization showers. Fourth, this is then subtracted from the initial distribution, in order to obtain the hadronized events originated from a three-body process

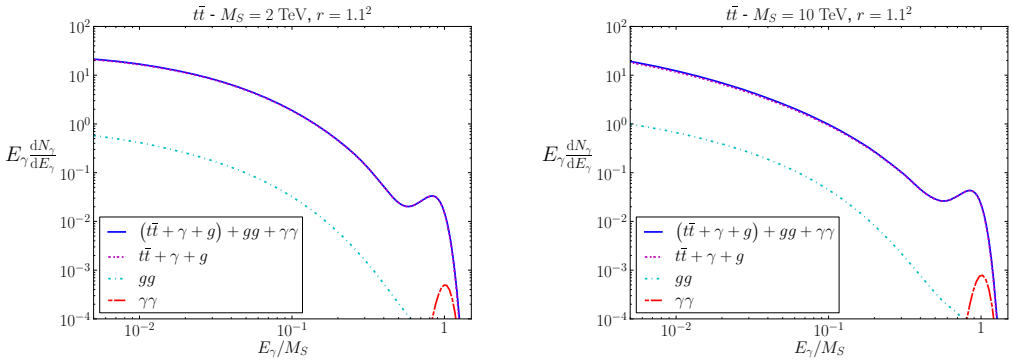

Figure 5.12: Characteristic gamma-ray spectrum from annihilation into $t\bar{t}$.

with a soft gluon in the final state. Finally we add back the hard part from the full theory, which includes VIB effects, and get the final gamma-ray spectrum.

The annihilation of pairs of S proceeds into different final states: quark-antiquark pair (with or without the emission of a single gluon or a photon, they are indistinguishable events to us as we consider the full inclusive three-body cross section), a pair of gammas, a pair of gluons. Therefore the total photon spectrum is eventually given by the sum of the photon spectrum originating from each possible final state,

$$\frac{dN_\gamma^{tot}}{dE_\gamma} = \frac{1}{\sigma_{t\bar{t}+\gamma+g}} \frac{dN_\gamma}{dE_\gamma}\bigg|_{t\bar{t}+\gamma+g} + \frac{1}{\sigma_{\gamma\gamma}} \frac{dN_\gamma}{dE_\gamma}\bigg|_{\gamma\gamma} + \frac{1}{\sigma_{gg}} \frac{dN_\gamma}{dE_\gamma}\bigg|_{gg} , \tag{5.44}$$

weighted with their respective branching ratios. For the sake of illustration, we now consider different SM fermionic final states for which the fermion mass may be a relevant parameter. Specifically, in the left (right) panel of Fig. 5.11 we show the spectra obtained with $\tau^+\tau^-$ ($b\bar{b}$) final states, while both panels of Fig. 5.12 are for top final states. All spectra shown have $z \approx (m_q/M_S)^2$ and $r = \left(M_\psi/M_S\right)^2 = 1.1^2$ or $r = 1.2^2$, respectively, with M_S and M_ψ adjusted accordingly. We have included for completeness the contribution from annihilation at one-loop into two gluons and into $\gamma\gamma$, assuming a gamma-ray detector with resolution $\Delta E_\gamma/E_\gamma = 10\%$. The parameters of the DM model are chosen so as to illustrate the possible presence of a feature in the final gamma-ray spectrum, not taking into account other possible constraints, *i.e.* relic abundance, direct, indirect and collider constraints.

5.5 SUMMARY AND RESULTS

We have studied radiative corrections to a simple DM scenario, where a real scalar particle annihilating into SM fermions through a heavy vector-like fermion. This topic has been already covered in several phenomenological studies [67, 288, 294–296] that focused on coupling to light quarks or leptons, but we expanded the discussion to the case of massive final states. Due to infrared and collinear divergences that affect bremsstrahlung of massless gauge bosons, the extension of these results to heavy quarks (or annihilation into a $\tau^+\tau^-$ pair) poses some technical problems. In particular, following the proposal of Ref. [297], we have adapted an effective approach suited for emission of soft gamma or gluons and that circum-

vent several unnecessary steps in the regularization of infrared divergences. From an effective approach perspective, much of the calculations map to the equivalent problem of radiative corrections to Higgs decay into SM fermions [303, 304]. In order to determine the gamma-ray spectra resulting from DM annihilation, we have discussed several simple approximations both for the differential and total three-body cross sections. We used them together with software tools CalcHEP and PYHTIA, which otherwise do not take into account VIB other than for the massless case. Our result for the total three-body cross section entered the bigger analysis of our Ref. [298], in which an extensive study of the available parameter space for the top-philic vector-like portal was performed. Considering constraints from relic abundance, collider production, indirect and direct detection, we show that a only a fraction the parameter space for this simple model is currently tested, see Fig. (11) in Ref. [298].

6

SUMMARY AND CONCLUSION

The success that the Standard Model (SM) achieved over the last fifty years in describing particle physics is an unprecedented achievement in the history of science. Its consistent mathematical framework for electromagnetic, weak and strong forces has been tested to great accuracy over a plethora of high energy phenomena and was able to predict the existence of several particles. Yet the SM explains only three out of the known four forces in nature, with gravity still out of the picture, yielding - among others - the consequence that the particle nature of dark matter is still a mystery to us. Despite the great experimental effort among various kinds of complementary searches, what it is estimated to represent about 27 % of the energy budget of our universe does not interact in any known way with ordinary matter.

In 2012 the long anticipated discovery of a particle exhibiting the properties of the scalar boson of the SM finally occurred during the Run 1 of the LHC. This completed the observation of the SM mass spectrum and confirmed the goodness of this theory to yet a higher degree of precision. Not without a certain irony though, the very experiment which made possible such a scientific triumph, disappointed many of the expectations that physicists in relation to BSM physics. To date in fact, analyses of the collisions happening at Run 2 of LHC did not show any evidence of new particles. This caused more than an eyebrow to raise in front of theories which were long believed to be the most promising candidates to extend the SM and to find an answer to the questions which it leaves pending, among which the one regarding a valid DM particle.

In particular, the most minimal models implementing supersymmetry are subject to increasing tension with the data. While this surely causes some discontent in the particle physics community, some among the theorists may even consider this null result a blessing. Model building in particle physics enjoys a bigger freedom of exploring models which produce a phenomenology that escapes the current searches. For what concerns our research more closely, this strengthens the motivation to explore dark matter scenarios which are either less minimal extensions of the MSSM or do not rely on SUSY.

For the first and main part of this manuscript, we choose to pursue the first option and study extended supersymmetric theories which, together with the usual "mirrored" particle content of the MSSM, includes an extra superfield, the axion. As outlined in detail in Ch. 2, the reason to add this new particle stems from a theoretical shortcoming of the SM. According to its gauge symmetries in fact, the operator $\sim \bar{\theta}\widetilde{F}^{\mu\nu}_{a}F^{a}_{\mu\nu}$ in the Lagrangian is allowed. While the $\bar{\theta}$ parameter is naturally expected to be of order one, observations of CP-violation set an upper bound of $\bar{\theta} < 10^{-10}$. Postulating the presence of an extra broken $U(1)_{PQ}$ global symmetry for the SM and an extra pseudoscalar particle, the axion, offers an elegant dynamical solution to this issue. We present the original DFSZ axion model, which has the most minimal particle content in the class of invisible axion models. Those are the models where f_a, the scale for the breaking of $U(1)_{PQ}$, is set to energies higher than $\sim 10^9$ GeV, otherwise they would be ruled out by astrophysics. In order to con-

sistently achieve both $U(1)_{PQ}$ breaking and SUSY breaking in such axion models, it is necessary to add two extra axion-like superfields.

In Ch. 3 we critically review the possibility that the axino, the supersymmetric partner of the axion, could explain the 3.5 keV line observed in 2014 by means of its radiative decay with a final state photon. After a brief analysis of the more general case of a decaying sterile neutrino, we show how the measured dark matter flux can be matched by a fermionic SM singlet that mixes with active neutrinos. We take into account constraints from the axino relic density and from a light gravitino, which is naturally present in the context of SUGRA. Using effective axion-gauge interactions, we show how the signal can be produced in both the R-parity conserving and the R-parity violating SUSY case, where the axino decay products that accompany the photon are a bino or a neutrino, respectively. The R-parity conserving case is strongly disfavoured by BBN and CMB bounds. In the second case we study how the cosmological constraints on neutrino masses can be translated into upper limits for the neutralino mixings and, in turn, for the decay rate of the axino into a photon and a neutrino. We also assess the implications of having the lightest neutralino mass well below the TeV range. Eventually we find that only a narrow region between 100 MeV and 10 GeV is allowed. While this region evades all current bounds, our study casts overall serious doubts on the axino hypothesis for the keV line.

In Ch. 4 we move on to discuss a complete supersymmetric model with a DFSZ axion. We include the LLE and LQD R-parity violating operators in our superpotential, as well as the terms with only the axion-like singlets and the ones connecting the two sectors. The model provides two DM candidates, the axion and the axino. The former is a warm dark matter candidate, which is well motivated by the small structure problem, while the latter is cold dark matter in the mass range we consider. At the expense of tuning a single parameter in the superpotential, we make the axino mass vary in the range $m_{\tilde{a}} \sim \mathcal{O}(1-100)$ keV. In this mass window the axino is stable thanks to its long lifetime resulting from its dominant channels into three neutrinos or into a neutrino plus an axion. Its subdominant channels with a photon in the final state allows us to constrain the model with X-ray and gamma-ray signals, which exclude certain regions in the $f_a - m_{\tilde{a}}$ plane, together with the bound from overproduction of mixed axion-axino dark matter. We distinguish the two scenarios in which the production mechanism of axion dark matter happens mostly through either cosmic string decay or misalignment mechanism, depending whether the reheating temperature is larger or smaller than $f_a \sim O(10^{10} - 10^{12})$ GeV. We study in detail the various loop decays that contribute to the decay width of the axino into a photon plus a neutrino, obtaining precise analytical estimates. For the specific case of the dark matter being solely constituted by the axino, we obtain bounds on the RpV parameters λ_{233} and λ'_{i33}, with $i = 2, 3$. We provide a benchmark point where the axino decay can explain the 3.5 keV line, although the debate about its possible astrophysical nature is still open. Future developments could include exploring further details of these models in relation to neutrino physics or possible collider features.

In Ch. 5 we move to a different scenario for dark matter and study the simplified model dubbed *vector-like portal*. Here the DM is a real scalar particle S annihilating into SM quarks or leptons through a fermionic heavy mediator. We are interested in the case of spectral signatures from virtual internal internal bremsstrahlung,

which can be very pronounced when the mediator and the dark matter are almost degenerate in mass. They can also drive the relic abundance, due to the chiral suppression of the two-body process. We focus specifically on the technical aspects of the calculation of the cross section for the three-body process for the case of heavy final states, which is useful for a top-philic scenario. In particular, we show how considering an effective approach for the case of low dark matter velocity simplifies the process, although maintaining the necessary cancellation of IR and UV divergences among the soft, hard and virtual modes. Several approximations for the differential cross sections are discussed, then applied in order to produce VIB in the photonic spectra from hadronization through Monte Carlo simulations. Our analysis enters in the extensive study of our Ref. [298], where all constraints from complementary searches to the top-philic scenario are considered. Currently only a small fraction of the available paramer space for this model is tested. Increased energy reach at colliders are needed for further analyses.

Particle physics models assuming new physics at the TeV scale are currently under pressure. With only two years left for LHC to run, the hopes for finding anything different from a null result are getting lower. Perhaps the assumption of new TeV-scale particle(s) that we used throughout our work might indeed be almost completely falsified, leaving us with the necessity of completely rethink our approach to the subject. On the other hand, axion searches (star cooling, solar axions, light shining through walls, ...) will keep setting limits on the axion mass and/or the value of the scale f_a, while direct and indirect DM searches will continue test the validity of the WIMP dark matter paradigm. New exciting territories in particle physics phenomenology are waiting around the corner, even if one may have to give up some of our long-standing beliefs about how nature works.

A

APPENDIX

A.1 AXINO-GAUGINO MIXING

In Sec. 4.4 most of the amplitudes involved in the radiative decay of the axino bear a strong dependence on its mixing with some of the other neutralino mass eigenstates. In Ch. 4 we rely on well-motivated estimates for these quantities, but in order to obtain their precise values one should diagonalize the neutralino mass matrix $\mathcal{M}_N$. While an exact analytical algorithm exists for the case of the MSSM [311], adding one more mass eigenstate, as for the case of the Next-to-Minimal Supersymmetric Standard Model (NMSSM), does not allow for a closed-form solution. In this section we show how the approximate block-diagonalization procedure of Ref. [312] for the NMSSM 5x5 neutralino mass matrix can be used to obtain a numerical value for the axino-gaugino mixing. The only requirement is a small mixing between the the singlet and the doublet states, which in our case corresponds to the mixing between any of the two Higgs doublets and the axion field A. From $\mathcal{M}_N$ in Eq. (4.23) we see that such mixing is indeed small, since $\frac{c_1 v_{u,d}}{\sqrt{2}} \approx \frac{\mu_{eff}}{f_a} \lesssim 10^{-7}$. Recalling that the axino mass eigenstate consists of a linear combination of the fermionic components of the fields A and $\bar{A}$ only, we define the following neutralino mass 5x5 sub-matrix:

$$\mathcal{M}_5 = \begin{bmatrix} M_1 & 0 & \frac{g_1 v_u}{2} & -\frac{g_1 v_d}{2} & 0 \\ 0 & M_2 & -\frac{g_2 v_u}{2} & \frac{g_2 v_d}{2} & 0 \\ \frac{g_1 v_u}{2} & -\frac{g_2 v_u}{2} & 0 & -\frac{c_1 v_A}{\sqrt{2}} & -\frac{c_1 v_d}{\sqrt{2}} \\ -\frac{g_1 v_d}{2} & \frac{g_2 v_d}{2} & -\frac{c_1 v_A}{\sqrt{2}} & 0 & -\frac{c_1 v_u}{\sqrt{2}} \\ 0 & 0 & -\frac{c_1 v_d}{\sqrt{2}} & -\frac{c_1 v_u}{\sqrt{2}} & m_{\tilde{a}} \end{bmatrix}, \tag{A.1}$$

where the axino mass $m_{\tilde{a}}$ is the lightest eigenvalue which results from the diagonalization of the 3x3 lower-right block of the neutralino mass matrix $\mathcal{M}_N$ in Eq. (4.23). The diagonalization of $\mathcal{M}_5$ proceeds in two steps: first, the 4x4 matrix V rotates only the MSSM upper-left 4x4 block into a diagonal form; next a second matrix block-diagonalizes the full resulting 5x5 matrix, in a way that the 4x4 MSSM sub-matrix $\mathcal{M}_{\tilde{\chi}^0}$ is still diagonal up to corrections of the second order in the singlet-doublet mixing parameter μ_{eff}/f_a.

The 5x5 unitary matrix U which combines these two steps is

$$U = \begin{bmatrix} \mathbb{1}_4 - \frac{1}{2}(V\Lambda)(V\Lambda)^T & (V\Lambda) \\ -(V\Lambda)^T & 1 - \frac{1}{2}(V\Lambda)^T(V\Lambda) \end{bmatrix} \begin{bmatrix} V & 0 \\ 0 & 1 \end{bmatrix}, \tag{A.2}$$

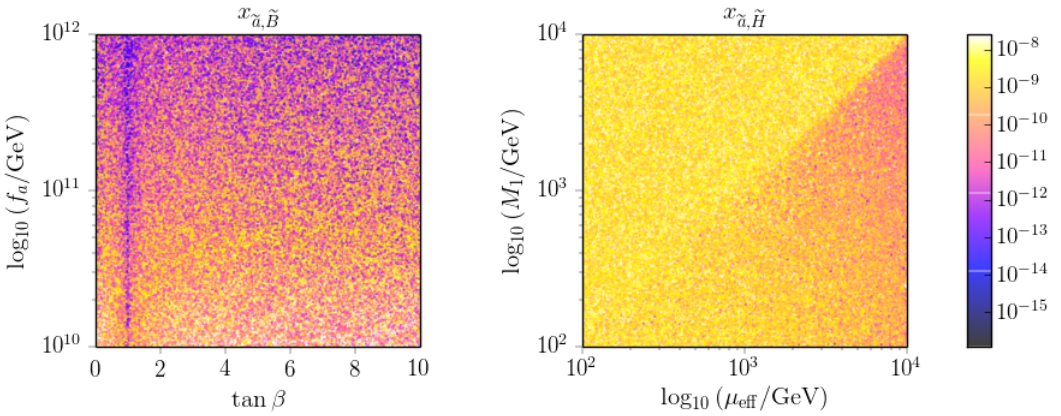

Figure A.1: Distribution of the mixings $x_{\tilde{a},\tilde{B}}$ and $x_{\tilde{a},\tilde{H}}$ obtained by numerical evaluation of the eigenvalues of $\mathcal{M}_4$. We run 10^5 points randomly varying $10^2\,\mathrm{GeV} < M_{1,2}, \mu_{\mathrm{eff}} < 10^4\mathrm{GeV}$, $1 < \tan\beta < 10$, $10^{10}\,\mathrm{GeV} < f_a < 10^{12}\,\mathrm{GeV}$, $1\,\mathrm{keV} < m_{\tilde{a}} < 10^2\,\mathrm{keV}$. From our estimate in Eq. (4.32) [Eq. (4.33)] we expect $x_{\tilde{a},\tilde{H}}$ [$x_{\tilde{a},\tilde{B}}$] to lie somewhere in the range between approximately 10^{-10} and 10^{-8} GeV [10^{-12} and 10^{-10} GeV], depending on the value of f_a.

with

$$\Lambda = -\frac{m_{\tilde{a}}}{\det\left(\mathcal{M}_4 - \mathbb{1}_4 m_{\tilde{a}}\right)} \begin{bmatrix} (M_2 - m_{\tilde{a}})\, g_1 \frac{v}{2} \mu_{\mathrm{eff}} \cos 2\beta \\ (M_1 - m_{\tilde{a}})\, g_2 \frac{v}{2} \mu_{\mathrm{eff}} \cos 2\beta \\ (M_1 - m_{\tilde{a}})\,(M_2 - m_{\tilde{a}})\,(\mu_{\mathrm{eff}} \sin\beta - m_{\tilde{a}} \cos\beta) - M_\star^3 \cos\beta \\ (M_1 - m_{\tilde{a}})\,(M_2 - m_{\tilde{a}})\,(\mu_{\mathrm{eff}} \cos\beta - m_{\tilde{a}} \sin\beta) - M_\star^3 \sin\beta \end{bmatrix}, \tag{A.3}$$

and $M_\star^3 = \frac{v^2}{4}\left[(M_1 - m_{\tilde{a}})\, g_2^2 + (M_2 - m_{\tilde{a}})\, g_1^2\right]$. The axino-gaugino mixings can then be read off from the off-diagonal entry $\sum_{j=1}^{4} V_{ij}\Lambda_j$ of U, with $j = \widetilde{B}_0, \widetilde{W}_0, \widetilde{H}_u^0, \widetilde{H}_d^0$. In Fig. A.1 we show two examples of how a more careful analysis can change significantly such quantities, and thus ultimately the phenomenology of the model. This possibly constitutes caveats to our above reasoning. In the left panel we observe that a value of $\tan\beta$ close to 1 strongly suppresses the value of $x_{\tilde{a},\tilde{B}}$, such that our previous estimates are off by several orders of magnitude. In the right panel instead we see how allowing for larger values of μ_{eff} might lower $x_{\tilde{a},\tilde{H}}$, if $M_1 < \mu$.

A.2 S_0 AND LIMITING BEHAVIOURS

The expression for the differential cross section in Eq. (5.32) contains the function $S_0(\chi)$, a very lengthy expression which can be found in the appendix of our work [298]. Here we provide it only in the limit of $z = m_q^2/M_S^2 \to 0$, where it reduces to

$$S_0(\chi)|_{z=0} = \frac{1-\chi}{(Y-2\chi)\,(Y-\chi)^3}\left[\frac{(Y-\chi)}{Y}\chi\left(Y^2 - 2Y\chi + 2\chi^2\right) + \frac{Y}{2}(Y-2\chi)^2 \ln\frac{Y-2\chi}{Y}\right], \tag{A.4}$$

with the shorthand $Y \equiv 1+r-z$. For annihilation in an s-wave, the LO cross section vanishes, $\sigma v_{q\bar{q}}|_{z=0} = 0$. Thus all the complications induced by IR divergences drop, and one recovers the known expressions for VIB for the differential cross section for massless fermionic final states [295],

$$\frac{d\sigma^{(0)}_{\rm VIB}}{d\omega} = \frac{N_c y_f^4}{8\pi M_S^3}\frac{\alpha_S C_F}{\pi}\frac{1-\chi}{1+r}\frac{1}{(1+r-2\chi)(1+r-\chi)^3}\Bigg[2(1+r-\chi)\chi \times \left((1+r)^2 - 2(1+r)\chi + 2\chi^2\right) - (1+r)^2(1+r-2\chi)^2 \ln\frac{1+r}{1+r-2\chi}\Bigg], \tag{A.5}$$

as well as the total cross section

$$\sigma v^{(0)}_{\rm VIB} = \frac{N_c y_f^4}{8\pi M_S^2}\frac{\alpha_S C_F}{\pi}\left\{(r+1)\left[\frac{\pi^2}{6} - \ln^2\frac{1+r}{2r} - 2{\rm Li}_2\left(\frac{1+r}{2r}\right)\right] + \frac{4r+3}{r+1} + \frac{4r^2-3r-1}{2r}\ln\frac{r-1}{r+1}\right\}. \tag{A.6}$$

While approaching the limit $r \to 1$ of degenerate S and ψ,

$$\sigma v^{(0)}_{\rm VIB} \to \frac{N_c y_f^4}{8\pi M_S^2}\frac{\alpha_S C_F}{\pi}\left(\frac{7}{2} - \frac{\pi^2}{3}\right). \tag{A.7}$$

in the opposite limit $r \gg 1$, VIB can be neglected.

With a factor of $\sigma v_{q\bar{q}}$ replacing the tree level decay rate of the Higgs, we recover the expression of Ref. [303] (taking into account their errata)

$$\sigma v^{\rm NLO}_{q\bar{q}} = \sigma v_{q\bar{q}}\frac{C_F\alpha_S}{\pi}\left\{\frac{A(\beta_0)}{\beta_0} + \frac{3+34\beta_0^2-13\beta_0^4}{16\beta_0^3}\ln\frac{1+\beta_0}{1-\beta_0} + \frac{3}{8\beta_0^2}\left(-1+7\beta_0^2\right)\right\}, \tag{A.8}$$

where

$$A(\beta_0) = \left(1+\beta_0^2\right)\left[4{\rm Li}_2\left(\frac{1-\beta_0}{1+\beta_0}\right) + 2{\rm Li}_2\left(-\frac{1-\beta_0}{1+\beta_0}\right) - 3\ln\frac{2}{1+\beta_0}\ln\frac{1+\beta_0}{1-\beta_0} - 2\ln\beta_0\ln\frac{1+\beta_0}{1-\beta_0}\right] - 3\beta_0\ln\frac{4}{1-\beta_0^2} - 4\beta_0\ln\beta_0\,. \tag{A.9}$$

A.3 PHASE-SPACE INTEGRATION FOR THE SOFT MODES

This appendix addresses some technical aspects of the calculation performed in Sec. 5.3, specifically for the quantity $\Delta\tilde{\sigma}v|^{\rm eff}_{\rm soft}$. The reason why we choose to present the procedure followed in order to obtain this particular quantity rather than any other one lies in the fact that it exemplifies all the general techniques used throughout the paper, yet it involves expressions which are compact enough to be readable. We will follow closely the procedure outlined for the QED case in [305]. Our starting point is the amplitude of Eq. (5.21): it describes the annihilation of a pair of S into two quarks with the associated emission of a soft gluon. It corresponds to the FSR amplitude in the first line in the expansion of Eq. (5.13), also depicted

in Figs. 5.3a and 5.3b. After we sum over final spins and polarization states[1] the amplitude squared for this process can be factorised as

$$\langle|\overline{\mathcal{M}}^{\text{eff}}_{\text{soft}}|\rangle^2 = 16N_c\frac{g_f^2y^4}{r^2}\frac{m_q^2}{M_S^4(1+r-z)}(p_1\cdot p_2-m_q^2)\sum_\lambda|\mathcal{J}_{\text{eik}}|^2, \tag{A.10}$$

where the square of the eikonal factor of Eq. (5.16) reads

$$\sum_\lambda|\mathcal{J}_{\text{eik}}|^2 = -m_q^2\left(\frac{1}{(p_1\cdot k+\lambda^2)^2}+\frac{1}{(p_2\cdot k+\lambda^2)^2}\right)+\frac{2p_1\cdot p_2}{(p_1\cdot k+\lambda^2)(p_2\cdot k+\lambda^2)}\,, \tag{A.11}$$

k is the gluon momentum and λ is the fictitious mass of the photon. We now define two kinematic variables

$$\omega\equiv E_g\quad,\quad x\equiv E_q-E_{\overline{q}}\quad, \tag{A.12}$$

such that we can write, with $M=2M_S$ from now on,

$$E_q=-x+\frac{M-\omega}{2}\quad,\quad E_{\overline{q}}=x+\frac{M-\omega}{2}\quad, \tag{A.13}$$

and the resulting scalar products are

$$\begin{aligned}2\,p_1\cdot k &= M(\omega-2x)-\lambda^2\,,\\ 2\,p_2\cdot k &= M(\omega+2x)-\lambda^2\,,\\ 2\,p_1\cdot p_2 &= M^2-2M\omega-2m_q^2+\lambda^2\,.\end{aligned} \tag{A.14}$$

In terms of our new variables in Eq. (A.12) and in the approximation in which both incoming DM particles are at rest, the usual phase-space integral for the three final states,

$$I_3=\frac{1}{(2\pi^5)}\int\frac{d^3k}{d\omega^3}\frac{d^3p_1}{dE_q^3}\frac{d^3p_2}{dE_{\overline{q}}^3}\delta^4(M-k-p_1-p_2) \tag{A.15}$$

can be written as

$$I_3=\frac{1}{256\pi^5}\int d\Omega\int d\phi\int_{\lambda^2}^{\omega_m}d\omega\int_{x_-}^{x_+}dx\,. \tag{A.16}$$

For the integration limits we have defined the quantities

$$\omega_m=\frac{M^2-4m_q^2+\lambda^2}{2M}\quad,\quad x_\pm=\pm\frac{1}{2}\sqrt{\omega^2-\lambda^2}\underbrace{\sqrt{\frac{\beta_0^2-2\frac{\omega}{M}+\frac{\lambda^2}{M^2}}{1-2\frac{\omega}{M}+\frac{\lambda^2}{M^2}}}}_{\equiv\beta}\,. \tag{A.17}$$

1 We consider massless polarizations for the photon even though we introduce a small photon mass λ^2 to handle the IR divergences. We can do this because of the *Ward identity*: massive polarisations depends on the photon momentum, therefore they vanish when they multiply the total amplitude.

Since we are here interested only in the soft modes of the emitted particle, we will only consider the corner of the parameter space with gluon energies up to $\omega_0 \ll \omega_m$. Using the definitions in Eqs. (A.14), the integrals over the variable x,

$$\int_{x_-}^{x_+} dx \frac{1}{(2p_1\cdot k-\lambda^2)(2p_2\cdot k-\lambda^2)} = \frac{1}{2M^2\omega} \underbrace{\ln\left(\frac{\omega+\beta\sqrt{\omega^2-\lambda^2}}{\omega-\beta\sqrt{\omega^2-\lambda^2}}\right)}_{\equiv f(\omega)}, \tag{A.18}$$

$$\int_{x_-}^{x_+} dx \frac{1}{(2p_{1,2}\cdot k-\lambda^2)^2} = \frac{1}{M^2} \underbrace{\frac{\beta\sqrt{\omega^2-\lambda^2}}{\omega^2(1-\beta^2)+\beta^2\lambda^2}}_{\equiv g(\omega)}, \tag{A.19}$$

can be used to perform the integral over x for the eikonal factor

$$\int_{x_-}^{x_+} dx \sum_\lambda |\mathcal{I}_{eik}|^2 = \frac{M^2-2M\omega-2m_q^2+\kappa^2}{2M^2\omega} f(\omega) - 2\frac{m_q^2}{M^2} g(\omega)\,. \tag{A.20}$$

Altogether we are left with

$$\begin{aligned}
\Delta\tilde{\sigma}v|^{eff}_{soft} &= \frac{1}{256\pi^5} \cancel{\int d\Omega}^{4\pi} \cancel{\int d\phi}^{2\pi} \int_{\kappa^2}^{\omega_0} d\omega \int_{x_-}^{x_+} dx \langle|\overline{\mathcal{M}}^{eff}_{soft}|\rangle^2 \qquad (A.21)\\
&= \frac{1}{32\pi^5}\frac{g_f^2 y^4}{r^2}\frac{m_q^2}{M_S^4(1+r-z)} \int_{\kappa^2}^{\omega_0} d\omega (M^2+2M\omega-2m_q^2+\kappa^2) \int_{x_-}^{x_+} dx \sum_\lambda |\mathcal{I}_{eik}|^2\\
&= \frac{\alpha_S}{\pi}\langle\sigma v_{q\bar{q}}\rangle \int_{\lambda^2}^{\omega_0} \left[\frac{1+\beta^2}{\beta}\frac{f(\omega)}{\omega} - 2\frac{1-\beta^2}{\beta} g(\omega)\right],
\end{aligned}$$

where $\langle\sigma v_{q\bar{q}}\rangle$ is the s-wave component of the two-body cross section of Eq. (5.2), with the obvious substitution $Q^2\alpha \to C_F\alpha_s$. In the last step we have sent to zero linear terms in λ^2. We have also neglected finite terms that give a null contribution when integrated between λ^2 and $\omega_0 \ll \omega_m$. Setting $\lambda^2 = 0$ exactly in the remnant terms would let them diverge, so we need to treat them differently. Starting from the simplest function,

$$g(\omega)\Big|_{\lambda^2=0} = \frac{1}{\omega}\frac{\beta}{1-\beta^2}\,, \tag{A.22}$$

we see it contains a logarithmic divergence when integrated:

$$\begin{aligned}
G \equiv \int_0^{\omega_0} d\omega g(\omega)\Big|_{\lambda=0} &= 2(1-\beta_0^2)\int_{\beta(0)=\beta_0}^{\beta(\omega_0)} d\beta \frac{\beta}{(1-\beta^2)^2(\beta^2-\beta_0^2)}\\
&= \left[\frac{\beta}{1-\beta^2} + \frac{1}{2}\frac{1+\beta_0^2}{1-\beta_0^2}\ln\left(\frac{1+\beta}{1-\beta}\right) - \frac{\beta_0}{1-\beta_0^2}\ln\left(\frac{\beta+\beta_0}{\beta_0-\beta}\right)\right]_{\beta_0}^{\beta(\omega_0)}. \qquad (A.23)
\end{aligned}$$

In order to isolate the divergent part in the integral, let us define a similar quantity:

$$g_0(\omega) = \frac{\beta_0\sqrt{\omega^2-\lambda^2}}{\omega^2(1-\beta^2)+\beta^2\lambda^2} \tag{A.24}$$

$$\implies \quad G_0 \equiv \int_0^{\omega_0} d\omega g_0(\omega)\Big|_{\lambda=0} = -\frac{\beta_0}{1-\beta_0^2}\left[\ln\left(\frac{1-\beta^2}{\beta_0^2-\beta^2}\right)\right]_{\beta_0}^{\beta(\omega_0)}. \tag{A.25}$$

The difference $G - G_0$ is now finite when $\beta = \beta_0$:

$$G - G_0 = \left[\frac{\beta}{1-\beta^2} + \frac{1}{2}\frac{1+\beta_0^2}{1-\beta_0^2} \ln\left(\frac{1+\beta}{1-\beta}\right) + \frac{\beta_0}{1-\beta_0^2} \ln\left(\frac{(1-\beta^2)}{\cancel{(\beta_0-\beta)}(\beta_0+\beta)} \frac{\cancel{\beta_0-\beta}}{\beta_0+\beta} \right) \right]_{\beta_0}^{\beta(\omega_0)} . \tag{A.26}$$

We therefore split the $g(\omega)$ function as

$$\int_0^{\omega_0} d\omega g(\omega) = G - G_0 + \lim_{\lambda\to 0} G_t \, , \tag{A.27}$$

where, after having defined $t(\omega) = \frac{\sqrt{\omega^2-\lambda^2}}{\omega}$:

$$\begin{aligned} G_t &= \int_\lambda^{\omega_0} d\omega \frac{\beta_0\sqrt{\omega^2-\lambda^2}}{\omega^2(1-\beta_0^2)+\beta_0\lambda^2} \\ &= \frac{1}{2}\frac{\beta_0}{1-\beta_0^2}\left[\ln\left(\frac{1+t}{1-t}\right) - \frac{1}{\beta_0}\ln\left(\frac{1+\beta_0 t}{1-\beta_0 t}\right)\right]_{\beta(\lambda)}^{\beta(\omega_0)} \qquad (A.28) \\ &= G_{t(\omega_0)} - G_{t(\lambda)}. \qquad (A.29) \end{aligned}$$

The integration was performed on the speed rather than on the energy, since $\omega = \lambda/\sqrt{1-t^2}$. For the lower extreme $t(\lambda) = \sqrt{1-\frac{\lambda^2}{\lambda^2}} = 0$, therefore $G_{t(\lambda)} = 0$ even before taking the massless limit. The upper extreme instead returns the IR-divergence as

$$\lim_{\lambda^2\to 0} G_{t(\omega_0)} = \frac{1}{2}\frac{\beta_0}{1-\beta_0^2}\left[\ln\left(\frac{4\omega_0^2}{\lambda^2}\right) - \frac{1}{\beta_0}\ln\left(\frac{1+\beta_0}{1-\beta_0}\right)\right] \tag{A.30}$$

To deal with the other ill-behaving function $\frac{f(\omega)}{\omega}$ we start working with indefinite integrals first:

$$F \equiv \int d\omega \frac{f(\omega)}{\omega}\bigg|_{\kappa=0} = -2(1-\beta_0^2)\int d\beta \frac{\beta}{(1-\beta^2)(\beta_0^2-\beta^2)} \ln\left(\frac{1+\beta}{1-\beta}\right) \tag{A.31}$$

The function F clearly contains the same singularity at $\beta = \beta_0$. If we now use partial fractioning to write

$$\frac{\beta}{(1-\beta^2)(\beta_0^2-\beta^2)} = \frac{1}{2}\frac{1}{1-\beta_0^2}\left[\frac{1}{1+\beta} - \frac{1}{1-\beta} + \frac{1}{\beta_0-\beta} - \frac{1}{\beta_0+\beta}\right] . \tag{A.32}$$

The primitives for the resulting 4 integrals can be found in Ref. [305]:

$$F_1 \equiv \int d\beta \frac{1}{1+\beta} \ln\left(\frac{1+\beta}{1-\beta}\right) = \frac{1}{2}\ln^2(1+\beta) - \mathrm{Li}_2\left(\frac{1-\beta}{2}\right) + \ln(1-\beta)\ln\left(\frac{2}{1+\beta}\right) \tag{A.33}$$

$$F_2 \equiv \int d\beta \frac{1}{1-\beta} \ln\left(\frac{1+\beta}{1-\beta}\right) = \mathrm{Li}_2\left(\frac{1-\beta}{2}\right) - \ln 2 \ln(1-\beta) + \frac{1}{2}\ln^2(1-\beta) + \cancel{\frac{\pi^2}{6}}^{\text{constant}} \tag{A.34}$$

$$\begin{aligned} F_3 \equiv \int d\beta \frac{1}{\beta_0-\beta} \ln\left(\frac{1+\beta}{1-\beta}\right) &= -\ln(\beta_0-\beta)\ln\left(\frac{1+\beta_0}{1-\beta_0}\right) - \ln(1-\beta)\ln(1-\beta_0) \\ &\quad + \frac{1}{2}\ln^2(1-\beta) + \mathrm{Li}_2\left(\frac{\beta_0-\beta}{1+\beta_0}\right) + \mathrm{Li}_2\left(\frac{\beta_0-\beta}{1-\beta}\right) \end{aligned} \tag{A.35}$$

$$\begin{aligned} F_4 \equiv \int d\beta \frac{1}{\beta_0+\beta} \ln\left(\frac{1+\beta}{1-\beta}\right) &= -\mathrm{Li}_2\left(\frac{1-\beta_0}{1+\beta}\right) - \mathrm{Li}_2\left(\frac{1-\beta}{1+\beta_0}\right) + \ln(\beta+\beta_0)\ln\left(\frac{1+\beta}{1-\beta}\right) \\ &\quad - \frac{1}{2}\ln^2(1+\beta) + \ln(1+\beta_0)\ln(1-\beta) \quad . \end{aligned} \tag{A.36}$$

This way the original integral is now given by $F = -F_1 + F_2 - F_3 + F_4$. The divergent part is now the first term in F_3. Similarly to what we have done before, but still working with indefinite integrals here, we introduce the term

$$\begin{aligned} F_0 &\equiv \ln\left(\frac{1+\beta_0}{1-\beta_0}\right) \int \frac{d\omega}{\omega}\bigg|_{\kappa=0} = -\ln\left(\frac{1+\beta_0}{1-\beta_0}\right)\ln\left(\frac{\beta_0^2-\beta^2}{1-\beta^2}\right) \\ &= \ln\left(\frac{1+\beta_0}{1-\beta_0}\right)\ln\left(\frac{\beta+\beta_0}{1-\beta^2}\right) - \ln\left(\frac{1+\beta_0}{1-\beta_0}\right)\log(\beta_0-\beta) \quad , \end{aligned} \tag{A.37}$$

where the last term cancels exactly the IR-divergence in the sum

$$\begin{aligned} F - F_0 = {} & 2\mathrm{Li}_2\left(\frac{1-\beta}{2}\right) - \mathrm{Li}_2\left(\frac{\beta_0-\beta}{1+\beta_0}\right) - \mathrm{Li}_2\left(\frac{\beta_0-\beta}{1-\beta}\right) - \mathrm{Li}_2\left(\frac{1-\beta_0}{1+\beta}\right) - \mathrm{Li}_2\left(\frac{1-\beta}{1+\beta_0}\right) \\ & - \ln^2(1-\beta) + \ln\left(1-\beta_0^2\right)\ln(1-\beta) - 2\ln 2\ln(1-\beta) + \ln(1-\beta)\ln(1+\beta) \\ & + \ln\left(\frac{1-\beta^2}{\beta+\beta_0}\right)\ln\left(\frac{1+\beta_0}{1-\beta_0}\right) + \ln(\beta+\beta_0)\ln\left(\frac{1+\beta}{1-\beta}\right) \quad . \end{aligned} \tag{A.38}$$

We will again write

$$\int_0^{\omega_0} d\omega \frac{f(\omega)}{\omega} = [F - F_0]_0^{\omega_0} + \lim_{\lambda\to 0} F_t\Big|_\lambda^{\omega_0} \, ,$$

where the final term reads

$$
\begin{aligned}
F_t &= \int \frac{d\omega}{\omega} \ln\left(\frac{1+\beta_0 t(\omega)}{1-\beta_0 t(\omega)}\right) \overset{y=\beta_0 t}{=} \int dy \frac{y}{\beta_0^2 - y^2} \ln\left(\frac{1+y}{1-y}\right) \\
&= \frac{1}{2}\int dy \left(\frac{1}{\beta_0 - y} - \frac{1}{\beta_0 + y}\right) \ln\left(\frac{1+y}{1-y}\right) \\
&= \mathrm{Li}_2\left(\frac{\beta_0(1-t)}{1-\beta_0}\right) + \mathrm{Li}_2\left(\frac{\beta_0(1-t)}{1-\beta_0 t}\right) + \mathrm{Li}_2\left(\frac{1-\beta_0}{1+\beta_0 t}\right) + \mathrm{Li}_2\left(\frac{1-\beta_0 t}{1+\beta_0}\right) \\
&+ \cancelto{\text{const.}}{\ln(1-\beta_0)\ln\beta_0} + \ln(1-\beta_0)\ln(1-t) - \cancelto{\text{const.}}{\ln(1+\beta_0)\ln(\beta_0)} - \ln(1+\beta_0)\ln(1-t) \\
&+ \frac{1}{2}\ln^2(1-\beta_0 t) + \frac{1}{2}\ln^2(1+\beta_0 t) - \ln(1-\beta_0 t)\ln\left(1-\beta_0^2\right) - \ln\left[\beta_0(1+t)\right]\ln\left(\frac{1+\beta_0 t}{1-\beta_0 t}\right)
\end{aligned}
$$

The upper limit $\omega = \omega_0$ of the corresponding definite integral contains a divergent term from

$$
\ln\left[1 - t(\omega_0)\right] \overset{\lambda\to 0}{\sim} \ln\left(\frac{\lambda^2}{2\omega_0^2}\right) \quad , \tag{A.39}
$$

while the other terms can be obtained setting $t(\omega_0) = 1$ directly:

$$
\begin{aligned}
\lim_{\lambda\to 0} F_{t(\omega_0)} = \frac{1}{2}\Bigg[& 2\mathrm{Li}_2\left(\frac{1-\beta_0}{1+\beta_0}\right) + \frac{1}{2}\ln^2(1-\beta_0) + \frac{1}{2}\ln^2(1+\beta_0) - \ln(1-\beta_0)\ln\left(1-\beta_0^2\right) \\
& - \ln\left(\frac{\lambda^2}{2\omega_0^2}\right)\ln\left(\frac{1+\beta_0}{1-\beta_0}\right) - \ln(2\beta_0)\ln\left(\frac{1+\beta_0}{1-\beta_0}\right)\Bigg]
\end{aligned} \tag{A.40}
$$

In the lower limit the dependence on the photon mass disappears,

$$
F_{t(\lambda)=0} = \frac{1}{2}\left[\frac{\pi^2}{3} + \ln\beta_0 \ln\left(\frac{1+\beta_0}{1-\beta_0}\right) - \ln^2(1+\beta_0)\right] , \tag{A.41}
$$

where we have used the first one among the following properties of the dilogarithmic function:

$$
\mathrm{Li}_2(z) + \mathrm{Li}_2(1-z) = \frac{\pi^2}{6} - \ln z \ln(1-z) , \tag{A.42}
$$

$$
\mathrm{Li}_2(1-z) + \mathrm{Li}_2(1-\frac{1}{z}) = -\frac{1}{2}\ln^2 z , \tag{A.43}
$$

$$
\mathrm{Li}_2(z) + \mathrm{Li}_2(\frac{1}{z}) = \frac{\pi^2}{6} - \frac{1}{2}\ln^2 z . \tag{A.44}
$$

$$
\tag{A.45}
$$

Eqs. (A.43), (A.44) and (A.45) are all to be used again once we go back to Eq. (A.21), taking the limit for $\omega_0 \ll m_q$. In this special case all the contribution coming from integrals other then the divergent ones we have just studied won't contribute,

because our integration interval shrinks to a point. Only functions with a pole at that point will then have non zero value in such a limit. Eq. (5.24) follows from

$$\begin{aligned}\Delta\tilde{\sigma}v|^{\mathrm{eff}}_{\mathrm{soft}} &= \frac{\alpha_S}{\pi}\langle\sigma v_{q\bar{q}}\rangle\int_{\lambda^2}^{\omega_0}\left[\frac{1+\beta^2}{\beta}\frac{f(\omega)}{\omega}-2\frac{1-\beta^2}{\beta}g(\omega)\right]\\ &= \frac{\alpha_S}{\pi}\langle\sigma v_{q\bar{q}}\rangle\int_{\lambda^2}^{\omega_0}\left\{\frac{1+\beta^2}{\beta}\left[\lim_{\lambda\to 0}F_{t(\omega_0)}-F_{t(\lambda)=0}\right]-2\frac{1-\beta^2}{\beta}\lim_{k\to 0}G_{t(\omega_0)}\right\}.\end{aligned} \tag{A.46}$$

BIBLIOGRAPHY

[1] M. Planck. "On the Law of Distribution of Energy in the Normal Spectrum." In: *Annalen Phys.* 4 (1901), p. 553.

[2] A. Einstein. "Concerning an heuristic point of view toward the emission and transformation of light." In: *Annalen Phys.* 17 (1905), pp. 132–148.

[3] S. L. Glashow. "Partial Symmetries of Weak Interactions." In: *Nucl. Phys.* 22 (1961), pp. 579–588. DOI: 10.1016/0029-5582(61)90469-2.

[4] S. Weinberg. "A Model of Leptons." In: *Phys. Rev. Lett.* 19 (1967), pp. 1264–1266. DOI: 10.1103/PhysRevLett.19.1264.

[5] A. Salam and J. C. Ward. "Electromagnetic and weak interactions." In: *Phys. Lett.* 13 (1964), pp. 168–171. DOI: 10.1016/0031-9163(64)90711-5.

[6] F. Englert and R. Brout. "Broken Symmetry and the Mass of Gauge Vector Mesons." In: *Phys. Rev. Lett.* 13 (9 1964), pp. 321–323. DOI: 10.1103/PhysRevLett.13.321. URL: https://link.aps.org/doi/10.1103/PhysRevLett.13.321.

[7] P. W. Higgs. "Broken Symmetries and the Masses of Gauge Bosons." In: *Phys. Rev. Lett.* 13 (16 1964), pp. 508–509. DOI: 10.1103/PhysRevLett.13.508. URL: https://link.aps.org/doi/10.1103/PhysRevLett.13.508.

[8] G. S. Guralnik, C. R. Hagen, and T. W. B. Kibble. "Global Conservation Laws and Massless Particles." In: *Phys. Rev. Lett.* 13 (20 1964), pp. 585–587. DOI: 10.1103/PhysRevLett.13.585. URL: https://link.aps.org/doi/10.1103/PhysRevLett.13.585.

[9] J. Goldstone. "Field Theories with Superconductor Solutions." In: *Nuovo Cim.* 19 (1961), pp. 154–164. DOI: 10.1007/BF02812722.

[10] Y. Nambu. "Axial vector current conservation in weak interactions." In: *Phys. Rev. Lett.* 4 (1960). [,107(1960)], pp. 380–382. DOI: 10.1103/PhysRevLett.4.380.

[11] G. Arnison et al. "Experimental Observation of Lepton Pairs of Invariant Mass Around 95-GeV at the CERN SPS Collider." In: *Phys. Lett.* B126 (1983). [,7.55(1983)], pp. 398–410. DOI: 10.1016/0370-2693(83)90188-0.

[12] P. Bagnaia et al. "Evidence for Zo —> e+ e- at the CERN anti-p p Collider." In: *Phys. Lett.* B129 (1983). [,7.69(1983)], pp. 130–140. DOI: 10.1016/0370-2693(83)90744-X.

[13] G. 't Hooft. "Renormalizable Lagrangians for Massive Yang-Mills Fields." In: *Nucl. Phys.* B35 (1971). [,201(1971)], pp. 167–188. DOI: 10.1016/0550-3213(71)90139-8.

[14] G. 't Hooft and M. Veltman. "Regularization and renormalization of gauge fields." In: *Nuclear Physics B* 44.1 (1972), pp. 189 –213. ISSN: 0550-3213. DOI: https://doi.org/10.1016/0550-3213(72)90279-9. URL: http://www.sciencedirect.com/science/article/pii/0550321372902799.

[15] D. J. Gross and F. Wilczek. "Ultraviolet Behavior of Nonabelian Gauge Theories." In: *Phys. Rev. Lett.* 30 (1973). [,271(1973)], pp. 1343–1346. DOI: 10.1103/PhysRevLett.30.1343.

[16] H. D. Politzer. "Reliable Perturbative Results for Strong Interactions?" In: *Phys. Rev. Lett.* 30 (1973). [,274(1973)], pp. 1346–1349. DOI: 10.1103/PhysRevLett.30.1346.

[17] H. Fritzsch, M. Gell-Mann, and H. Leutwyler. "Advantages of the Color Octet Gluon Picture." In: *Phys. Lett.* 47B (1973), pp. 365–368. DOI: 10.1016/0370-2693(73)90625-4.

[18] B. R. Stella and H.-J. Meyer. "(9.46 GeV) and the gluon discovery (a critical recollection of PLUTO results)." In: *The European Physical Journal H* 36.2 (2011), p. 203. ISSN: 2102-6467. DOI: 10.1140/epjh/e2011-10029-3. URL: https://doi.org/10.1140/epjh/e2011-10029-3.

[19] R. D. Peccei. "Discrete and global symmetries in particle physics." In: *Lect. Notes Phys.* 521 (1999), pp. 1–50. DOI: 10.1007/BFb010552, 10.1007/BFb0105521. arXiv: hep-ph/9807516 [hep-ph].

[20] M. Tanabashi et al. "Review of Particle Physics." In: *Phys. Rev. D* 98 (3 2018), p. 030001. DOI: 10.1103/PhysRevD.98.030001. URL: https://link.aps.org/doi/10.1103/PhysRevD.98.030001.

[21] D. Wallace. "The Quantization of gravity: An Introduction." In: (2000). arXiv: gr-qc/0004005 [gr-qc].

[22] F. Zwicky. "Die Rotverschiebung von extragalaktischen Nebeln." In: *Helv.Phys.Acta* 6 (1933), pp. 110–127.

[23] "On the Masses of Nebulae and of Clusters of Nebulae." In: *Astrophysical Journal* 86 (1937), p. 217. DOI: {10.1086/143864}.

[24] Babcock. "The rotation of the Andromeda Nebula." In: *Lick Observatory Bulletin* 19 (1939), pp. 41–51.

[25] V. C. Rubin and W. K. J. Ford. "Rotation of the Andromeda Nebula from a Spectroscopic Survey of Emission Regions." In: *apj* 159 (1970), p. 379.

[26] D. Fabricant, M. Lecar, and P. Gorenstein. "X-ray measurements of the mass of M87." In: *apj* 241 (Oct. 1980), pp. 552–560. DOI: 10.1086/158369.

[27] E. R. Newton, P. J. Marshall, and T. Treu. "Enhanced Lensing Rate by Clustering of Massive Galaxies: Newly Discovered Systems in the Slacs Fields." In: *apj* 696.2 (2009), p. 1125. URL: http://stacks.iop.org/0004-637X/696/i=2/a=1125.

[28] R. B. Metcalf, L. A. Moustakas, A. J. Bunker, and I. R. Parry. "Spectroscopic gravitational lensing and limits on the dark matter substructure in Q2237+0305." In: *apj* 607 (2004), pp. 43–59. DOI: 10.1086/383243. arXiv: astro-ph/0309738 [astro-ph].

[29] L. A. Moustakas and R. B. Metcalf. "Detecting dark matter substructure spectroscopically in strong gravitational lenses." In: *Mon.Not.Roy.Astron.Soc.* 339 (2003), p. 607. DOI: 10.1046/j.1365-8711.2003.06055.x. arXiv: astro-ph/0206176 [astro-ph].

[30] J. N. Bahcall, C. Flynn, A. Gould, and S. Kirhakos. "M dwarfs, microlensing, and the mass budget of the galaxy." In: *Astrophys.J.* 435 (1994), pp. L51–L54. arXiv: astro-ph/9406019 [astro-ph].

[31] H. Hoekstra, H. Yee, and M. Gladders. "Current status of weak gravitational lensing." In: *New Astron.Rev.* 46 (2002), pp. 767–781. DOI: 10.1016/S1387-6473(02)00245-2. arXiv: astro-ph/0205205 [astro-ph].

[32] P. Cote, M. Mateo, E. Olszewski, and K. Cook. "Internal kinematics of the andromeda II dwarf spheroidal galaxy." In: (1999). arXiv: astro-ph/9907003 [astro-ph].

[33] M. Mateo. "Dwarf galaxies of the Local Group." In: *Ann.Rev.Astron.Astrophys.* 36 (1998), pp. 435–506. DOI: 10.1146/annurev.astro.36.1.435. arXiv: astro-ph/9810070 [astro-ph].

[34] A. A. Penzias and R. W. Wilson. "A Measurement of excess antenna temperature at 4080-Mc/s." In: *Astrophys. J.* 142 (1965), pp. 419–421. DOI: 10.1086/148307.

[35] R. H. Dicke, P. J. E. Peebles, P. G. Roll, and D. T. Wilkinson. "Cosmic Black-Body Radiation." In: *Astrophys. J.* 142 (1965), pp. 414–419. DOI: 10.1086/148306.

[36] C. Bennett et al. "Nine-Year Wilkinson Microwave Anisotropy Probe (WMAP) Observations: Final Maps and Results." In: (2012). arXiv: 1212.5225 [astro-ph.CO].

[37] Y. Akrami et al. "Planck 2018 results. I. Overview and the cosmological legacy of Planck." In: (2018). arXiv: 1807.06205 [astro-ph.CO].

[38] V. A. Rubakov and D. S. Gorbunov. *Introduction to the Theory of the Early Universe*. Singapore: World Scientific, 2017. ISBN: 9789813209879, 9789813209886, 9789813220058. DOI: 10.1142/10447. URL: http://www.DESY.eblib.com/patron/FullRecord.aspx?p=737614.

[39] M. Kamionkowski and D. N. Spergel. "Large angle cosmic microwave background anisotropies in an open universe." In: *Astrophys.J.* 432 (1994), p. 7. DOI: 10.1086/174543. arXiv: astro-ph/9312017 [astro-ph].

[40] M. Kamionkowski, B. Ratra, D. N. Spergel, and N. Sugiyama. "CBR anisotropy in an open inflation, CDM cosmogony." In: *Astrophys.J.* 434 (1994), pp. L1–L4. arXiv: astro-ph/9406069 [astro-ph].

[41] B. Paczynski. "Gravitational microlensing at large optical depth." In: *apj* 301 (1986), pp. 503–516. DOI: 10.1086/163919.

[42] B. J. Carr. "Observational constraints on baryonic dark matter." In: *Particle astrophysics: The Early universe and cosmic structures. Proceedings, 25th Rencontres de Moriond, Les Arcs, France, March 4-11, 1990*. [,141(1990)]. 1990, pp. 141–160. URL: https://inspirehep.net/record/307838/files/Pages_from_C90-03-04--1_141.pdf.

[43] S. D. White, C. Frenk, and M. Davis. "Clustering in a Neutrino Dominated Universe." In: *Astrophys.J.* 274 (1983), pp. L1–L5.

[44] C. Weinheimer. "Proceedings of 10th International Workshop on Neutrino Telescopes, Venice, Italy." In: (2003). DOI: 10.1016/j.physrep.2004.08.031. arXiv: hep-ph/0306057 [hep-ph].

[45] B. W. Lee and S. Weinberg. "Cosmological Lower Bound on Heavy-Neutrino Masses." In: *Phys. Rev. Lett.* 39 (4 1977), pp. 165–168. DOI: 10.1103/PhysRevLett.39.165. URL: http://link.aps.org/doi/10.1103/PhysRevLett.39.165.

[46] D. O. Caldwell, R. Eisberg, D. Grumm, M. S. Witherell, B. Sadoulet, et al. "Laboratory Limits on Galactic Cold Dark Matter." In: *Phys.Rev.Lett.* 61 (1988), p. 510. DOI: 10.1103/PhysRevLett.61.510.

[47] G. Jungman, M. Kamionkowski, and K. Griest. "Supersymmetric dark matter." In: *Phys.Rept.* 267 (1996), pp. 195–373. DOI: 10.1016/0370-1573(95)00058-5. arXiv: hep-ph/9506380 [hep-ph].

[48] T. Falk, K. A. Olive, and M. Srednicki. "Heavy sneutrinos as dark matter." In: *Phys.Lett.* B339 (1994), pp. 248–251. DOI: 10.1016/0370-2693(94)90639-4. arXiv: hep-ph/9409270 [hep-ph].

[49] W. Buchmuller, K. Hamaguchi, and M. Ratz. "Gauge couplings at high temperature and the relic gravitino abundance." In: *Phys.Lett.* B574 (2003), pp. 156–161. DOI: 10.1016/j.physletb.2003.09.017. arXiv: hep-ph/0307181 [hep-ph].

[50] K. Choi, K. Hwang, H. B. Kim, and T. Lee. "Cosmological gravitino production in gauge mediated supersymmetry breaking models." In: *Phys.Lett.* B467 (1999), pp. 211–217. DOI: 10.1016/S0370-2693(99)01156-9. arXiv: hep-ph/9902291 [hep-ph].

[51] T. Gherghetta, G. Giudice, and A. Riotto. "Nucleosynthesis bounds in gauge mediated supersymmetry breaking theories." In: *Phys.Lett.* B446 (1999), pp. 28–36. DOI: 10.1016/S0370-2693(98)01527-5. arXiv: hep-ph/9808401 [hep-ph].

[52] M. S. Turner. "Windows on the axion." In: *Physics Reports* 197.2 (1990), pp. 67 –97. ISSN: 0370-1573. DOI: http://dx.doi.org/10.1016/0370-1573(90)90172-X. URL: http://www.sciencedirect.com/science/article/pii/037015739090172X.

[53] G. G. Raffelt. "Astrophysical methods to constrain axions and other novel particle phenomena." In: *Phys.Rept.* 198 (1990), pp. 1–113. DOI: 10.1016/0370-1573(90)90054-6.

[54] S. Bonometto, F. Gabbiani, and A. Masiero. "Mixed dark matter from axino distribution." In: (1993). arXiv: astro-ph/9305010 [astro-ph].

[55] L. Covi, J. E. Kim, and L. Roszkowski. "Axinos as cold dark matter." In: *Phys.Rev.Lett.* 82 (1999), pp. 4180–4183. DOI: 10.1103/PhysRevLett.82.4180. arXiv: hep-ph/9905212 [hep-ph].

[56] T. Marrodán Undagoitia and L. Rauch. "Dark matter direct-detection experiments." In: *J. Phys.* G43.1 (2016), p. 013001. DOI: 10.1088/0954-3899/43/1/013001. arXiv: 1509.08767 [physics.ins-det].

[57] T. R. Slatyer. "Energy Injection And Absorption In The Cosmic Dark Ages." In: *Phys. Rev.* D87.12 (2013), p. 123513. DOI: 10.1103/PhysRevD.87.123513. arXiv: 1211.0283 [astro-ph.CO].

[58] J. M. Gaskins. "A review of indirect searches for particle dark matter." In: *Contemp. Phys.* 57.4 (2016), pp. 496–525. DOI: 10.1080/00107514.2016.1175160. arXiv: 1604.00014 [astro-ph.HE].

[59] J. Conrad. "Indirect Detection of WIMP Dark Matter: a compact review." In: *Interplay between Particle and Astroparticle physics (IPA2014) London, United Kingdom, August 18-22, 2014*. 2014. arXiv: 1411.1925 [hep-ph]. URL: https://inspirehep.net/record/1326617/files/arXiv:1411.1925.pdf.

[60] S. Y. Hoh, J. Komaragiri, and W. A.T.B. W. Abdullah. "Dark Matter Searches at the Large Hadron Collider." In: *AIP Conf. Proc.* 1704.1 (2016), p. 020005. DOI: 10.1063/1.4940063. arXiv: 1512.07376 [hep-ex].

[61] G. Busoni, A. De Simone, E. Morgante, and A. Riotto. "On the Validity of the Effective Field Theory for Dark Matter Searches at the LHC." In: *Phys. Lett.* B728 (2014), pp. 412–421. DOI: 10.1016/j.physletb.2013.11.069. arXiv: 1307.2253 [hep-ph].

[62] A. De Simone and T. Jacques. "Simplified models vs. effective field theory approaches in dark matter searches." In: *Eur. Phys. J.* C76.7 (2016), p. 367. DOI: 10.1140/epjc/s10052-016-4208-4. arXiv: 1603.08002 [hep-ph].

[63] J. Abdallah et al. "Simplified Models for Dark Matter Searches at the LHC." In: *Phys. Dark Univ.* 9-10 (2015), pp. 8–23. DOI: 10.1016/j.dark.2015.08.001. arXiv: 1506.03116 [hep-ph].

[64] L. Bergstrom. "Radiative Processes in Dark Matter Photino Annihilation." In: *Phys. Lett.* B225 (1989), pp. 372–380. DOI: 10.1016/0370-2693(89)90585-6. URL: http://dx.doi.org/10.1016/0370-2693(89)90585-6.

[65] L. Bergstrom, T. Bringmann, and J. Edsjo. "New Positron Spectral Features from Supersymmetric Dark Matter - a Way to Explain the PAMELA Data?" In: *Phys. Rev.* D78 (2008), p. 103520. DOI: 10.1103/PhysRevD.78.103520. arXiv: 0808.3725 [astro-ph].

[66] T. Bringmann, L. Bergstrom, and J. Edsjo. "New Gamma-Ray Contributions to Supersymmetric Dark Matter Annihilation." In: *JHEP* 01 (2008), p. 049. DOI: 10.1088/1126-6708/2008/01/049. arXiv: 0710.3169 [hep-ph].

[67] F. Giacchino, L. Lopez-Honorez, and M. H. G. Tytgat. "Scalar Dark Matter Models with Significant Internal Bremsstrahlung." In: *JCAP* 1310 (2013), p. 025. DOI: 10.1088/1475-7516/2013/10/025. arXiv: 1307.6480 [hep-ph].

[68] A. Boyarsky, O. Ruchayskiy, D. Iakubovskyi, and J. Franse. "Unidentified Line in X-Ray Spectra of the Andromeda Galaxy and Perseus Galaxy Cluster." In: *Phys. Rev. Lett.* 113 (2014), p. 251301. DOI: 10.1103/PhysRevLett.113.251301. arXiv: 1402.4119 [astro-ph.CO].

[69] E. Bulbul, M. Markevitch, A. Foster, R. K. Smith, M. Loewenstein, and S. W. Randall. "Detection of an Unidentified Emission Line in the Stacked X-Ray Spectrum of Galaxy Clusters." In: *Astrophys. J.* 789 (2014), p. 13. DOI: 10.1088/0004-637X/789/1/13. arXiv: 1402.2301 [astro-ph.CO].

[70] O. Urban, N. Werner, S. W. Allen, A. Simionescu, J. S. Kaastra, and L. E. Strigari. "A Suzaku Search for Dark Matter Emission Lines in the X-Ray Brightest Galaxy Clusters." In: *Mon. Not. Roy. Astron. Soc.* 451.3 (2015), pp. 2447–2461. DOI: 10.1093/mnras/stv1142. arXiv: 1411.0050 [astro-ph.CO].

[71] T. E. Jeltema and S. Profumo. "Discovery of a 3.5 keV line in the Galactic Centre and a critical look at the origin of the line across astronomical targets." In: *Mon. Not. Roy. Astron. Soc.* 450.2 (2015), pp. 2143–2152. DOI: 10.1093/mnras/stv768. arXiv: 1408.1699 [astro-ph.HE].

[72] E. Bulbul, M. Markevitch, A. R. Foster, R. K. Smith, M. Loewenstein, and S. W. Randall. "Comment on "Dark Matter Searches Going Bananas: the Contribution of Potassium (And Chlorine) to the 3.5 keV Line"." In: (2014). arXiv: 1409.4143 [astro-ph.HE].

[73] A. Boyarsky, J. Franse, D. Iakubovskyi, and O. Ruchayskiy. "Comment on the Paper "Dark Matter Searches Going Bananas: the Contribution of Potassium (And Chlorine) to the 3.5 keV Line" by T. Jeltema and S. Profumo." In: ().

[74] T. Jeltema and S. Profumo. "Reply to Two Comments on "Dark Matter Searches Going Bananas the Contribution of Potassium (And Chlorine) to the 3.5 keV Line"." In: ().

[75] E. Carlson, T. Jeltema, and S. Profumo. "Where Do the 3.5 keV Photons Come From? A Morphological Study of the Galactic Center and of Perseus." In: *JCAP* 1502.02 (2015), p. 009. DOI: 10.1088/1475-7516/2015/02/009. arXiv: 1411.1758 [astro-ph.HE].

[76] O. Ruchayskiy, A. Boyarsky, D. Iakubovskyi, E. Bulbul, D. Eckert, J. Franse, D. Malyshev, M. Markevitch, and A. Neronov. "Searching for Decaying Dark Matter in Deep XMM–Newton Observation of the Draco Dwarf Spheroidal." In: *Mon. Not. Roy. Astron. Soc.* 460.2 (2016), pp. 1390–1398. DOI: 10.1093/mnras/st$W_1$026. arXiv: 1512.07217 [astro-ph.HE].

[77] T. E. Jeltema and S. Profumo. "Deep Xmm Observations of Draco Rule Out at the 99% Confidence Level a Dark Matter Decay Origin for the 3.5 keV Line." In: *Mon. Not. Roy. Astron. Soc.* 458.4 (2016), pp. 3592–3596. DOI: 10.1093/mnras/st$W_5$78. arXiv: 1512.01239 [astro-ph.HE].

[78] E. Bulbul, M. Markevitch, A. Foster, E. Miller, M. Bautz, M. Loewenstein, S. W. Randall, and R. K. Smith. "Searching for the 3.5 keV Line in the Stacked Suzaku Observations of Galaxy Clusters." In: *Astrophys. J.* 831.1 (2016), p. 55. DOI: 10.3847/0004-637X/831/1/55. arXiv: 1605.02034 [astro-ph.HE].

[79] S. P. Liew. "Axino Dark Matter in Light of an Anomalous X-Ray Line." In: *JCAP* 1405 (2014), p. 044. DOI: 10.1088/1475-7516/2014/05/044. arXiv: 1403.6621 [hep-ph].

[80] J.-C. Park, S. C. Park, and K. Kong. "X-Ray Line Signal from 7 keV Axino Dark Matter Decay." In: *Phys. Lett.* B733 (2014), pp. 217–220. DOI: 10.1016/j.physletb.2014.04.037. arXiv: 1403.1536 [hep-ph].

[81] K.-Y. Choi and O. Seto. "X-ray line signal from decaying axino warm dark matter." In: *Phys. Lett.* B735 (2014), pp. 92–94. DOI: 10.1016/j.physletb.2014.06.008. arXiv: hep-ph/1403.1782 [hep-ph].

[82] B. Dutta, I. Gogoladze, R. Khalid, and Q. Shafi. "3.5 keV X-ray line and R-Parity Conserving Supersymmetry." In: *JHEP* 1411 (2014), p. 018. DOI: 10.1007/JHEP11(2014)018. arXiv: hep-ph/1407.0863 [hep-ph].

[83] S. Dimopoulos, S. Raby, and F. Wilczek. "Supersymmetry and the scale of unification." In: *Phys. Rev. D* 24 (6 1981), pp. 1681–1683. DOI: 10.1103/PhysRevD.24.1681. URL: https://link.aps.org/doi/10.1103/PhysRevD.24.1681.

[84] H. Georgi and S. L. Glashow. "Unity of All Elementary-Particle Forces." In: *Phys. Rev. Lett.* 32 (8 1974), pp. 438–441. DOI: 10.1103/PhysRevLett.32.438. URL: https://link.aps.org/doi/10.1103/PhysRevLett.32.438.

[85] H. Fritzsch and P. Minkowski. "Unified interactions of leptons and hadrons." In: *Annals of Physics* 93.1 (1975), pp. 193 –266. ISSN: 0003-4916. DOI: https://doi.org/10.1016/0003-4916(75)90211-0. URL: http://www.sciencedirect.com/science/article/pii/0003491675902110.

[86] P. Langacker. "Grand unified theories and proton decay." In: *Physics Reports* 72.4 (1981), pp. 185 –385. ISSN: 0370-1573. DOI: https://doi.org/10.1016/0370-1573(81)90059-4. URL: http://www.sciencedirect.com/science/article/pii/0370157381900594.

[87] L. Susskind. "Dynamics of Spontaneous Symmetry Breaking in the Weinberg-Salam Theory." In: *Phys. Rev.* D20 (1979), pp. 2619–2625. DOI: 10.1103/PhysRevD.20.2619.

[88] S. Weinberg. "Implications of Dynamical Symmetry Breaking." In: *Phys. Rev.* D13 (1976). [Addendum: Phys. Rev.D19,1277(1979)], pp. 974–996. DOI: 10.1103/PhysRevD.19.1277,10.1103/PhysRevD.13.974.

[89] G. 't Hooft. "Naturalness, chiral symmetry, and spontaneous chiral symmetry breaking." In: *NATO Sci. Ser. B* 59 (1980), pp. 135–157. DOI: 10.1007/978-1-4684-7571-5_9.

[90] E. Gildener. "Gauge-symmetry hierarchies." In: *Phys. Rev. D* 14 (6 1976), pp. 1667–1672. DOI: 10.1103/PhysRevD.14.1667. URL: https://link.aps.org/doi/10.1103/PhysRevD.14.1667.

[91] M. J. G. Veltman. "The Infrared - Ultraviolet Connection." In: *Acta Phys. Polon.* B12 (1981), p. 437.

[92] M. Drees, R. Godbole, and P. Roy. *Theory and phenomenology of sparticles: An account of four-dimensional N=1 supersymmetry in high energy physics*. 2004.

[93] L. Randall and R. Sundrum. "A Large mass hierarchy from a small extra dimension." In: *Phys. Rev. Lett.* 83 (1999), pp. 3370–3373. DOI: 10.1103/PhysRevLett.83.3370. arXiv: hep-ph/9905221 [hep-ph].

[94] N. Arkani-Hamed, S. Dimopoulos, and G. R. Dvali. "The Hierarchy problem and new dimensions at a millimeter." In: *Phys. Lett.* B429 (1998), pp. 263–272. DOI: 10.1016/S0370-2693(98)00466-3. arXiv: hep-ph/9803315 [hep-ph].

[95] S. Dimopoulos and J. Preskill. "Massless Composites With Massive Constituents." In: *Nucl. Phys.* B199 (1982), pp. 206–222. DOI: 10.1016/0550-3213(82)90345-5.

[96] D. B. Kaplan, H. Georgi, and S. Dimopoulos. "Composite Higgs Scalars." In: *Phys. Lett.* 136B (1984), pp. 187–190. DOI: 10.1016/0370-2693(84)91178-X.

[97] J. Wess and B. Zumino. "Supergauge transformations in four dimensions." In: *Nuclear Physics B* 70.1 (1974), pp. 39 –50. ISSN: 0550-3213. DOI: https://doi.org/10.1016/0550-3213(74)90355-1. URL: http://www.sciencedirect.com/science/article/pii/0550321374903551.

[98] H. Nilles. "Supersymmetry, supergravity and particle physics." In: *Physics Reports* 110.1 (1984), pp. 1 –162. ISSN: 0370-1573. DOI: https://doi.org/10.1016/0370-1573(84)90008-5. URL: http://www.sciencedirect.com/science/article/pii/0370157384900085.

[99] S. R. Coleman and J. Mandula. "All Possible Symmetries of the S Matrix." In: *Phys. Rev.* 159 (1967), pp. 1251–1256. DOI: 10.1103/PhysRev.159.1251.

[100] R. Haag, J. T. Lopuszanski, and M. Sohnius. "All Possible Generators of Supersymmetries of the s Matrix." In: *Nucl. Phys.* B88 (1975). [,257(1974)], p. 257. DOI: 10.1016/0550-3213(75)90279-5.

[101] J. T. Lopuszanski. "On some properties of physical symmetries." In: *J. Math. Phys.* 12 (1971), pp. 2401–2412. DOI: 10.1063/1.1665551.

[102] S. P. Martin. "A Supersymmetry Primer." In: *Adv. Ser. Direct. High Energy Phys.* 18 (1997), p. 1. DOI: 10.1142/9789812839657_0001, 10.1142/9789814307505_0001. arXiv: hep-ph/9709356 [hep-ph].

[103] H. Georgi and S. L. Glashow. "Gauge theories without anomalies." In: *Phys. Rev.* D6 (1972), p. 429. DOI: 10.1103/PhysRevD.6.429.

[104] H. K. Dreiner. "An Introduction to explicit R-parity violation." In: (1997). [Adv. Ser. Direct. High Energy Phys.21,565(2010)], pp. 462–479. DOI: 10.1142/9789814307505_0017. arXiv: hep-ph/9707435 [hep-ph].

[105] A. H. Chamseddine, R. L. Arnowitt, and P. Nath. "Locally Supersymmetric Grand Unification." In: *Phys. Rev. Lett.* 49 (1982), p. 970. DOI: 10.1103/PhysRevLett.49.970.

[106] L. J. Hall, J. D. Lykken, and S. Weinberg. "Supergravity as the Messenger of Supersymmetry Breaking." In: *Phys. Rev.* D27 (1983), pp. 2359–2378. DOI: 10.1103/PhysRevD.27.2359.

[107] R. Barbieri, S. Ferrara, and C. A. Savoy. "Gauge Models with Spontaneously Broken Local Supersymmetry." In: *Phys. Lett.* 119B (1982), p. 343. DOI: 10.1016/0370-2693(82)90685-2.

[108] M. Dine and W. Fischler. "A Phenomenological Model of Particle Physics Based on Supersymmetry." In: *Phys. Lett.* 110B (1982), pp. 227–231. DOI: 10.1016/0370-2693(82)91241-2.

[109] C. R. Nappi and B. A. Ovrut. "Supersymmetric Extension of the SU(3) x SU(2) x U(1) Model." In: *Phys. Lett.* 113B (1982), pp. 175–179. DOI: 10.1016/0370-2693(82)90418-X.

[110] L. Alvarez-Gaume, M. Claudson, and M. B. Wise. "Low-Energy Supersymmetry." In: *Nucl. Phys.* B207 (1982), p. 96. DOI: 10.1016/0550-3213(82)90138-9.

[111] M. Dine and A. E. Nelson. "Dynamical supersymmetry breaking at low-energies." In: *Phys. Rev.* D48 (1993), pp. 1277–1287. DOI: 10.1103/PhysRevD.48.1277. arXiv: hep-ph/9303230 [hep-ph].

[112] M. Dine, A. E. Nelson, and Y. Shirman. "Low-energy dynamical supersymmetry breaking simplified." In: *Phys. Rev.* D51 (1995), pp. 1362–1370. DOI: 10.1103/PhysRevD.51.1362. arXiv: hep-ph/9408384 [hep-ph].

[113] M. Dine, A. E. Nelson, Y. Nir, and Y. Shirman. "New tools for low-energy dynamical supersymmetry breaking." In: *Phys. Rev.* D53 (1996), pp. 2658–2669. DOI: 10.1103/PhysRevD.53.2658. arXiv: hep-ph/9507378 [hep-ph].

[114] V. A. Rubakov and M. E. Shaposhnikov. "Do We Live Inside a Domain Wall?" In: *Phys. Lett.* 125B (1983), pp. 136–138. DOI: 10.1016/0370-2693(83)91253-4.

[115] V. A. Rubakov and M. E. Shaposhnikov. "Extra Space-Time Dimensions: Towards a Solution to the Cosmological Constant Problem." In: *Phys. Lett.* 125B (1983), p. 139. DOI: 10.1016/0370-2693(83)91254-6.

[116] L. Randall and R. Sundrum. "An Alternative to compactification." In: *Phys. Rev. Lett.* 83 (1999), pp. 4690–4693. DOI: 10.1103/PhysRevLett.83.4690. arXiv: hep-th/9906064 [hep-th].

[117] L. Randall and R. Sundrum. "Out of this world supersymmetry breaking." In: *Nucl. Phys.* B557 (1999), pp. 79–118. DOI: 10.1016/S0550-3213(99)00359-4. arXiv: hep-th/9810155 [hep-th].

[118] G. F. Giudice, M. A. Luty, H. Murayama, and R. Rattazzi. "Gaugino mass without singlets." In: *JHEP* 12 (1998), p. 027. DOI: 10.1088/1126-6708/1998/12/027. arXiv: hep-ph/9810442 [hep-ph].

[119] G. R. Farrar and P. Fayet. "Phenomenology of the Production, Decay, and Detection of New Hadronic States Associated with Supersymmetry." In: *Phys. Lett.* 76B (1978), pp. 575–579. DOI: 10.1016/0370-2693(78)90858-4.

[120] G. L. Kane, C. F. Kolda, L. Roszkowski, and J. D. Wells. "Study of Constrained Minimal Supersymmetry." In: *Phys. Rev.* D49 (1994), pp. 6173–6210. DOI: 10.1103/PhysRevD.49.6173. arXiv: hep-ph/9312272 [hep-ph].

[121] P. Bechtle et al. "How Alive is Constrained SUSY Really?" In: *Nucl. Part. Phys. Proc.* 273-275 (2016), pp. 589–594. DOI: 10.1016/j.nuclphysbps.2015.09.088. arXiv: 1410.6035 [hep-ph].

[122] D. Dercks, H. Dreiner, M. E. Krauss, T. Opferkuch, and A. Reinert. "R-Parity Violation at the Lhc." In: *Eur. Phys. J.* C77.12 (2017), p. 856. DOI: 10.1140/epjc/s10052-017-5414-4. arXiv: 1706.09418 [hep-ph].

[123] E. Aprile et al. "First Dark Matter Search Results from the XENON1T Experiment." In: *Phys. Rev. Lett.* 119.18 (2017), p. 181301. DOI: 10.1103/PhysRevLett.119.181301. arXiv: 1705.06655 [astro-ph.CO].

[124] D. S. Akerib et al. "Results from a Search for Dark Matter in the Complete Lux Exposure." In: *Phys. Rev. Lett.* 118.2 (2017), p. 021303. DOI: 10.1103/PhysRevLett.118.021303. arXiv: 1608.07648 [astro-ph.CO].

[125] A. Tan et al. "Dark Matter Results from First 98.7 Days of Data from the Pandax-Ii Experiment." In: *Phys. Rev. Lett.* 117.12 (2016), p. 121303. DOI: 10.1103/PhysRevLett.117.121303. arXiv: 1607.07400 [hep-ex].

[126] S. Weinberg. "Supersymmetry at Ordinary Energies. 1. Masses and Conservation Laws." In: *Phys. Rev.* D26 (1982), p. 287. DOI: 10.1103/PhysRevD.26.287.

[127] H. K. Dreiner, C. Luhn, and M. Thormeier. "What is the Discrete Gauge Symmetry of the Mssm?" In: *Phys. Rev.* D73 (2006), p. 075007. DOI: 10.1103/PhysRevD.73.075007. arXiv: hep-ph/0512163 [hep-ph].

[128] H. K. Dreiner, C. Luhn, H. Murayama, and M. Thormeier. "Proton Hexality from an Anomalous Flavor U(1) and Neutrino Masses: Linking to the String Scale." In: *Nucl. Phys.* B795 (2008), pp. 172–200. DOI: 10.1016/j.nuclphysb.2007.11.014. arXiv: 0708.0989 [hep-ph].

[129] L. E. Ibanez and G. G. Ross. "Discrete Gauge Symmetry Anomalies." In: *Phys. Lett.* B260 (1991), pp. 291–295. DOI: 10.1016/0370-2693(91)91614-2.

[130] Y. Grossman and H. E. Haber. "(S)Neutrino Properties in R-Parity Violating Supersymmetry. 1. CP Conserving Phenomena." In: *Phys. Rev.* D59 (1999), p. 093008. DOI: 10.1103/PhysRevD.59.093008. arXiv: hep-ph/9810536 [hep-ph].

[131] H. K. Dreiner, C. Luhn, H. Murayama, and M. Thormeier. "Baryon Triality and Neutrino Masses from an Anomalous Flavor U(1)." In: *Nucl. Phys.* B774 (2007), pp. 127–167. DOI: 10.1016/j.nuclphysb.2007.03.028. arXiv: hep-ph/0610026 [hep-ph].

[132] H. K. Dreiner, J. Soo Kim, and M. Thormeier. "A Simple Baryon Triality Model for Neutrino Masses." In: (2007). arXiv: 0711.4315 [hep-ph].

[133] M. A. Bernhardt, S. P. Das, H. K. Dreiner, and S. Grab. "Sneutrino as Lightest Supersymmetric Particle in B_3 Msugra Models and Signals at the Lhc." In: *Phys. Rev.* D79 (2009), p. 035003. DOI: 10.1103/PhysRevD.79.035003. arXiv: 0810.3423 [hep-ph].

[134] B. C. Allanach, A. Dedes, and H. K. Dreiner. "R Parity Violating Minimal Supergravity Model." In: *Phys. Rev.* D69 (2004). [Erratum: Phys. Rev. D72, 079902 (2005)], p. 115002. DOI: 10.1103/PhysRevD.69.115002,10.1103/PhysRevD.72.079902. arXiv: hep-ph/0309196 [hep-ph].

[135] L. J. Hall and M. Suzuki. "Explicit R-Parity Breaking in Supersymmetric Models." In: *Nucl. Phys.* B231 (1984), pp. 419–444. DOI: 10.1016/0550-3213(84)90513-3.

[136] E. Nardi. "Renormalization Group Induced Neutrino Masses in Supersymmetry without R-Parity." In: *Phys. Rev.* D55 (1997), pp. 5772–5779. DOI: 10.1103/PhysRevD.55.5772. arXiv: hep-ph/9610540 [hep-ph].

[137] A. Abada and M. Losada. "Constraints on a General Three Generation Neutrino Mass Matrix from Neutrino Data: Application to the MSSM with R-Parity Violation." In: *Nucl. Phys.* B585 (2000), pp. 45–78. DOI: 10.1016/S0550-3213(00)00397-7. arXiv: hep-ph/9908352 [hep-ph].

[138] M. Hirsch, M. A. Diaz, W. Porod, J. C. Romao, and J. W. F. Valle. "Neutrino Masses and Mixings from Supersymmetry with Bilinear R Parity Violation: a Theory for Solar and Atmospheric Neutrino Oscillations." In: *Phys. Rev.* D62 (2000). [Erratum: Phys. Rev. D65, 119901 (2002)], p. 113008. DOI: 10.1103/PhysRevD.62.113008,10.1103/PhysRevD.65.119901. arXiv: hep-ph/0004115 [hep-ph].

[139] S. Davidson and M. Losada. "Neutrino Masses in the R-parity Violating MSSM." In: *JHEP* 05 (2000), p. 021. DOI: 10.1088/1126-6708/2000/05/021. arXiv: hep-ph/0005080 [hep-ph].

[140] A. H. Chamseddine and H. K. Dreiner. "Anomaly Free Gauged R Symmetry in Local Supersymmetry." In: *Nucl. Phys.* B458 (1996), pp. 65–89. DOI: 10.1016/0550-3213(95)00583-8. arXiv: hep-ph/9504337 [hep-ph].

[141] H. M. Lee, S. Raby, M. Ratz, G. G. Ross, R. Schieren, K. Schmidt-Hoberg, and P. K. S. Vaudrevange. "A unique $\mathbb{Z}_4^R$ symmetry for the MSSM." In: *Phys. Lett.* B694 (2011), pp. 491–495. DOI: 10.1016/j.physletb.2010.10.038. arXiv: 1009.0905 [hep-ph].

[142] H. M. Lee, S. Raby, M. Ratz, G. G. Ross, R. Schieren, K. Schmidt-Hoberg, and P. K. S. Vaudrevange. "Discrete R Symmetries for the MSSM and Its Singlet Extensions." In: *Nucl. Phys.* B850 (2011), pp. 1–30. DOI: 10.1016/j.nuclphysb.2011.04.009. arXiv: 1102.3595 [hep-ph].

[143] H. K. Dreiner, T. Opferkuch, and C. Luhn. "Froggatt-Nielsen models with a residual $\mathbb{Z}_4^R$ symmetry." In: *Phys. Rev.* D88.11 (2013), p. 115005. DOI: 10.1103/PhysRevD.88.115005. arXiv: 1308.0332 [hep-ph].

[144] M.-C. Chen, M. Ratz, and V. Takhistov. "R Parity Violation from Discrete R Symmetries." In: *Nucl. Phys.* B891 (2015), pp. 322–345. DOI: 10.1016/j.nuclphysb.2014.12.011. arXiv: 1410.3474 [hep-ph].

[145] R. D. Peccei. "The Strong CP Problem and Axions." In: *Lect. Notes Phys.* 741 (2008), pp. 3–17. DOI: 10.1007/978-3-540-73518-2_1. arXiv: hep-ph/0607268 [hep-ph].

[146] G. 't Hooft. "Symmetry Breaking Through Bell-Jackiw Anomalies." In: *Phys. Rev. Lett.* 37 (1976), pp. 8–11. DOI: 10.1103/PhysRevLett.37.8.

[147] G. 't Hooft. "Computation of the Quantum Effects Due to a Four-Dimensional Pseudoparticle." In: *Phys. Rev.* D14 (1976). [Erratum: Phys. Rev.D18,2199(1978)], pp. 3432–3450. DOI: 10.1103/PhysRevD.18.2199.3, 10.1103/PhysRevD.14.3432.

[148] R. J. Crewther, P. Di Vecchia, G. Veneziano, and E. Witten. "Chiral Estimate of the Electric Dipole Moment of the Neutron in Quantum Chromodynamics." In: *Phys. Lett.* 88B (1979). [Erratum: Phys. Lett.91B,487(1980)], p. 123. DOI: 10.1016/0370-2693(80)91025-4,10.1016/0370-2693(79)90128-X.

[149] C. A. Baker et al. "An Improved experimental limit on the electric dipole moment of the neutron." In: *Phys. Rev. Lett.* 97 (2006), p. 131801. DOI: 10.1103/PhysRevLett.97.131801. arXiv: hep-ex/0602020 [hep-ex].

[150] F. Wilczek. "Problem of Strong P and T Invariance in the Presence of Instantons." In: *Phys. Rev. Lett.* 40 (1978), pp. 279–282. DOI: 10.1103/PhysRevLett.40.279.

[151] S. Weinberg. "A New Light Boson?" In: *Phys. Rev. Lett.* 40 (1978), pp. 223–226. DOI: 10.1103/PhysRevLett.40.223.

[152] R. D. Peccei and H. R. Quinn. "CP Conservation in the Presence of Instantons." In: *Phys. Rev. Lett.* 38 (1977), pp. 1440–1443. DOI: 10.1103/PhysRevLett.38.1440.

[153] R. D. Peccei and H. R. Quinn. "Constraints Imposed by CP Conservation in the Presence of Instantons." In: *Phys. Rev.* D16 (1977), pp. 1791–1797. DOI: 10.1103/PhysRevD.16.1791.

[154] A. Strumia and F. Vissani. "Neutrino masses and mixings and..." In: (2006). arXiv: hep-ph/0606054 [hep-ph].

[155] P. Minkowski. "mu –>gt; e gamma at a Rate of One Out of 1-Billion Muon Decays?" In: *Phys.Lett.* B67 (1977), p. 421. DOI: 10.1016/0370-2693(77)90435-X.

[156] R. N. Mohapatra and G. Senjanovic. "Neutrino masses and mixings in gauge models with spontaneous parity violation." In: *Phys. Rev. D* 23 (1 1981), pp. 165–180. DOI: 10.1103/PhysRevD.23.165. URL: http://link.aps.org/doi/10.1103/PhysRevD.23.165.

[157] J. Schechter and J. W. F. Valle. "Neutrino Decay and Spontaneous Violation of Lepton Number." In: *Phys. Rev.* D25 (1982), p. 774. DOI: 10.1103/PhysRevD.25.774.

[158] M. Nowakowski and A. Pilaftsis. "W and Z boson interactions in supersymmetric models with explicit R-parity violation." In: *Nucl. Phys.* B461 (1996), pp. 19–49. DOI: 10.1016/0550-3213(95)00594-3. arXiv: hep-ph/9508271 [hep-ph].

[159] A. Hocker and W. J. Marciano. "The Muon Anomalous Magnetic Moment." In: (2008).

[160] A. Sakharov. "Violation of CP Invariance, C Asymmetry, and Baryon Asymmetry of the Universe." In: *Pisma Zh.Eksp.Teor.Fiz.* 5 (1967), pp. 32–35. DOI: 10.1070/PU1991v034n05ABEH002497.

[161] J. A. Harvey and M. S. Turner. "Cosmological baryon and lepton number in the presence of electroweak fermion number violation." In: *Phys.Rev.* D42 (1990), pp. 3344–3349. DOI: 10.1103/PhysRevD.42.3344.

[162] D. Huterer and D. L. Shafer. "Dark energy two decades after: Observables, probes, consistency tests." In: *Rept. Prog. Phys.* 81.1 (2018), p. 016901. DOI: 10.1088/1361-6633/aa997e. arXiv: 1709.01091 [astro-ph.CO].

[163] S. L. Adler. "Axial vector vertex in spinor electrodynamics." In: *Phys. Rev.* 177 (1969), pp. 2426–2438. DOI: 10.1103/PhysRev.177.2426.

[164] J. S. Bell and R. Jackiw. "A PCAC puzzle: pio –> gamma gamma in the sigma model." In: *Nuovo Cim.* A60 (1969), pp. 47–61. DOI: 10.1007/BF02823296.

[165] S. L. Adler and W. A. Bardeen. "Absence of higher order corrections in the anomalous axial vector divergence equation." In: *Phys. Rev.* 182 (1969), pp. 1517–1536. DOI: 10.1103/PhysRev.182.1517.

[166] Y. Nambu and G. Jona-Lasinio. "Dynamical Model of Elementary Particles Based on an Analogy with Superconductivity. 1." In: *Phys. Rev.* 122 (1961), pp. 345–358. DOI: 10.1103/PhysRev.122.345.

[167] W. A. Bardeen. "Anomalous Currents in Gauge Field Theories." In: *Nucl. Phys.* B75 (1974), pp. 246–258. DOI: 10.1016/0550-3213(74)90546-X.

[168] M. Srednicki. *Quantum field theory*. Cambridge University Press, 2007. ISBN: 9780521864497, 9780511267208.

[169] R. J. Crewther. "Effects of Topological Charge in Gauge Theories." In: *Acta Phys. Austriaca Suppl.* 19 (1978), pp. 47–153. DOI: 10.1007/978-3-7091-8538-4_3.

[170] R. Jackiw and C. Rebbi. "Vacuum Periodicity in a Yang-Mills Quantum Theory." In: *Phys. Rev. Lett.* 37 (1976), pp. 172–175. DOI: 10.1103/PhysRevLett.37.172.

[171] R. D. Peccei. "The Strong CP Problem." In: *Adv. Ser. Direct. High Energy Phys.* 3 (1989), pp. 503–551. DOI: 10.1142/9789814503280_0013.

[172] S. Yu. Khlebnikov and M. E. Shaposhnikov. "Extra Space-time Dimensions: Towards a Solution to the Strong CP Problem." In: *Phys. Lett.* B203 (1988), pp. 121–124. DOI: 10.1016/0370-2693(88)91582-1.

[173] G. Schierholz. "Towards a dynamical solution of the strong CP problem." In: *Nucl. Phys. Proc. Suppl.* 37A.1 (1994), pp. 203–210. DOI: 10.1016/0920-5632(94)90751-X. arXiv: hep-lat/9403012 [hep-lat].

[174] M. A. B. Beg and H. S. Tsao. "Strong P, T Noninvariances in a Superweak Theory." In: *Phys. Rev. Lett.* 41 (1978), p. 278. DOI: 10.1103/PhysRevLett.41.278.

[175] H. Georgi. "A Model of Soft CP Violation." In: *Hadronic J.* 1 (1978), p. 155.

[176] R. N. Mohapatra and G. Senjanovic. "Natural Suppression of Strong p and t Noninvariance." In: *Phys. Lett.* 79B (1978), pp. 283–286. DOI: 10.1016/0370-2693(78)90243-5.

[177] D. B. Kaplan and A. V. Manohar. "Current Mass Ratios of the Light Quarks." In: *Phys. Rev. Lett.* 56 (1986), p. 2004. DOI: 10.1103/PhysRevLett.56.2004.

[178] K. Choi, C. W. Kim, and W. K. Sze. "Mass Renormalization by Instantons and the Strong CP Problem." In: *Phys. Rev. Lett.* 61 (1988), p. 794. DOI: 10.1103/PhysRevLett.61.794.

[179] J. Gasser and H. Leutwyler. "Quark Masses." In: *Phys. Rept.* 87 (1982), pp. 77–169. DOI: 10.1016/0370-1573(82)90035-7.

[180] M. Dine. "TASI lectures on the strong CP problem." In: *Flavor physics for the millennium. Proceedings, Theoretical Advanced Study Institute in elementary particle physics, TASI 2000, Boulder, USA, June 4-30, 2000*. 2000, pp. 349–369. arXiv: hep-ph/0011376 [hep-ph].

[181] W. A. Bardeen, R. D. Peccei, and T. Yanagida. "CONSTRAINTS ON VARIANT AXION MODELS." In: *Nucl. Phys.* B279 (1987), pp. 401–428. DOI: 10.1016/0550-3213(87)90003-4.

[182] Y. Asano, E. Kikutani, S. Kurokawa, T. Miyachi, M. Miyajima, Y. Nagashima, T. Shinkawa, S. Sugimoto, and Y. Yoshimura. "Search for a Rare Decay Mode K+ —> pi+ Neutrino anti-neutrino and Axion." In: *Phys. Lett.* 107B (1981). [,411(1981)], p. 159. DOI: 10.1016/0370-2693(81)91172-2.

[183] J. E. Kim. "Weak Interaction Singlet and Strong CP Invariance." In: *Phys. Rev. Lett.* 43 (1979), p. 103. DOI: 10.1103/PhysRevLett.43.103.

[184] M. A. Shifman, A. I. Vainshtein, and V. I. Zakharov. "Can Confinement Ensure Natural CP Invariance of Strong Interactions?" In: *Nucl. Phys.* B166 (1980), pp. 493–506. DOI: 10.1016/0550-3213(80)90209-6.

[185] G. G. Raffelt. "Astrophysical Axion Bounds." In: *Lect. Notes Phys.* 741 (2008), pp. 51–71. DOI: 10.1007/978-3-540-73518-2_3. arXiv: hep-ph/0611350 [hep-ph].

[186] E. W. Kolb and M. S. Turner. "The Early Universe." In: *Front. Phys.* 69 (1990), pp. 1–547.

[187] P. Sikivie. "Of Axions, Domain Walls and the Early Universe." In: *Phys. Rev. Lett.* 48 (1982), pp. 1156–1159. DOI: 10.1103/PhysRevLett.48.1156.

[188] K.-Y. Choi, L. Covi, J. E. Kim, and L. Roszkowski. "Axino Cold Dark Matter Revisited." In: *JHEP* 04 (2012), p. 106. DOI: 10.1007/JHEP04(2012)106. arXiv: 1108.2282 [hep-ph].

[189] F. D'Eramo, L. J. Hall, and D. Pappadopulo. "Radiative Pq Breaking and the Higgs Boson Mass." In: *JHEP* 06 (2015), p. 117. DOI: 10.1007/JHEP06(2015)117. arXiv: 1502.06963 [hep-ph].

[190] R. F. Dashen. "Chiral SU(3) x SU(3) as a symmetry of the strong interactions." In: *Phys. Rev.* 183 (1969), pp. 1245–1260. DOI: 10.1103/PhysRev.183.1245.

[191] W. A. Bardeen and S. H. H. Tye. "Current Algebra Applied to Properties of the Light Higgs Boson." In: *Phys. Lett.* 74B (1978), pp. 229–232. DOI: 10.1016/0370-2693(78)90560-9.

[192] J. E. Kim and H. P. Nilles. "The mu Problem and the Strong CP Problem." In: *Phys. Lett.* 138B (1984), pp. 150–154. DOI: 10.1016/0370-2693(84)91890-2.

[193] H. P. Nilles and S. Raby. "Supersymmetry and the strong CP problem." In: *Nucl. Phys.* B198 (1982), pp. 102–112. DOI: 10.1016/0550-3213(82)90547-8.

[194] K. Rajagopal, M. S. Turner, and F. Wilczek. "Cosmological Implications of Axinos." In: *Nucl. Phys.* B358 (1991), pp. 447–470. DOI: 10.1016/0550-3213(91)90355-2.

[195] J. E. Kim. "A Common Scale for the Invisible Axion, Local SUSY GUTs and Saxino Decay." In: *Phys. Lett.* 136B (1984), pp. 378–382. DOI: 10.1016/0370-2693(84)92023-9.

[196] H. K. Dreiner, F. Staub, and L. Ubaldi. "From the Unification Scale to the Weak Scale: a Self Consistent Supersymmetric Dine-Fischler-Srednicki-Zhitnitsky Axion Model." In: *Phys. Rev.* D90.5 (2014), p. 055016. DOI: 10.1103/PhysRevD.90.055016. arXiv: 1402.5977 [hep-ph].

[197] L. Covi, H.-B. Kim, J. E. Kim, and L. Roszkowski. "Axinos as Dark Matter." In: *JHEP* 05 (2001), p. 033. DOI: 10.1088/1126-6708/2001/05/033. arXiv: hep-ph/0101009 [hep-ph].

[198] K. J. Bae, K. Choi, and S. H. Im. "Effective Interactions of Axion Supermultiplet and Thermal Production of Axino Dark Matter." In: *JHEP* 08 (2011), p. 065. DOI: 10.1007/JHEP08(2011)065. arXiv: 1106.2452 [hep-ph].

[199] S. Colucci, H. K. Dreiner, F. Staub, and L. Ubaldi. "Heavy concerns about the light axino explanation of the 3.5 keV X-ray line." In: *Phys. Lett.* B750 (2015), pp. 107–111. DOI: 10.1016/j.physletb.2015.09.009. arXiv: 1507.06200 [hep-ph].

[200] R. N. Mohapatra and P. B. Pal. "Massive neutrinos in physics and astrophysics. Second edition." In: *World Sci. Lect. Notes Phys.* 60 (1998). [World Sci. Lect. Notes Phys.72,1(2004)], pp. 1–397.

[201] T. Asaka, S. Blanchet, and M. Shaposhnikov. "The nuMSM, dark matter and neutrino masses." In: *Phys. Lett.* B631 (2005), pp. 151–156. DOI: 10.1016/j.physletb.2005.09.070. arXiv: hep-ph/0503065 [hep-ph].

[202] T. Yanagida. "Horizontal Symmetry and Masses of Neutrinos." In: *Prog. Theor. Phys.* 64 (1980), p. 1103. DOI: 10.1143/PTP.64.1103.

[203] R. N. Mohapatra and G. Senjanovic. "Neutrino Mass and Spontaneous Parity Violation." In: *Phys. Rev. Lett.* 44 (1980), p. 912. DOI: 10.1103/PhysRevLett.44.912.

[204] S. F. King. "Neutrino mass models." In: *Rept. Prog. Phys.* 67 (2004), pp. 107–158. DOI: 10.1088/0034-4885/67/2/R01. arXiv: hep-ph/0310204 [hep-ph].

[205] M. Drewes et al. "A White Paper on keV Sterile Neutrino Dark Matter." In: *JCAP* 1701.01 (2017), p. 025. DOI: 10.1088/1475-7516/2017/01/025. arXiv: 1602.04816 [hep-ph].

[206] P. A. R. Ade et al. "Planck 2015 results. XIII. Cosmological parameters." In: *Astron. Astrophys.* 594 (2016), A13. DOI: 10.1051/0004-6361/201525830. arXiv: 1502.01589 [astro-ph.CO].

[207] A. Boyarsky, O. Ruchayskiy, and M. Shaposhnikov. "The Role of sterile neutrinos in cosmology and astrophysics." In: *Ann. Rev. Nucl. Part. Sci.* 59 (2009), pp. 191–214. DOI: 10.1146/annurev.nucl.010909.083654. arXiv: 0901.0011 [hep-ph].

[208] S. Tremaine and J. E. Gunn. "Dynamical Role of Light Neutral Leptons in Cosmology." In: *Phys. Rev. Lett.* 42 (1979), pp. 407–410. DOI: 10.1103/PhysRevLett.42.407.

[209] V. D. Barger, R. J. N. Phillips, and S. Sarkar. "Remarks on the Karmen Anomaly." In: *Phys. Lett.* B352 (1995). [Erratum: Phys. Lett. B356, 617 (1995)], pp. 365–371. DOI: 10.1016/0370-2693(95)00486-5,10.1016/0370-2693(95)00831-5. arXiv: hep-ph/9503295 [hep-ph].

[210] P. B. Pal and L. Wolfenstein. "Radiative Decays of Massive Neutrinos." In: *Phys. Rev.* D25 (1982), p. 766. DOI: 10.1103/PhysRevD.25.766.

[211] D. E. Gruber, J. L. Matteson, L. E. Peterson, and G. V. Jung. "The spectrum of diffuse cosmic hard x-rays measured with heao-1." In: *Astrophys. J.* 520 (1999), p. 124. DOI: 10.1086/307450. arXiv: astro-ph/9903492 [astro-ph].

[212] K. Abazajian, G. M. Fuller, and M. Patel. "Sterile neutrino hot, warm, and cold dark matter." In: *Phys. Rev.* D64 (2001), p. 023501. DOI: 10.1103/PhysRevD.64.023501. arXiv: astro-ph/0101524 [astro-ph].

[213] K. Abazajian, G. M. Fuller, and W. H. Tucker. "Direct detection of warm dark matter in the X-ray." In: *Astrophys. J.* 562 (2001), pp. 593–604. DOI: 10.1086/323867. arXiv: astro-ph/0106002 [astro-ph].

[214] A. Boyarsky, A. Neronov, O. Ruchayskiy, M. Shaposhnikov, and I. Tkachev. "Where to find a dark matter sterile neutrino?" In: *Phys. Rev. Lett.* 97 (2006), p. 261302. DOI: 10.1103/PhysRevLett.97.261302. arXiv: astro-ph/0603660 [astro-ph].

[215] A. Boyarsky, O. Ruchayskiy, D. Iakubovskyi, A. V. Maccio', and D. Malyshev. "New evidence for dark matter." In: (2009). arXiv: 0911.1774 [astro-ph.CO].

[216] M. Loewenstein, A. Kusenko, and P. L. Biermann. "New Limits on Sterile Neutrinos from Suzaku Observations of the Ursa Minor Dwarf Spheroidal Galaxy." In: *Astrophys. J.* 700 (2009), pp. 426–435. DOI: 10.1088/0004-637X/700/1/426. arXiv: 0812.2710 [astro-ph].

[217] A. Boyarsky, A. Neronov, O. Ruchayskiy, and M. Shaposhnikov. "Constraints on sterile neutrino as a dark matter candidate from the diffuse x-ray background." In: *Mon. Not. Roy. Astron. Soc.* 370 (2006), pp. 213–218. DOI: 10.1111/j.1365-2966.2006.10458.x. arXiv: astro-ph/0512509 [astro-ph].

[218] M. Loewenstein and A. Kusenko. "Dark Matter Search Using XMM-Newton Observations of Willman 1." In: *Astrophys. J.* 751 (2012), p. 82. DOI: 10.1088/0004-637X/751/2/82. arXiv: 1203.5229 [astro-ph.CO].

[219] H. Yuksel, J. F. Beacom, and C. R. Watson. "Strong Upper Limits on Sterile Neutrino Warm Dark Matter." In: *Phys. Rev. Lett.* 101 (2008), p. 121301. DOI: 10.1103/PhysRevLett.101.121301. arXiv: 0706.4084 [astro-ph].

[220] S. Riemer-Sorensen and S. H. Hansen. "Decaying dark matter in Draco." In: *Astron. Astrophys.* 500 (2009), pp. L37–L40. DOI: 10.1051/0004-6361/200912430. arXiv: 0901.2569 [astro-ph.CO].

[221] M. Kawasaki and K. Nakayama. "Axions: Theory and Cosmological Role." In: *Ann. Rev. Nucl. Part. Sci.* 63 (2013), pp. 69–95. DOI: 10.1146/annurev-nucl-102212-170536. arXiv: 1301.1123 [hep-ph].

[222] L. Covi and J. E. Kim. "Axinos as Dark Matter Particles." In: *New J. Phys.* 11 (2009), p. 105003. DOI: 10.1088/1367-2630/11/10/105003. arXiv: 0902.0769 [astro-ph.CO].

[223] K. J. Bae, E. J. Chun, and S. H. Im. "Cosmology of the DFSZ Axino." In: *JCAP* 1203 (2012), p. 013. DOI: 10.1088/1475-7516/2012/03/013. arXiv: 1111.5962 [hep-ph].

[224] C. Cheung, G. Elor, and L. J. Hall. "The Cosmological Axino Problem." In: *Phys. Rev.* D85 (2012), p. 015008. DOI: 10.1103/PhysRevD.85.015008. arXiv: 1104.0692 [hep-ph].

[225] R. T. Co, F. D'Eramo, and L. J. Hall. "Gravitino Or Axino Dark Matter with Reheat Temperature as High as 10^{16} GeV." In: *JHEP* 03 (2017), p. 005. DOI: 10.1007/JHEP03(2017)005. arXiv: 1611.05028 [hep-ph].

[226] M. Viel, J. Lesgourgues, M. G. Haehnelt, S. Matarrese, and A. Riotto. "Constraining warm dark matter candidates including sterile neutrinos and light gravitinos with WMAP and the Lyman-alpha forest." In: *Phys. Rev.* D71 (2005), p. 063534. DOI: 10.1103/PhysRevD.71.063534. arXiv: astro-ph/0501562 [astro-ph].

[227] M. Bolz, A. Brandenburg, and W. Buchmuller. "Thermal production of gravitinos." In: *Nucl. Phys.* B606 (2001). [Erratum: Nucl. Phys.B790,336(2008)], pp. 518–544. DOI: 10.1016/S0550-3213(01)00132-8,10.1016/j.nuclphysb.2007.09.020. arXiv: hep-ph/0012052 [hep-ph].

[228] H. K. Dreiner, M. Hanussek, J. S. Kim, and S. Sarkar. "Gravitino cosmology with a very light neutralino." In: *Phys. Rev.* D85 (2012), p. 065027. DOI: 10.1103/PhysRevD.85.065027. arXiv: 1111.5715 [hep-ph].

[229] Z. Hou, R. Keisler, L. Knox, M. Millea, and C. Reichardt. "How Massless Neutrinos Affect the Cosmic Microwave Background Damping Tail." In: *Phys. Rev.* D87 (2013), p. 083008. DOI: 10.1103/PhysRevD.87.083008. arXiv: 1104.2333 [astro-ph.CO].

[230] H. K. Dreiner, C. Hanhart, U. Langenfeld, and D. R. Phillips. "Supernovae and light neutralinos: SN1987A bounds on supersymmetry revisited." In: *Phys. Rev.* D68 (2003), p. 055004. DOI: 10.1103/PhysRevD.68.055004. arXiv: hep-ph/0304289 [hep-ph].

[231] H. K. Dreiner, S. Heinemeyer, O. Kittel, U. Langenfeld, A. M. Weber, and G. Weiglein. "Mass Bounds on a Very Light Neutralino." In: *Eur. Phys. J.* C62 (2009), pp. 547–572. DOI: 10.1140/epjc/s10052-009-1042-y. arXiv: 0901.3485 [hep-ph].

[232] H. K. Dreiner, S. Grab, D. Koschade, M. Kramer, B. O'Leary, and U. Langenfeld. "Rare meson decays into very light neutralinos." In: *Phys. Rev.* D80 (2009), p. 035018. DOI: 10.1103/PhysRevD.80.035018. arXiv: 0905.2051 [hep-ph].

[233] M. Hirsch and J. Valle. "Neutrinoless double beta decay in supersymmetry with bilinear R parity breaking." In: *Nucl. Phys.* B557 (1999), pp. 60–78. DOI: 10.1016/S0550-3213(99)00368-5. arXiv: hep-ph/9812463 [hep-ph].

[234] T. Banks, Y. Grossman, E. Nardi, and Y. Nir. "Supersymmetry without R-parity and without lepton number." In: *Phys. Rev.* D52 (1995), pp. 5319–5325. DOI: 10.1103/PhysRevD.52.5319. arXiv: hep-ph/9505248 [hep-ph].

[235] M. Hirsch and J. Valle. "Supersymmetric origin of neutrino mass." In: *New J. Phys.* 6 (2004), p. 76. DOI: 10.1088/1367-2630/6/1/076. arXiv: hep-ph/0405015 [hep-ph].

[236] H. K. Dreiner and G. G. Ross. "R-parity violation at hadron colliders." In: *Nucl. Phys.* B365 (1991), pp. 597–613. DOI: 10.1016/0550-3213(91)90443-2.

[237] W. Hu and J. Silk. "Thermalization and spectral distortions of the cosmic background radiation." In: *Phys. Rev.* D48 (1993), pp. 485–502. DOI: 10.1103/PhysRevD.48.485.

[238] J. R. Ellis, G. B. Gelmini, J. L. Lopez, D. V. Nanopoulos, and S. Sarkar. "Astrophysical constraints on massive unstable neutral relic particles." In: *Nucl. Phys.* B373 (1992), pp. 399–437. DOI: 10.1016/0550-3213(92)90438-H.

[239] S. Alekhin et al. "A facility to Search for Hidden Particles at the CERN SPS: the SHiP physics case." In: *Rept. Prog. Phys.* 79.12 (2016), p. 124201. DOI: 10.1088/0034-4885/79/12/124201. arXiv: 1504.04855 [hep-ph].

[240] J. A. Conley, H. K. Dreiner, and P. Wienemann. "Measuring a Light Neutralino Mass at the ILC: Testing the MSSM Neutralino Cold Dark Matter Model." In: *Phys. Rev.* D83 (2011), p. 055018. DOI: 10.1103/PhysRevD.83.055018. arXiv: 1012.1035 [hep-ph].

[241] S. Colucci, H. K. Dreiner, and L. Ubaldi. "The Supersymmetric R-Parity Violating Dine-Fischler-Srednicki-Zhitnitsky Axion Model." In: (2018). arXiv: 1807.02530 [hep-ph].

[242] J. Preskill, M. B. Wise, and F. Wilczek. "Cosmology of the Invisible Axion." In: *Phys. Lett.* 120B (1983), pp. 127–132. DOI: 10.1016/0370-2693(83)90637-8.

[243] R. Holman, G. Lazarides, and Q. Shafi. "Axions and the Dark Matter of the Universe." In: *Phys. Rev.* D27 (1983), p. 995. DOI: 10.1103/PhysRevD.27.995.

[244] K.-Y. Choi, J. E. Kim, and L. Roszkowski. "Review of Axino Dark Matter." In: *J. Korean Phys. Soc.* 63 (2013), pp. 1685–1695. DOI: 10.3938/jkps.63.1685. arXiv: 1307.3330 [astro-ph.CO].

[245] K. Tamvakis and D. Wyler. "Broken Global Symmetries in Supersymmetric Theories." In: *Phys. Lett.* 112B (1982), pp. 451–454. DOI: 10.1016/0370-2693(82)90846-2.

[246] T. Goto and M. Yamaguchi. "Is Axino Dark Matter Possible in Supergravity?" In: *Phys. Lett.* B276 (1992), pp. 103–107. DOI: 10.1016/0370-2693(92)90547-H.

[247] E. J. Chun, J. E. Kim, and H. P. Nilles. "Axino Mass." In: *Phys. Lett.* B287 (1992), pp. 123–127. DOI: 10.1016/0370-2693(92)91886-E. arXiv: hep-ph/9205229 [hep-ph].

[248] E. J. Chun and A. Lukas. "Axino Mass in Supergravity Models." In: *Phys. Lett.* B357 (1995), pp. 43–50. DOI: 10.1016/0370-2693(95)00881-K. arXiv: hep-ph/9503233 [hep-ph].

[249] P. Moxhay and K. Yamamoto. "Peccei-Quinn Symmetry Breaking by Radiative Corrections in Supergravity." In: *Phys. Lett.* 151B (1985), pp. 363–366. DOI: 10.1016/0370-2693(85)91655-7.

[250] J. E. Kim and M.-S. Seo. "Mixing of Axino and Goldstino, and Axino Mass." In: *Nucl. Phys.* B864 (2012), pp. 296–316. DOI: 10.1016/j.nuclphysb.2012.06.018. arXiv: 1204.5495 [hep-ph].

[251] G. Honecker and W. Staessens. "On Axionic Dark Matter in Type IIA String Theory." In: *Fortsch. Phys.* 62 (2014), pp. 115–151. DOI: 10.1002/prop.201300036. arXiv: 1312.4517 [hep-th].

[252] G. F. Giudice and R. Rattazzi. "Theories with Gauge Mediated Supersymmetry Breaking." In: *Phys. Rept.* 322 (1999), pp. 419–499. DOI: 10.1016/S0370-1573(99)00042-3. arXiv: hep-ph/9801271 [hep-ph].

[253] T. Banks, M. Dine, and M. Graesser. "Supersymmetry, Axions and Cosmology." In: *Phys. Rev.* D68 (2003), p. 075011. DOI: 10.1103/PhysRevD.68.075011. arXiv: hep-ph/0210256 [hep-ph].

[254] L. M. Carpenter, M. Dine, G. Festuccia, and L. Ubaldi. "Axions in Gauge Mediation." In: *Phys. Rev.* D80 (2009), p. 125023. DOI: 10.1103/PhysRevD.80.125023. arXiv: 0906.5015 [hep-th].

[255] H. Georgi, D. B. Kaplan, and L. Randall. "Manifesting the Invisible Axion at Low-Energies." In: *Phys. Lett.* 169B (1986), pp. 73–78. DOI: 10.1016/0370-2693(86)90688-X.

[256] F. Staub. "SARAH." In: (2008). arXiv: 0806.0538 [hep-ph].

[257] F. Staub. "From Superpotential to Model Files for FeynArts and CalcHep/CompHep." In: *Comput. Phys. Commun.* 181 (2010), pp. 1077–1086. DOI: 10.1016/j.cpc.2010.01.011. arXiv: 0909.2863 [hep-ph].

[258] F. Staub. "Automatic Calculation of supersymmetric Renormalization Group Equations and Self Energies." In: *Comput. Phys. Commun.* 182 (2011), pp. 808–833. DOI: 10.1016/j.cpc.2010.11.030. arXiv: 1002.0840 [hep-ph].

[259] H. K. Dreiner and M. Thormeier. "Supersymmetric Froggatt-Nielsen models with baryon and lepton number violation." In: *Phys. Rev.* D69 (2004), p. 053002. DOI: 10.1103/PhysRevD.69.053002. arXiv: hep-ph/0305270 [hep-ph].

[260] Y. Grossman and H. E. Haber. "Neutrino Masses and Sneutrino Mixing in R-Parity Violating Supersymmetry." In: 1999. arXiv: hep-ph/9906310 [hep-ph]. URL: http://www-public.slac.stanford.edu/sciDoc/docMeta.aspx?slacPubNumber=SLAC-PUB-8173.

[261] M. Kawasaki and T. Moroi. "Gravitino production in the inflationary universe and the effects on big bang nucleosynthesis." In: *Prog. Theor. Phys.* 93 (1995), pp. 879–900. DOI: 10.1143/PTP.93.879, 10.1143/ptp/93.5.879. arXiv: hep-ph/9403364 [hep-ph].

[262] O. Wantz and E. P. S. Shellard. "Axion Cosmology Revisited." In: *Phys. Rev.* D82 (2010), p. 123508. DOI: 10.1103/PhysRevD.82.123508. arXiv: 0910.1066 [astro-ph.CO].

[263] K. J. Bae, J.-H. Huh, and J. E. Kim. "Update of axion CDM energy." In: *JCAP* 0809 (2008), p. 005. DOI: 10.1088/1475-7516/2008/09/005. arXiv: 0806.0497 [hep-ph].

[264] M. S. Turner. "Cosmic and Local Mass Density of Invisible Axions." In: *Phys. Rev.* D33 (1986), pp. 889–896. DOI: 10.1103/PhysRevD.33.889.

[265] P. Sikivie. "Axion Cosmology." In: *Lect. Notes Phys.* 741 (2008). [,19(2006)], pp. 19–50. DOI: 10.1007/978-3-540-73518-2_2. arXiv: astro-ph/0610440 [astro-ph].

[266] A. Albrecht and N. Turok. "Evolution of Cosmic Strings." In: *Phys. Rev. Lett.* 54 (1985), pp. 1868–1871. DOI: 10.1103/PhysRevLett.54.1868.

[267] D. P. Bennett and F. R. Bouchet. "Evidence for a Scaling Solution in Cosmic String Evolution." In: *Phys. Rev. Lett.* 60 (1988), p. 257. DOI: 10.1103/PhysRevLett.60.257.

[268] M. Kuster, G. Raffelt, and B. Beltran. "Axions: Theory, Cosmology, and Experimental Searches. Proceedings, 1St Joint Ilias-Cern-Cast Axion Training, Geneva, Switzerland, November 30-December 2, 2005." In: *Lect. Notes Phys.* 741 (2008), pp.1–258.

[269] B. Mukhopadhyaya and S. Roy. "Radiative Decay of the Lightest Neutralino in an R-Parity Violating Supersymmetric Theory." In: *Phys. Rev.* D60 (1999), p. 115012. DOI: 10.1103/PhysRevD.60.115012. arXiv: hep-ph/9903418 [hep-ph].

[270] L. Lavoura. "General Formulae for $f_1 \to f_2\gamma$." In: *Eur. Phys. J.* C29 (2003), pp. 191–195. DOI: 10.1140/epjc/$S^2$003-01212-7. arXiv: hep-ph/0302221 [hep-ph].

[271] S. Dawson. "R-Parity Breaking in Supersymmetric Theories." In: *Nucl. Phys.* B261 (1985), pp. 297–318. DOI: 10.1016/0550-3213(85)90577-2.

[272] "Search for Selectrons and Smuons at $\sqrt{s} = 13$ TeV." In: *CMS-PAS-SUS-17-009* (2017).

[273] B. C. Allanach, A. Dedes, and H. K. Dreiner. "Bounds on R-Parity Violating Couplings at the Weak Scale and at the GUT Scale." In: *Phys. Rev.* D60 (1999), p. 075014. DOI: 10.1103/PhysRevD.60.075014. arXiv: hep-ph/9906209 [hep-ph].

[274] P. Arias, D. Cadamuro, M. Goodsell, J. Jaeckel, J. Redondo, and A. Ringwald. "Wispy Cold Dark Matter." In: *JCAP* 1206 (2012), p. 013. DOI: 10.1088/1475-7516/2012/06/013. arXiv: 1201.5902 [hep-ph].

[275] R. Essig, E. Kuflik, S. D. McDermott, T. Volansky, and K. M. Zurek. "Constraining Light Dark Matter with Diffuse X-Ray and Gamma-Ray Observations." In: *JHEP* 11 (2013), p. 193. DOI: 10.1007/JHEP11(2013)193. arXiv: 1309.4091 [hep-ph].

[276] Q.-H. Cao, C.-R. Chen, C. S. Li, and H. Zhang. "Effective Dark Matter Model: Relic density, CDMS II, Fermi LAT and LHC." In: *JHEP* 08 (2011), p. 018. DOI: 10.1007/JHEP08(2011)018. arXiv: 0912.4511 [hep-ph].

[277] J. Goodman, M. Ibe, A. Rajaraman, W. Shepherd, T. M. P. Tait, and H.-B. Yu. "Constraints on Dark Matter from Colliders." In: *Phys. Rev.* D82 (2010), p. 116010. DOI: 10.1103/PhysRevD.82.116010. arXiv: 1008.1783 [hep-ph].

[278] A. Rajaraman, W. Shepherd, T. M. P. Tait, and A. M. Wijangco. "LHC Bounds on Interactions of Dark Matter." In: *Phys. Rev.* D84 (2011), p. 095013. DOI: 10.1103/PhysRevD.84.095013. arXiv: 1108.1196 [hep-ph].

[279] P. J. Fox, R. Harnik, J. Kopp, and Y. Tsai. "Missing Energy Signatures of Dark Matter at the LHC." In: *Phys. Rev.* D85 (2012), p. 056011. DOI: 10.1103/PhysRevD.85.056011. arXiv: 1109.4398 [hep-ph].

[280] P. J. Fox, R. Harnik, J. Kopp, and Y. Tsai. "LEP Shines Light on Dark Matter." In: *Phys. Rev.* D84 (2011), p. 014028. DOI: 10.1103/PhysRevD.84.014028. arXiv: 1103.0240 [hep-ph].

[281] I. M. Shoemaker and L. Vecchi. "Unitarity and Monojet Bounds on Models for DAMA, CoGeNT, and CRESST-II." In: *Phys. Rev.* D86 (2012), p. 015023. DOI: 10.1103/PhysRevD.86.015023. arXiv: 1112.5457 [hep-ph].

[282] O. Buchmueller, M. J. Dolan, and C. McCabe. "Beyond Effective Field Theory for Dark Matter Searches at the LHC." In: *JHEP* 01 (2014), p. 025. DOI: 10.1007/JHEP01(2014)025. arXiv: 1308.6799 [hep-ph].

[283] D. Racco, A. Wulzer, and F. Zwirner. "Robust collider limits on heavy-mediator Dark Matter." In: *JHEP* 05 (2015), p. 009. DOI: 10.1007/JHEP05(2015)009. arXiv: 1502.04701 [hep-ph].

[284] D. Abercrombie et al. "Dark Matter Benchmark Models for Early LHC Run-2 Searches: Report of the ATLAS/CMS Dark Matter Forum." In: (2015). Ed. by A. Boveia, C. Doglioni, S. Lowette, S. Malik, and S. Mrenna. arXiv: 1507.00966 [hep-ex].

[285] A. Albert et al. "Towards the next generation of simplified Dark Matter models." In: *Phys. Dark Univ.* 16 (2017), pp. 49–70. DOI: 10.1016/j.dark.2017.02.002. arXiv: 1607.06680 [hep-ex].

[286] P. Fileviez Perez and M. B. Wise. "Baryon Asymmetry and Dark Matter Through the Vector-Like Portal." In: *JHEP* 05 (2013), p. 094. DOI: 10.1007/JHEP05(2013)094. arXiv: 1303.1452 [hep-ph].

[287] H. Goldberg. "Constraint on the Photino Mass from Cosmology." In: *Phys. Rev. Lett.* 50 (1983). [Erratum: Phys. Rev. Lett.103,099905(2009)], p. 1419. DOI: 10.1103/PhysRevLett.50.1419.

[288] T. Toma. "Internal Bremsstrahlung Signature of Real Scalar Dark Matter and Consistency with Thermal Relic Density." In: *Phys. Rev. Lett.* 111 (2013), p. 091301. DOI: 10.1103/PhysRevLett.111.091301. arXiv: 1307.6181 [hep-ph]. URL: http://dx.doi.org/10.1103/PhysRevLett.111.091301.

[289] R. Flores, K. A. Olive, and S. Rudaz. "Radiative Processes in Lsp Annihilation." In: *Phys. Lett.* B232 (1989), pp. 377–382. DOI: 10.1016/0370-2693(89)90760-0. URL: http://dx.doi.org/10.1016/0370-2693(89)90760-0.

[290] T. Bringmann, X. Huang, A. Ibarra, S. Vogl, and C. Weniger. "Fermi LAT Search for Internal Bremsstrahlung Signatures from Dark Matter Annihilation." In: *JCAP* 1207 (2012), p. 054. DOI: 10.1088/1475-7516/2012/07/054. arXiv: 1203.1312 [hep-ph].

[291] N. F. Bell, J. B. Dent, T. D. Jacques, and T. J. Weiler. "Dark Matter Annihilation Signatures from Electroweak Bremsstrahlung." In: *Phys. Rev.* D84 (2011), p. 103517. DOI: 10.1103/PhysRevD.84.103517. arXiv: 1101.3357 [hep-ph].

[292] M. Garny, A. Ibarra, M. Pato, and S. Vogl. "Internal bremsstrahlung signatures in light of direct dark matter searches." In: *JCAP* 1312 (2013), p. 046. DOI: 10.1088/1475-7516/2013/12/046. arXiv: 1306.6342 [hep-ph].

[293] M. Garny, A. Ibarra, and S. Vogl. "Signatures of Majorana dark matter with t-channel mediators." In: *Int. J. Mod. Phys.* D24.07 (2015), p. 1530019. DOI: 10.1142/S0218271815300190. arXiv: 1503.01500 [hep-ph].

[294] F. Giacchino, L. Lopez-Honorez, and M. H. G. Tytgat. "Bremsstrahlung and Gamma Ray Lines in 3 Scenarios of Dark Matter Annihilation." In: *JCAP* 1408 (2014), p. 046. DOI: 10.1088/1475-7516/2014/08/046. arXiv: 1405.6921 [hep-ph].

[295] A. Ibarra, T. Toma, M. Totzauer, and S. Wild. "Sharp Gamma-ray Spectral Features from Scalar Dark Matter Annihilations." In: *Phys. Rev.* D90.4 (2014), p. 043526. DOI: 10.1103/PhysRevD.90.043526. arXiv: 1405.6917 [hep-ph].

[296] F. Giacchino, A. Ibarra, L. Lopez Honorez, M. H. G. Tytgat, and S. Wild. "Signatures from Scalar Dark Matter with a Vector-like Quark Mediator." In: *JCAP* 1602.02 (2016), p. 002. DOI: 10.1088/1475-7516/2016/02/002. arXiv: 1511.04452 [hep-ph].

[297] T. Bringmann, A. J. Galea, and P. Walia. "Leading QCD Corrections for Indirect Dark Matter Searches: a Fresh Look." In: *Phys. Rev.* D93.4 (2016), p. 043529. DOI: 10.1103/PhysRevD.93.043529. arXiv: 1510.02473 [hep-ph].

[298] S. Colucci, B. Fuks, F. Giacchino, L. Lopez Honorez, M. H. G. Tytgat, and J. Vandecasteele. "Top-philic Vector-Like Portal to Scalar Dark Matter." In: (2018). arXiv: 1804.05068 [hep-ph].

[299] T. Kinoshita. "Mass singularities of Feynman amplitudes." In: *J. Math. Phys.* 3 (1962), pp. 650–677. DOI: 10.1063/1.1724268.

[300] F. Bloch and A. Nordsieck. "Note on the Radiation Field of the electron." In: *Phys. Rev.* 52 (1937), pp. 54–59. DOI: 10.1103/PhysRev.52.54.

[301] V. Barger, Y. Gao, W. Y. Keung, and D. Marfatia. "Generic dark matter signature for gamma-ray telescopes." In: *Phys. Rev.* D80 (2009), p. 063537. DOI: 10.1103/PhysRevD.80.063537. arXiv: 0906.3009 [hep-ph].

[302] V. Barger, W.-Y. Keung, and D. Marfatia. "Bremsstrahlung in dark matter annihilation." In: *Phys. Lett.* B707 (2012), pp. 385–388. DOI: 10.1016/j.physletb.2012.01.001. arXiv: 1111.4523 [hep-ph].

[303] M. Drees and K.-i. Hikasa. "Note on qcd corrections to hadronic higgs decay." In: *Phys. Lett.* B240 (1990). [Erratum: Phys. Lett.B262,497(1991)], p. 455. DOI: 10.1016/0370-2693(90)91130-4.

[304] E. Braaten and J. P. Leveille. "Higgs Boson Decay and the Running Mass." In: *Phys. Rev.* D22 (1980), p. 715. DOI: 10.1103/PhysRevD.22.715.

[305] B. De Wit and J. Smith. *Field Theory in Particle Physics Volume 1*. Amsterdam, Netherlands: North-Holland, 1986.

[306] M. E. Peskin and D. V. Schroeder. *An Introduction to quantum field theory*. Reading, USA: Addison-Wesley, 1995. ISBN: 9780201503975, 0201503972. URL: http://www.slac.stanford.edu/~mpeskin/QFT.html.

[307] M. Drees and K.-i. Hikasa. "Heavy Quark Thresholds in Higgs Physics." In: *Phys. Rev.* D41 (1990), p. 1547. DOI: 10.1103/PhysRevD.41.1547.

[308] T. Sjöstrand, S. Ask, J. R. Christiansen, R. Corke, N. Desai, P. Ilten, S. Mrenna, S. Prestel, C. O. Rasmussen, and P. Z. Skands. "An Introduction to PYTHIA 8.2." In: *Comput. Phys. Commun.* 191 (2015), pp. 159–177. DOI: 10.1016/j.cpc.2015.01.024. arXiv: 1410.3012 [hep-ph].

[309] A. Birkedal, K. Matchev, and M. Perelstein. "Dark matter at colliders: A Model independent approach." In: *Phys. Rev.* D70 (2004), p. 077701. DOI: 10.1103/PhysRevD.70.077701. arXiv: hep-ph/0403004 [hep-ph].

[310] A. Belyaev, N. D. Christensen, and A. Pukhov. "CalcHEP 3.4 for collider physics within and beyond the Standard Model." In: *Comput. Phys. Commun.* 184 (2013), pp. 1729–1769. DOI: 10.1016/j.cpc.2013.01.014. arXiv: 1207.6082 [hep-ph].

[311] S. Y. Choi, J. Kalinowski, G. A. Moortgat-Pick, and P. M. Zerwas. "Analysis of the neutralino system in supersymmetric theories." In: *Eur. Phys. J.* C22 (2001). [Addendum: Eur. Phys. J. C23, 769 (2002)], pp. 563–579. DOI: 10.1007/s100520100808. arXiv: hep-ph/0108117 [hep-ph].

[312] S. Y. Choi, D. J. Miller, and P. M. Zerwas. "The Neutralino Sector of the Next-To-Minimal Supersymmetric Standard Model." In: *Nucl. Phys.* B711 (2005), pp. 83–111. DOI: 10.1016/j.nuclphysb.2005.01.006. arXiv: hep-ph/0407209 [hep-ph].